Spatio-temporal variation in the spring freshet of major circumpolar Arctic river systems

by

Roxanne Ahmed
B.Eng., University of Victoria, 2011

A Thesis Submitted in Partial Fulfillment
of the Requirements for the Degree of

MASTER OF SCIENCE

In the Department of Geography

Supervisory Committee

Spatio-temporal variation in the spring freshet of major circumpolar Arctic river systems

by

Roxanne Ahmed
B.Eng., University of Victoria, 2011

Supervisory Committee
Dr. Terry D. Prowse (Department of Geography)
Supervisor

Dr. Barrie R. Bonsal (Department of Geography)
Departmental member

Dr. Yonas B. Dibike (Department of Geography)
Departmental member

Abstract

Supervisory Committee
Dr. Terry D. Prowse (Department of Geography)
Supervisor
Dr. Barrie R. Bonsal (Department of Geography)
Departmental member
Dr. Yonas B. Dibike (Department of Geography)
Departmental member

The spring freshet is the dominant annual hydrologic event occurring on largely nival Arctic river systems. It provides the greatest proportion of freshwater influx to the Arctic Ocean, amongst all other atmospheric input sources. To assess whether any shift in the seasonality of spring freshets has occurred, and how climatic drivers and flow regulation govern trends in sub-basin freshets and their contribution to outlet flow, a temporal and spatial analysis of 106 hydrometric stations located across four major Arctic-draining river systems is performed to extract information regarding the timing, magnitude and volume of the spring freshet of the four largest Arctic-draining rivers; namely, the Mackenzie River in Canada, and the Ob, Yenisei and Lena rivers in Eurasia. Total annual freshwater influx to the Arctic Ocean from these basins increased by 14% during 1980-2009. Despite freshet volume displaying a net increase, its proportional contribution to annual flow has decreased. In fact, rising winter, spring and fall discharge proportions, combined with lower peak freshet magnitudes, potentially increased freshet durations, and lower summer proportions indicate a shift towards flatter, more gradual annual hydrographs with earlier pulse onsets. Discharge assessed on a sub-basin level during 1962-2000 and 1980-2000 reveals regional differences in trends, with higher-relief drainage areas displaying the strongest trends. Sub-basin trends generally agree with those at the outlets, particularly in sub-basins without upstream flow regulation. Flow regulation has had a greater impact on observed trends in freshet volume compared to peak freshet magnitude. Timing measures are found to be strongly linked to spring temperatures. Volume relationships are also apparent with winter precipitation, however, these are less distinct. Moreover, flow regulation appears to suppress climatic drivers of freshet volume but has a lesser effect on timing measures. Significant relationships are found with several major atmospheric and oceanic teleconnections indices. This study provides valuable information regarding the dominant controls of freshet generation, whilst highlighting potential impacts of freshet variability on the freshwater balance of the Arctic Ocean.

Table of Contents

Acknowledgements

First and foremost, I would like to extend my gratitude towards my supervisor Dr. Terry Prowse for his commitment, humour, thoughtful insight and admirable mentorship throughout my time at W-CIRC. Equal thanks go to Dr. Barrie Bonsal for his input and dedication, and for all the helpful advice he has provided. Dr. Yonas Dibike, thank you for your mentorship over my last five years at W-CIRC, and for hiring me on as a co-op student in the first place. My life's path has truly changed since those humble beginnings as a co-op student at W-CIRC, and for that I am indebted to you. To the rest of those who have crossed my path at W-CIRC, thank you for your companionship and expertise. In particular, I'd like to thank fellow grad students Brandi Newton, Allison Bawden, Hayley Linton and Gillian Walker. Thanks to Scott Jackson for providing me with a solid basis to undertake this thesis research. My friends and family have been an integral part of my support systems, and for that I am grateful. Finally, and perhaps most importantly, I'd like to thank Chris Jensen, for his patience, guidance, and for always keeping me on belay.

Financial assistance from the Water and Climate Impacts Research Centre, Environment Canada, the University of Victoria, the Natural Sciences and Engineering Research Council and the Northern Scientific Training Program is gratefully acknowledged.

CHAPTER 1: INTRODUCTION

1.1 Background

1.1.1 Introduction

Recently, rate of change in Arctic climate has been higher compared to other parts of the globe (e.g., Larsen et al., 2014, ACIA, 2005; White et al., 2007). Arctic hydrological processes affect the regional marine and terrestrial ecology, cryosphere components including the sea ice regime, and also have an important influence on the salinity stratification and freshwater storage budget of the Arctic Ocean (Arnell, 2005; Kattsov et al., 2007). Variability in the hydrologic regime can impact these systems, as well as, have global implications. An example of this is the global thermohaline circulation, which is partly influenced by movement of low-salinity waters in the Arctic Ocean (e.g., Loeng et al., 2005). A change in the freshwater budget of the Arctic Ocean has potential to alter freshwater export and deep oceanic convection in the North Atlantic, with consequences to the thermohaline circulation (e.g., Aagard and Carmack 1989; Carmack 2000; Peterson et al., 2002; Arnell 2005). Since ecological and marine crysopheric considerations as well as freshwater storage and release mechanisms have increasingly been shown to be seasonally dependent (e.g., Loeng et al., 2005; Carmack et al., 2006; McClelland et al., 2011), it is important to evaluate the variability of major freshwater fluxes to the Arctic. In particular, the spring freshet deserves consideration because it is the dominant annual hydrologic event on nival-regime dominated Arctic river systems, and, of all the freshwater fluxes, provides the greatest proportion of freshwater influx to the Arctic Ocean amongst all other atmospheric sources.

1.1.2 Research need

Currently, the annual volume of freshwater input to the Arctic Ocean from river runoff is approximately known (e.g., Lammers et al., 2001; Prowse and Flegg, 2000); however, no research has yet been undertaken to quantify and analyse the trends in timing, peak magnitude and volume of the spring freshet, or of the climatic and atmospheric circulation patterns that control these trends. This is a critical knowledge gap since previous research only describes the effect of total annual runoff or the peak magnitude of freshet runoff (e.g., Shiklomanov et al., 2007) and yet, the timing and volume of the spring freshet dictates when the majority of terrestrial freshwater discharge enters the Arctic Ocean. In fact, Shiklomanov et al. (2007) stressed a need to further investigate relationships of freshet volume as well as peak magnitude with overall annual discharge. Additionally, climate change scenarios generally predict high-latitude increases in precipitation, particularly during autumn and winter, which manifest as snow in the terrestrial Arctic drainage. This northward transfer of precipitation will expectedly cause an increase in runoff to the Arctic Ocean (e.g., Larsen et al., 2014, Anisimov et al., 2007; Kattsov et al., 2007), most of which will occur as snowmelt runoff during the spring freshet. It is therefore critically important to investigate recent trends in the freshet as well as other seasonal runoff characteristics.

1.1.3 Study area and data

This study focuses on the four major Arctic draining rivers; namely, the Mackenzie River in Canada, and the Lena, Yenisei and Ob rivers in Eurasia, herein referred to as MOLY (see Figure 1). Combined, these four rivers contribute almost 1900 km^3 of freshwater to the Arctic Ocean per year, or about 60% of annual flow volume from all Arctic contributing areas (Grabs et al., 2000; Prowse and Flegg, 2000) and are considered the “big four” of Arctic-draining rivers.

Total contributing areas of the four major river systems, including un-gauged drainage areas, are as follows: Mackenzie 1,800,000 km^2 (Finnis et al., 2009); Ob 2,975,000 km^2 (Yang et al., 2004b); Lena 2,488,000 km^2 (Yang et al., 2002); and Yenisei 2,554,482 km^2 (Zhang et al., 2003).

This work is designed to provide a comprehensive analysis of the spatial and temporal variation of spring freshets from watersheds located in the four major drainage systems of the circumpolar Arctic. However, because of their relative remoteness, Arctic regions are plagued by a distinct lack of hydrometric data availability (Shiklomanov et al., 2002). As a result, the study is somewhat limited both temporally and spatially. Moreover, extensive flow regulation in many of the basins may potentially obscure the climatic and atmospheric relationships to spring freshet measures. Thus, the study classifies sub-basins into regulated, minimally-regulated and unregulated drainage areas. Further basin details and study area maps are provided in Chapter 2.

1.2 Thesis Objectives

This thesis is intended to address some of the research gaps mentioned in Section 1.1.2. The broad goal of the proposed research is to quantify the spatial and temporal variation in the annual major pulses of spring discharge (i.e., the spring freshet) entering the Arctic Ocean through the four major Arctic river systems (MOLY) and their associated sub-basins, as well as examine the climatic and atmospheric relationships with the freshet. This goal will be addressed via three key objectives:

(I) Quantify the trends in freshet timing and magnitude in outlet stations of the four major river basins (MOLY) around the circumpolar Arctic. This will determine whether there were any changes (e.g., increasing or decreasing annual or

seasonal flows) and, importantly, whether a shift in seasonality of peak flows has occurred. Temporal sequencing of circumpolar freshet events will also be examined.

(II) Investigate the MOLY freshet flows entering the Arctic Ocean at a finer scale, by determining the trends in peak magnitude, volume, and timing of spring freshets in regulated, minimally regulated and unregulated sub-basins as well as changes in hydrograph shape. Trends on a sub-basin level will be compared to those which have occurred at the outlets.

(III) Examine relationships of variability in spring freshets with regional temperature and precipitation patterns, as well as, several large-scale atmospheric/oceanic teleconnection indices including the Arctic Oscillation (AO), North Atlantic Oscillation (NAO), Pacific Decadal Oscillation (PDO) and El Niño-Southern Oscillation (ENSO).

1.3 Thesis Structure

The thesis consists of six chapters, some of which are written in a journal manuscript style. Chapter 1 provides general background and identifies the research need including specific objectives of the study. Chapter 2 presents a detailed review of relevant literature as it pertains to the overall objectives of the thesis. Specific emphasis is placed on impacts of Arctic freshwater with particular focus on spring freshets. Chapters 3, 4 and 5 are structured as journal-style manuscripts, with sections on introductory material, basin descriptions and methodology. Chapters 3, 4 and 5 address thesis objectives I, II and II, respectively. A summary and conclusion of the main findings from the thesis is given in Chapter 6. Due to the journal-style

manuscript structuring of the some of the chapters, some text is repeated, particularly with respect to introductory material, study area and methodology.

References

Aagaard, K., Carmack, E.C., 1989. The role of fresh water in ocean circulation and climate. J. Geophys. Res. 94, 14,485–14,498.

ACIA, 2005. Arctic Climate Impact Assessment - Scientific Report. Cambridge University Press, New York.

Anisimov, O., Vaughan, D.G., Callaghan, T., Furgal, C., Marchant, H., Prowse, T.D., Vilhjalmsson, H., Walsh, J.E., 2007. Polar regions (Arctic and Antarctic). In: Parry, M.L., Canziani, O.F., Palutikof, J.P., van der Linden, P.J., Hanson, C.E. (Eds.), Climate Change 2007: Impacts, Adaptation and Vulnerability. Contribution of Working Group II to the Fourth Assessment Report of the Intergovernmental Panel on Climate Change. Cambridge University Press, Cambridge, pp. 653–685.

Arnell, N.W., 2005. Implications of climate change for freshwater inflows to the Arctic Ocean. J. Geophys. Res. 110, D07105.

Carmack, E.C., 2000. The freshwater budget of the Arctic Ocean: Sources, storage and sinks. In: Lewis, E.L. (Ed.), The Freshwater Budget of the Arctic Ocean. Kluwer, Dordrecht, Netherlands, pp. 91–126.

Carmack, E.C., Barber, D.G., Christensen, J.R., Macdonald, R.W., Rudels, B., Sakshaug, E., 2006. Climate variability and physical forcing of the food webs and the carbon budget of pan-Arctic shelves. Prog. Oceanogr. 71, 145–181.

Finnis, J., Cassano, J., Holland, M., Uotila, P., 2009. Synoptically forced hydroclimatology of major Arctic watersheds in general circulation models, Part 1 : the Mackenzie River Basin. Int. J. Climatol. 29, 1226–1243.

Grabs, W.E., Portmann, F., De Couet, T., 2000. Discharge observation networks in Arctic regions: Computation of the river runoff into the Arctic Ocean, its seasonality and variability. In: Lewis, E.L. (Ed.), The Freshwater Budget of the Arctic Ocean. Kluwer, Dordrecht, Netherlands, pp. 249–267.

Kattsov, V.M., Walsh, J.E., Chapman, W.L., Govorkova, V. a., Pavlova, T. V., Zhang, X., 2007. Simulation and Projection of Arctic Freshwater Budget Components by the IPCC AR4 Global Climate Models. J. Hydrometeorol. 8, 571–589.

Larsen, J.N., O.A. Anisimov, A. Constable, A.B. Hollowed, N. Maynard, P. Prestrud, T.D. Prowse, and J.M.R. Stone, 2014: Polar regions. In: Climate Change 2014: Impacts, Adaptation, and Vulnerability. Part B: Regional Aspects. Contribution of Working Group II to the Fifth Assessment Report of the Intergovernmental Panel on Climate Change [Barros, V.R., C.B. Field, D.J. Dokken, M.D. Mastrandrea, K.J. Mach, T.E. Bilir, M. Chatterjee, K.L. Ebi, Y.O. Estrada, R.C. Genova, B. Girma, E.S. Kissel, A.N. Levy, S. MacCracken, P.R. Mastrandrea, and L.L. White (eds.)]. Cambridge University Press, Cambridge, United Kingdom and New York, NY, USA, pp. 1567-1612.

Lammers, R.B., Shiklomanov, A.I., Vörösmarty, C.J., Fekete, B.M., Peterson, B.J., 2001. Assessment of contemporary Arctic river runoff based on observational discharge records. J. Geophys. Res. 106, 3321–3334.

Loeng, H., Brander, K., Carmack, E., Denisenko, S., Drinkwater, K., Hansen, B., Kovacs, K., Livingston, P., Mclaughlin, F., Bellerby, R., Browman, H., Furevik, T., Grebmeier, J.M., Jansen, E., Jónsson, S., Jørgensen, L.L., 2005. Ch. 9: Marine Systems. In: Symon, C., Arris, L., Heal, B. (Eds.), Arctic Climate Impact Assessment. Cambridge University Press, New York, pp. 453–538.

McClelland, J.W., Holmes, R.M., Dunton, K.H., Macdonald, R.W., 2011. The Arctic Ocean Estuary. Estuaries and Coasts 35, 353–368.

Peterson, B.J., Holmes, R.M., McClelland, J.W., Vörösmarty, C.J., Lammers, R.B., Shiklomanov, A.I., Shiklomanov, I.A., Rahmstorf, S., 2002. Increasing river discharge to the Arctic Ocean. Science (80-.). 298, 2171–2173.

Prowse, T.D., Flegg, P.O., 2000. Arctic river flow: A review of contributing areas. In: Lewis, E.L. (Ed.), The Freshwater Budget of the Arctic Ocean. Kluwer, Dordrecht, Netherlands, pp. 269–280.

Shiklomanov, A.I., Lammers, R.B., Rawlins, M.A., Smith, L.C., Pavelsky, T.M., 2007. Temporal and spatial variations in maximum river discharge from a new Russian data set. J. Geophys. Res. 112, G04S53.

Shiklomanov, A.I., Lammers, R.B., Vorosmarty, C.J., 2002. Widespread decline in hydrological monitoring threatens pan-Arctic research. Eos (Washington. DC). 83, 13: 16–17.

White, D., Hinzman, L., Alessa, L., Cassano, J., Chambers, M., Falkner, K., Francis, J., Gutowski, W.J., Holland, M., Holmes, R.M., Huntington, H., Kane, D., Kliskey, A., Lee, C., McClelland, J., Peterson, B., Rupp, T.S., Straneo, F., Steele, M., Woodgate, R., Yang, D., Yoshikawa, K., Zhang, T., 2007. The Arctic freshwater system: changes and impacts. J. Geophys. Res. 112, G04S54.

Yang, D., Kane, D.L., Hinzman, L.D., Zhang, X., Zhang, T., Ye, H., 2002. Siberian Lena River hydrologic regime and recent change. J. Geophys. Res. 107, 4694.

Yang, D., Ye, B., Shiklomanov, A., 2004. Discharge characteristics and changes over the Ob River watershed in Siberia. J. Hydrometeorol. 5, 595–610.

Zhang, X., Ikeda, M., Walsh, J., 2003. Arctic sea ice and freshwater changes driven by the atmospheric leading mode in a coupled sea ice-ocean model. J. Clim. 16, 2159–2177.

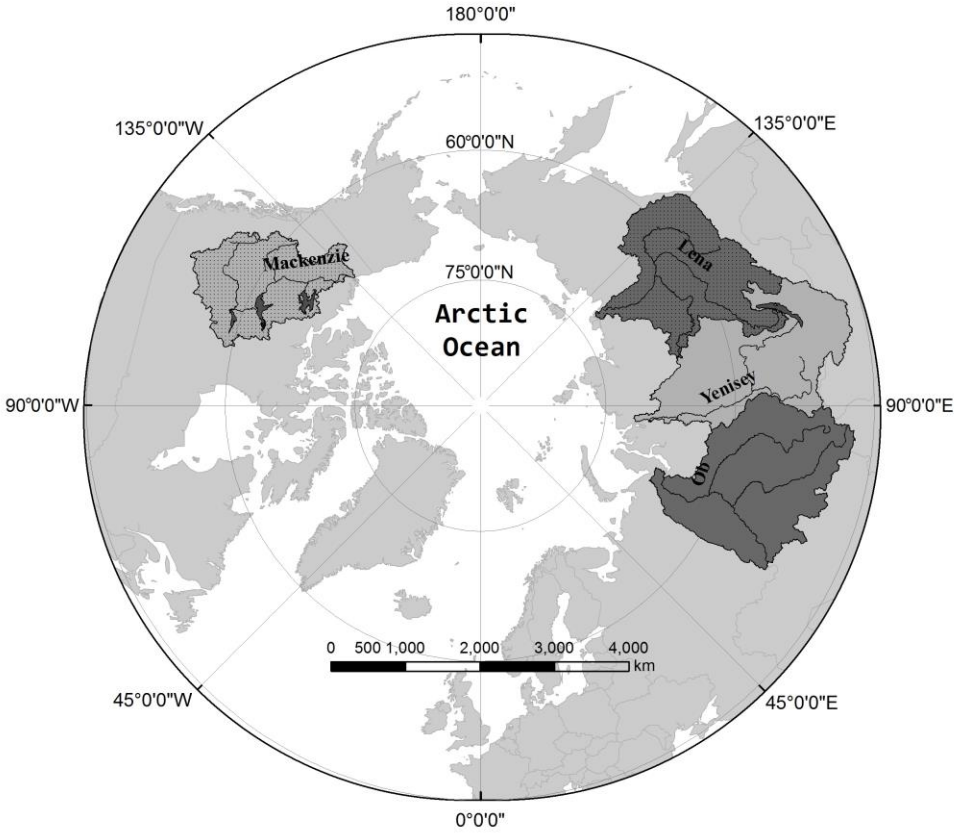

Figure 1. Circumpolar drainage basins of the Mackenzie, Ob, Yenisei and Lena rivers.

CHAPTER 2: LITERATURE REVIEW

Abstract

The influx of terrestrial freshwater to the Arctic Ocean has the potential to influence global climate through modification of the intensity of the thermohaline circulation. It can also have important impacts on the Arctic cryosphere and, marine and terrestrial biota. At the same time, climate is changing faster in the Arctic compared to other parts of the globe. This warrants the importance of a better understanding of climate-discharge linkages in Arctic-draining rivers, which are the dominant source of freshwater input to the Arctic Ocean. Strikingly, although previous studies have focused on annual or monthly flow, seasonality of flow has never been investigated, despite its relative importance to the Arctic Ocean. Seasonality can affect freshwater runoff trajectory upon entering the Arctic Ocean, influencing whether freshwater is placed into storage or released, and correspondingly can have spinoffs to global climate. Seasonality also has important impacts to Arctic sea ice production and ablation. To date, no research has collectively evaluated trends in the magnitude and sequential timing of the spring freshets – the dominant, seasonal hydrologic event occurring on these nival river systems – or of the atmospheric circulation patterns and meteorological variables that control them.

This literature review provides an overview of the freshwater budget of the Arctic Ocean and highlights the importance of the spring freshet as a component of the freshwater budget. Characteristics of the contributing terrestrial drainage basins are discussed as well as data collection and accuracy issues surrounding Arctic hydrological and hydro-climatic data. The objective is to provide the necessary background required prior to evaluating the occurrence and climatic relationships associated with spatial and temporal variations in the spring freshet of major Arctic river systems.

2.1 Introduction

Arctic hydrological processes are integral to the Arctic marine and terrestrial ecology, cryosphere, and sea ice regime as well as Arctic Ocean stratification and freshwater storage (Arnell, 2005; Kattsov et al., 2007). Variability in the hydrologic regimes of Arctic-draining rivers can impact all these systems, as well as have global implications. Importantly, the marine Arctic plays a role in the global climate system through thermohaline circulation, which is partly influenced by movement of low-salinity waters in the Arctic Ocean (e.g., Loeng et al., 2005). This occurs chiefly through export of relatively fresher water from the Arctic Ocean southwards into the North Atlantic, through Fram Strait and the Canadian Arctic Archipelago (CAA), thus integrating the Arctic hydrological system with global thermohaline circulation (e.g., Aagard and Carmack 1989; Carmack 2000; Peterson et al., 2002; Arnell 2005). Hence, a change in the freshwater budget of the Arctic Ocean has potential to alter freshwater export and deep oceanic convection in the North Atlantic, with possible consequences to the circulation (e.g., Aagard and Carmack 1989; Kattsov et al., 2007; McClelland et al., 2011). The Arctic Ocean also affects global climate through its impact on surface heat balance. Snow and ice cover in the Arctic form a positive radiative feedback loop in which open water leads to decreased albedo, which leads to enhanced warming causing more ice melting and finally, results in more open water (Carmack, 2000). Since ecological and marine crysopheric considerations as well as freshwater storage and release mechanisms have increasingly been shown to be seasonally dependent (e.g., Loeng et al., 2005; Carmack et al., 2006; McClelland et al., 2011), it is incumbent to examine the spatial and temporal variability and correspondingly, the seasonality of major freshwater inputs to the Arctic Ocean.

In the nival-dominated regimes of the pan-Arctic region, the greatest component of the Arctic Ocean freshwater balance is influx from Arctic-draining rivers (Aagaard and Carmack, 1989). Meanwhile, the annual spring freshet following snowmelt and river-ice breakup is the dominant hydrologic event occurring on these Arctic river systems. Considering the potential consequences of the timing and magnitude of this major annual event, there is a need to determine the temporal trends as well as spatial variability of spring freshets of Arctic rivers. It is also critical to investigate spring freshet linkages with atmospheric circulation patterns, and other climatic controls such as temperature and precipitation patterns, to determine what impacts these relationships can have on spring freshet trends and variability.

2.2 The Freshwater Budget of the Arctic Ocean

The area of the Arctic Ocean has been determined to cover as much as $14.2*10^6$ km^2 (Lammers et al., 2001) although Serreze et al. (2006) estimate the area as $9.6*10^6$ km^2 and Dyurgerov and Carter (2004) define the area as $9.0*10^6$ km^2. The differences are due to what the authors consider inclusive of the Arctic Ocean; for example, including Hudson and James Bay, Baffin Bay and parts of the northern North Atlantic extends the ocean area and terrestrial domain (Serreze et al., 2006). The latter definition ($9.0*10^6$ km^2) comprises about 2.5% of global ocean area and receives more freshwater per unit area than any other global ocean (Dyurgerov and Carter, 2004), making it very sensitive to changes in freshwater flux. The ocean is largely landlocked and receives freshwater inflows from a total catchment area ranging from approximately $17*10^6$ km^2 to $31*10^6$ km^2, again depending on the definition used for geographical extent of terrestrial contributing area (Prowse and Flegg, 2000; Shiklomanov et al., 2000; Dyurgerov and Carter, 2004; Serreze et al., 2006). Using the mean liquid fresh water storage estimate of 80,000 km^3 as defined in Aagaard and Carmack (1989), the Arctic Ocean

only comprises about 1% of global ocean volume, yet it receives approximately 11% of global river discharge (McClelland et al., 2011), making it highly sensitive to river inflows particularly on the shallow continental shelf regions of Russia (Lammers et al., 2001; Shiklomanov et al., 2000). The volume of freshwater stored in the Arctic Ocean is approximately equal to the freshwater content of all global lakes and rivers, and the amount of freshwater stored is about 10-15 times greater than the amount exported annually (Aagard and Carmack, 1989).

2.2.1 Linkages with the global hydrological cycle

The Arctic Ocean plays a key role in the global hydrological cycle by receiving, transforming, storing and exporting fresh water. Whereas stratification of surface layers in temperate seas is mainly controlled by temperature, cold surface waters of Arctic and sub-Arctic seas are relatively fresh and stratified by salinity (Carmack et al., 2008). Consequently, stratification of surface waters in sub-polar seas is strongly influenced by freshwater export from the Arctic Ocean, through liquid water and ice outflow. Weak stratification of surface waters in sub-polar seas such as in the northern Atlantic Ocean coupled with freshwater export from the Arctic Ocean regulates deep oceanic convection, which is a major driver of global thermohaline circulation (Dickson et al., 2000). As it is a sensitive balance, rapid freshening of North Atlantic deep water (NADW) accompanied by a decrease in water salinity has been predicted to have consequences to this circulation (Dickson et al., 2002). Serreze et al. (2006) compiled information from numerous studies (Aagaard and Carmack, 1989; Curry and Mauritzen, 2005; Dukhovskoy et al., 2004; Hakkinen, 1999; Holland et al., 2001; Proshutinsky et al., 2002; Steele et al., 1996; Wehl, 1968), which predict a change in freshwater outflow from the Arctic Ocean potentially disrupting the large-scale Meridional Overturning Circulation (MOC) by increasing upper ocean stratification in important convective regions. Freshwater sensitivity experiments,

using a variety of coupled ocean and climate models, suggest that North Atlantic deep water formation cannot be sustained after an increase of 0.06 to 0.15 Sverdrup (whereby 1 Sverdrup (Sv) = 1×10^6 m^3/s) of additional freshwater, emphasizing the urgency of investigating land, ocean and atmospheric interactions as part of the Arctic hydrological cycle (Peterson et al., 2002).

2.2.2 Budget components

Understanding the freshwater budget of the Arctic Ocean requires investigation of major budget components, including river runoff, freshwater import through Bering Strait, precipitation minus evaporation, liquid water and ice export through Fram Strait, ice export through Fram Strait, and largely liquid export through the Canadian Arctic Archipelago (CAA) (Aagard and Carmack 1989). See Figure 1 for an illustration of these and other major ocean features. The budget results in a net surplus, although Aagard and Carmack (1989) and Serreze et al. (2006) state that the imbalance is indistinguishable from zero due to the inherent uncertainties in budget terms. Atmospheric freshwater input is received from direct precipitation (P) and runoff (R) minus evaporation (E). Relatively fresh water (compared to the reference salinity of 34.8) from the Pacific Ocean is imported through Bering Strait, driven by pressure gradients caused by salinity and temperature differences between the Pacific and Arctic Oceans – another example of the potential importance of freshwater input seasonality. As discussed, river discharge comprises the greatest proportion of freshwater input to the Arctic Ocean, accounting for up to 38% of mean annual freshwater contribution. Pacific inflow contributes 30% while direct precipitation contributes 24% (Carmack, 2000; Serreze et al., 2006), although Aagard and Carmack (1989) have noted the considerable uncertainty in measuring P-E fluxes. Mean annual freshwater export totals 51% through Fram Strait, with 26% of this as liquid water and 25% as

sea ice, and 35% through the CAA (Carmack, 2000; Serreze et al., 2006). However, these estimates are based on a compilation of budget terms from different analyses using varying periods of record ranging in length from <10 years to 50+ years, requiring the estimates to be taken with caution.

During the formation of sea ice, water distilled as brine is rejected into the underlying ocean. Although young first-year sea ice has a higher average salinity, the salinity of multi-year ice decreases to around 1-6 parts per thousand (ppt) as a result of brine exclusion. Thus, the outflow of ice through Fram Strait is significant despite the sea ice cover typically being only 1-4 m thick (Serreze et al., 2006). Seasonally, ice export through Fram Strait is greatest during winter. Liquid water inflows through Bering Strait and outflows through the CAA generally reach their peak during summer. Direct precipitation over the Arctic Ocean tends to peak in late summer and early autumn (Walsh et al., 1994).

The structure of salinity stratification within the Arctic Ocean is characterized by a seasonally variable surface mixed layer in the upper 30 to 50 m of the water column, underlain by cold stratified layers forming the Arctic halocline, followed by a warmer, salty Atlantic layer and finally deepwater below 1600 m. Vertical stability provided by the salinity stratification allows formation of an ice cover on the ocean (Carmack, 2000). The salty Atlantic layer is largely formed from North Atlantic inflows through Fram Strait. In the western Arctic, the surface mixed layer is generally fresher and the halocline extends deeper and with more structure compared to the eastern Arctic, largely due to the influence of Pacific inflows which form a "cold halostad" that lies above lower halocline waters of Eastern Arctic origin (McClelland et al., 2011; Shimada et al., 2005). In total, liquid freshwater storage in the Arctic Ocean is estimated to be around 80,000 km^3. The Canadian Basin holds approximately 46,000 km^3 of the 58,000

km^3 of fresh water stored in the deep basins, with the Eurasian Basin holding the remainder. 22,000 km^3 is held on the continental shelves (Aagaard and Carmack, 1989). The halocline in the Canadian Basin is deeper with a lower surface salinity, while on the Eurasian side, salinity rapidly increases with depth, reaching approximately 35 ppt at 200 m, and temperature remaining below -1.5°C until approximately 150 m (Aagaard and Carmack, 1989).

In a study that used salinity, $\delta^{18}O$ and nutrient data collected in 2003 and 2004, Yamamoto-Kawai et al. (2008) found relatively fresh Pacific water entering via Bering Strait to be the main freshwater source in the Canadian Basin below 50 m depth, and Bering Strait through-flow to provide up to 75% of the input from Pacific and meteoric sources. Freshwater exported through Fram Strait via the Transpolar Drift mainly originates from Eurasian river runoff and Pacific waters, whilst freshwater exported through the CAA is mainly comprised of North American river runoff (such as from the Mackenzie River) and Pacific Ocean freshwater (Jahn et al., 2009). Water held in the Beaufort Gyre has an approximate residency time of 10 years whilst water exported through the Transpolar Drift has a residency of only about 2 years (McClelland et al., 2011). Overall, ice and liquid freshwater sourced from the Canadian Basin contributes about 40% of freshwater export from the Arctic Ocean to the North Atlantic Ocean (Yamamoto-Kawai et al., 2008).

2.2.3 Impacts of river influx

According to Aagard and Carmack (1989), runoff from Arctic-draining rivers totals 3300 km^3/year, although the time period used to obtain this calculation is not given. The greatest contribution is from four major rivers: Yenisei (603 km^3/yr), Ob (530 km^3/yr), Lena (520 km^3/yr) and Mackenzie (340 km^3/yr). Figure 1 shows the location of these four major drainage basins relative to the Arctic Ocean. Typically, intra-annual variability in runoff contribution from rivers

is high, with the Yenisei and Lena rivers showing a fortyfold increase in peak spring flows versus winter flows and the Mackenzie showing a fivefold increase in peak flows. In Arctic nival rivers, up to 60% of flows are released during the spring freshet (Lammers et al., 2001). Runoff climatology is different amongst regions, with the winter-spring melt transition occurring in March-May in the Barents Sea and Hudson Bay regions and April-June in the Kara, Laptev, East Siberian and Beaufort seas (McClelland et al., 2011).

Several authors have documented changes in freshwater inflows to the Arctic Ocean and their causes. In particular, river discharge to the Arctic Ocean has experienced a recent increase, with potential to alter the freshwater budget of the Arctic Ocean (Arnell, 2005). One such study found that increasing river discharge combined with a surplus precipitation minus evaporation balance contributed an additional ~20,000 km^3 of freshwater to the Arctic and North Atlantic oceans from the 1960s to the 1990s, while sea ice attrition and glacial melt added another ~17,000 km^3 (Peterson et al., 2006). As alluded to in Section 2.2.1, a change in the freshwater balance of the Arctic Ocean could alter the density structure of the largely salt-stratified Arctic basin halocline with effects on downwards convection of warm surface waters in the North Atlantic Ocean and subsequent reduction in North Atlantic deep water formation (e.g., Carmack, 2000; Anisimov et al., 2001; Peterson et al., 2002), resulting in potentially major regional climatic effects from a slowdown of the thermohaline circulation.

Peterson et al. (2002) found that Eurasian river discharge had increased by approximately 7% over the period 1936-1999. This amounted to a volumetric increase of 128 km^3 of freshwater annually by the end of the study period, or an increase of 2.0 ± 0.7 km^3/year, and was linked with trends in global surface air temperature and the North Atlantic Oscillation. Another study (Dickson et al., 2002) investigated the glacial meltwater contribution to Arctic freshwater

inflow and provided comparisons of glacier mass balance data to pan-Arctic river discharge. Pan-Arctic river discharge was found to have increased due to generally positive discharge anomalies from the 1960s up to the 1980s, and then experienced an overall decline from about 1980-1990 as a result of negative discharge anomalies. In the 1990s, discharge anomalies once again became positive. They stated that increasing river runoff combined with continuous glacial contribution could compound ventilation and convectional circulation of North Atlantic deep water, resulting in unforeseen regional changes. McPhee et al. (2009) described a rapid change in the freshwater content of the Arctic Ocean. In their study, aerial hydrographic surveys conducted in spring of 2008 found that freshwater content in the western Arctic had increased by 8,500 km^3, or 26%, when compared to winter climatological values. They reasoned that river runoff plus precipitation and influx of fresher Pacific water were the dominant sources of the increase, rather than localized sea ice melting.

In addition to emphasizing the impacts of variability in freshwater runoff, it should be noted that terrestrial runoff trajectories within the Arctic Ocean have important implications as well, and are added key examples of the importance of runoff seasonality. Runoff that enters the Arctic Ocean is not uniformly distributed; it follows a circulation path that will determine if the freshwater becomes primarily stored or released. Freshwater stored within the Arctic Ocean largely resides in the Canadian Basin, with the greatest amount held in the Beaufort Gyre, a dynamic feature driven by anticyclonic wind forcing that resides in the Canadian Basin north of Alaska (Serreze et al., 2006; Carmack et al., 2008). Of note is that the anticyclonic circulation of the Beaufort Gyre is an exception; circulation elsewhere in the Arctic Ocean is cyclonic (Carmack et al., 2008). Under strong anticyclonic forcing, freshwater is pushed into storage from various proximal sources while weak forcing releases freshwater (Proshutinsky et al.,

2002). Polyakov et al. (2008) found that over the last century, the salinity of the central Arctic Ocean increased while waters over the Siberian shelf showed a freshening trend. This was partially due to variations of the large-scale atmospheric circulation processes influencing the trajectories of terrestrial runoff entering the Arctic Ocean; Steele and Boyd (1998) and Johnson and Polyakov (2001) showed that exchange mechanisms between the central ocean and shelf regions were driven by cyclonic versus anticyclonic phases of atmospheric circulation regimes, and that recent eastward diversion of Siberian river runoff in Arctic waters was a result of tendencies towards cyclonic atmospheric circulation patterns. Furthermore, Polyakov et al. (2008) found that these variations in large scale atmospheric and oceanic circulation affecting runoff trajectory can have a profound effect on freshwater outflow to sub-polar seas. A release of just 5% of freshwater stored in the Beaufort Gyre could cause a salinity change similar to the Great Salinity Anomaly which occurred in the 1970s, when the upper 500 to 800m layer of the northern North Atlantic Sea experienced widespread freshening largely due to a pulse of sea ice outflow, consequently stopping oceanic convection in the Labrador Sea for one year (Dickson et al., 1988; Aagard and Carmack, 1989). Atmospheric connections to runoff forcing are further discussed in Section 2.3.

2.3 Atmospheric Connections and Climatic Flow Drivers

According to Walsh (2000), large-scale atmospheric circulation patterns affect Arctic hydrologic variability over a variety of timescales ranging from daily, to decadal, and longer. This is due to the three major ways in which the circulation patterns affect freshwater inflows; namely, direct P and E on surface waters through atmospheric moisture inflow patterns and convergence over the Arctic Ocean; P and E over terrestrial watersheds contributing river runoff;

and finally, wind-forcing driving advection of sea-ice and freshwater into and around the Arctic Ocean.

The following four different climate indices have been previously shown to affect climate in the study region and are discussed in the following paragraphs: Arctic Oscillation (AO), North Atlantic Oscillation (NAO), Pacific Decadal Oscillation (PDO), and El Niño-Southern Oscillation (ENSO). ENSO is the leading pattern of inter-annual climate variability in the Pacific (Trenberth, 1997). The PDO index is derived as the leading principal component of monthly SST anomalies in the Pacific Ocean north of 20°N, separated from global SST anomalies to distinguish the pattern from any climate warming signal (Mantua et al., 1997). The AO is defined as the leading principal component of sea level pressure (SLP) anomalies north of 20°N and varies considerably in intra-seasonal time scales in mid- to high-latitudes (Thompson and Wallace, 1998). The NAO is the normalized difference in surface pressure (SP) between stations in Azores and Iceland (Hurrell, 1995).

In Canada, freshwater trends and variability have been linked to phases of the AO, ENSO and PDO (Bonsal et al., 2006). For example, more intense, positive phases of the PDO and ENSO have been shown to be a factor in decreased precipitation and subsequently, decreased river discharge in northern Canada (Déry, 2005). The PDO in particular has been shown to affect hydrologic variability in western North American regions which may be encompassed by the Mackenzie basin (e.g., Hamlet and Lettenmaier, 1999; Neal et al., 2002). El Niño conditions and positive phases of PDO are representative of a deeper Aleutian Low, which has been linked to warmer winter and spring temperatures and subsequently, earlier snowmelt and freshwater ice break-up events in Western Canada (Bonsal et al., 2006). The opposite tendencies are associated with La Niña/negative phases of PDO.

In the case of the three Siberian basins, spring river discharge has been positively correlated with winter and spring AO, an effect likely due to a high correlation of spring air temperature with the AO (Ye et al., 2004). The AO has a strong center of action over the central Arctic Ocean, but displays weaker centers of opposing sign over the northern Atlantic and northern Pacific oceans (Serreze et al., 2002), thus exhibiting a weaker influence on climatic conditions over these regions. The positive phase of the AO is associated with anomalously high sea-level pressure in the mid-latitudes and lower pressure in the Arctic, causing confinement of cold air to the high Arctic and resulting in warmer Northern Hemisphere winters (Stoner et al., 2009). Positive indices of NAO are representative of a stronger Icelandic Low, leading to colder winters and springs (and hence later freshwater ice break-up dates) over western Atlantic regions and vice versa (e.g., Hurrell, 1995; Bonsal et al., 2006) . Like the AO, the NAO is most active in winter months, bringing cold, dry Arctic air over northern Canada during its positive phase (Kingston et al., 2006). Although the NAO and AO are highly correlated and nearly identical in the temporal domain, with both demonstrating similar structures (Thompson and Wallace, 1998), there is evidence of distinct regional differences (e.g., Rogers et al., 2001). For example, effects of the NAO tend to be regionalized while AO effects are on a more global scale (Sveinsson et al., 2008), with the NAO in particular being shown to affect variability in temperature and precipitation over the Northern Hemisphere (Hurrell, 1995).

Descriptive plots of surface air temperature (SAT) and precipitation anomalies regressed onto normalized anomalies of November through April AO, ENSO and PDO during the period 1950 – 1996, obtained from the Joint Institute for the Study of the Atmosphere and Ocean (JISAO) (see http://jisao.washington.edu/analyses0500/#details), show that the positive phase of AO is associated with positive SAT anomalies and positive precipitation anomalies over most

parts of the Mackenzie and Eurasian basins during winter months. The warm phase of ENSO (El Niño) is associated with positive SAT and precipitation anomalies over Mackenzie while Eurasian basins show mostly negative SAT with some positive SAT anomalies in the southern portions of the basins. Precipitation anomalies are mostly negative over Eurasian basins, with some regional indications of positive anomalies. PDO in its warm phase is associated with positive SAT anomalies in the Mackenzie and Eurasian basins, with very high anomalies over the Mackenzie. Distribution of precipitation anomalies vary, with mostly positive anomalies in the Mackenzie and Ob basins, and a mix of positive and negative precipitation anomalies in the Yenisei and Lena basins. Of important note is that since many teleconnections indices are highly correlated, for example NAO with AO, any interpretation of streamflow or circulation linkages with atmospheric oscillation patterns should take this into consideration (Sveinsson et al., 2008).

Burn (2008) explored the climatic influences on streamflow timing in three sub-watersheds of the Mackenzie River headwaters, evaluating trends in streamflow timing for 26 hydrometric stations over a variety of time periods. Following Maurer (2004), a composite analysis was used to examine timing relationships with climate indices, in which the 10 highest and 10 lowest values of climate indices were identified along with corresponding years of streamflow timing measures. The measures were evaluated using a t-test to determine if the timing measures differed significantly from the series mean. This approach is recommended since climate signals from large-scale teleconnections are not always linearly related to the hydro-climatic variable in question; for example, a strong correlation may exist in one phase but may be non-existent or weak in the other. The results revealed that the spring freshet occurred earlier in the headwater catchments, and that some of the observed trends could be attributed to trends in meteorological variables.

As mentioned in Section 2.2.3, atmospheric circulation patterns influence runoff trajectories within the Arctic Ocean (Jahn et al., 2009; McClelland et al., 2011). In particular, the Arctic Oscillation (AO) index influences whether runoff is transported to the interior ocean or outward for export; a high AO index drives water eastward into the Beaufort Gyre, while a low AO index tends to drive water into the Transpolar Drift (Johnson and Polyakov, 2001). Recently, Russian river discharge was found to experience an eastward diversion related to an alteration in atmospheric circulation (Dickson et al., 2000). A study by Macdonald et al. (1999) showed the redistribution of river inflows from eastern to western Siberia was partially credited with causing freshening of the surface layers of the Beaufort Sea in the 1990s. However, McClelland et al. (2011) noted that possible increases in freshwater inputs from increasing river discharge may not be noticed until the Beaufort Gyre begins to store and release larger quantities of freshwater at the decadal scale in response to atmospheric circulation variability indicators such as the Arctic Oscillation. Despite this, Greene et al. (2008) cited several studies which stated that changes in wind-driven forcing of the Beaufort Gyre, in combination with enhanced river inflow and sea ice melting, had resulted in alternating state of increased freshwater export and increased freshwater storage in the Arctic.

2.4 Ecological Implications of Arctic Freshwater

According to the IPCC Third Assessment Report (Anisimov et al., 2001), the Arctic region is particularly vulnerable to climate change due to its thermally sensitive cryosphere. Atmospheric freshwater transport within and between oceanic basins is an important part of the climate system of the Earth (Stigebrandt, 2000). The process of salinity distribution – which forms the "haline" part of thermohaline circulation – is sensitive to climate change effects which cause freshening of the Earth's polar regions (e.g., Toggweiler and Key, 2003). A weakened

Arctic circulation could affect aquatic ecosystems, since the circulation brings deep, nutrient-rich waters to the surface (Toggweiler and Key, 2001). Stronger stratification in the Arctic Ocean will enhance warming and reduce surface mixing, but will disrupt vertical transportation of nutrients (Francis et al., 2009). Changes in Arctic Ocean circulation patterns and freshwater export since the 1990s have been associated with biogeographic range expansions of boreal plankton, such as a renewal of pan-Arctic range exchanges of Pacific and Atlantic species (Greene et al., 2008). Additionally, it was found that during the same period, a dramatic regime shift occurred in the northwest Atlantic shelf ecosystems ranging from the Labrador Sea to the Mid-Atlantic Bight, in which stratification and freshening of the shelf waters were potentially linked with abundances and seasonal cycles of phytoplankton and zooplankton (Greene et al., 2008).

There are numerous other biological implications associated with spring freshet discharge. Riparian zones are affected by the frequency and severity of the spring flood, and while flooding is often portrayed in a negative context (e.g., Jasek, 2003; Shiklomanov et al., 2007), it has been shown that spring flooding is an important recharge mechanism for perched basins hydraulically separated from main flow channels (e.g., Marsh and Hey, 1989; Prowse and Conly, 1998). It has been suggested that increased river discharge will result in enhanced nutrient and sediment fluxes, with consequences to Arctic marine ecosystems (Kattsov et al., 2007; Tank et al., 2011). McClelland et al. (2011) stated that in general, terrestrial river water entering the Arctic Ocean is rich in organic matter and depleted in inorganic nitrogen. As such, organic matter concentrations in runoff increase dramatically during the spring freshet, while inorganic nitrate and silica concentrations decrease. River inputs act to dilute the Arctic Ocean with respect to nitrate and phosphate, and enrich it with respect to dissolved organic carbon and

silica. Concentrations of suspended matter in runoff are distinctly higher in basins draining mountainous regions; for example, waters originating from the Mackenzie basin have a higher sediment content than many of the Eurasian basins. Phytoplankton concentrations peak on the freshwater side of the Ob, Yenisei and Lena estuaries, yet are relatively consistent across freshwater to saltwater transitions in the Mackenzie estuary, likely due to greater light attenuation from high sediment load. Since coastal estuarine regions are under ice cover for up to 9 months of the year, nutrients delivered under low winter flow remain under the ice and support winter secondary production. When the spring freshet occurs, water with high organic material concentrations and low inorganic materials mix and disperse with water built up during the winter, with consequences to estuarine communities (Macdonald, 2000; McClelland et al., 2011). Terrestrial organic carbon from rivers can oxidize and produce CO_2, contributing to the processes of Arctic Ocean acidification (AMAP, 2013). These variations in organic material concentrations emphasize the importance of the seasonality of spring river discharge on distribution, timing and magnitude of ecosystem production in Arctic coastal communities (Loeng et al., 2005; Carmack et al., 2006).

One of the most significant defining features of the Arctic Ocean is its sea-ice cover (Serreze et al., 2007). The sea-ice regime plays a role in Arctic Ocean salinity dynamics, adding salt during sea-ice production and releasing fresh water during ablation (Macdonald, 2000). A change in the freshwater balance (possibly due to river discharge) will have effects on the cold halocline layer which insulates the floating sea-ice cover from the warmer, saltier Atlantic layer below; a reduction in the cold halocline layer can therefore have considerable effects on the sea-ice cover (Steele and Boyd, 1998). Rises in air temperature due to climate change will reduce snow cover and sea-ice extent, decreasing the albedo and causing positive radiative feedback

which acts to further reduce ice and snow cover. Thinner sea-ice cover and larger open-water areas allow for stronger heat flux from the ocean to the atmosphere, particularly during autumn and early winter. This increased transfer of heat locally increases the air temperature, moisture content, cloud cover and precipitation, and reduces the vertical static stability in the lower troposphere (Vihma, 2014). Furthermore, large rivers, such as the Mackenzie, Ob, Lena and Yenisei, transport an immense amount of heat from their respective continental watersheds to the Arctic Ocean (Lammers et al., 2007; Liu et al., 2005; Yang et al., 2014). This extensive intrusion of warm terrestrial Arctic river waters into the Arctic Ocean rapidly warms the ocean's surface layers, enhancing the localized melting of sea ice (Nghiem et al., 2014). This is yet another example of the importance of seasonality in Arctic river discharge.

Impacts of reduced sea-ice cover to the Arctic regions include warmer autumns and winters, increased wave action in open waters exacerbating coastal erosion, and disrupted polar bear abundance due to a loss of habitat (Serreze et al., 2007). Reduced sea-ice cover allows for more light penetration, which intuitively results in enhanced phytoplankton activity; however, reduced sea-ice cover will also allow for stronger vertical wind mixing over open water areas, thus countering any increased phytoplankton activity (Francis et al., 2009).

2.5 Flow and Budget Predictions

Future climate change projections reveal an increase in precipitation (e.g., Anisimov et al., 2007, Larsen et al., 2014) which, along with air temperature increases, may cause a shift from a nival-dominated Arctic regime to a more pluvial one. Total annual terrestrial freshwater contribution to the Arctic Ocean, as predicted by models using various future greenhouse gas scenarios, is expected to increase by up to 10 – 30% by the year 2100 (Anisimov et al., 2007). A warming climate would induce monotonic changes in streamflow, but these may be enhanced by

climatic oscillations causing variability in meteorological factors and thus potentially obscure any climatically-induced monotonic trends in streamflow (Woo et al., 2006). As such, a presence of significant streamflow trends in historical records does not necessarily indicate a direct influence of climatic factors and should be approached with caution.

In general, climate models predict that as anthropogenic greenhouse gas emissions increase, an intensification of the Arctic hydrological cycle will result, causing a northward migration of precipitation and consequently an increase in high latitude river runoff (Wu et al., 2005). According to Arora and Boer (2001), the global hydrological cycle is expected to intensify by 3% by the end of this century. In a study that examined outputs of 10 models used in the Intergovernmental Panel on Climate Change Fourth Assessment Report, Holland et al. (2007) found that simulated budget changes from the period 1950 to 2050 showed an overall acceleration of the Arctic hydrological cycle, as a result of a net increase in freshwater inputs from precipitation minus evaporation, river runoff and ice melt. Liquid freshwater storage within the Arctic Ocean increased, with a corresponding increase in freshwater export primarily through Fram Strait. This was, however, countered by a decrease of freshwater storage and export in sea ice. All of the models agreed on greenhouse gas loading as the cause of the changes. In another study that ran simulations of the freshwater balance of the Arctic Ocean in the latter half of the 21st century, Koenigk et al. (2007) stated that the dominance of sea ice export through Fram Strait will disappear and export will become increasingly dominated by liquid water transport. Historically, Holland et al. (2007) cited observations that showed freshening of the northern North Atlantic in the latter part of the twentieth century was linked to increased Arctic river discharge, direct precipitation, sea ice melt and subsequent export.

2.6 Characteristics of the Study Basins

As described in Dyurgerov and Carter (2004), the pan-Arctic region contains nearly half of the global alpine and subpolar glacial area. Terrestrial Arctic watersheds may extend farther south than what is considered the Arctic region, with some major Canadian and Eurasian basins extending south of 50°N (Loeng et al., 2005). As a result, discharge characteristics from rivers vary if the geographic location of a sub-basin subscribes to a nival, pluvial or hybrid regime. Discharge variability is also dependent on vegetation, elevation and terrain that affect hydrological retention. For example, rivers with large lakes at their headwaters will have more moderated seasonal discharge characteristics than those without (Carmack, 2000). Total Arctic contributing areas of the four major river systems (Figure 1), including ungauged drainage areas, are as follows: Mackenzie 1,800,000 km^2 (Finnis et al., 2009); Ob 2,975,000 km^2 (Yang et al., 2004b); Lena 2,488,000 km^2 (Yang et al., 2002); and Yenisei 2,554,482 km^2 (Zhang et al., 2003).

2.6.1 Physiography

The Mackenzie River basin, in North America, encompasses portions of the provinces of British Columbia, Alberta and Saskatchewan as well as the Northwest Territories and Yukon and is the largest Arctic-draining North American river. Basin relief is shown in Figure 2. The human population of the Mackenzie Basin is less than 400,000. The basin comprises four physiographical regions, divided into Delta, Western Cordillera, Interior Plains and Precambrian Shield (Woo and Thorne, 2003). It occupies approximately 20% of Canadian landmass with around two-thirds of the area underlain by permafrost (Dyke et al., 1997). Western Cordillera regions include a series of mountain chains and high plateaus and valleys, with mountainous terrain exceeding 2000 m in elevation; meanwhile in the central and eastern Interior Plains and

Canadian Shield terrain varies from flat wetland and grassland to rolling valley-wetlands and Precambrian bedrock outcroppings (Woo and Thorne, 2003). Total gauged drainage area for the Mackenzie River, taken at the hydrometric station located at Arctic Red River, is 1,680,000 km^2. Daily discharge gauged at this location is only available beginning in 1973. Mean annual discharge of the Mackenzie River, gauged at Arctic Red River (see Figure 2), is 8,926 m^3s^{-1} during the period 1973 – 2000 (R-ArcticNET v4.0). Prowse and Flegg (2000) showed that during the selected period of 1975- 1984, the outlet regions of major northern rivers made up the majority of that river basin's ungauged area. Vegetation in the basin varies from boreal forest to alpine and Arctic tundra, and is largely unregulated with the exception of the Peace sub-basin (Stewart, 2000). Land cover composition is forest (63%), wetland (18%), shrub (18%), grassland (4%) and cropland (3%) (Revenga et al., 1998).

Basin relief of Eurasian basins is given in Figure 3. In Eurasia, the Ob River basin gauged at Salehard comprises an area of 2,950,000 km^2. Mean annual discharge of the Ob River, gauged at Salehard during 1930 - 1999, is 12,492 m^3s^{-1} (R-ArcticNET v4.0). The Ob River flows northwest across western Siberia from its source in the Altai Mountains (Yang et al., 2004b). Approximately 4-10% of the basin is underlain by permafrost (Zhang et al., 2008). A large portion of the basin land cover is wetland, swamp and marshland with mixed deciduous and coniferous forest transitioning to grassland and cropland in the south (Bowling et al., 2000). Compared to the Lena and Yenisei, the Ob basin has more industrialized and agricultural areas (Dynesius and Nilsso, 1994) with composition as follows: cropland (36%), forest (30%), wetland (11%), grassland (10%), shrub (5%), developed (5%), and irrigated cropland (3%) (Revenga et al., 1998). Unlike largely undeveloped basins like the Lena and the Mackenzie, the Ob basin has a population of 27 million with significant agriculture development particularly in the steppe

zones in the southern portion of the basin, which are important areas to wheat farming in Russia (Yang et al., 2004b). A large portion of the Western Siberian Lowlands lies within the Ob River basin (Nuttall, 2005); the gentle relief, peat deposits and wetland vegetation affect and mediate the flow within the region (McClelland et al., 2011). In the 1950s to 1980s, one major reservoir and three mid-size dams were built with a total capacity of 61.6 km^3, or about 15% of total annual discharge at the outlet (Yang et al., 2004b).

The Yenisei River basin, gauged at Igarka, drains an area of 2,440,000 km^2 and daily discharge data are available from 1936 to 2005, although there are several significant gaps in cold-season data during the period 1969 to 1979. Mean annual discharge of the Yenisei River, gauged at Igarka from 1936 - 1999, is 18,395 m^3s^{-1} (R-ArcticNET v4.0). The Yenisei River flows north from its origin in the Baikal Mountains and Central Siberian Plateau. Southern portions of the Yenisei Basin encompass the Western and Eastern Sayan mountain ranges as well as Lake Baikal, and up to 80% of the basin is located in the Central Siberian Plateau, with elevations ranging from 500-700 metres a.s.l. The basin is bordered by the Yenisei Ridge in the west and the Putorana Mountains in the northeast (Lydolph et al., 1977). Total population of the basin is 5 million, with 10 cities having a minimum population of 100,000 people. Approximately 36-55% of the basin is underlain by permafrost (Zhang et al., 2008) with composition of forest (49%), grassland (18%), shrub (15%), cropland (13%) and wetland (3%) (Revenga et al., 1998). There is significant human activity and economic development in the region (Dynesius and Nilsso, 1994) and it contains at least six major reservoirs with a capacity exceeding 25 km^3, built between the 1950s and 1980s (Yang et al., 2004a), and up to 64 reservoirs in the Yenisei-Angara basin (Stuefer et al., 2011). In a study which compared observed, regulated discharge data to a naturalized discharge data set which removed the effects

of flow regulation, it was found that regulation in the Yenisei was significant enough to affect the mean annual discharge response to precipitation during the period 1980 to 2004 (Stuefer et al., 2011). Flow regulation affects seasonal patterns of discharge to the Arctic Ocean by reducing the peak discharge during spring and summer months and releasing additional stored spring and summer water from reservoirs in winter months, and it has been shown that increases in winter discharge in some Eurasian basins can be attributed to this release (McClelland, 2004; Yang et al., 2004b; Ye et al., 2003).

The Lena River basin, gauged at Kusur, drains an area of 2,430,000 km^2. Mean annual discharge of the Lena River, from 1934 - 2000, is 16,760m^3s^{-1} (R-ArcticNET v4.0). The Lena River, flowing north from its origin in the Baikal Mountains, has mountainous regions in the eastern and southern portions (Ma et al., 2000; Ye et al., 2003). It includes the Baikal Mountains in the south, Yakut Lowlands below the mouth of the Aldan tributary and Verkhoyansk Mountains to the east (Lydolph et al., 1977). There is significant permafrost coverage in the Lena basin, with approximately 78-93% of the basin underlain by permafrost (Zhang et al., 2008). The high permafrost coverage results in low subsurface storage capacity, meaning that winter flows are very low and spring peaks are very high, with the June peak approaching 55 times the winter low discharge (Yang et al., 2002). Terrestrial land cover composition is forest (84%), shrub (9%), grassland (3%), cropland (2%) and wetland (1%) (Revenga et al., 1998). It has the least amount of economic development and human activity compared to the Yenisey and Ob (Dynesius and Nilsso, 1994) and also has the least regulated flow, with only one major reservoir, that was built in the 1960s (Liu et al., 2005). Total basin population is 2.3 million people with one major city, Yakutsk.

2.6.2 Climate

The four study basins considered in this study represent significantly different hydro-climatic characteristics. The Mackenzie Basin covers several climatic regions, including cold temperate, mountain, sub-Arctic and Arctic zones (Woo and Thorne, 2003). Mean surface air temperature (SAT) averaged over the entire basin is -25°C in January and 13.8°C in July (Serreze, 2003). Precipitation ranges from greater than 1000 mm in the southwest of the basin to only 200 mm in the delta region (Woo and Thorne, 2003). Climate in the Ob Basin is characterized by a cold continental and sub-Arctic to Arctic climate. It is the warmest of the four basins, with a mean SAT of -18.7°C in January and 18.1°C in July. However, summer maximum temperatures in the arid south can reach 40°C while winter temperatures in the Altai Mountains can fall as low as -60°C. Precipitation, which falls mainly as rain during the summer, can reach up to 1,575 mm annually in the Altai Mountains, while much of the rest of the basin receives 300 – 600 mm annually (Serreze, 2003). Climate in the Yenisei Basin ranges from continental in the southern and central portions to sub-Arctic in the north. Average winter temperatures range from -20°C in the southern regions to -32°C in the northern regions, while summer average temperatures range from 20°C in the south to 12°C in the north. Mean SAT is -26.5°C in January and 15.2°C in July. Precipitation, which falls primarily as rain during the warmer months, ranges from 400 – 500 mm annually in the north, 500 – 750 mm in the central regions, and up to 1200 mm annually in the south (Serreze, 2003). Similarly, climate in the Lena Basin ranges from continental to subarctic and arctic. The Lena Basin is the coldest of the four basins. Winters are cold, clear and calm, with temperatures falling as low as -70°C. Summer temperatures range from 10 to 20°C. Mean SAT in January is -35°C and 14.7°C in July. The southern mountain ranges receive up to 600-700 mm of precipitation annually, while the central

basin receives 200 – 400 mm and 100 mm falls annually in the delta regions. Like the other basins, most precipitation falls as rain during the summer (Lydolph et al., 1977; Serreze, 2003).

Climate in the study basins, similarly to other Arctic regions, is highly subject to variability and change. Due to extensive snow and sea-ice cover, climate feedbacks and interactions are accelerated in Arctic regions, causing an effect known as Arctic amplification (Serreze and Francis, 2006). Since the 1960s, surface air temperatures in the Arctic have risen at approximately double the global rate (Anisimov et al., 2007). In the Mackenzie basin, climate in the region has undergone a significant warming trend, with temperatures increasing by more than 1.5°C in the latter half of the 20th century (e.g., Woo et al., 2007; Yip et al., 2012). Meanwhile, in the Eurasian basins, there has been notable winter warming, precipitation increases in winter and fall, and an increase in overall ground temperature over the last several decades (Yang et al., 2002). In general, recent warming in the study regions covering northern Asia and north-western North America is most apparent during winter and spring, with the smallest changes occurring in the fall (McBean et al., 2005). Precipitation records have shown indications of an overall increasing trend in Arctic regions over the last century, although the trends are highly variable and have high uncertainty due to sparse monitoring in polar regions (Anisimov et al., 2007). As discussed, variability in Arctic climate can have not only regional effects, but may also have impacts on a global scale.

2.6.3 Flow regulation

The Yenisei basin is the most substantially regulated of the four basins, with at least six major reservoirs with a capacity greater than 25 km^3 located along the Yenisei and Angara stems (Yang et al., 2004a; Stuefer et al., 2011). The next most regulated basin is the Ob, which contains one major reservoir with a storage capacity greater than 25 km^3, and three midsize dams

(Yang et al., 2004b). Of the Eurasian basins, the Lena is least affected by flow regulation, with only one major reservoir located along the Vilyuy tributary. The Mackenzie basin is also considered moderately affected, despite only one major reservoir located along the Peace tributary. Large lakes in the Mackenzie basin (e.g., Great Slave L. and Great Bear L.) provide substantial storage capacity, acting to reduce high spring peaks and sustain lower flows resulting in a more consistent runoff pattern throughout the year, similar to the effect of flow regulation (Woo and Thorne, 2003). Percentage area of each basin directly upstream of a major reservoir is as follows: Mackenzie 3.9%; Ob 11.6%; Yenisei 46.5% and Lena 4.2%. Locations of major hydroelectric dams or reservoirs in the Mackenzie and Eurasian basins are shown in Figure 1.

2.6.4 Sub-basin classification

Regulation is a necessary consideration when investigating trends in the magnitude and timing of the spring freshet. However, removing the effects of flow regulation by means of hydraulic modelling is not tractable within the scope of this study. To accommodate this, sub-basin stations have been classified into three categories. Unregulated stations (H_U) do not have any flow impoundment in their upstream catchment areas. These catchment areas are considered regionally representative of a natural, unregulated basin with stable hydrologic conditions. Regulated stations (H_R) are located downstream of a major reservoir and have an average seasonal runoff pattern that is strongly influenced by the upstream flow impoundment. Lastly, minimally regulated stations (H_M) have upstream flow impoundment but have a signal that has been noticeably diminished by contribution from unaffected H_U basins. For example, the outlet station of the Mackenzie River, gauged near Inuvik, NT, is located approximately 3,120 km downstream of the W.A.C. Bennett Dam, gauged near Hudson's Hope, BC. Given the distance,

the flow gauged near Inuvik integrates a virtually insignificant percentage of impounded flow from the W.A.C. Bennett Dam.

Of course, there is a subjective element involved in differentiating between stations classified as H_R or H_M. Determining whether the regulation signal has been significantly diminished to classify as H_M requires comparing the station's average hydrograph to that of an H_R-classified upstream station, and also to unaffected H_U-classified upstream contributing basins. Note that H_U stations gauging the outlet of any large water body such as a natural lake have a similar flow regime and will exhibit comparable flow characteristics to that of an H_R station. The assigned classifications of each of the 106 analyzed stations with their associated sub-basin drainage areas are shown in Figure 4 for the Mackenzie basin and Figure 5 for the Eurasian basins. Approximately 85% of total gauged drainage area is classified as H_U in the Mackenzie. Due to limited station availability and expansive flow regulation in the Eurasian regions, only 9% of gauged area is classified as H_U in the Ob basin, 12% in the Yenisei and 8% in the Lena basin.

Sub-basins are also classified using a simple characterization based on geography and topology. These regions are given in Figure 2 for the Mackenzie basin and Figure 3 for the Eurasian basins. Appendix A gives the hypsometric curves for each sub-basin separated by regional classification. These curves are useful in interpreting the effects elevation and topographic relief may have on freshet characteristics and trends.

In the Mackenzie basin, the southern region contains a high proportion of high-relief alpine drainage typical of the North American Cordillera, with one major dam in the southwest. The western region also consists of high-relief, high-elevation alpine zones including portions of

the Mackenzie Mountains. The eastern region contains interior plains and Precambrian Canadian Shield while the northern region incorporates the plains surrounding Great Bear Lake and the Mackenzie Mountains to the west. In the Ob basin, the western and eastern regions consist largely of Western Siberian lowlands, although the western region covers a small section of the Altai Mountains at the headwaters of the Irtish River. Vast expanses of wetlands cover these regions. The southern region contains the largest proportion of high-relief drainage in the entire Ob basin. There are only three stations located in the Ob lowlands characterized as the northern region. In the Yenisei, the western region contains the Altai Mountains while the southern region contains the Sayan mountain ranges as well as Lake Baikal. Eastern drainages include higher-relief smaller watersheds below Lake Baikal, covering the Baikal Mountains to the east. The northern Yenisei basins include portions of the higher-elevation Central Siberian Plateau. Finally, the western regions of the Lena basin include the impounded Vilyuy River and Central Siberian Plateau. Southern basins cover some portions of the Baikal Mountains while the sole eastern basin drains a portion of the Verkhoyansk Mountains. Due to limited data availability, there are no northern-classified sub-basins in the Lena basin.

2.7 Data

2.7.1 Data sources

Daily discharge data used are obtained from the Environment Canada Hydrometric Database (HYDAT) for stations in the Mackenzie basin and from the Regional, Hydrometeorological Data Network for Russia (R-ArcticNET Russia v4.0) (Lammers and Shiklomanov, cited 2012) for the Ob, Lena and Yenisei basins. R-ArcticNET Russia (v4.0) contains information from 139 Russian Arctic gauges compiled from original archives of the State Hydrological Institute (SHI) and the Arctic and Antarctic Research Institute (AARI), St.

Petersburg, Russia. Due to limited temporal availability, not all available stations are utilized. Selection of hydrometric stations is discussed in Chapters 4 and 5. As a result of the limited temporal availability, two time periods are utilized to maximize the number of stations selected for inclusion; 1962 – 2000 and 1980 – 2000. These two periods are hence referred to as t_1 and t_2, respectively. Currently, the temporal range of Eurasian station data for most Lena, Yenisei or Ob sub-basins obtained from R-ArcticNET Russia (v4.0) does not extend past the year 2000, whilst many stations in the Mackenzie basin have incomplete or missing data in the period 1970 – 1979. Hence, the shorter period t_2 is chosen to maximize spatial coverage of stations with available data, while the longer period t_1 is used to increase the power of significance testing and t-tests for stations that have available data. All four outlet stations have available data to 2009.

Runoff, in terms of magnitude and timing, is primarily affected by air temperature and precipitation (e.g., Yip et al., 2012). Temperature can affect the timing characteristics (e.g., pulse onset and duration) of the spring freshet, while winter precipitation accumulation can affect the magnitude of the freshet. Since air temperature and precipitation accumulation have impacts on freshet discharge on a more seasonal, rather than daily, basis, climatic data are extracted from archives on a monthly scale and averaged into seasons. These data are available at the spatial scales required for this analysis, although weekly snow flow analyses have been performed for many large Arctic rivers (e.g., Khan et al., 2008). Relationships between spring freshet discharge characteristics and climatic variables are explored in Chapter 5, using a Pearson's *r* correlation analysis. This type of analysis reveals any regional sensitivity of spring freshet runoff to climatic variation, and whether basin regulation is an important influence.

There are several different climatic datasets available, providing temperature and precipitation data over the study regions at a variety of resolutions. Available climatic datasets

consist of re-analysis data, gridded observational data and Global Climate Model (GCM) data. Climatic correlations were performed using a very high resolution dataset covering the Mackenzie region only, as well as high resolution and coarse resolution datasets with global coverage. Comparison of the findings indicates whether the resolution of the climatic dataset has an impact on results. These comparisons are given in Appendix C.

As a result of the comparisons, climatic correlations presented in Chapter 5 are performed using the CRU TS3.21: Climatic Research Unit (CRU) Time-Series (TS) Version 3.21 of High Resolution Gridded Data of Month-by-month Variation in Climate (Jan. 1901 – Dec. 2012), since it is based on climatic observations and gave the highest number of significant results. This dataset is made publicly available through the British Atmospheric Data Centre (BADC) (see http://badc.nerc.ac.uk/data/cru/). CRU TS3.21 is a gridded climatic dataset constructed at a high spatial resolution of 0.5 x 0.5 degrees covering all global land areas, excluding Antarctica, from monthly observations of global meteorological stations. Mean, minimum and maximum temperature and total precipitation time series of an earlier predecessor of the dataset, CRU TS3.10, compared favourably to other available global gridded datasets with the only exceptions occurring in regions or temporal periods with sparser observational data (Harris et al., 2014).

Results using alternative datasets, as discussed, are presented in Appendix C. A 10 × 10 km very-high resolution, spline-interpolated dataset of daily precipitation and daily maximum and minimum temperature covering the period 1950 – 2010, referred to as NRCAN (2012) (Hutchinson et al., 2009; McKenney et al., 2011), is also used for the Mackenzie basin. For the Eurasian basins, the ERA-40 dataset is utilized in addition to CRU TS3.21. ERA-40 is a re-analysis product of meteorological observations covering the period September 1957 to August 2002, produced by the European Centre for Medium-Range Weather Forcasts (ECMWF)

(Uppala et al., 2005). Resolution is based on the T159 Gaussian grid, corresponding to a coarse spatial resolution of approximately 1.125° x 1.125°. Bengtsson et al. (2004) noted that care must be taken when using re-analysis data such as ERA-40 in longer-term climate analyses due to inhomogeneities inherent in the available observational data.

Climate indices for AO, NAO, PDO and ENSO are obtained from the National Oceanic and Atmospheric Administration (http://www.esrl.noaa.gov/psd/data/climateindices/list/) as monthly standardized anomalies. In this study, the common Niño 3.4 index of sea surface temperature (SST) anomalies is used to classify ENSO conditions, which capture the region bounded between 5°S – 5°N and 170°W – 120°W. Positive SST anomalies, taken from 5-month running means and exceeding 0.4° C for 6 months or more, are associated with El Niño events, while the opposite patterns are associated with La Niña (Trenberth, 1997).

2.7.2 Hydrometric data accuracy

Discharge measurements in rivers require establishment of rating curves with accurate elementary measurements such as depth, width and velocity for a number of points across the river (Shiklomanov et al., 2006). Such measurement techniques may differ between Canadian and Russian agencies. According to Lammers et al. (2001), variations in discharge data are expected depending on local site conditions, type of gauge used and the number of measurements taken along the river cross section. Differing analytical techniques and periods of active discharge monitoring have discouraged comparisons of North American and Eurasian discharge trends as a whole entity (White et al., 2007). North American agencies typically use vertical-axis meters which sample at a few points along a vertical cross-section, while Eurasian agencies typically use horizontal-axis meters which use more points in the vertical cross-section (Pelletier, 1990). Discharge measurement errors range from +2 to +5% under open-water

conditions for rivers without flood plains and rise to +5 to +12% for rivers with flood plains (Rantz, 1982); meanwhile, rivers in mountainous regions can have maximum errors of up to 25% (Lammers et al., 2001). During periods of low temperatures, discharge estimates become even more uncertain due to anchor ice, frazil ice and backwater conditions; Wedel (1990) reported errors of +10% under rough ice conditions.

Reliability of discharge measurements in Arctic rivers is further confounded by sparse flow metering, often occurring only two or more times per year to represent extreme high and low flows (Carmack, 2000). Shiklomanov et al. (2002) state that amongst the "active" Russian hydrometeorological stations, about 5-8% have reportedly not directly measured discharge for 3 to 5 years, and that frequency of on-site flow metering has decreased at almost all Russian gauges. Both Canadian and Russian agencies use a similar method of estimating discharge, whereby corresponding water levels measured at the same time are used in conjunction with flow measurements to create a stage/discharge curve, presuming a relationship between flow and water level. Measurements taken throughout the rest of the year are of water level only, and flow is calculated indirectly using the relationship. This method is obviously limited, and cannot account for variations in winter ice-cover roughness affecting hydraulic flow resistance and frazil dam formation raising water levels. During high flows, frictional resistance in river channels is highly variable and overflow conditions are common. Currently, there are no international standards for Arctic river gauging and a comparative study of different flow metering methodologies is still required (Carmack, 2000).

High latitude regions are plagued by a lack of hydrometric data availability, and have a sparse hydrometric network compared to those in more temperate regions. Often, flow records span only a few decades (Woo et al., 2006). Shiklomanov et al. (2002) cite the problems

regarding widespread decline in monitoring stations, particularly in far eastern Siberia. They have documented a 40% decline in active monitoring gauges, and state that a reduction in recent years of 7% of monitoring area may seem inconsequential but, in perspective, it is equivalent to an area of 1.5 million km^2, about the size of the state of Alaska. Grabs et al. (2000) note that de-population in high-latitude areas, particularly in the former Soviet Union, has resulted in a declining station network and created difficulties in obtaining existing data. Environmental and infrastructure considerations hamper establishment and maintenance of Arctic region stations, including materials supply, instrument maintenance, and observer availability as well as all the described problems with taking measurements under ice cover or during break up. They state that it is reasonable to assume a probable scale of error of approximately 15% on inland stations and up to 30% for coastal and delta stations. Despite these limitations, sufficient data exists for the purposes of this study, and any measurement errors inherent to the hydrometric data are not considered significant enough to discount meaningful results.

References

Aagaard, K., Carmack, E.C., 1989. The role of fresh water in ocean circulation and climate. J. Geophys. Res. 94, 14,485–14,498.

AMAP, 2013. AMAP Assessment 2013: Arctic Ocean Acidification. Arctic Monitoring and Assessment Programme (AMAP), Oslo, Norway. viii + 99 pp.

Anisimov, O., Fitzharris, B., Hagen, J.O., Jefferies, R., Marchant, H., Nelson, F., Prowse, T.D., Vaughan, D.G., 2001. Polar regions (Arctic and Antarctic). In: McCarthy, J.J., Canziani, O.F., Leary, N.A., Dokken, D.J., White, K.S. (Eds.), Climate Change 2001: Impacts, Adaptation and Vulnerability. Contribution of Working Group II to the Third Assessment Report of the Intergovernmental Panel on Climate Change. Cambridge University Press, Cambridge, pp. 803–841.

Anisimov, O., Vaughan, D.G., Callaghan, T., Furgal, C., Marchant, H., Prowse, T.D., Vilhjalmsson, H., Walsh, J.E., 2007. Polar regions (Arctic and Antarctic). In: Parry, M.L., Canziani, O.F., Palutikof, J.P., van der Linden, P.J., Hanson, C.E. (Eds.), Climate Change 2007: Impacts, Adaptation and Vulnerability. Contribution of Working Group II to the Fourth Assessment Report of the Intergovernmental Panel on Climate Change. Cambridge University Press, Cambridge, pp. 653–685.

Arnell, N.W., 2005. Implications of climate change for freshwater inflows to the Arctic Ocean. J. Geophys. Res. 110, D07105.

Arora, V.K., Boer, G.J., 2001. Effects of simulated climate change on the hydrology of major river basins. J. Geophys. Res. 106, 3335–3336.

Bengtsson, L., Hodges, K.I., Hagemann, S., 2004. Sensitivity of the ERA40 reanalysis to the observing system: determination of the global atmospheric circulation from reduced observations. Tellus A 56, 456–471.

Bonsal, B.R., Prowse, T.D., Duguay, C.R., Lacroix, M.P., 2006. Impacts of large-scale teleconnections on freshwater-ice break/freeze-up dates over Canada. J. Hydrol. 330, 340–353.

Bowling, L.C., Lettenmaier, D.P., Matheussen, B. V., 2000. Hydroclimatology of the Arctic drainage basin. In: Lewis, E. (Ed.), The Freshwater Budget of the Arctic Ocean. Kluwer, Dordrecht, Netherlands, pp. 57–90.

Burn, D.H., 2008. Climatic influences on streamflow timing in the headwaters of the Mackenzie River Basin. J. Hydrol. 352, 225–238.

Carmack, E., Mclaughlin, F., Yamamoto-Kawai, M., Itoh, M., Shimada, K., Krishfield, R., Proshutinsky, A., 2008. Freshwater storage in the Northern Ocean and the special role of the Beaufort Gyre. In: Dickson, R.R. et al. (Ed.), Arctic-Subarctic Ocean Fluxes: Defining the Role of the Northern Seas in Climate. Springer, New York, pp. 145–169.

Carmack, E.C., 2000. The freshwater budget of the Arctic Ocean: Sources, storage and sinks. In: Lewis, E.L. (Ed.), The Freshwater Budget of the Arctic Ocean. Kluwer, Dordrecht, Netherlands, pp. 91–126.

Carmack, E.C., Barber, D.G., Christensen, J.R., Macdonald, R.W., Rudels, B., Sakshaug, E., 2006. Climate variability and physical forcing of the food webs and the carbon budget of pan-Arctic shelves. Prog. Oceanogr. 71, 145–181.

Curry, R., Mauritzen, C., 2005. Dilution of the northern North Atlantic Ocean in recent decades. Science (80-.). 1772–1774.

Déry, S.J., 2005. Decreasing river discharge in northern Canada. Geophys. Res. Lett. 32, L10401.

Dickson, B., Osborn, T., Hurrell, J.W., Meincke, J., Blindheim, J., Adlandsvik, B., Vinje, T., Alekseev, G., Maslowski, W., 2000. The Arctic Ocean response to the North Atlantic Oscillation. J. Clim. 13, 2671–2696.

Dickson, B., Yashayaev, I., Meincke, J., Turrell, B., Dye, S., Holfort, J., 2002. Rapid freshening of the deep North Atlantic Ocean over the past four decades. Nature 416, 832–7.

Dickson, R., Meincke, J., Malmberg, S., Lee, A., 1988. The “great salinity anomaly” in the northern North Atlantic 1968–1982. Prog. Oceanogr. 20, 103–151.

Dukhovskoy, D.S., Johnson, M.A., Proshutinsky, A., 2004. Arctic decadal variability: An auto-oscillatory system of heat and fresh water exchange. Geophys. Res. Lett. 31, L03302.

Dynesius, M., Nilsso, C., 1994. Fragmentation and flow regulation of river systems in the northern third of the world. Science (80-.). 266, 753–762.

Dyurgerov, M.B., Carter, C.L., 2004. Observational Evidence of Increases in Freshwater Inflow to the Arctic Ocean. Arctic, Antarct. Alp. Res. 36, 117–122.

Finnis, J., Cassano, J., Holland, M., Uotila, P., 2009. Synoptically forced hydroclimatology of major Arctic watersheds in general circulation models, Part 1 : the Mackenzie River Basin. Int. J. Climatol. 29, 1226–1243.

Francis, J.A., White, D.M., Cassano, J.J., Gutowski, W.J., Hinzman, L.D., Holland, M.M., Steele, M.A., Vörösmarty, C.J., 2009. An arctic hydrologic system in transition: Feedbacks and impacts on terrestrial, marine, and human life. J. Geophys. Res. 114, G04019.

Grabs, W.E., Portmann, F., De Couet, T., 2000. Discharge observation networks in Arctic regions: Computation of the river runoff into the Arctic Ocean, its seasonality and variability. In: Lewis, E.L. (Ed.), The Freshwater Budget of the Arctic Ocean. Kluwer, Dordrecht, Netherlands, pp. 249–267.

Greene, C.H., Pershing, A.J., Cronin, T.M., Ceci, N., 2008. Arctic climate change and its impacts on the ecology of the North Atlantic. Ecology 89, S24–S38.

Hakkinen, S., 1999. A simulation of the thermohaline effects of a Great Salinity Anomaly. J. Clim. 1781–1795.

Hamlet, A.F., Lettenmaier, D.P., 1999. Columbia River streamflow forecasting based on ENSO and PDO climate signals. J. Water Resour. Plan. Manag. 125, 333–341.

Harris, I., Jones, P.D., Osborn, T.J., Lister, D.H., 2014. Updated high-resolution grids of monthly climatic observations - the CRU TS3.10 Dataset. Int. J. Climatol. 34, 623–642.

Holland, M.M., Bitz, C.M., Eby, M., Weaver, A.J., 2001. The role of ice-ocean interactions in the variability of the North Atlantic thermohaline circulation. J. Clim. 656–675.

Holland, M.M., Finnis, J., Barrett, A.P., Serreze, M.C., 2007. Projected changes in Arctic Ocean freshwater budgets. J. Geophys. Res. 112, G04S55.

Hurrell, J.W., 1995. Decadal Trends in the North Atlantic Oscillation: Regional Temperatures and Precipitation. Science (80-.). 269, 676–679.

Hutchinson, M.F., McKenney, D.W., Lawrence, K., Pedlar, J.H., Hopkinson, R.F., Milewska, E., Papadopol, P., 2009. Development and testing of Canada-wide interpolated spatial models of daily minimum–maximum temperature and precipitation for 1961–2003. J. Appl. Meteorol. Climatol. 48, 725–741.

Jahn, A., Tremblay, B., Newton, R., Holland, M.M., Lawrence, A., 2009. Arctic freshwater export variability : A model study. In: Proceedings of 17th International Northern Research

Basins Symposium and Workshop. Iqaluit-Pangnirtung-Kuujjuaq, Canada, August 12-18, 2009, pp. 153–163.

Jasek, M., 2003. Ice jam release surges, ice runs, and breaking fronts: field measurements, physical descriptions, and research needs. Can. J. Civ. Eng. 30, 113–127.

Johnson, M.A., Polyakov, I. V, 2001. The Laptev Sea as a source for recent Arctic Ocean salinity changes. Geophys. Res. Lett. 28, 2017–2020.

Kattsov, V.M., Walsh, J.E., Chapman, W.L., Govorkova, V. a., Pavlova, T. V., Zhang, X., 2007. Simulation and Projection of Arctic Freshwater Budget Components by the IPCC AR4 Global Climate Models. J. Hydrometeorol. 8, 571–589.

Khan, V., Holko, L., Rubinstein, K., Breiling, M., 2008. Snow Cover Characteristics over the Main Russian River Basins as Represented by Reanalyses and Measured Data. J. Appl. Meteorol. Climatol. 47, 1819–1833.

Kingston, D.G., Lawler, D.M., McGregor, G.R., 2006. Linkages between atmospheric circulation, climate and streamflow in the northern North Atlantic: research prospects. Prog. Phys. Geogr. 30, 143–174.

Koenigk, T., Mikolajewicz, U., Haak, H., Jungclaus, J., 2007. Arctic freshwater export in the 20th and 21st centuries. J. Geophys. Res. 112, G04S41.

Lammers, R.B., Pundsack, J.W., Shiklomanov, A.I., 2007. Variability in river temperature, discharge, and energy flux from the Russian pan-Arctic landmass. J. Geophys. Res. 112, G04S59.

Lammers, R.B., Shiklomanov, A.I., 2013. A Regional, Hydrometeorological Data Network for Russia. Available online at http://www.r-arcticnet.sr.unh.edu/v4.0/index.html.

Lammers, R.B., Shiklomanov, A.I., Vörösmarty, C.J., Fekete, B.M., Peterson, B.J., 2001. Assessment of contemporary Arctic river runoff based on observational discharge records. J. Geophys. Res. 106, 3321–3334.

Larsen, J.N., O.A. Anisimov, A. Constable, A.B. Hollowed, N. Maynard, P. Prestrud, T.D. Prowse, and J.M.R. Stone, 2014: Polar regions. In: Climate Change 2014: Impacts, Adaptation, and Vulnerability. Part B: Regional Aspects. Contribution of Working Group II to the Fifth Assessment Report of the Intergovernmental Panel on Climate Change [Barros, V.R., C.B. Field, D.J. Dokken, M.D. Mastrandrea, K.J. Mach, T.E. Bilir, M. Chatterjee, K.L. Ebi, Y.O. Estrada, R.C. Genova, B. Girma, E.S. Kissel, A.N. Levy, S. MacCracken,

P.R. Mastrandrea, and L.L. White (eds.)]. Cambridge University Press, Cambridge, United Kingdom and New York, NY, USA, pp. 1567-1612.

Liu, B., Yang, D., Ye, B., Berezovskaya, S., 2005. Long-term open-water season stream temperature variations and changes over Lena River Basin in Siberia. Glob. Planet. Change 48, 96–111.

Loeng, H., Brander, K., Carmack, E., Denisenko, S., Drinkwater, K., Hansen, B., Kovacs, K., Livingston, P., Mclaughlin, F., Bellerby, R., Browman, H., Furevik, T., Grebmeier, J.M., Jansen, E., Jónsson, S., Jørgensen, L.L., 2005. Ch. 9: Marine Systems. In: Symon, C., Arris, L., Heal, B. (Eds.), Arctic Climate Impact Assessment. Cambridge University Press, New York, pp. 453–538.

Lydolph, P.E., Temple, D., Temple, D., 1977. Geograhpy of the U.S.S.R. Wiley, New York.

Ma, X., Fukushima, Y., Hiyama, T., Hashimoto, T., Ohata, T., 2000. A macro- • scale hydrological analysis of the Lena River basin. Hydrol. Process. 14, 639–651.

Macdonald, R.W., 2000. Arctic estuaries and ice: a positive-negative estuarine couple. In: Lewis, E. (Ed.), The Freshwater Budget of the Arctic Ocean. Kluwer, Dordrecht, Netherlands, pp. 383–407.

Macdonald, R.W., Carmack, E.C., McLaughlin, F. a., Falkner, K.K., Swift, J.H., 1999. Connections among ice, runoff and atmospheric forcing in the Beaufort Gyre. Geophys. Res. Lett. 26, 2223.

Mantua, N.J., Hare, S.R., Zhang, Y., Wallace, J.M., Francis, R.C., 1997. A Pacific interdecadal climate oscillation with impacts on salmon production. Bull. Am. Meteorol. Soc. 78, 1069–1079.

Marsh, P., Hey, M., 1989. The Flooding Hydrology of Mackenzie Delta Lakes 42, 41–49.

Maurer, E.P., Lettenmaier, D.P., Mantua, N.J., 2004. Variability and potential sources of predictability of North American runoff. Water Resour. Res. 40, W09306.

McBean, G., Alekseev, G., Chen, D., Førland, E., Fyfe, J., Groisman, P.Y., King, R., Melling, H., Vose, R., Whitfield, P.H., 2005. Arctic climate: past and present. In: Symon, C., Arris, L., Heal, B. (Eds.), Arctic Climate Impacts Assessment (ACIA). Cambridge University Press, Cambridge, pp. 21–60.

McClelland, J.W., 2004. Increasing river discharge in the Eurasian Arctic: Consideration of dams, permafrost thaw, and fires as potential agents of change. J. Geophys. Res. 109, D18102.

McClelland, J.W., Holmes, R.M., Dunton, K.H., Macdonald, R.W., 2011. The Arctic Ocean Estuary. Estuaries and Coasts 35, 353–368.

McKenney, D.W., Hutchinson, M.F., Papadopol, P., Lawrence, K., Pedlar, J.H., Campbell, K., Milewska, E., Hopkinson, R.F., Price, D., Owen, T., 2011. Customized spatial climate models for North America. Bull. Am. Meteorol. Soc. 92, 1611–1622.

McPhee, M.G., Proshutinsky, A., Morison, J.H., Steele, M., Alkire, M.B., 2009. Rapid change in freshwater content of the Arctic Ocean. Geophys. Res. Lett. 36, L10602.

Neal, E.G., Walter, M.T., Coffeen, C., 2002. Linking the Pacific Decadal Oscillation to seasonal stream discharge patterns in Southeast Alaska. J. Hydrol. 188–197.

Nghiem, S., Hall, D., Rigor, I., 2014. Effects of Mackenzie River discharge and bathymetry on sea ice in the Beaufort Sea. Geophys. Res. … 873–879.

Nuttall, M., 2005. Encyclopedia of the Arctic. Routledge.

Pelletier, P.M., 1990. A review of techniques used by Canada and other northern countries for measurement and computation of streamflow under ice conditions. Nord. Hydrol. 21, 317–340.

Peterson, B.J., Holmes, R.M., McClelland, J.W., Vörösmarty, C.J., Lammers, R.B., Shiklomanov, A.I., Shiklomanov, I.A., Rahmstorf, S., 2002. Increasing river discharge to the Arctic Ocean. Science (80-.). 298, 2171–2173.

Peterson, B.J., McClelland, J., Curry, R., Holmes, R.M., Walsh, J.E., Aagaard, K., 2006. Trajectory shifts in the Arctic and subarctic freshwater cycle. Science (80-.). 313, 1061–1066.

Polyakov, I. V., Alexeev, V.A., Belchansky, G.I., Dmitrenko, I.A., Ivanov, V. V., Kirillov, S.A., Korablev, A.A., Steele, M., Timokhov, L.A., Yashayaev, I., 2008. Arctic Ocean Freshwater Changes over the Past 100 Years and Their Causes. J. Clim. 21, 364–384.

Proshutinsky, A., Bourke, R.H., McLaughlin, F.A., 2002. The role of the Beaufort Gyre in Arctic climate variability: Seasonal to decadal climate scales. Geophys. Res. Lett. 29, 15–1– 15–4.

Proshutinsky, A., Bourke, R.H., McLaughlin, F.A., 2002. The role of the Beaufort Gyre in Arctic climate variability: Seasonal to decadal climate scales. Geophys. Res. Lett. 29, 15–1 – 15–4.

Prowse, T.D., Conly, F.M., 1998. Effects of climatic variability and flow regulation on ice-jam flooding of a northern delta. Hydrol. Process. 12, 1589–1610.

Prowse, T.D., Flegg, P.O., 2000. Arctic river flow: A review of contributing areas. In: Lewis, E.L. (Ed.), The Freshwater Budget of the Arctic Ocean. Kluwer, Dordrecht, Netherlands, pp. 269–280.

Rantz, S.E., 1982. Measurement and Computation of Streamflow : Volume 2 . Computation of Discharge. In: Geological Survey Water-Supply Paper 2175. United States Government Printing Office, Washington, DC.

Revenga, C., Murray, S., Abramovitz, J., Hammond, A., 1998. Watersheds of the world: ecological value and vulnerability. World Resources Institute, Washington, DC.

Rogers, A.N., Bromwich, D.H., Sinclair, E.N., Cullather, R.I., 2001. The atmospheric hydrologic cycle over the Arctic basin from reanalyses, Part 2. J. Clim. 14, 2414–2429.

Serreze, M.C., 2003. Arctic Climate. In: Holton, J.R., Curry, J.A., Pyle, J.A. (Eds.), Encyclopedia of Atmospheric Sciences. Academic Press, p. 171.

Serreze, M.C., Barrett, A.P., Slater, A.G., Woodgate, R.A., Aagaard, K., Lammers, R.B., Steele, M., Moritz, R., Meredith, M., Lee, C.M., 2006. The large-scale freshwater cycle of the Arctic. J. Geophys. Res. 111, C11010.

Serreze, M.C., Bromwich, D.H., Clark, M.P., Etringer, A.J., Zhang, T., Lammers, R., 2002. Large-scale hydro-climatology of the terrestrial Arctic drainage system. J. Geophys. Res. 108, 8160.

Serreze, M.C., Francis, J.A., 2006. The Arctic Amplification Debate. Clim. Change 76, 241–264.

Serreze, M.C., Holland, M.M., Stroeve, J., 2007. Perspectives on the Arctic's shrinking sea-ice cover. Science (80-.). 315, 1533–1536.

Shiklomanov, A.I., Lammers, R.B., Rawlins, M.A., Smith, L.C., Pavelsky, T.M., 2007. Temporal and spatial variations in maximum river discharge from a new Russian data set. J. Geophys. Res. 112, G04S53.

Shiklomanov, A.I., Lammers, R.B., Vorosmarty, C.J., 2002. Widespread decline in hydrological monitoring threatens pan-Arctic research. Eos (Washington. DC). 83, 13: 16–17.

Shiklomanov, A.I., Yakovleva, T.I., Lammers, R.B., Karasev, I.P., Vörösmarty, C.J., Linder, E., 2006. Cold region river discharge uncertainty—estimates from large Russian rivers. J. Hydrol. 326, 231–256.

Shiklomanov, I.A., Shiklomanov, A.I., Lammers, R.B., Peterson, B.J., Vorosmarty, C.J., 2000. The dynamics of river water inflow to the Arctic Ocean. In: Lewis, E.L. (Ed.), The Freshwater Budget of the Arctic Ocean. Kluwer, Dordrecht, Netherlands, pp. 281–296.

Shimada, K., Motoyo, I., Nishino, S., Mclaughlin, F., Carmack, E.C., Proshutinsky, A., 2005. Halocline structure in the Canada Basin of the Arctic Ocean. Geophys. Res. Lett. 32, L03605.

Steele, M., Boyd, T., 1998. Retreat of the cold halocline layer in the Arctic Ocean. J. Geophys. Res. 103, 10419–10435.

Steele, M., Thomas, D., Rothrock, D., Martin, S., 1996. A simple model study of the Arctic Ocean freshwater balance. J. Geophys. Res. 20, 833–848.

Stewart, R.E., 2000. The variable climate of the Mackenzie River Basin: its water cycle and fresh water discharge. In: Lewis, E. (Ed.), The Freshwater Budget of the Arctic Ocean. Kluwer, Dordrecht, Netherlands, pp. 367–381.

Stigebrandt, A., 2000. Oceanic freshwater fluxes in the climate system. In: Lewis, E. (Ed.), The Freshwater Budget of the Arctic Ocean. Kluwer, Dordrecht, Netherlands, pp. 1–20.

Stoner, A.M.K., Hayhoe, K., Wuebbles, D.J., 2009. Assessing General Circulation Model Simulations of Atmospheric Teleconnection Patterns. J. Clim. 22, 4348–4372.

Stuefer, S., Yang, D., Shiklomanov, A., 2011. Effect of streamflow regulation on mean annual discharge variability of the Yenisei River. In: Cold Region Hydrology in a Changing Climate (Proceedings of Symposium H02 Held during IUGG2011 in Melbourne, Australia, July 2011). IAHS Publ. 346, pp. 27–32.

Sveinsson, O., Lall, U., Gaudet, J., Kushnir, Y., Zebiak, S., Fortin, V., 2008. Analysis of climatic states and atmospheric circulation patterns that influence Quebec spring streamflows. J. Hydrol. Eng. 411–425.

Tank, S.E., Manizza, M., Holmes, R.M., McClelland, J.W., Peterson, B.J., 2011. The processing and impact of dissolved riverine nitrogen in the Arctic Ocean. Estuaries and Coasts 35, 401–415.

Thompson, D.W.J., Wallace, J.M., 1998. The Arctic Oscillation signature in the wintertime geopotential height and temperature fields. Geophys. Res. Lett. 25, 1297–1300.

Toggweiler, J.R., Key, R.M., 2001. Ocean Circulation: Thermohaline Circulation. In: Encyclopedia of Atmospheric Sciences, Vol. 4. Academic Press, San Diego, CA, pp. 1549–1555.

Trenberth, K., 1997. The definition of El Nino. Bull. Am. Meteorol. Soc. 78, 2771–2777.

Uppala, S.M., Kallberg, P.W., Simmons, A.J., Andrae, U., Bechtold, V.D.C., Fiorino, M., Gibson, J.K., Haseler, J., Hernandez, A., Kelly, G.A., Li, X., Onogi, K., Saarinen, S., Sokka, N., Allan, R.P., Andersson, E., Arpe, K., Balmaseda, M.A., Beljaars, A.C.M., Berg, L. Van De, Bidlot, J., Bormann, N., Caires, S., Chevallier, F., Dethof, A., Dragosavac, M., Fisher, M., Fuentes, M., Hagemann, S., Hólm, E., Hoskins, B.J., Isaksen, L., Janssen, P.A.E.M., Jenne, R., Mcnally, A.P., Mahfouf, J.-F., Morcrette, J.-J., Rayner, N.A., Saunders, R.W., Simon, P., Sterl, A., Trenberth, K.E., Untch, A., Vasiljevic, D., Viterbo, P., Woollen, J., 2005. The ERA-40 re-analysis. Q. J. R. Meteorol. Soc. 131, 2961–3012.

Vihma, T., 2014. Effects of Arctic Sea Ice Decline on Weather and Climate: A Review. Surv. Geophys. 35, 1175–1214.

Walsh, J.E., 2000. Global atmospheric circulation patterns and relationships to Arctic freshwater fluxes. In: Lewis, E. (Ed.), The Freshwater Budget of the Arctic Ocean. Kluwer, Dordrecht, Netherlands, pp. 21–43.

Walsh, J.E., Zhou, X., Portis, A., Serreze, M.C., 1994. Atmospheric contribution to hydrologic variations in the Arctic. Atmosphere-Ocean 733–755.

Wedel, J.H., 1990. Regional Hydrology. In: Prowse, T.D., Ommanney, C.S.L. (Eds.), Northern Hydrology: Canadian Perspectives. National Hydrology Research Institute, Saskatoon, SK, pp. 207–226.

Wehl, P.K., 1968. The role of the oceans in climate change: A theory of the ice ages. Meteorol. Monogr 8, 38–62.

White, D., Hinzman, L., Alessa, L., Cassano, J., Chambers, M., Falkner, K., Francis, J., Gutowski, W.J., Holland, M., Holmes, R.M., Huntington, H., Kane, D., Kliskey, A., Lee, C., McClelland, J., Peterson, B., Rupp, T.S., Straneo, F., Steele, M., Woodgate, R., Yang, D., Yoshikawa, K., Zhang, T., 2007. The Arctic freshwater system: changes and impacts. J. Geophys. Res. 112, G04S54.

Woo, M., Mollinga, M., Smith, S.L., 2007. Climate warming and active layer thaw in the boreal and tundra environments of the Mackenzie 743, 733–743.

Woo, M., Thorne, R., 2003. Streamflow in the Mackenzie basin, Canada. Arctic 56, 328–340.

Woo, M., Thorne, R., Szeto, K., 2006. Reinterpretation of streamflow trends based on shifts in large-scale atmospheric circulation. Hydrol. Process. 20, 3995–4003.

Wu, P., Wood, R., Stott, P., 2005. Human influence on increasing Arctic river discharges. Geophys. Res. Lett. 32, L02703.

Yamamoto-Kawai, M., McLaughlin, F. a., Carmack, E.C., Nishino, S., Shimada, K., 2008. Freshwater budget of the Canada Basin, Arctic Ocean, from salinity, δ 18 O, and nutrients. J. Geophys. Res. 113, C01007.

Yang, D., Kane, D.L., Hinzman, L.D., Zhang, X., Zhang, T., Ye, H., 2002. Siberian Lena River hydrologic regime and recent change. J. Geophys. Res. 107, 4694.

Yang, D., Marsh, P., Shaoqing, G., 2014. Heat flux calculations for Mackenzie and Yukon Rivers. Polar Sci. 8, 232–241.

Yang, D., Ye, B., Kane, D.L., 2004a. Streamflow changes over Siberian Yenisei River Basin. J. Hydrol. 296, 59–80.

Yang, D., Ye, B., Shiklomanov, A., 2004b. Discharge characteristics and changes over the Ob River watershed in Siberia. J. Hydrometeorol. 5, 595–610.

Ye, B., Yang, D., Kane, D.L., 2003. Changes in Lena River streamflow hydrology: Human impacts versus natural variations. Water Resour. Res. 39, 1200.

Ye, H., Yang, D., Zhang, T., Zhang, X., Ladochy, S., Ellison, M., 2004. The impact of climatic conditions on seasonal river discharges in Siberia. J. Hydrometeorol. 5, 286–295.

Yip, Q.K.Y., Burn, D.H., Seglenieks, F., Pietroniro, A., Soulis, E.D., 2012. Climate Impacts on Hydrological Variables in the Mackenzie River Basin. Can. Water Resour. J. 37, 209–230.

Zhang, T., Barry, R.G., Knowles, K., Heginbottom, J.A., Brown, J., 2008. Statistics and characteristics of permafrost and ground-ice distribution in the Northern Hemisphere. Polar Geogr. 31, 47–68.

Zhang, X., Ikeda, M., Walsh, J., 2003. Arctic sea ice and freshwater changes driven by the atmospheric leading mode in a coupled sea ice-ocean model. J. Clim. 16, 2159–2177.

List of Figures

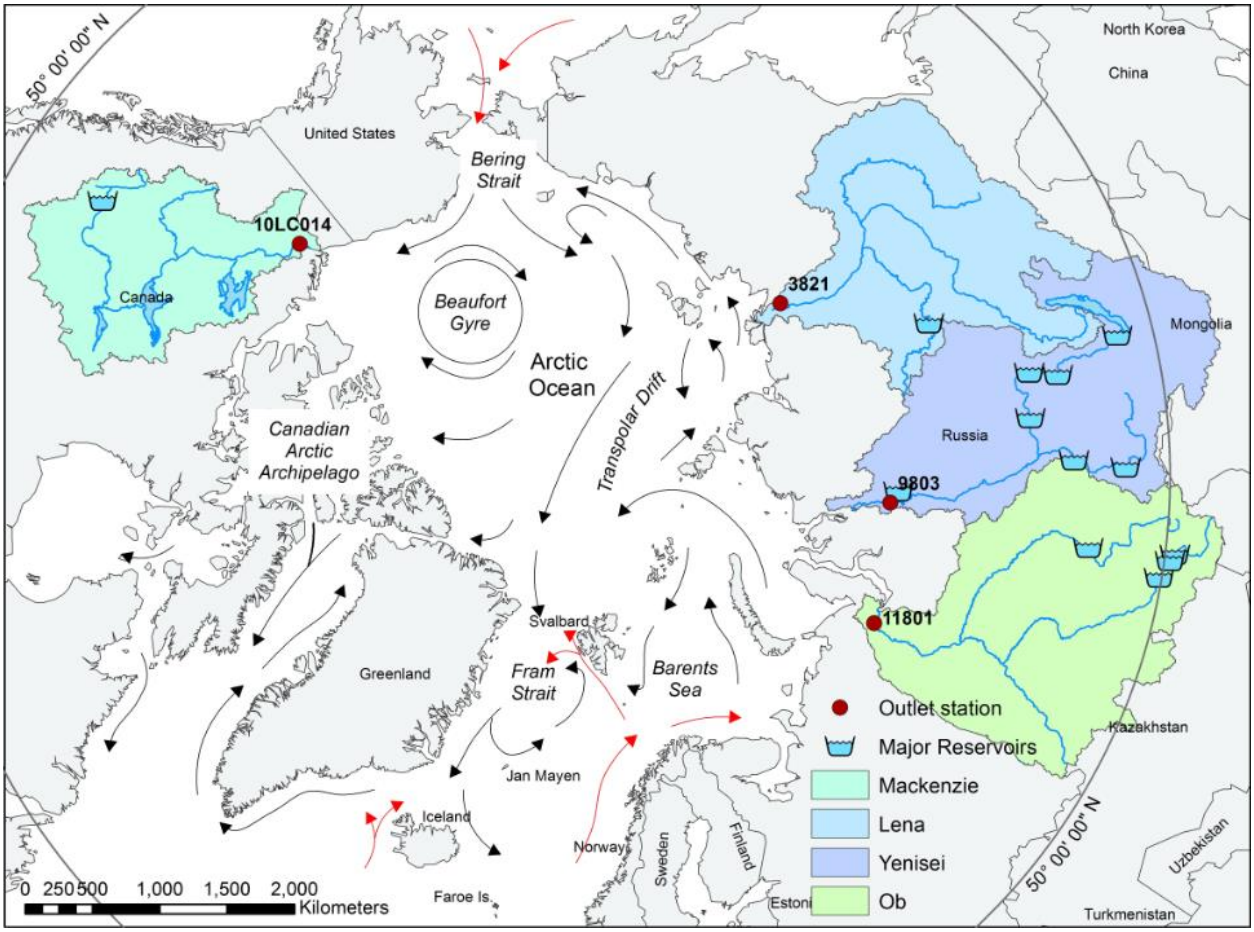

Figure 1. Map showing the Arctic Ocean, ocean features, major surface currents, major reservoirs and drainage basins and outlet stations of the Mackenzie, Ob, Yenisei and Lena rivers. Red arrows denote warmer currents, while black arrows denote colder currents. Figure adapted from Figure 6 in McClelland et al. (2011).

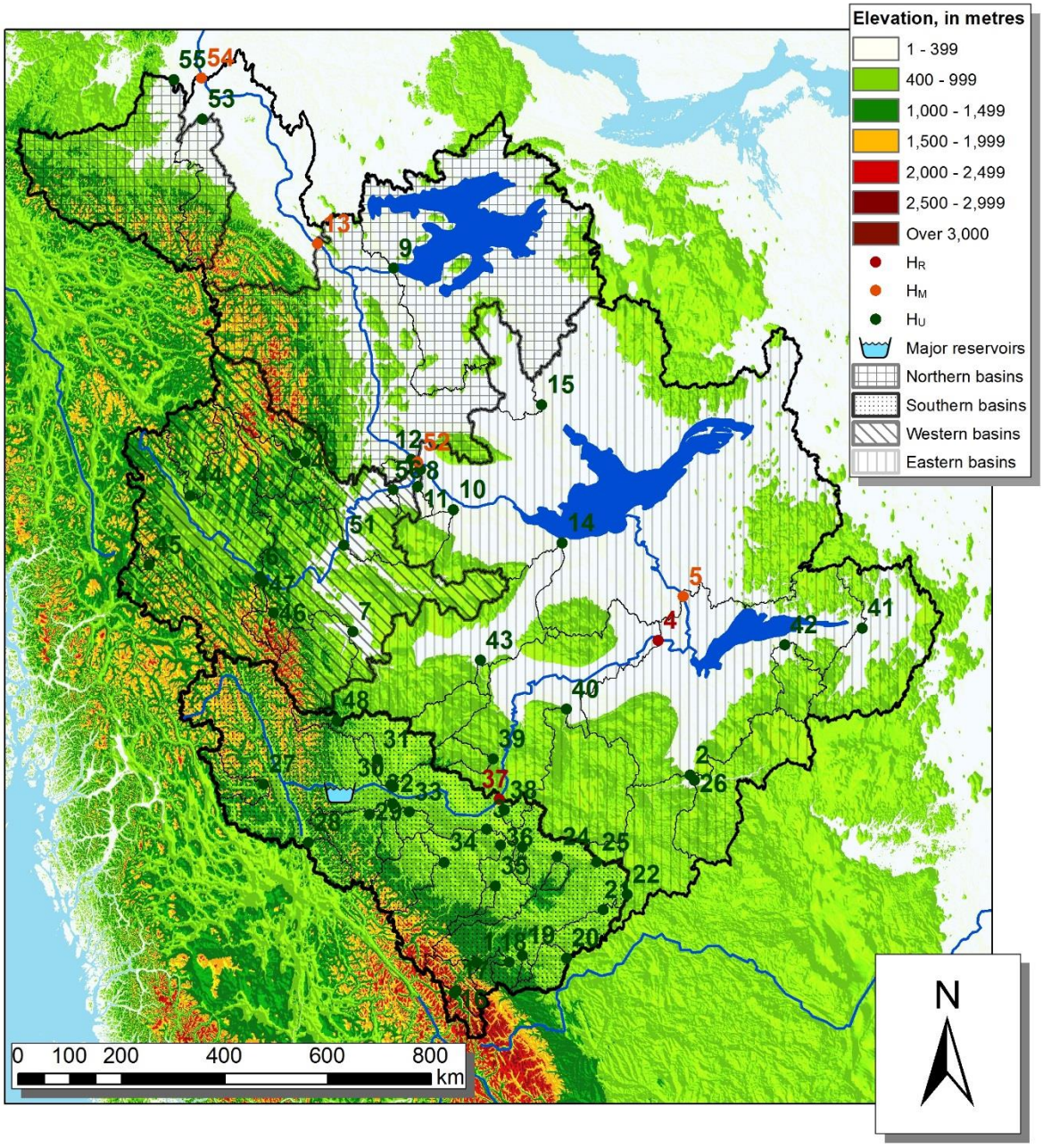

Figure 2. Topographical map of the Mackenzie basin showing regional classification of sub-basins into Northern, Southern, Western and Eastern regions. Outlet stations are not included in the classification.

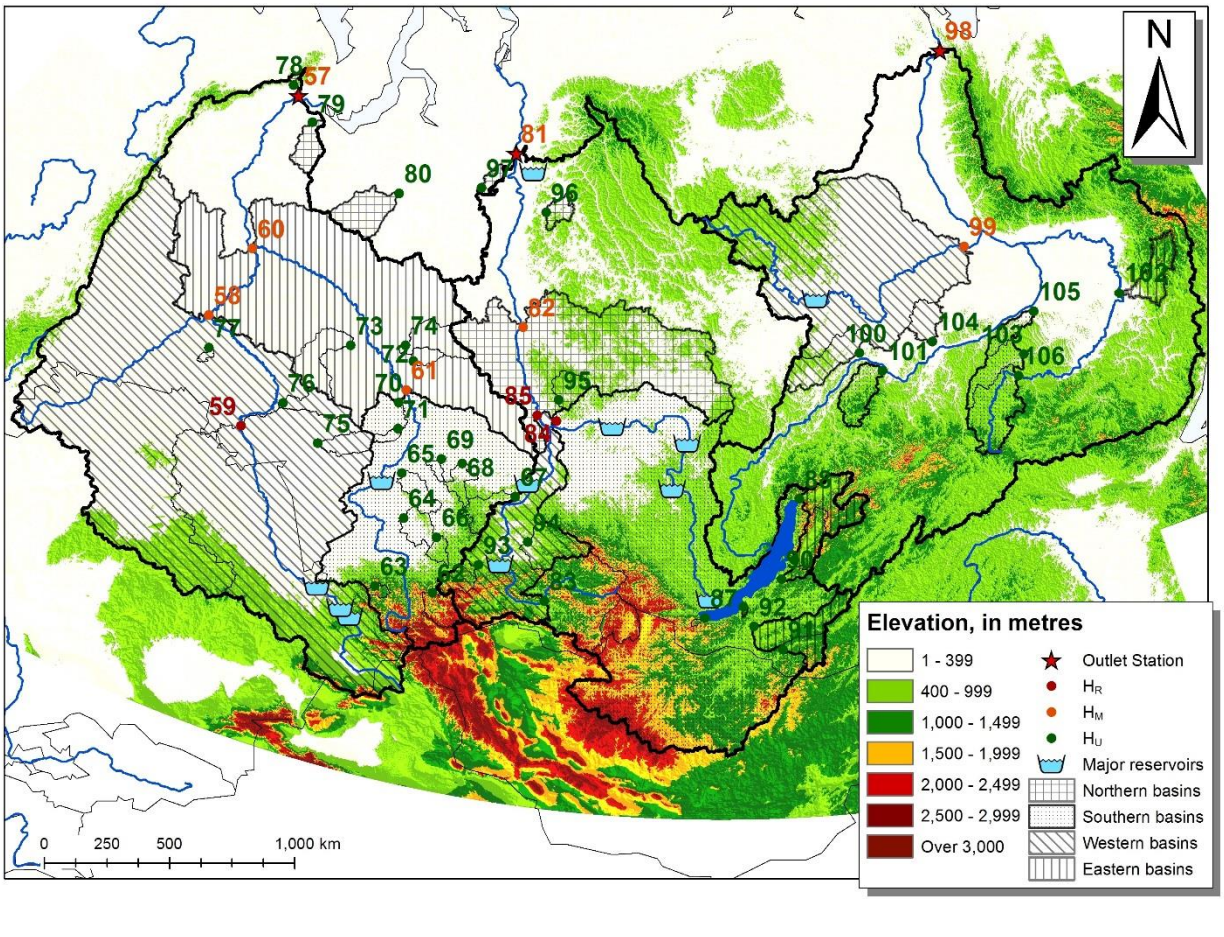

Figure 3. Topographical map of the Eurasian basins showing regional classification of sub-basins into Northern, Southern, Western and Eastern regions. Outlet stations are not included in the classification.

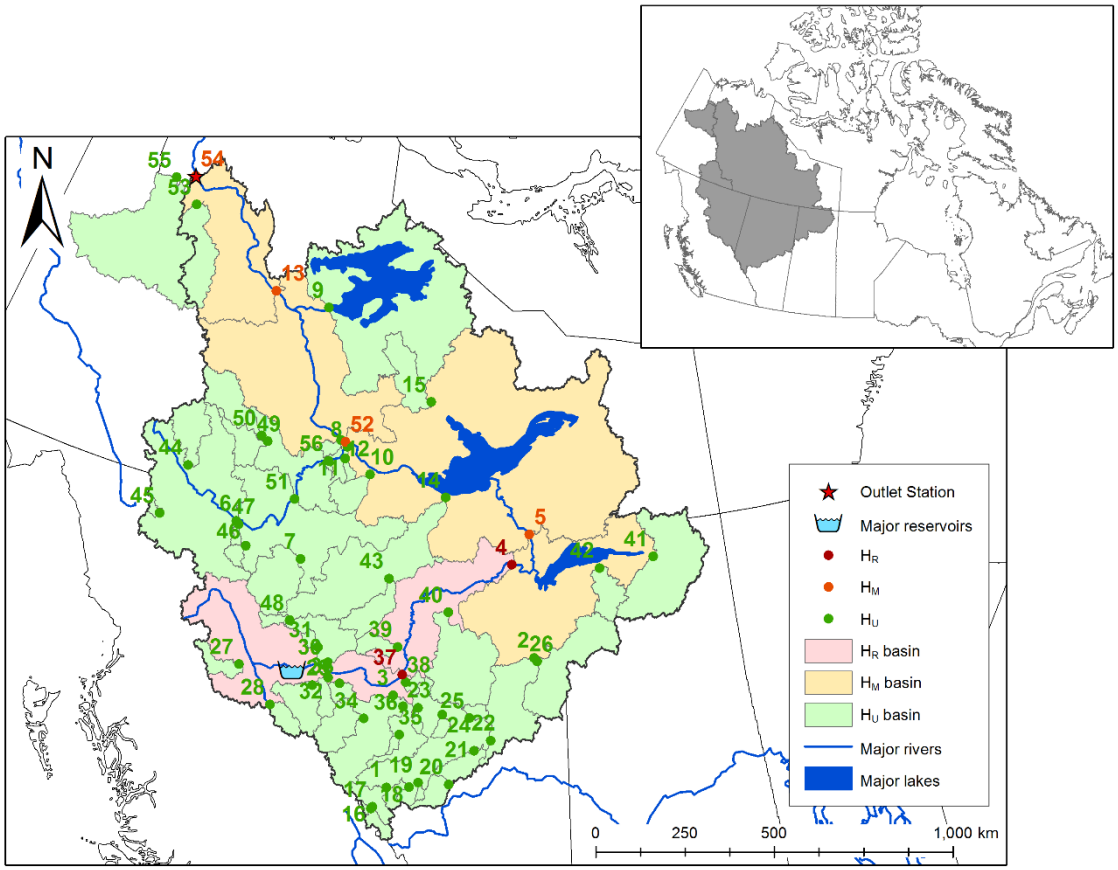

Figure 4. Study area of the Mackenzie basin showing station locations labeled with a unique identifier and station sub-basin drainage areas. Stations and basins are colour-coded and classified as regulated (H_R), minimally regulated (H_M) or unregulated (H_U).

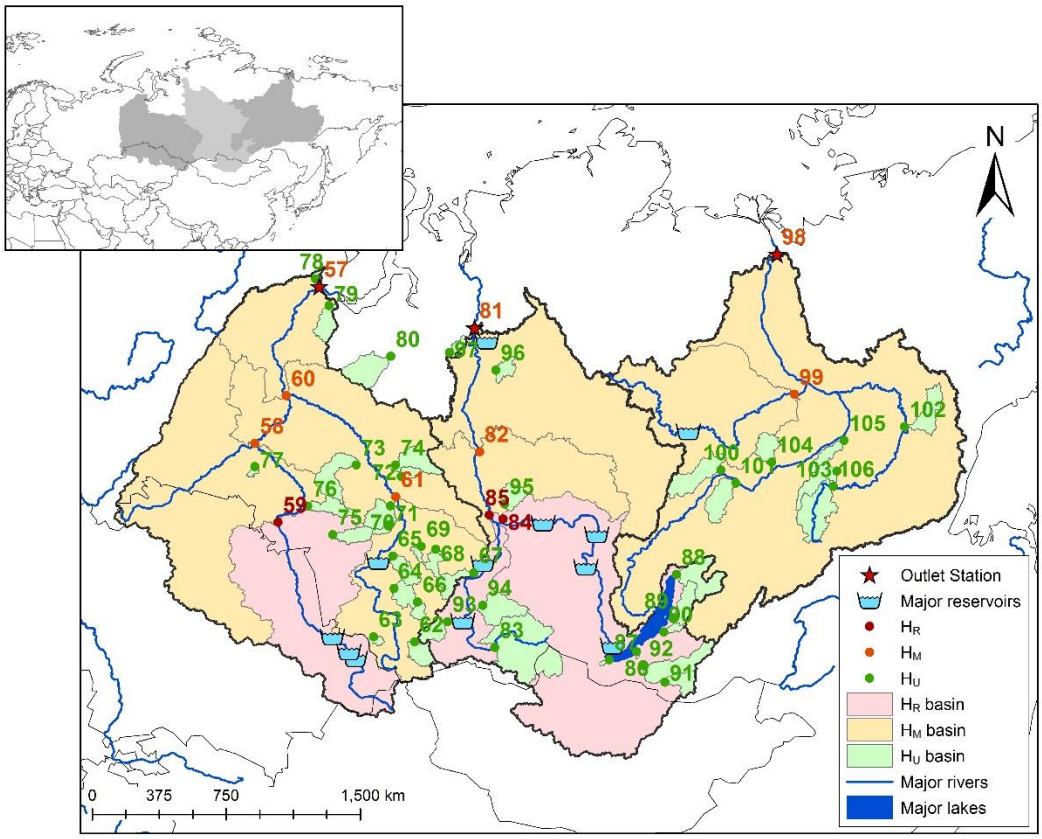

Figure 5. Study area of the (left to right in inset map) Ob, Yenisei and Lena basins showing station locations labeled with a unique identifier and station sub-basin drainage areas. Stations and basins are colour-coded and classified as regulated (H_R), minimally regulated (H_M) or unregulated (H_U).

CHAPTER 3: TRENDS IN SEASONAL RUNOFF COMPONENTS OF FOUR MAJOR ARCTIC-DRAINING RIVERS

Abstract

Runoff from Arctic rivers constitutes a major freshwater influx to the Arctic Ocean. In these nival-dominated river systems, the majority of annual discharge is released during the spring snowmelt period. Since the circulation regime of the salinity-stratified Arctic Ocean is connected to global earth-ocean dynamics through thermohaline circulation, variability in this input can have important impacts to the global climate system.

Daily discharge data for the four largest Arctic-draining river watersheds (Mackenzie, Ob, Lena and Yenisei; herein referred to as MOLY) are analyzed to determine trends in discharge timing and magnitude for the entire length of available records, as well as during a recent 30-year period. Emphasis is placed on the spring freshet. Combined flows are assessed to determine overall changes to circumpolar freshwater input to the Arctic Ocean.

During the period 1980 – 2009, total freshwater influx to the Arctic Ocean increased by up to 89 km^3/10yr. Meanwhile, freshet contribution given as a fraction of annual flow decreased by 1.7% during 1980 – 2009, while winter, spring and fall showed increases (1.3%, 2.5% and 2.5%, respectively). Summer revealed a strong decrease (5.8%) in proportional discharge. This decrease, coupled with an increase in spring discharge and earlier pulse onset dates, indicates a general shift towards a flatter, more gradual hydrograph with earlier peak discharges. From this study it can be concluded that the annual increase in MOLY discharge is not solely due to increased spring freshet discharge, but is a combination of increases across all timing measures.

Keywords: Arctic, hydrological trends, spring freshet, hydro-climatology

3.1 Introduction

Terrestrial freshwater contribution to the Arctic Ocean from Arctic-draining rivers plays an important role in several physical processes, affecting systems on both global and regional scales. Variability in this contribution can have wide-ranging effects on global feedback interactions, hydrological extremes and contaminant and nutrient pathways (Anisimov et al., 2007). For example, runoff from Arctic-draining rivers influences salinity stratification within the Arctic Ocean. This stratification regime governs freshwater export from the Arctic Ocean through the northern North Atlantic Ocean, and is an integral part of the global ocean circulation regime. A change in stratification of surface waters can affect North Atlantic Deep Water (NADW) formation which, coupled with Atlantic Meridional Overturning Circulation (AMOC), is a critical driving force in the global thermohaline circulation (e.g., Aagaard and Carmack, 1989; Anisimov et al., 2001; Dickson et al., 2000, 2002; Proshutinsky et al., 2002; Loeng et al., 2005; Serreze et al., 2006). During the spring freshet, Arctic runoff plays an important role as a nutrient supplier to near-shore and estuarine ecosystems, providing an influx of organic carbon during the spring freshet, yet diluting waters with respect to inorganic nitrate and silica compounds (Kattsov et al., 2007; McClelland et al., 2011; Tank et al., 2011).

In Arctic-draining rivers, the annual spring freshet following snowmelt and river ice break-up provides up to 60% of the total annual flow volume (Lammers et al., 2001). Seasonality and magnitude of this event play a key role in the processes which govern freshwater storage and circulation in the Arctic Ocean. For example, discharge seasonality can affect freshwater runoff trajectory upon entering the Arctic Ocean, influencing whether freshwater is placed into storage or released. Seasonality also has important impacts to Arctic sea ice

production and ablation, as well as distribution, timing and magnitude of ecosystem production in Arctic coastal communities (Carmack et al., 2006; Loeng et al., 2005).

It is well-documented that changes in Arctic river discharge have been occurring. During the period 1936 to 1999, discharge from Eurasian basins draining to the Arctic Ocean increased annually by 2.0 ± 0.7 km^3yr^{-1}, which resulted in a cumulative increase of 128 km^3 more freshwater released annually by the end of the period as compared to the beginning (Peterson et al., 2002). This increase in freshwater discharge was tempered by an overall yearly decrease in Canadian discharge to high-latitude seas (including the Labrador Sea, Eastern and Western Hudson Bay, Arctic Ocean and Bering Strait) of -3.1 km^3 yr^{-1} during the period 1964-2003, although Canadian discharge directly to the Arctic Ocean showed a non-statistically significant increase (Déry, 2005). Meanwhile, global climate model projections show an overall increase of river influx to the Arctic Ocean of approximately 10 – 30% by the year 2100 (Walsh et al., 2005).

Despite the relative importance of seasonality to numerous Arctic physical processes, previous studies focused on changes in total annual runoff contribution, rather than temporal distribution of runoff timing. Given that Arctic climate change is occurring at an accelerated rate compared to the global average (e.g., Larsen et al., 2014; Anisimov et al., 2007; Serreze and Francis, 2006), there is a research need to assess potential changes in the seasonal runoff characteristics of major Arctic river systems providing freshwater influx to the Arctic Ocean. Reported changes in Arctic river discharge are not spatially uniform, with indications of increased discharges from Eurasian basins and decreased discharges from North American basins. Given these regional variations, this study aims to determine what changes, if any, have occurred in combined spring freshet contribution from major basins, and whether there are any

temporal correspondences in these changes. Seasonality of individual basin discharge is also investigated. These objectives are achieved by analyzing daily discharge data of the four largest Arctic-draining rivers: the Mackenzie Basin in Canada, and the Ob, Lena and Yenisei river basins in Eurasia, herein referred to as MOLY. Combined, these four rivers contribute almost 1900 km^3 of freshwater to the Arctic Ocean per year, or about 60% of annual flow volume from all Arctic contributing areas (Grabs et al., 2000; Prowse and Flegg, 2000). Discharge data are analyzed over the entire available length of record for each river, and collectively, during the period 1980 – 2009.

3.2 Basin Characteristics

The pan-Arctic drainage basins and outlet stations of the Mackenzie, Ob, Yenisei and Lena rivers are shown in Figure 1, while outlet station characteristics are given in Table 1. Total contributing areas of the four major river systems, including ungauged drainage areas, are as follows: Mackenzie 1,800,000 km^2 (Finnis et al., 2009); Ob 2,975,000 km^2 (Yang et al., 2004b); Lena 2,488,000 km^2 (Yang et al., 2002); and Yenisei 2,554,482 km^2 (Zhang et al., 2003). The pan-Arctic region contains nearly half of the global alpine and sub-polar glacial area (Dyurgerov and Carter, 2004). Meanwhile, some major Eurasian Arctic basins extend below 50°N, further south than what is traditionally considered within the Arctic region (Loeng et al., 2005) (see Figure 1). As a result, discharge behaviour at each of the four major drainage outlets is influenced along its course by sub-basin tributaries which may adhere to variety of hydrological regimes such as nival, pluvial, prolacustrine, hybrid or other. For example, hydrologic retention due to extensive wetland coverage or large lakes within a catchment, such as found in the Ob or Mackenzie basins, will lead to a more moderated seasonal discharge characteristic than basins without such retention (Carmack, 2000).

Reservoir regulation is known to impact seasonal distribution of discharge (Yang et al., 2004a; Ye et al., 2003). Each of the MOLY watersheds experiences some degree of flow regulation within their catchments, ranging from only one major reservoir in each of the Mackenzie and Lena basins, to four or more major reservoirs in the Ob and Yenisei basins (Stuefer et al., 2011; Yang et al., 2004a; 2004b). In terms of flow regulation, the Yenisei basin is the most substantially regulated, with at least six major reservoirs having a capacity greater than 25 km^3 located along the Yenisei and Angara stems (Yang et al., 2004a; Stuefer et al., 2011). It is considered "strongly affected" by flow regulation and fragmentation according to an assessment of anthropogenic changes in river flow and river channel continuity of large river systems (Dynesius and Nilsso, 1994). The next most regulated is the Ob basin, containing one major reservoir with capacity greater than 25 km^3 and three midsize dams (Yang et al., 2004b). The Ob basin is moderately affected based on its classification of flow regulation and fragmentation. Of the Eurasian basins, the Lena is least affected by flow regulation, with only one major reservoir located along the Vilyuy tributary. It is moderately affected in terms of regulation and fragmentation (Dynesius and Nilsso, 1994). The Mackenzie basin is also moderately affected, despite having only one major reservoir located along the Peace tributary. Large lakes in the Mackenzie basin (e.g., Great Slave L. and Great Bear L.) provide substantial storage capacity, acting to reduce high spring peaks and sustain lower flows resulting in a more consistent runoff pattern throughout the year, similar to the effect of flow regulation (Woo and Thorne, 2003). The percentage of each basin's area that is located directly upstream of a major reservoir (obtained by delineating the drainage areas of the reservoirs), is as follows: Mackenzie 3.9%; Ob 11.6%; Yenisei 46.5% and Lena 4.2%. See Figure 1 for locations of major reservoirs.

3.3 Data and Analysis

3.3.1 Data sources

Daily discharge data are obtained from the Environment Canada Hydrometric Database (HYDAT) for stations in the Mackenzie basin and from the Regional, Hydrometeorological Data Network for Russia (R-ArcticNET Russia v4.0) (Lammers and Shiklomanov, cited 2012) for the Ob, Lena and Yenisei basins. Availability of Arctic hydrometric data is temporally limited, with all outlet stations having published records to 2009 only, and records in many smaller basins not extending past 2000. Complete records for the Mackenzie outlet station begin in 1973, while the Yenisei outlet station has several extensive gaps during the period 1963 – 1979. As a result, the period 1980 – 2009 is chosen for analysis of combined MOLY flow, while individual stations are assessed for the entire available record. Available record periods are given in Table 1.

3.3.2 Spring freshet definition

Two methods are used to define the volume of discharge released during the spring freshet period: i) flows occurring during the period April through July (AMJJ), referred to as V_1 and ii) integrated flow from the date of the spring pulse onset to the hydrograph centre of mass calculated from pulse onset to the last day of the calendar year, referred to as V_2. July is used as the end-date of the V_1 period since some basins display high discharge rates well into the summer months. The date of the spring pulse onset is determined as the date at which cumulative departure from mean annual flow was most negative. This yields the date when flows on subsequent days are greater than the year average (Cayan et al., 2001; Stewart et al., 2005); see Appendix B for an illustration of the algorithm as well as visual indicators of the pulse onset, freshet end date, peak magnitude and V_1 and V_2 definitions of the spring freshet for a sample year of the Yenisei River outlet station.

Visual inspection of the results verified that this is a reliable method for identifying the start date of spring freshet as shown in the example in Appendix B. Choosing the freshet end date by visual means is subjective and influenced by precipitation, temperature and other factors; therefore, the hydrograph centre of mass adjusted by pulse onset as the freshet end date is used as a consistent method for determination of the freshet end date. Other descriptors used to analyse freshet characteristics are given in Table 2.

3.3.3 Trend analysis

The Mann-Kendall (Mann, 1945; Kendall, 1975) test is used to assess the temporal trends in freshet timing and magnitude. This non-parametric test is often used for detecting trends in hydrologic time series that may be affected by seasonal climatic variability, missing data or extremes (Hirsch and Slack, 1984) and makes no prior assumptions about normality of data. In addition, a Trend-Free Pre-Whitening (TFPW) approach (Yue et al., 2002) is used to correct data for serial autocorrelation following the methods of Burn and Cunderlik (2004). This approach first fits a monotonic trend for a data series which is then removed prior to pre-whitening the data series. The monotonic trend is then re-added to the residual de-trended and pre-whitened data series, whereby the Mann-Kendall test statistic and local significance are calculated. All trends are considered statistically significant at the 5% level.

3.4 Results

3.4.1 Freshet characteristics

Over the period 1980 – 2009, average freshet start date is May 12, 14, 28 and 19 for the Mackenzie, Ob, Lena and Yenisei rivers, respectively. According to freshet definition V_2, during 1980 – 2009 an average of 48% of total annual flow is released during the freshet period for the Mackenzie River, 51% for the Ob, 57% for the Lena and 52% for the Yenisei. Table 3 shows the

percentage of total MOLY freshwater volume released by each river for V_1 and V_2 freshet definitions as well as during the months of April through July. Overall, total proportional freshet volume contributions are greatest from the Lena and Yenisei during V_1 or V_2 freshet definitions, with the Yenisei reaching its peak proportional contribution in the month of April and the Lena slightly delayed, reaching its proportional peak contribution in June and July. The Lena River is largely unregulated and therefore characterized by a sharp spring peak and low winter flows typical of a nival basin with extensive permafrost coverage (Kane, 1997). By contrast, extensive regulation of the Yenisei River dampens the spring freshet with flows being enhanced from storage releases at other times of the year such as late fall and mid-winter (Yang et al., 2004a). The Mackenzie and Ob stations exhibit a more consistent spring contribution characteristic of flow regimes moderated by the existence of large lakes or wetland areas.

3.4.2 Changes in timing and magnitude

Observed changes in discharge are generally most notable during the shorter period of 1980 – 2009 versus the entire length of available records. All outlets show either a decreasing (i.e. earlier) trend or no trend in pulse onset date (Table 4 and Figure 2), although only the Mackenzie and Lena stations exhibit a significant trend resulting in an earlier pulse onset by 1.2 to 1.4 days per decade, respectively, over their longer records. Freshet length (Table 4, not plotted) shows either a slight decreasing trend (Ob) or no trend over the longer record, while all outlets have an increasing but non-significant trend in freshet length. Although peak freshet magnitude trends are generally decreasing, no significant changes are detected (Table 4, not plotted) with exception of a minor, non-significant increase in the Ob basin during 1980-2009.

In terms of released discharge magnitude, little change is detected in freshet volume (V_2) over the longer records, but all outlets show an increase in freshet volume during 1980 – 2009

(Table 4, Figure 3). Increases are significant in all stations except for the Yenisei, with the Lena station indicating a significant increasing trend of up to an additional 18.9 km^3/10 year over the 30-year period. Annual volume also increases in both time periods, although only the Lena station exhibits a significant increase of up to 28.8 km^3/10 year from 1936 – 2009. During 1980 – 2009, however, all stations with exception of the Ob show an increase of greater than 20 km^3/10 years by the end of the period (Table 4, Figure 4).

To assess whether discharge seasonality has shifted for individual stations, fraction of flows released during the freshet and winter (December – February) (V_{DJF}), spring (March – May) (V_{MAM}), summer (June – August) (V_{JJA}) and fall (September – November) (V_{SON}) (Figure 5 to Figure 9, respectively) are calculated and shown as a percentage of total annual flow for each station. Table 5 gives trends in the percentage changes during each timing measure. Over all periods, percentage of flow released during the freshet (V_2) decreases in all stations, although none of those trends are significant. Meanwhile, winter and spring percentages generally increase, while summer proportions decrease. An increase in V_{MAM} percentage coupled with a decrease in V_{JJA} percentage is notable since it indicates a shift in timing of overall peak discharges. Although pulse onset occurs in May for all stations, overall discharges typically peak in June. Despite a decrease in freshet discharge proportion, peak discharges are shifting towards an earlier release. Fall discharges show either a slight increase (Mackenzie) or decrease (Ob, Lena) during the longer records, while during 1980 – 2009 all stations indicate an increase in fall discharge.

3.4.3 Changes in combined circumpolar discharge

Total annual discharge from all four basins combined significantly increased by approximately 89 km^3/10yr over the period 1980 – 2009 (Figure 10a). To better assess the

seasonal contributions to this overall annual increase, trends for all seasonal measures (V_1, V_2, V_{DJF}, V_{MAM}, V_{JJA}, and V_{SON}) are determined. From Figure 10b and Figure 10c, it is apparent that, while freshet discharge V_2 shows a statistically significant increase of up to 33 km^3/10yr, other seasons also display increasing discharges over the same period. With the exception of summer (+16 km^3/10yr, p = 0.254), all increases are statistically significant at the 5% level. Spring, fall and winter show increases of 29 km^3/10yr, 35 km^3/10yr and 16 km^3/10yr, respectively.

Despite variation in individual proportions of seasonal flow, there is consistency in combined sequencing of discharge compared to individual flows (Figure 11). Freshet contribution as a fraction of combined annual flow for MOLY stations is shown to decrease by approximately 1.7% during 1980 – 2009, although this trend is not significant. Winter proportional contribution increased significantly by 1.3%, while spring fraction also shows an increase, but is not significant. Combined summer fractional flows show a significant decrease of up to 5.8%, which is consistent with earlier findings indicating highly decreased summer proportions for individual outlet stations. Fall fractions show a statistically significant increase of approximately 2.5%.

3.5 Conclusions

This analysis of the outlet stations of the four largest Arctic-draining rivers indicates that the sum total annual discharge from these rivers has increased by up to 89 km^3/10yr over the period 1980 – 2009, amounting to an approximate 14% increase from the end of the period compared to the beginning. While this estimate is comparatively larger than the 7% increase found in a previous study using records from the six largest Eurasian rivers during 1936 – 2009 (see Peterson et al., 2002), the results found here are consistently greater during the shorter, more recent period of analysis used. As Figure 4 and Table 4 indicate, trends over the longer periods

tended to occur at a much slower rate than trends given in 1980 – 2009. This apparent rapid increase in freshwater volume contribution during 1980 - 2009 may be an effect of the short window of analysis used, but could also be due to changes in climatic conditions over the recent period.

Trends in combined MOLY seasonal flow are also investigated to determine whether this annual increase could be attributed to a rising freshet, rising winter low-flows, or some other combination of seasonal increases. While freshet discharge shows a significant increase of up to 33 km^3/10yr (Figure 10), this change is complemented by corresponding increases in winter, spring and fall. In fact, compared to other timing measures, fall indicates the greatest increase, of up to 35 km^3/10yr. This may be a result of delayed river ice freeze-up dates, or increased late-summer and autumn precipitation. Meanwhile, the fraction of discharge released during the freshet as a percentage of annual decreased by approximately 1.7% (Figure 11), while winter and fall proportions increased. A distinct shift towards earlier melt timing was also indicated by a strong decrease (5.8%) in proportional summer discharge countered by a corresponding increase (2.5%) in spring discharge.

Individually, trends in fraction of flow released seasonally agree with overall trends in circumpolar flow. Individual rivers show varying decreases in fraction of flow released during the freshet, coupled with increases in winter, spring and fall fractions and decreases in summer fractions. The only exception to this general tendency is seen in the Ob River, which indicates a decrease in winter and a slight increase in summer proportional flow. These deviations are not substantial enough to overcome the combined trends of all four rivers. Pulse onset dates occurred earlier, while freshet durations increased slightly and peak freshet magnitudes generally decreased. Rising winter and fall discharge proportions, combined with lower peak freshet

magnitudes, increased freshet durations, and lower summer proportions are indicative of a potential shift to a flatter, more gradual annual hydrograph with an earlier pulse onset. While this apparent shift in seasonality can clearly have important consequences to Arctic and global feedback systems, it remains yet to be determined whether these changes can be attributed to flow regulation or are climatic in nature. Despite the recent window of observation used for combined flow, many basins have had some form of flow regulation in place for extended periods, and the establishment of such regulation will likely have impacts on the longer-term records. In addition, studying trends over large, continental-scale basins will obscure any effects of regional climatic variation on smaller-sized basins. It is thus recommended to undertake an analysis of trends and climatic drivers on a sub-basin level to determine potential causes of shifting seasonality in Arctic freshwater influx.

3.6 Acknowledgements

This work was partially supported by a Discovery Grant and ArcticNet funding from the Natural Sciences and Engineering Council of Canada (NSERC) to one of the co-authors. The authors would also like to acknowledge the Arctic Rapid Integrated Monitoring System (ArcticRIMS) and the Regional Hydrometeorological Data Network for the Pan-Arctic Region (R-ArcticNet) for freely providing data.

References

Aagaard, K., Carmack, E.C., 1989. The role of fresh water in ocean circulation and climate. J. Geophys. Res. 94, 14,485–14,498.

Ahmed, R., Prowse, T.D., Dibike, Y.B., Bonsal, B.R., 2012. Temporal sequencing of annual spring runoff in major Arctic-draining rivers. In: Poster Session Presented at: American Geophysical Union Fall Meeting 2012. Dec. 3-7, 2012. San Francisco, CA.

Anisimov, O., Fitzharris, B., Hagen, J.O., Jefferies, R., Marchant, H., Nelson, F., Prowse, T.D., Vaughan, D.G., 2001. Polar regions (Arctic and Antarctic). In: McCarthy, J.J., Canziani, O.F., Leary, N.A., Dokken, D.J., White, K.S. (Eds.), Climate Change 2001: Impacts, Adaptation and Vulnerability. Contribution of Working Group II to the Third Assessment Report of the Intergovernmental Panel on Climate Change. Cambridge University Press, Cambridge, pp. 803–841.

Anisimov, O., Vaughan, D.G., Callaghan, T., Furgal, C., Marchant, H., Prowse, T.D., Vilhjalmsson, H., Walsh, J.E., 2007. Polar regions (Arctic and Antarctic). In: Parry, M.L., Canziani, O.F., Palutikof, J.P., van der Linden, P.J., Hanson, C.E. (Eds.), Climate Change 2007: Impacts, Adaptation and Vulnerability. Contribution of Working Group II to the Fourth Assessment Report of the Intergovernmental Panel on Climate Change. Cambridge University Press, Cambridge, pp. 653–685.

Burn, D.H., Cunderlik, J.M., 2004. Hydrological trends and variability in the Liard River basin. Hydrol. Sci. 49, 53–67.

Carmack, E.C., 2000. The freshwater budget of the Arctic Ocean: Sources, storage and sinks. In: Lewis, E.L. (Ed.), The Freshwater Budget of the Arctic Ocean. Kluwer, Dordrecht, Netherlands, pp. 91–126.

Carmack, E.C., Barber, D.G., Christensen, J.R., Macdonald, R.W., Rudels, B., Sakshaug, E., 2006. Climate variability and physical forcing of the food webs and the carbon budget of pan-Arctic shelves. Prog. Oceanogr. 71, 145–181.

Cayan, D.R., Kammerdiener, S.A., Dettinger, M.D., Caprio, J.M., Peterson, D.H., 2001. Changes in the Onset of Spring in the Western United States. Bull. Am. Meteorol. Soc. 82, 399–415.

Déry, S.J., 2005. Decreasing river discharge in northern Canada. Geophys. Res. Lett. 32, L10401.

Dickson, B., Osborn, T., Hurrell, J.W., Meincke, J., Blindheim, J., Adlandsvik, B., Vinje, T., Alekseev, G., Maslowski, W., 2000. The Arctic Ocean response to the North Atlantic Oscillation. J. Clim. 13, 2671–2696.

Dickson, B., Yashayaev, I., Meincke, J., Turrell, B., Dye, S., Holfort, J., 2002. Rapid freshening of the deep North Atlantic Ocean over the past four decades. Nature 416, 832–7.

Dynesius, M., Nilsso, C., 1994. Fragmentation and flow regulation of river systems in the northern third of the world. Science (80-.). 266, 753–762.

Dyurgerov, M.B., Carter, C.L., 2004. Observational Evidence of Increases in Freshwater Inflow to the Arctic Ocean. Arctic, Antarct. Alp. Res. 36, 117–122.

Finnis, J., Cassano, J., Holland, M., Uotila, P., 2009. Synoptically forced hydroclimatology of major Arctic watersheds in general circulation models, Part 1 : the Mackenzie River Basin. Int. J. Climatol. 29, 1226–1243.

Grabs, W.E., Portmann, F., De Couet, T., 2000. Discharge observation networks in Arctic regions: Computation of the river runoff into the Arctic Ocean, its seasonality and variability. In: Lewis, E.L. (Ed.), The Freshwater Budget of the Arctic Ocean. Kluwer, Dordrecht, Netherlands, pp. 249–267.

Hirsch, R.M., Slack, J.R., 1984. A non-parametric trend test for seasonal data with serial dependence. Water Resour. Res. 20, 727–732.

Kane, D.L., 1997. The impact of Arctic hydrologic perturbations on Arctic ecosystems induced by climate change. In: Oechel, W.C., Callaghan, T., Gilmanov, T.G., Holten, J.I., Maxwell, B., Molau, U., Sveinbjornsson, B. (Eds.), Global Change and Arctic Terrestrial Ecosystems. Springer-Verlag, New York, pp. 63–81.

Kattsov, V.M., Walsh, J.E., Chapman, W.L., Govorkova, V. a., Pavlova, T. V., Zhang, X., 2007. Simulation and Projection of Arctic Freshwater Budget Components by the IPCC AR4 Global Climate Models. J. Hydrometeorol. 8, 571–589.

Kendall, M., 1975. Rank Correlation Measures. Charles Griffin, London, UK.

Lammers, R.B., Shiklomanov, A.I., 2013. A Regional, Hydrometeorological Data Network for Russia. Available online at http://www.r-arcticnet.sr.unh.edu/v4.0/index.html.

Lammers, R.B., Shiklomanov, A.I., Vörösmarty, C.J., Fekete, B.M., Peterson, B.J., 2001. Assessment of contemporary Arctic river runoff based on observational discharge records. J. Geophys. Res. 106, 3321–3334.

Larsen, J.N., Anisimov, O.A., Constable, A., Hollowed, A.B., Maynard, N., Prestrud, P., Prowse, T.D., Stone, J.M.R., 2014. Polar regions. In: Barros, V.R., Field, C.B., Dokken, D.J., Mastrandrea, M.D., Mach, K.J., Bilir, T.E., Chatterjee, M., Ebi, K.L., Estrada, Y.O., Genova, R.C., Girma, B., Kissel, E.S., Levy, A.N., MacCracken, S., Mastrandrea, P.R., White, L.L. (Eds.), Climate Change 2014: Impacts, Adaptation, and Vulnerability. Part B: Regional Aspects. Contribution of Working Group II to the Fifth Assessment Report of the Intergovernmental Panel of Climate Change. Cambridge University Press, Cambridge, United Kingdom and New York, NY, USA, pp. 1567–1612.

Loeng, H., Brander, K., Carmack, E., Denisenko, S., Drinkwater, K., Hansen, B., Kovacs, K., Livingston, P., Mclaughlin, F., Bellerby, R., Browman, H., Furevik, T., Grebmeier, J.M., Jansen, E., Jónsson, S., Jørgensen, L.L., 2005. Ch. 9: Marine Systems. In: Symon, C., Arris, L., Heal, B. (Eds.), Arctic Climate Impact Assessment. Cambridge University Press, New York, pp. 453–538.

Mann, H.B., 1945. Nonparametric tests against trend. Econom. J. Econom. Soc. 13, 245–259.

McClelland, J.W., Holmes, R.M., Dunton, K.H., Macdonald, R.W., 2011. The Arctic Ocean Estuary. Estuaries and Coasts 35, 353–368.

Peterson, B.J., Holmes, R.M., McClelland, J.W., Vörösmarty, C.J., Lammers, R.B., Shiklomanov, A.I., Shiklomanov, I.A., Rahmstorf, S., 2002. Increasing river discharge to the Arctic Ocean. Science (80-.). 298, 2171–2173.

Proshutinsky, A., Bourke, R.H., McLaughlin, F.A., 2002. The role of the Beaufort Gyre in Arctic climate variability: Seasonal to decadal climate scales. Geophys. Res. Lett. 29, 15–1– 15–4.

Prowse, T.D., Flegg, P.O., 2000. Arctic river flow: A review of contributing areas. In: Lewis, E.L. (Ed.), The Freshwater Budget of the Arctic Ocean. Kluwer, Dordrecht, Netherlands, pp. 269–280.

Serreze, M.C., Barrett, A.P., Slater, A.G., Woodgate, R.A., Aagaard, K., Lammers, R.B., Steele, M., Moritz, R., Meredith, M., Lee, C.M., 2006. The large-scale freshwater cycle of the Arctic. J. Geophys. Res. 111, C11010.

Serreze, M.C., Francis, J.A., 2006. The Arctic Amplification Debate. Clim. Change 76, 241–264.

Stewart, I., Cayan, D., Dettinger, M., 2005. Changes toward earlier streamflow timing across western North America. J. Clim. 18, 1136–1155.

Stuefer, S., Yang, D., Shiklomanov, A., 2011. Effect of streamflow regulation on mean annual discharge variability of the Yenisei River. In: Cold Region Hydrology in a Changing Climate (Proceedings of Symposium H02 Held during IUGG2011 in Melbourne, Australia, July 2011). IAHS Publ. 346, pp. 27–32.

Tank, S.E., Manizza, M., Holmes, R.M., McClelland, J.W., Peterson, B.J., 2011. The processing and impact of dissolved riverine nitrogen in the Arctic Ocean. Estuaries and Coasts 35, 401–415.

Walsh, J.E., Anisimov, O., Hagen, J.O., Jakobsson, T., Oerlemans, J., Prowse, T.D., Romanovsky, V., Savelieva, N., Serreze, M.C., Shiklomanov, I.A., Solomon, S., 2005. Cryosphere and hydrology. In: Symon, C., Arris, L., Heal, B. (Eds.), Arctic Climate Impact Assessment (ACIA). Cambridge University Press, Cambridge, pp. 183–242.

Woo, M., Thorne, R., 2003. Streamflow in the Mackenzie basin, Canada. Arctic 56, 328–340.

Yang, D., Kane, D.L., Hinzman, L.D., Zhang, X., Zhang, T., Ye, H., 2002. Siberian Lena River hydrologic regime and recent change. J. Geophys. Res. 107, 4694.

Yang, D., Ye, B., Kane, D.L., 2004a. Streamflow changes over Siberian Yenisei River Basin. J. Hydrol. 296, 59–80.

Yang, D., Ye, B., Shiklomanov, A., 2004b. Discharge characteristics and changes over the Ob River watershed in Siberia. J. Hydrometeorol. 5, 595–610.

Ye, B., Yang, D., Kane, D.L., 2003. Changes in Lena River streamflow hydrology: Human impacts versus natural variations. Water Resour. Res. 39, 1200.

Yue, S., Pilon, P.J., Phinney, B., Cavadias, G., 2002. The influence of autocorrelation on the ability to detect trend in hydrological series. Hydrol. Process. 16, 1807–1829.

Zhang, X., Ikeda, M., Walsh, J., 2003. Arctic sea ice and freshwater changes driven by the atmospheric leading mode in a coupled sea ice-ocean model. J. Clim. 16, 2159–2177.

List of Tables

Table 1. Characteristics of outlet stations as labeled in Figure 1. *Note: Yenisei station is missing complete records in the years 1963-1965, 1968-1974, and 1977-1979. Records are not infilled.

Basin	ID	Name	Location (°N, °E)	Area (km^2)	Avail. Years
Mackenzie	10LC014	Mackenzie R. at Arctic Red R.	67.5, -133.8	1679100	1973-2009
Lena	3821	Lena at Kusur	56.8, -111.4	132585	1936-2009
Yenisei	9803	Yenisei at Igarka	55.7, -117.6	50300	1936-2009*
Ob	11801	Ob at Salekhard	59.1, -112.4	293000	1936-2009

Table 2. Metrics used to describe freshet characteristics.

Symbol	Description
F_P	Freshet pulse date
F_L	Freshet length
F_M	Peak freshet magnitude
V_1	April – July volume
V_2	Freshet volume
V_{APR}	April volume
V_{MAY}	May volume
V_{JUN}	June volume
V_{JUL}	July volume
V_{ANN}	Annual volume
V_{DJF}	December - February volume
V_{MAM}	March - May volume
V_{JJA}	June - August volume
V_{SON}	September - November volume

Table 3. Average proportional percentage contribution to total MOLY flow volume per river for different timing measures, 1980 – 2009

River	V_1 %	V_2 %	V_{APR} %	V_{MAY} %	V_{JUN} %	V_{JUL} %
Mackenzie	14	13	19	20	10	15
Lena	31	35	11	15	37	37
Yenisei	35	32	48	43	37	22
Ob	20	20	22	22	16	26

Table 4. Trends in various flow characteristics for MOLY outlet stations. Negative time values indicate trends toward earlier dates and vice versa. * denotes trend is significant at the 10% level and ** denotes trend is significant at the 5% level.

	Entire Period Trend					30-year Trend (1980-2009)				
	F_P	F_L	F_M	V_1	V_{ANN}	F_P	F_L	F_M	V_1	V_{ANN}
	d/10yr	d/10yr	m^3s^{-1}/10yr	km^3/10yr	km^3/10yr	d/10yr	d/10yr	m^3s^{-1}/10yr	km^3/10yr	km^3/10yr
Mackenzie	-1.2*	0.0	-767	0.0	9.0	-1.4	0.8	0	5.1**	21.5**
Ob	0.0	-0.7**	-123	0.0	5.4	0.0	0.8	290	5.3**	10.3
Lena	-1.4**	0.0	-622	3.5	28.8**	-0.9	2.4	-2000	18.9**	40.6**
Yenisei	--	--	--	--	--	-1.6	1.7	-1600	4.0	23.7**

Table 5. Trends in fraction of flow released during different seasons for MOLY outlet stations. Negative values indicate trends toward lower percentages and vice versa. * denotes trend is significant at the 10% level and ** denotes trend is significant at the 5% level.

	Entire Period Trend [% Change]					30-year Trend (1980-2009) [% Change]				
	V_2	*DJF*	*MAM*	*JJA*	*SON*	V_2	*DJF*	*MAM*	*JJA*	*SON*
Mackenzie	-0.8	1.5**	2.6	-4.3	0.7	-0.6	1.3	2.2	-3.4**	0.8
Ob	0.3	2.2**	2.7	-3.6*	-0.7	-1.2	-1.4	0.8	0.3	1.4
Lena	-1.6	2.0**	3.8**	-7.1**	-0.1	-2.7	0.5	2.5	-8.3	7.5**
Yenisei	--	--	--	--	--	-2.0	2.8**	4.3	-6.0*	2.1

List of Figures

Figure 6. Time versus percentage of flow released during winter (DJF), shown with trends and p-values for entire length of record (solid red line) and 1980-2009 (dashed red line). Percentage changes for different periods are given in Table 5.

Figure 7. Time versus percentage of flow released during spring (MAM), shown with trends and p-values for entire length of record (solid red line) and 1980-2009 (dashed red line). Percentage changes for different periods are given in Table 5.

Figure 8. Time versus percentage of flow released during summer (JJA), shown with trends and p-values for entire length of record (solid red line) and 1980-2009 (dashed red line). Percentage changes for different periods are given in Table 5.

Figure 9. Time versus percentage of flow released during autumn (SON), shown with trends and p-values for entire length of record (solid red line) and 1980-2009 (dashed red line). Percentage changes for different periods are given in Table 5.

Figure 10. Trend in MOLY total freshwater volume contribution to the Arctic Ocean during A) annually, B) during V1 and V2 freshet definitions, and C) seasonally for the period 1980 – 2009. Solid, unmarked lines denote trend, with change per decade and p-values given.

Figure 11. Time versus percentage of MOLY combined flow released during certain timing measures, shown with trends and p-values for 1980-2009.

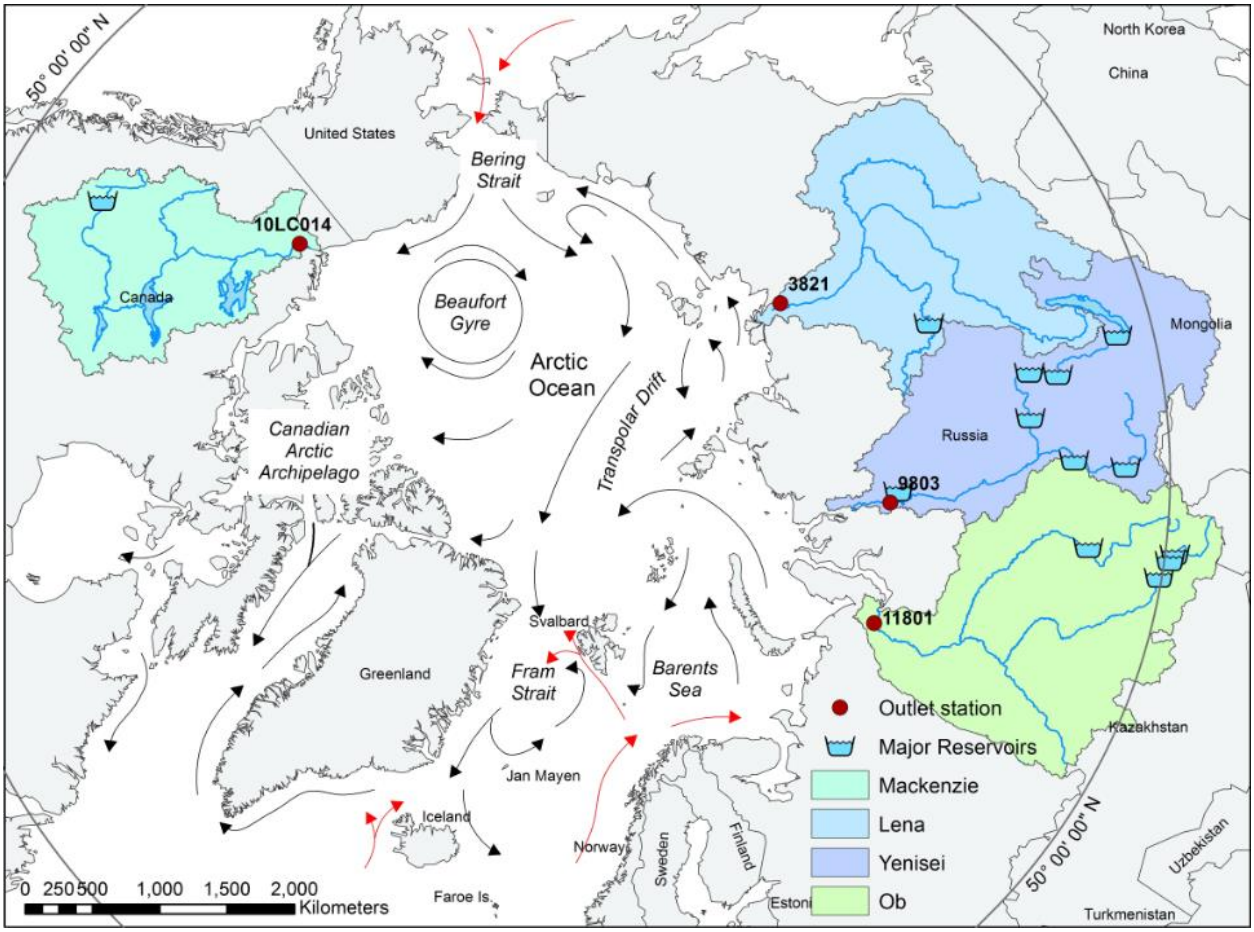

Figure 1. Map showing the Arctic Ocean, ocean features, major surface currents, major reservoirs and drainage basins and outlet stations of the Mackenzie, Ob, Yenisei and Lena rivers. Red arrows denote warmer currents, while black arrows denote colder currents. Adapted from Figure 6 in McClelland et al. (2011).

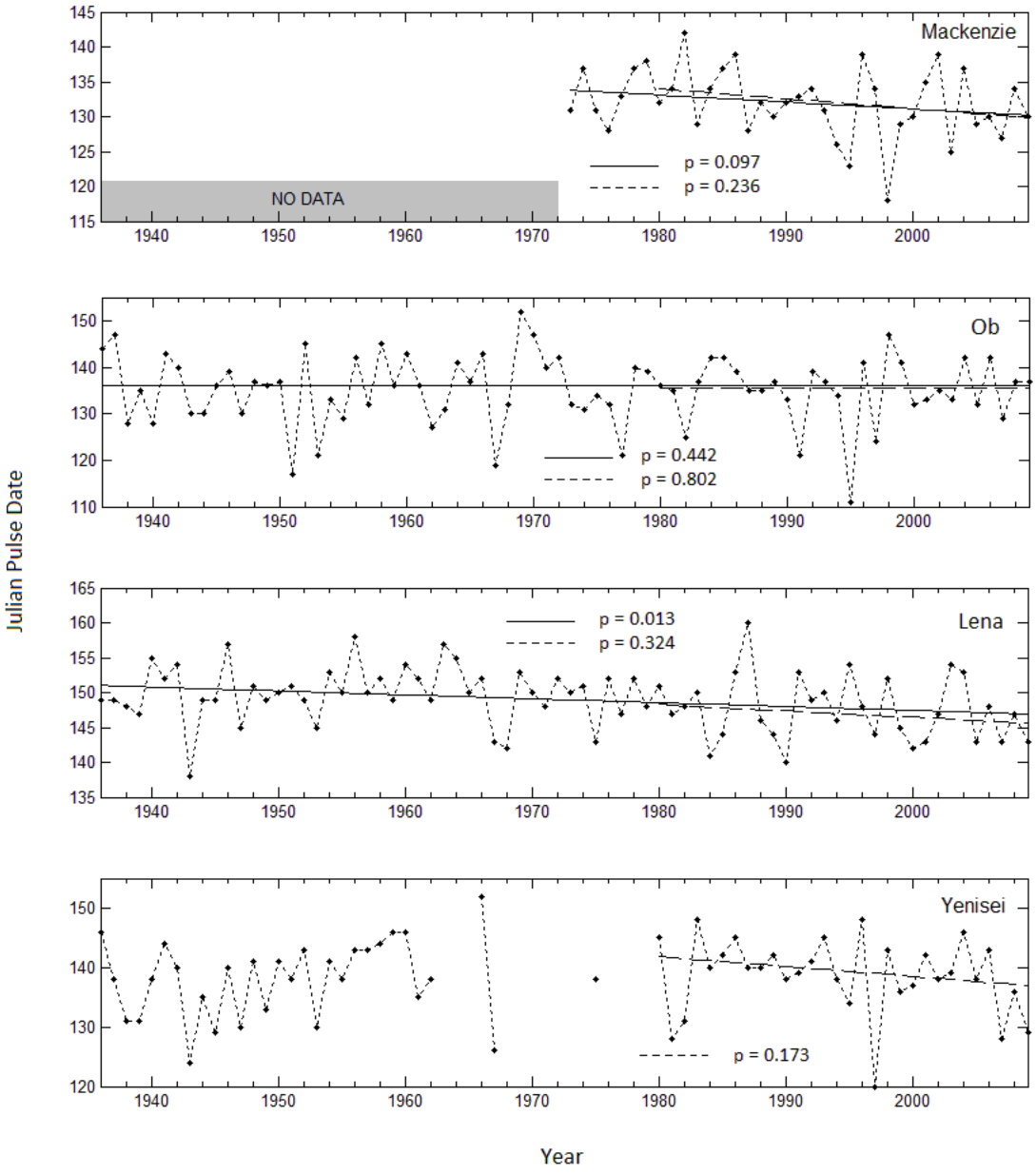

Figure 2. Trends in pulse dates with p-values for 1980 – 2009 and the entire available length of record. Only 1980 – 2009 trends are given for the Yenisei station due to missing data from 1969 – 1979; Mackenzie station trends are calculated for continuous data from 1973 – 2009 due to missing data prior to 1973. Black markers denote observed time series values connected with a dotted line, with the thick solid line indicating the longer record trend line and the dashed line indicating the 30 year trend line.

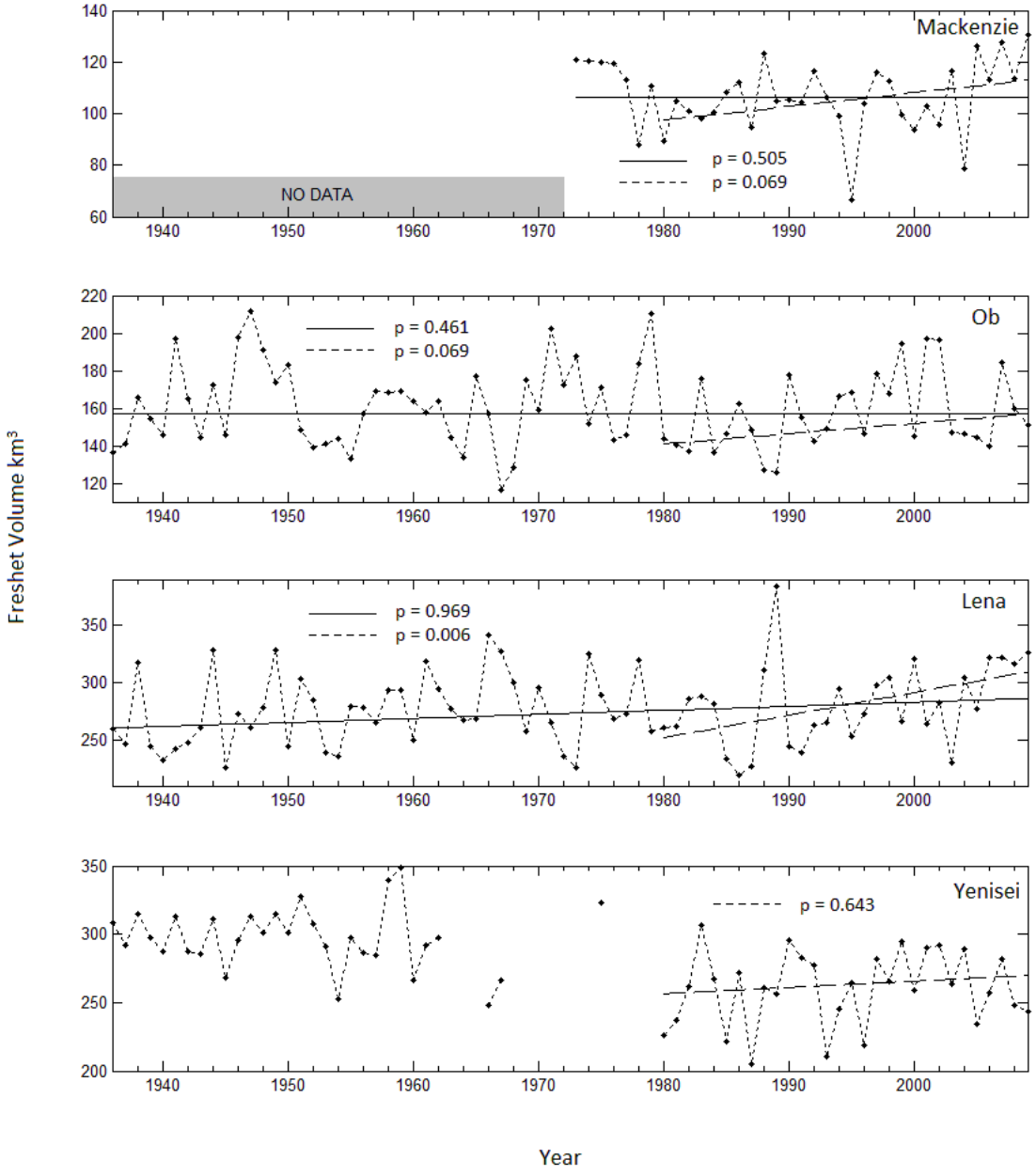

Figure 3. Trends in freshet volume (V_2) with p-values for 1980 – 2009 and the entire available length of record. Only 1980 – 2009 trends are given for the Yenisei station due to missing data from 1969 – 1979; Mackenzie station trends are calculated for continuous data from 1973 – 2009 due to missing data prior to 1973. Black markers denote observed time series values connected with a dotted line, with the thick solid line indicating the longer record trend line and the dashed line indicating the 30 year trend line.

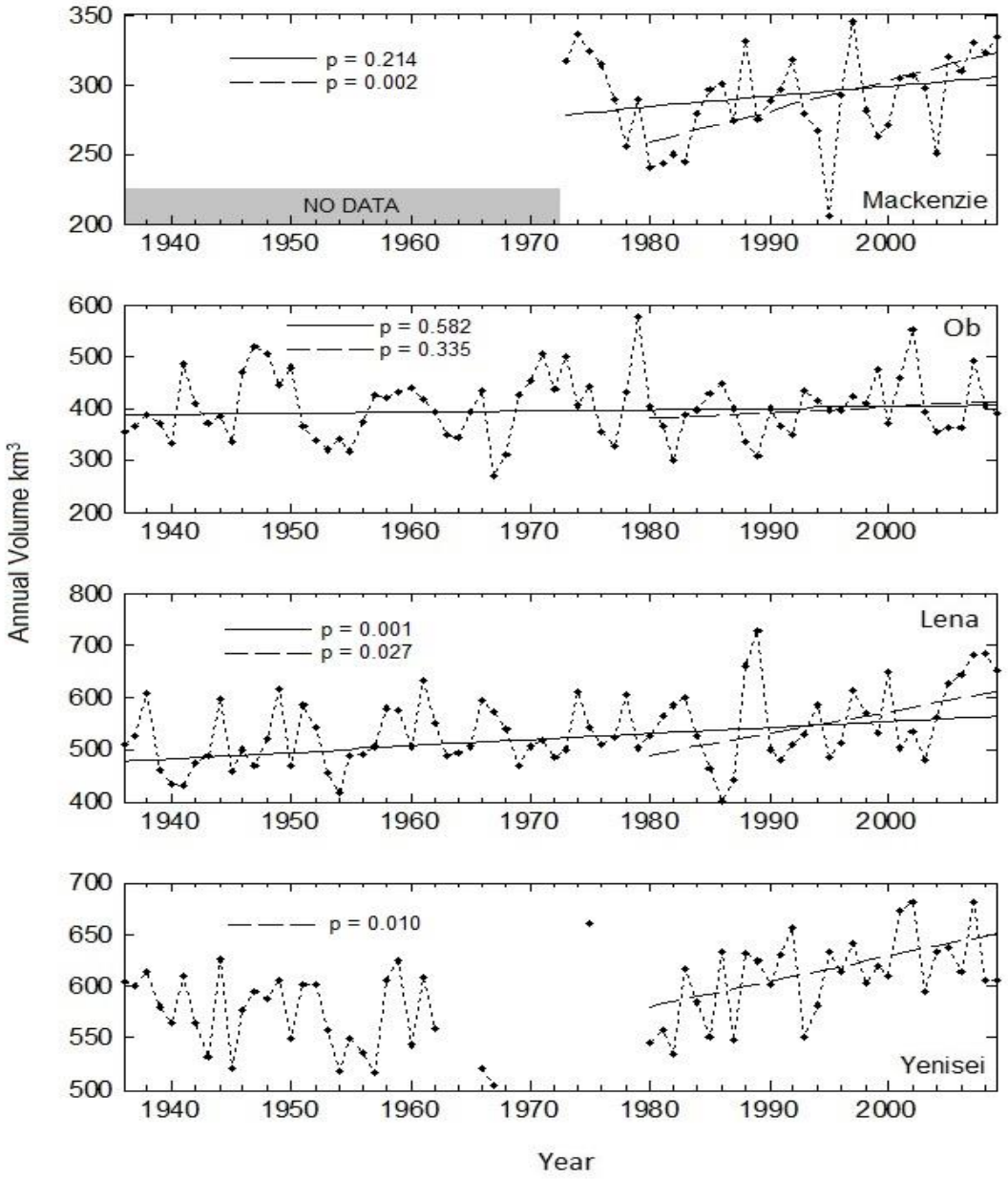

Figure 4. Trends in annual volume with p-values for 1980 – 2009 and the entire available length of record. Only 1980 – 2009 trends are given for the Yenisei station due to missing data from 1969 – 1979; Mackenzie station trends are calculated for continuous data from 1973 – 2009 due to missing data prior to 1973. Black markers denote observed time series values connected with a dotted line, with the thick solid line indicating the longer record trend line and the dashed line indicating the 30 year trend line.

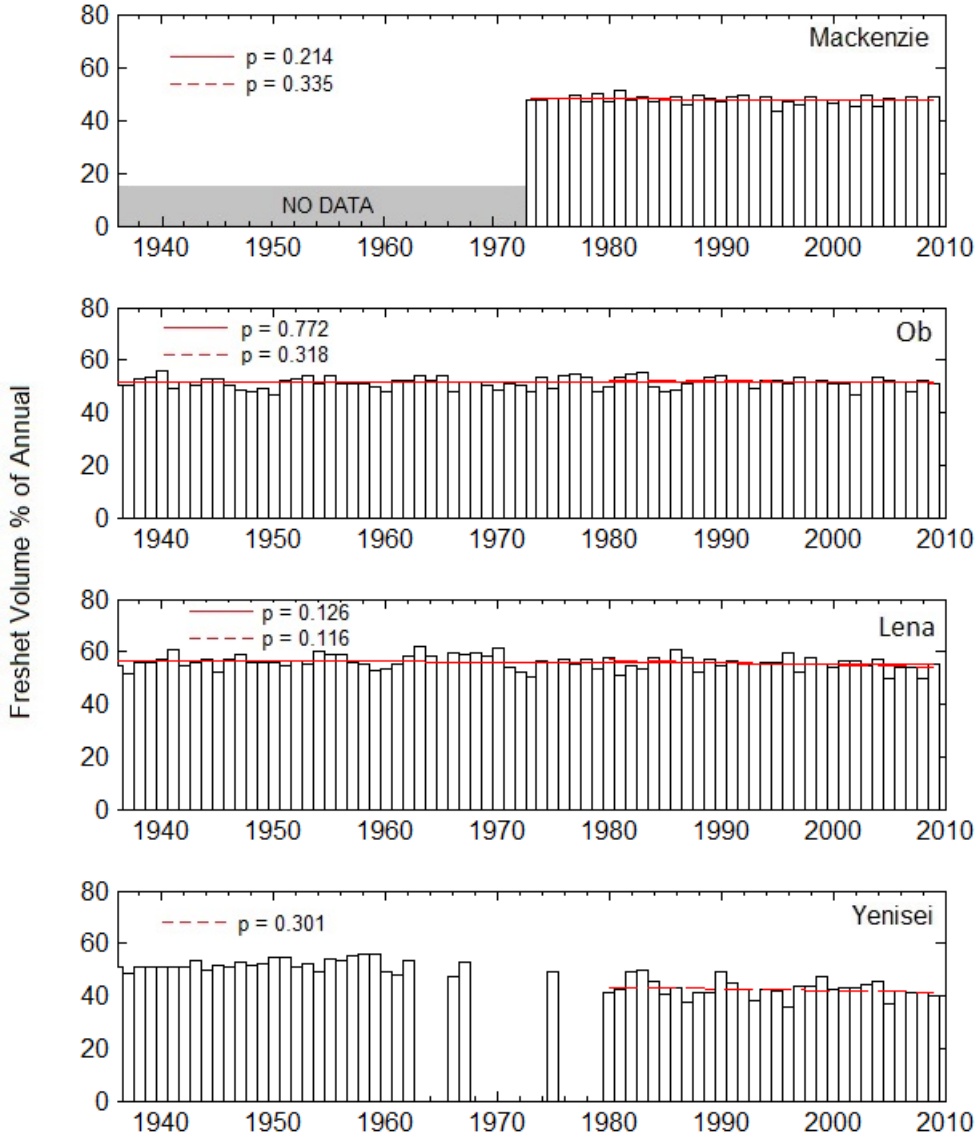

Figure 5. Time versus percentage of flow released during spring freshet (V_2 definition), shown with trends and p-values for entire length of record (solid red line) and 1980-2009 (dashed red line). Percentage changes for different periods are given in Table 5.

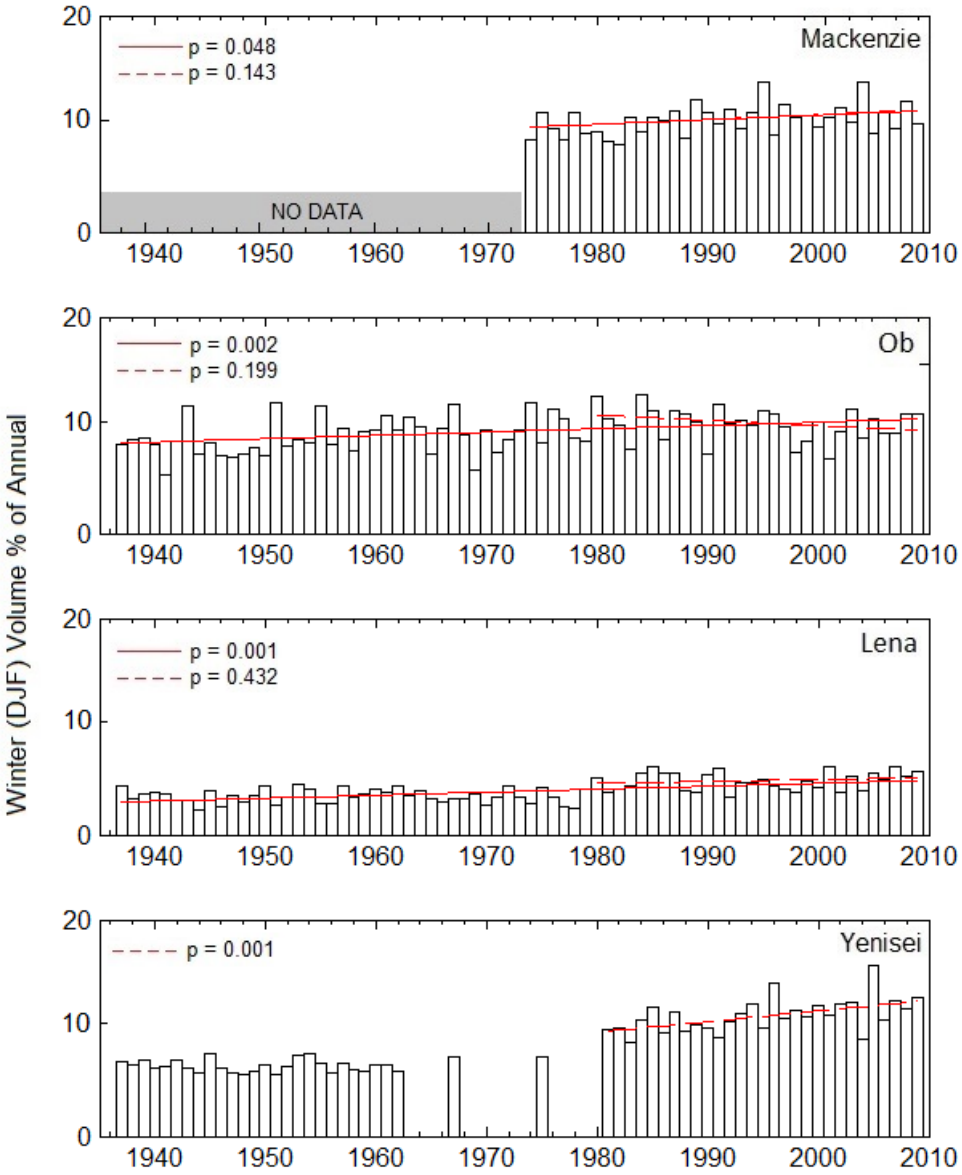

Figure 6. Time versus percentage of flow released during winter (DJF), shown with trends and p-values for entire length of record (solid red line) and 1980-2009 (dashed red line). Percentage changes for different periods are given in Table 5.

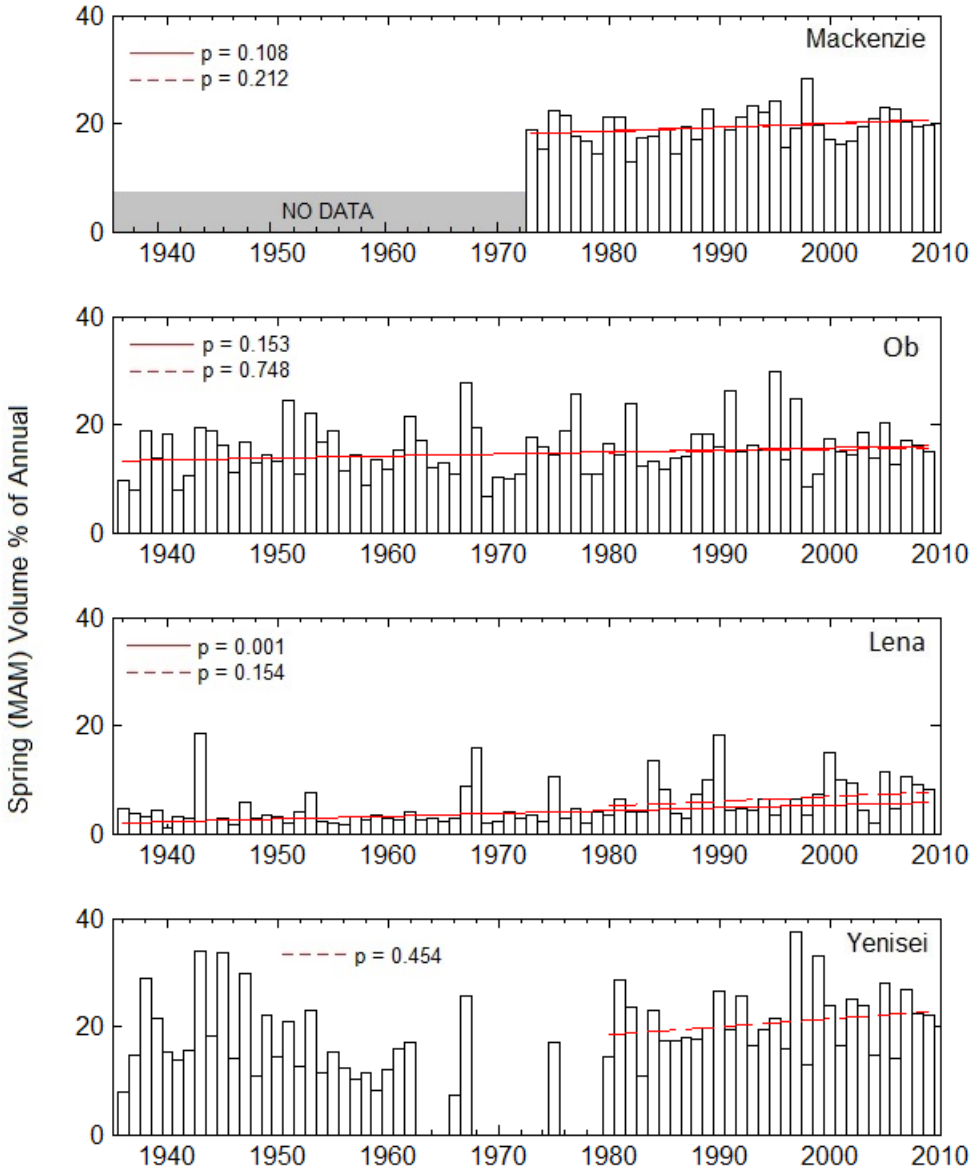

Figure 7. Time versus percentage of flow released during spring (MAM), shown with trends and p-values for entire length of record (solid red line) and 1980-2009 (dashed red line). Percentage changes for different periods are given in Table 5.

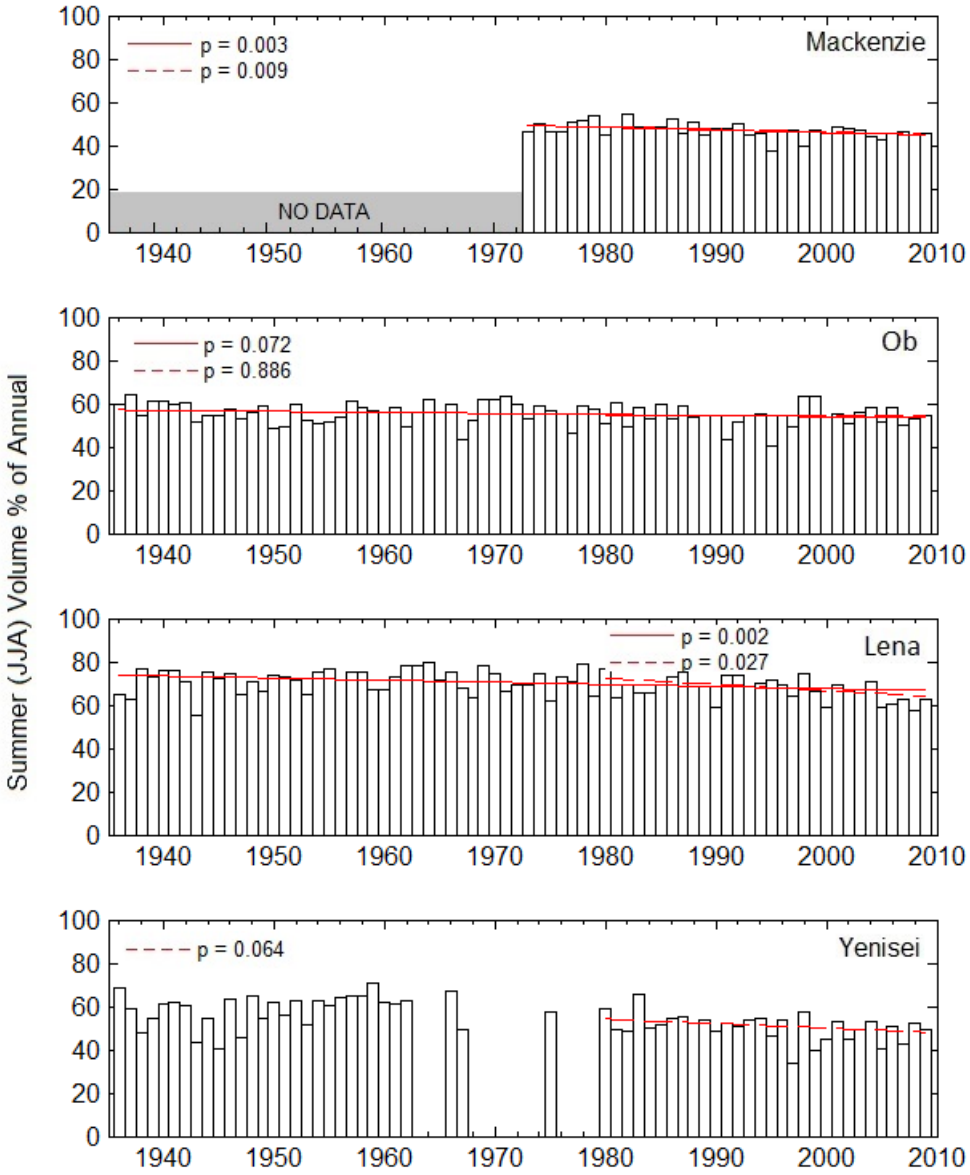

Figure 8. Time versus percentage of flow released during summer (JJA), shown with trends and p-values for entire length of record (solid red line) and 1980-2009 (dashed red line). Percentage changes for different periods are given in Table 5.

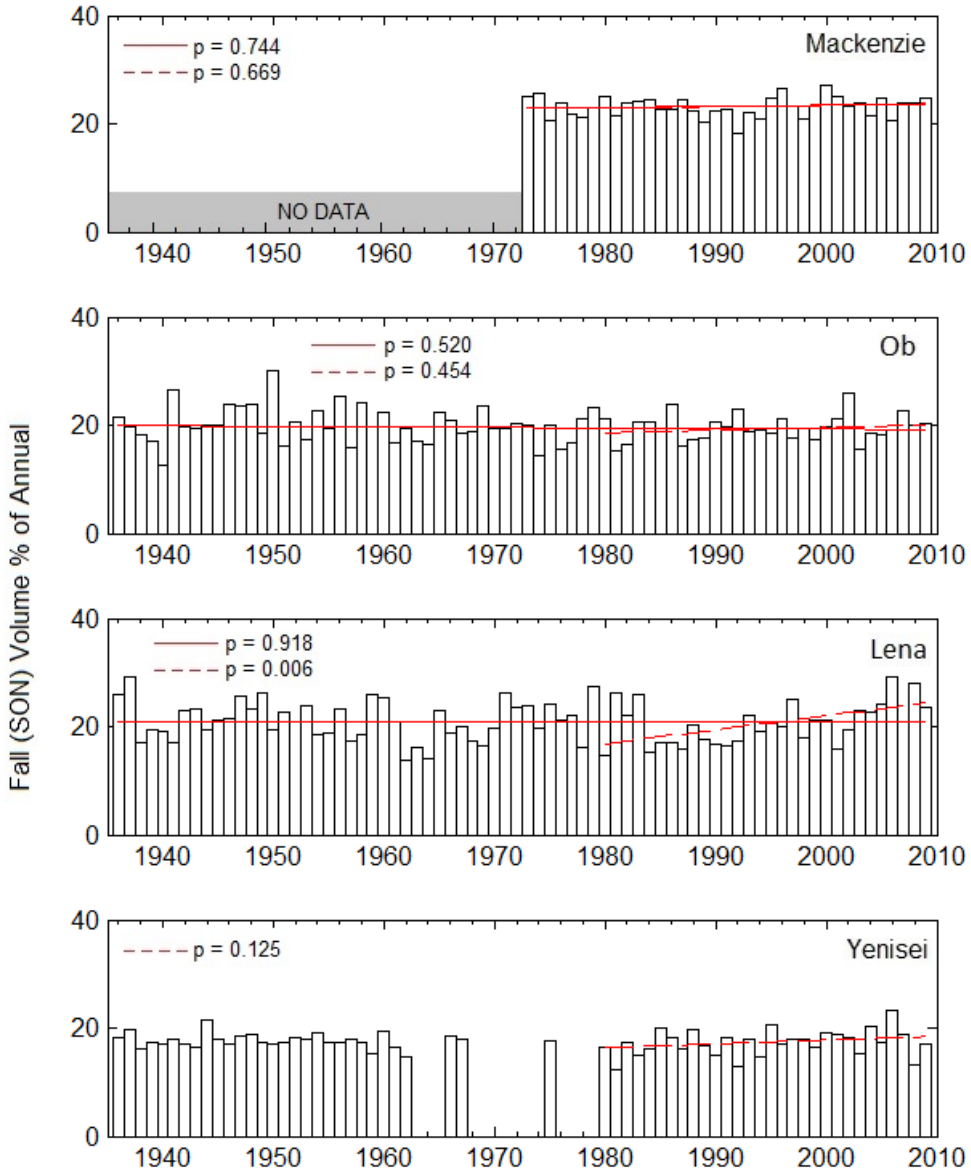

Figure 9. Time versus percentage of flow released during autumn (SON), shown with trends and p-values for entire length of record (solid red line) and 1980-2009 (dashed red line). Percentage changes for different periods are given in Table 5.

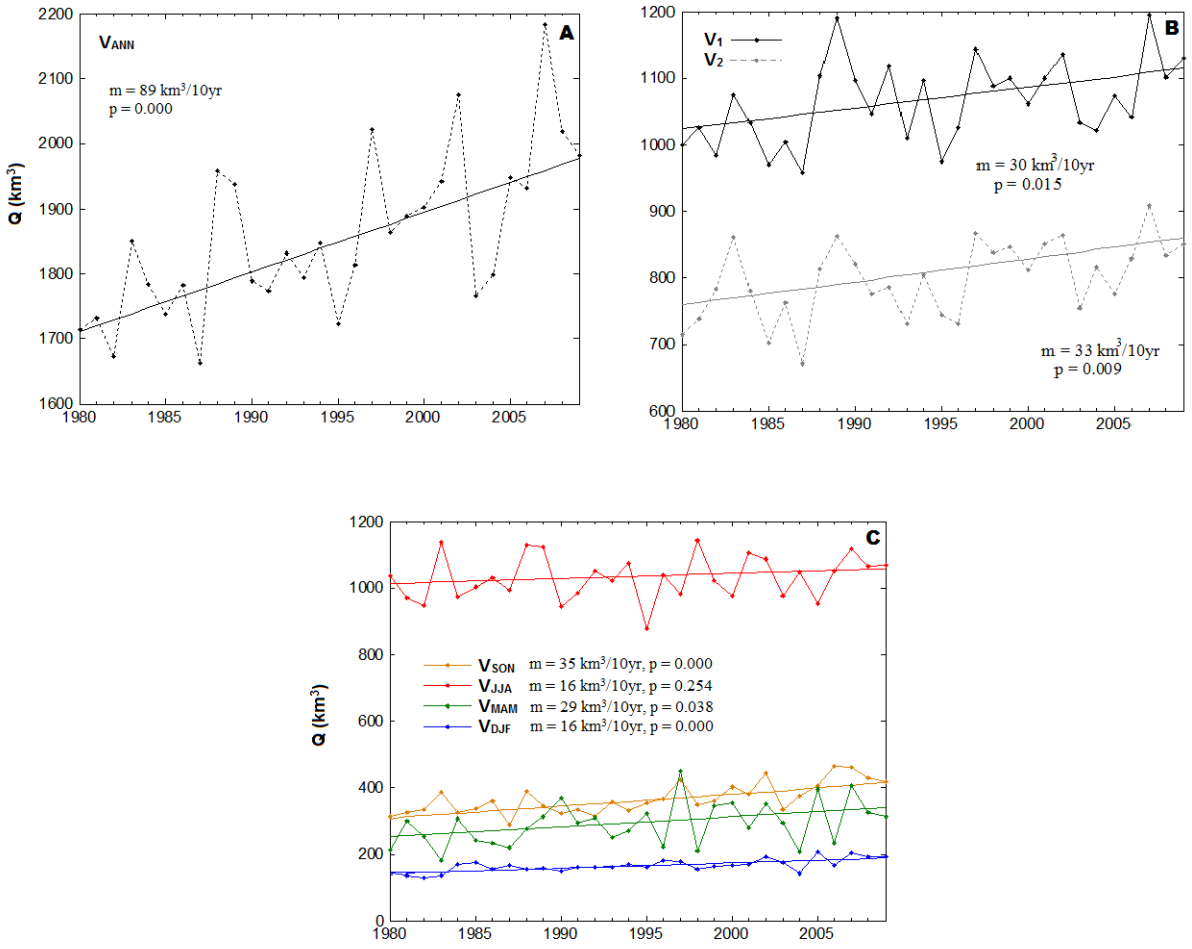

Figure 10. Trends in MOLY total freshwater volume contribution to the Arctic Ocean during A) annually, B) during V_1 and V_2 freshet definitions, and C) seasonally for the period 1980 – 2009. Solid, unmarked lines denote trends, with changes per decade and p-values given.

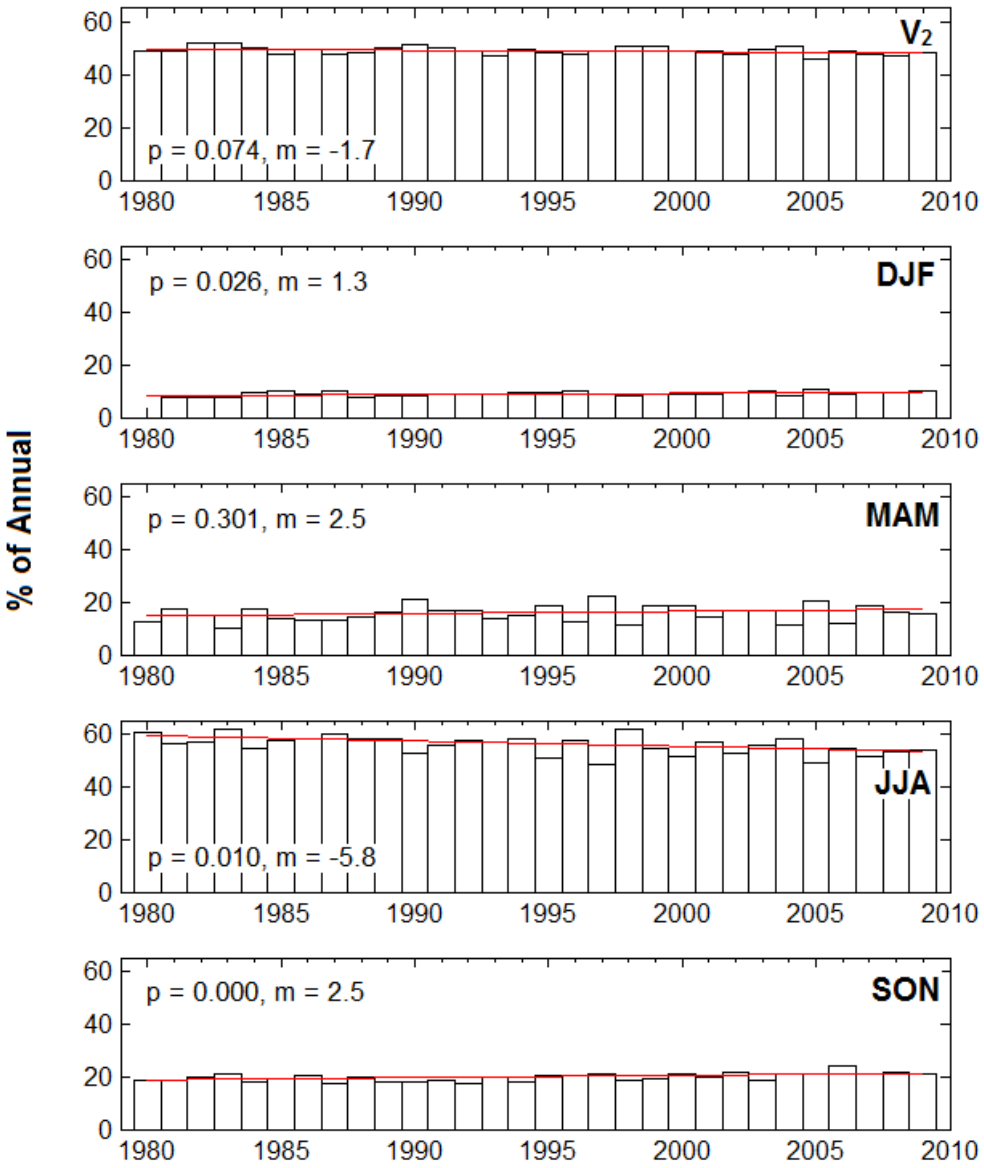

Figure 11. Time versus percentage of MOLY combined flow released during certain timing measures, shown with trends and p-values for 1980-2009.

CHAPTER 4: COMPARISON OF OUTLET AND SUB-BASIN HYDROGRAPHS FOR FOUR MAJOR ARCTIC-DRAINING RIVERS

Abstract

Warming in the Arctic has significant impacts on global climate through its positive feedbacks to the global climate system. One such potential impact is an increase in terrestrial freshwater influx from Arctic-draining rivers, which are a major source of freshwater input to the Arctic Ocean and have the potential to influence global climate through modification of the intensity of the thermohaline circulation. In these nival-dominated river systems, the majority of annual discharge is released during the spring freshet.

Using historic daily discharge data, this study determines spring freshet characteristics for sub-basins located within the four largest Arctic-draining watersheds (Mackenzie, Ob, Lena and Yenisei). Results of a previous study showed an observed change in discharge seasonality at the outlets of these rivers, marked by increasing cold-season flows, earlier pulse dates and a lower fraction of flow released during the spring freshet. By observing trends and hydrograph characteristics of sub-basins, separated by regional topography and regulation classification, it is determined that sub-basin flows match the general pattern of outlet discharge, with some regional variation. Importantly, the majority of significant trends are observed in stations with no upstream impoundment signal. Stations with a strong regulation signal do not display any significant relationships with freshet volume at the outlets, although regulation does not seem to suppress the relationship of outlet flows with short-term maximum spring peaks generated by high-relief terrain. It remains uncertain whether flow regulation removes the regional effect of hydro-climatic drivers, and how this translates to observed changes at the outlets.

Keywords: Arctic, hydrological trends, spring freshet, hydro-climatology, regulation

4.1 Introduction

The Arctic Ocean is largely an enclosed system, receiving freshwater from three main sources: continental river runoff, direct precipitation on the ocean surface, and import of lower-salinity Pacific waters through Bering Strait (Aagaard and Carmack, 1989; Carmack, 2000; Serreze et al., 2006). Other terrestrial and marine sources provide a minor contribution. Of these, river runoff comprises the greatest freshwater influx, providing as much as 50% or more compared to other sources based on varying definitions of Arctic Ocean contributing area (Prowse and Flegg, 2000). Consequently, freshwater distribution and storage in the ocean is particularly sensitive to river discharge, particularly since the Arctic Ocean receives ~11% of global river discharge while occupying only ~1% of global ocean volume (Aagaard and Carmack, 1989; Shiklomanov, 1998). This is an important consideration since stratification in the cold upper ocean is predominantly controlled by salinity, rather than temperature (Carmack et al., 2008). The largest contributing Arctic watersheds are the Mackenzie Basin in Canada, and the Ob, Lena and Yenisei river basins in Eurasia. Combined, these four rivers contribute almost 1900 km^3 of freshwater to the Arctic Ocean per year, or about 60% of annual flow volume from all Arctic contributing areas (Grabs et al., 2000; Prowse and Flegg, 2000a).

Stratification affecting freshwater export from the Arctic Ocean through the northern North Atlantic Ocean is an integral part of the global ocean circulation regime. A perturbation in the stratification of surface waters can have effects on North Atlantic Deep Water (NADW) formation; this phenomenon, coupled with Atlantic Meridional Overturning Circulation (AMOC), is a critical driving force in the global thermohaline circulation (e.g., Aagaard and Carmack, 1989; Anisimov et al., 2001; Dickson et al., 2000, 2002; Proshutinsky et al., 2002; Loeng et al., 2005; Serreze et al., 2006). In major Arctic-draining rivers, the annual spring

freshet following snowmelt and river ice break-up period provides as much as 60% of total annual flow volume and is a major hydrologic event (Lammers et al., 2001). Seasonality and magnitude of this event play a role in the processes which govern freshwater storage and circulation in the Arctic Ocean. For example, discharge seasonality can affect freshwater runoff trajectory upon entering the Arctic Ocean, influencing whether freshwater is placed into storage or released, and in turn, linking Arctic spring river discharge with oceanic heat transport to northern latitudes.

There are numerous other consequences to spring discharge. Runoff is a major nutrient supplier to near shore and estuarine ecosystems, providing an influx of organic carbon during the spring freshet, yet diluting waters with respect to inorganic nitrate and silica compounds (Kattsov et al., 2007; McClelland et al., 2011; Tank et al., 2011). Arctic aquatic ecosystems benefit from vertical transport of nutrient rich deep waters that occurs in overturning circulation (Toggweiler and Key, 2001). Riparian zones are affected by the frequency and severity of the spring flood, and while flooding is often portrayed in a negative context (e.g., Jasek, 2003; Shiklomanov et al., 2007), it has been shown that spring flooding is an important recharge mechanism for perched basins hydraulically separated from main flow channels (e.g., Marsh and Hey, 1989; Prowse and Conly, 1998). Indirectly, a change in the freshwater balance, possibly due to river discharge, can have effects on the cold halocline layer which acts to insulate the Arctic sea-ice cover from warmer, saltier waters below (Steele and Boyd, 1998). Furthermore, large rivers such as the Mackenzie, Ob, Lena or Yenisei, transport an immense amount of heat from their respective continental watersheds to the Arctic Ocean, particularly during the spring freshet. This extensive intrusion of comparatively warmer terrestrial Arctic river waters into the Arctic Ocean rapidly

warms the ocean's surface layers, enhancing the localized melting of sea ice (Nghiem et al., 2014).

Rate of change in Arctic climate has been higher compared to other parts of the globe (ACIA, 2005; White et al., 2007). The continuous decrease of snow and ice cover in the high latitudes enhances radiative feedbacks, causing an amplification of climate change effects in poleward regions (Polyakov et al., 2002; Serreze and Francis, 2006). Northward migration of precipitation patterns, increased evapotranspiration, more profound sea ice melting, glacial wastage, permafrost degradation and an expected increase in river runoff all point to an intensification of the Arctic hydrologic cycle. Greater subsurface infiltration into thawing permafrost stocks is causing an increase in traditionally low winter flows, while the annual spring flood is occurring earlier in conjunction with a more rapid snowmelt period (ACIA, 2005; Rawlins et al., 2010; Smith et al., 2007; Wu et al., 2005). In some basins, a warming Arctic climate points to a shift from a nival runoff regime to a more pluvial or hybrid regime, resulting in a flattening of the seasonal hydrograph as more precipitation falls as rain versus snow (Anisimov et al., 2001). These climate-induced changes in the hydrological cycle have an effect on the seasonality of the spring freshet and hence influence when the majority of freshwater discharge enters the Arctic Ocean.

Recently, Arctic river discharge has undergone a change. Shiklomanov et al. (2007) found that peak spring discharge magnitude had generally decreased across Eurasian basins. They stressed a need to further investigate relationships of freshet volume in addition to peak-magnitude with total annual discharge. During the period 1936 to 1999, annual discharge from Eurasian basins draining to the Arctic Ocean increased by 2.0 ± 0.7 km^3yr^{-1}, resulting in a cumulative increase of 128 km^3 more freshwater released annually by the end of the period as

compared to the beginning (Peterson et al., 2002). This increase in freshwater discharge was tempered by an overall yearly decrease in Canadian discharge to high-latitude seas (including the Labrador Sea, Eastern and Western Hudson Bay, Arctic Ocean and Bering Strait) of -3.1 $km^3 yr^{-1}$ during the period 1964-2003, although Canadian discharge directly to the Arctic Ocean showed a non-statistically significant increase (Déry, 2005). Eurasian increases have been associated with variations in the North Atlantic Oscillation (NAO) climate index and increases in mean, surface air temperature while North American decreases have been correlated with more intense positive phases of the Arctic Oscillation (AO) and negative phases of the Pacific Decadal and El Niño/Southern Oscillations (PDO/ENSO) (Peterson et al., 2002; Déry, 2005). Meanwhile, the results of Chapter 3 indicated that total annual discharge from the four largest Arctic-draining rivers had increased by up to 8.9 $km^3 yr^{-1}$ over the period 1980 – 2009. While this increase seems proportionally larger than the earlier study incorporating only major Eurasian basins, it was noted that observed trends varied substantially depending on the analysis window utilized.

Importantly, in Chapter 3 it was discovered that seasonality of flow had changed. Despite a significant increase in circumpolar freshet discharge of up to 3.3 $km^3 yr^{-1}$, this change was complemented by corresponding increases in all seasons (winter, spring, summer and fall). Only the summer increase of 1.6 $km^3 yr^{-1}$ was not statistically significant. In fact, discharge released during the spring freshet as a percentage of annual flow decreased by 1.7% while winter and fall proportions increased (1.3% and 2.5%, respectively). Rising winter and fall discharge proportions, combined with lower peak freshet magnitudes, increased freshet durations, and lower summer proportions all suggest a shift to a flatter, more gradual average hydrograph with an earlier pulse onset at the outlets. As discussed, this shift in seasonality can have numerous

impacts. Since the spring freshet remains an important annual event, further investigation is required.

Currently, it is unknown whether the observed changes in freshet magnitude and seasonality seen at the major river outlets are scalable on a regional level, and how the dominant controls of elevation, latitude and flow regulation impact contribution to outlet discharge. To clarify the role of these basic drivers of changing seasonality and magnitude in outlet discharge, this study analyzes trends and characteristics of the spring freshet in the hydrometric records of 106 sub-basin stations located within the Mackenzie, Ob, Lena and Yenisei river basins, separated by regulation classification and region. This will identify whether there are any regional differences in trends and in unregulated versus regulated stations, allowing for comparison of freshet characteristics in contributing sub-basins to outlet flows.

4.2 Basin Characteristics

The pan-Arctic drainage basins of the Mackenzie, Ob, Yenisei and Lena rivers are shown in Figure 1. Total contributing areas of the four major river systems, including ungauged drainage areas, are as follows: Mackenzie 1,800,000 km^2 (Finnis et al., 2009); Ob 2,975,000 km^2 (Yang et al., 2004b); Lena 2,488,000 km^2 (Yang et al., 2002); and Yenisei 2,554,482 km^2 (Zhang et al., 2003). The pan-Arctic region contains nearly half of the global alpine and sub-polar glacial area (Dyurgerov and Carter, 2004). Meanwhile, some major Eurasian Arctic basins extend below 50°N, further south than what is traditionally considered within the Arctic region (Loeng et al., 2005) (see Figure 1). As a result, discharge behaviour at each of the four major drainage outlets is influenced along its course by sub-basin tributaries which may adhere to variety of hydrological regimes such as nival, pluvial, prolacustrine, hybrid or other. For example, hydrologic retention due to extensive wetland coverage or large lakes within a

catchment, such as found in the Ob or Mackenzie basins, will lead to a more moderated seasonal discharge characteristic than basins without such retention (Carmack, 2000).

4.2.1 Flow regulation

Each of the MOLY watersheds experiences some degree of flow regulation within their catchments. The Yenisei basin is the most substantially regulated of the four basins, with at least six major reservoirs having a capacity greater than 25 km^3 located along the Yenisei and Angara stems (Yang et al., 2004a; Stuefer et al., 2011). The next most regulated is the Ob basin, containing one major reservoir with capacity greater than 25 km^3 and three midsize dams (Yang et al., 2004b). Of the Eurasian basins, the Lena is least affected by flow regulation, with only one major reservoir located along the Vilyuy tributary. The Mackenzie basin is also considered moderately affected, despite only one major reservoir located along the Peace tributary. Large lakes in the Mackenzie basin (e.g., Great Slave L. and Great Bear L.) provide substantial storage capacity, acting to reduce high spring peaks and sustain lower flows resulting in a more consistent runoff pattern throughout the year, similar to the effect of flow regulation (Woo and Thorne, 2003). Percentage of area in each basin directly upstream of a major reservoir, obtained by delineating the drainage area of each major reservoir, is as follows: Mackenzie 3.9%; Ob 11.6%; Yenisei 46.5% and Lena 4.2%. See Table 1 for characteristics of major reservoirs and Figure 1 for locations of major reservoirs. Flow regulation on a sub-basin level is discussed in Section 4.3.1.

4.3 Data and Analysis

4.3.1 Data sources

Daily discharge data are obtained from the Environment Canada Hydrometric Database (HYDAT) for stations in the Mackenzie basin and from the Regional, Hydrometeorological Data

Network for Russia (R-ArcticNET Russia v4.0) (Lammers and Shiklomanov, cited 2012) for the Ob, Lena and Yenisei basins. R-ArcticNET Russia (v4.0) contains information from 139 Russian Arctic gauges compiled from original archives of the State Hydrological Institute (SHI) and the Arctic and Antarctic Research Institute (AARI), St. Petersburg, Russia.

Quantifying discharge is difficult on rivers affected by ice-cover conditions, particularly during dynamic ice periods such as spring break-up when stage-discharge relationships are inconsistent (e.g., Shiklomanov et al., 2006; Beltaos, 2011). Discharge errors that might exist in the above data archives, however, are not considered significant in this study given that the period of dynamic breakup typically only affects the early stages of the rising limb of spring freshet. The bulk of the freshet discharge typically occurs well after breakup during subsequent periods of unobstructed flowing ice (Kääb and Prowse, 2011) and the late spring, open-water period when stage-discharge relationships are more reliable.

Availability of hydrometric data is temporally limited, particularly in the Mackenzie region. As a result, two time periods are utilized to maximize the number of stations selected for inclusion; 1962 – 2000 and 1980 – 2000. These two periods are hence referred to as t_1 and t_2, respectively. Currently, the temporal range of Eurasian station data for most Lena, Yenisei or Ob sub-basins obtained from R-ArcticNET Russia (v4.0) does not extend past the year 2000, whilst many stations in the Mackenzie basin have incomplete or missing data in the period 1970 – 1979. Hence, the shorter period t_2 is chosen to maximize spatial coverage of stations with available data, while the longer period t_1 is used to increase the power of significance testing and t-tests for stations that had available data. Table 2 identifies which stations in the Mackenzie region have available data during t_2 only. All Eurasian sub-basin stations have data from 1962 or

earlier. In total, there are 66 analyzed stations for t_1 and 106 analyzed stations for t_2. Relevant station information for all 106 stations is given in Table 2.

4.3.2 Sub-basin classification

Regulation is a necessary consideration when investigating trends in the magnitude and timing of the spring freshet. However, removing the effects of flow regulation by means of hydraulic modelling is not tractable within the scope of this study, nor would it be useful in determining the effects regulation may have on observed outlet discharge. To accommodate this, sub-basin stations have been classified into three categories. Unregulated stations (H_U) are not impounded in their upstream catchment areas. These catchment areas are considered regionally representative of a natural, unregulated basin with stable hydrologic conditions. Regulated stations (H_R) are located downstream of a major reservoir and have an average seasonal runoff pattern that is strongly influenced by the upstream flow impoundment. Lastly, minimally regulated stations (H_M) incorporate an upstream impounded flow signal that has been noticeably diminished by contribution from unaffected H_U basins. For example, the outlet station of the Mackenzie River, gauged near Inuvik, NT, is located approximately 3,120 km downstream of the W.A.C. Bennett Dam, gauged near Hudson's Hope, BC. Given the distance, the flow gauged near Inuvik integrates a virtually insignificant percentage of impounded flow from the W.A.C. Bennett Dam.

Of course, there is a subjective element involved in differentiating between stations classified as H_R or H_M. Determining whether the regulation signal has been significantly diminished to classify as H_M requires comparing the station's average hydrograph to that of an H_R-classified upstream station, and also to unaffected H_U-classified upstream contributing basins. Note that H_U stations gauging the outlet of any large water body such as a natural lake

will exhibit flow characteristics similar to that of an H_R station. The assigned classifications of each of the 106 analyzed stations are given in Table 2 with their associated sub-basin drainage areas shown in Figure 2 for the Mackenzie basin and Figure 3 for the Eurasian basins. Approximately 85% of total gauged drainage area is classified as H_U in the Mackenzie. Due to limited station availability and expansive flow regulation in the Eurasian regions, only 9% of gauged area is classified as H_U in the Ob basin, 12% in the Yenisei and 8% in the Lena basin.

Sub-basins are also classified using a simple characterization based on geography and topography. Sub-basins, where available, are roughly divided into northern, southern, eastern and western regions of similar topographical composition. For example, the southern region of the Mackenzie basin incorporates largely alpine drainage areas, while the eastern region mostly consists of plains and large lakes. These regions are given in Figure 4 for the Mackenzie basin and Figure 5 for the Eurasian basins. Appendix A gives the hypsometric curves for each sub-basin separated by regional classification. These curves are useful in interpreting the effects elevation and topographic relief may have on freshet characteristics and trends.

In the Mackenzie basin, the southern region contains a high proportion of high-relief alpine drainage typical of the North American Cordillera, with one major dam in the southwest. The western region also consists of high-relief, high-elevation alpine zones including portions of the Mackenzie Mountains. The eastern region contains interior plains and Precambrian Canadian Shield while the northern region incorporates the plains surrounding Great Bear Lake and the Mackenzie Mountains to the west. In the Ob basin, the western and eastern regions consist largely of Western Siberian lowlands, although the western region covers a small section of the Altai Mountains at the headwaters of the Irtish River. Vast expanses of wetlands cover these regions. The southern region contains the largest proportion of high-relief drainage in the

entire Ob basin. There are only three stations located in the Ob lowlands characterized as the northern region. In the Yenisei, the western region contains the Altai Mountains while the southern region contains the Sayan mountain ranges as well as Lake Baikal. Eastern drainages include higher-relief smaller watersheds below Lake Baikal, covering the Baikal Mountains to the east. The northern Yenisei basins include portions of the higher-elevation Central Siberian Plateau. Lastly, the western regions of the Lena basin include the impounded Vilyuy River and Central Siberian Plateau. Southern basins cover some portions of the Baikal Mountains while the sole eastern basin drains a portion of the Verkhoyansk Mountains. Due to limited data availability, there are no northern-classified sub-basins in the Lena basin.

It must be noted that basin size may affect the comparison of sub-basin hydrographs to outlet station records and other sub-basins. This is especially applicable to the analysis of Section 4.4.3, whereby basins of varying size are related to outlet flow. For example, large-sized basins typically exhibit different hydrological responses compared to small-sized basins, usually due to large-sized basins incorporating multiple hydrologic regimes. Ideally, to avoid any scaling effects, comparisons would be performed on basins of similar size only. However, this is not possible since sub-basin sites are constrained by availability of regional hydrometric data. Despite this limitation, it has been shown that the relationship of basin area to annual flow volume is relatively linear for large drainage areas, including differing definitions of geographic contributing area to the Arctic Ocean (Prowse and Flegg, 2000). Therefore, although the effects of basin scale cannot be eliminated within the scope of this study, it is not unreasonable to compare sub-basins of varying sizes, particularly if the compared basins have similar hydrologic regimes.

4.3.3 Flow estimation

Missing data in the hydrometric records are estimated using three different techniques. If there is an available upstream or downstream station gauging the same water course as the station with missing records, measurements from that recording gauge are used provided that it has a complete record over the period to be estimated. To account for lesser or additional contributing area, the estimated river runoff rate is scaled such that

$$R_P = R_F A_P / A_F \qquad (1)$$

where R denotes the runoff rate ($m^3 s^{-1}$) over an area A (m^2) and subscripts P and F identify the partial and full records, respectively (Déry et al., 2005). Similarly, stations with partial records that have no upstream or downstream station along the same tributary are assessed for areal runoff scaling by comparing the hydrologic response to the closest available basin, provided it has a similar hydrologic response. Whenever possible, missing records are assigned values from basins with similar morphology and scaled by basin area in the same fashion as (1) (Gibson et al., 2006).

If there are no suitable stations to use for runoff scaling, then missing discharge values are estimated from the mean daily value of discharge over the entire evaluated time period, adjusted by the deviation in discharge from the mean of all rivers in the larger basin (evaluated over the same time period) for which data are available on the missing day (Déry et al., 2005). At least three rivers which do not have concurrent missing data are used for reconstruction in all cases. Here, data are reconstructed according to

$$R_P = \frac{R_1 + R_2 + \cdots + R_N}{\overline{R_1} + \overline{R_2} + \cdots + \overline{R_N}} \times \overline{R_P} \qquad (2)$$

whereby R_P is the station with partial records for which missing data are to be reconstructed, $\overline{R_P}$ is the mean discharge for a specific day over the remaining time period, and $R_1 \ldots R_N$ and $\overline{R_1} \ldots \overline{R_N}$ are the time series of discharge for a particular day and the daily mean of the corresponding station for the evaluated time period, respectively. The percentages of missing data infilled for each station, where applicable, are given in Table 2.

4.3.4 Spring freshet definition

Two methods are used to define the volume of discharge released during the spring freshet period: i) flows occurring during the period April through July (AMJJ), referred to as V_1 and ii) integrated flow from the date of the spring pulse onset to the hydrograph centre of mass calculated from pulse onset to the last day of the calendar year, referred to as V_2. July is used as the end-date of the V_1 period since some basins display high discharge rates well into the summer months. The date of the spring pulse onset is determined as the date at which cumulative departure from mean annual flow was most negative. This yields the date when flows on subsequent days are greater than the year average (Cayan et al., 2001; Stewart et al., 2005); see Appendix B for an illustration of the algorithm as well as visual indicators of the pulse onset, freshet end date, peak magnitude and V_1 and V_2 definitions of the spring freshet for a sample year of the Yenisei River outlet station.

Visual inspection of the results as shown in the example in Appendix B verified that this is a reliable method for identifying the start date of spring freshet. Choosing the freshet end date by visual means is subjective and influenced by precipitation, temperature and other factors; thus, adopting the hydrograph centre of mass adjusted by pulse onset as the freshet end date guarantees a consistent metric for comparison of freshet trends amongst stations. Other metrics used to describe freshet characteristics are given in Table 3.

4.3.5 Trend analysis

The Mann-Kendall (Mann, 1945; Kendall, 1975) trend test is used to assess the temporal trends in freshet timing, peak freshet magnitude and volume for all stations. This non-parametric, rank-based test is often used for detecting trends in hydrologic time series that may be affected by seasonal climatic variability, missing data or extremes (Hirsch and Slack, 1984) and makes no prior assumptions about normality of data. In addition, a Trend-Free Pre-Whitening (TFPW) approach (Yue et al., 2002) is used to correct data for serial autocorrelation following the methods of Burn and Cunderlik (2004). This approach first fits a monotonic trend for a data series which is then removed prior to pre-whitening the data series. The monotonic trend is then re-added to the residual de-trended and pre-whitened data series, whereby the Mann-Kendall test statistic and local significance are calculated.

4.3.6 Flow relationships

Freshet characteristics for all sub-basin stations are assessed to determine which sub-basin stations serve as good predictors for corresponding years of anomalously high or low freshet magnitude and volume as gauged at the basin outlets. A non-parametric approach is used to ensure robustness of the t-test for stations which show evidence of non-normality as determined from one-sample Kolmogorov-Smirnov testing (Massey, 1951). The majority of stations display no evidence of non-normality; those stations which fail normality testing will have some loss of power for the t-test.

To determine the flow relationships, each sub-basin station's normalized Z-scores are sorted by year according to the top (or bottom) 25% of freshet magnitudes or volumes at their corresponding outlet stations. The t-test is then used to determine which sub-basins display a significantly higher or lower freshet magnitude or volume, based on the sub-basin series mean at

a 95% confidence level, during the top (or bottom) 25% freshet magnitudes or volumes at the outlet station of their respective basins.

4.4 Results

4.4.1 Hydrograph characteristics

Figure 6 shows the average hydrographs for stations in the Mackenzie basin, 1962 – 2000 and 1980 – 2000, grouped by region and regulation classification. Stations are referred to by their label IDs in brackets, as given in Table 2. Individual hydrographs are scaled differently to match the maximum discharge values. Note that not all stations in the Mackenzie region have data records for both time periods. Also illustrated are average freshet start dates and freshet end dates.

In the northern region, hydrographs typically adhere to a sub-Arctic or Arctic nival regime, characterized by an annual peak occurring during the spring freshet followed by a secondary peak or peaks driven by summer and autumn rainfall. A prolacustrine regime with subdued peak flows and higher seasonal low flows is seen at the outlet of Great Bear Lake (9). The moderately affected H_M stations at the outlet and northern Mackenzie stem (13) have higher cold-season base flows than the smaller streams, which often exhibit negligible winter base flow (e.g., French and Slaymaker, 1993). In the southern region, average hydrographs demonstrate a typically alpine pluvial flow regime with low winter base flows and several summer and fall rainfall peaks. These secondary rainfall peaks are particularly evident on stations with smaller drainage areas (e.g., less than 5000 km^2) and unaffected by flow regulation. Some higher latitude stations (e.g., 27, 28 & 29) demonstrate a sub-Arctic nival regime. Station (37) located below the W.A.C. Bennett Dam indicates a strong presence of flow regulation as noted by less substantial peaks and higher cold-season flows. For stations with both time periods, spring peaks

are generally lower during t_2 while rainfall-driven peaks have increased in magnitude. Owing to generally higher latitudes, western stations mostly adhere to a sub-Arctic nival regime, with the smallest basins (11 & 56) having a hybrid regime characterized by a significant secondary rainfall peak. There are no H_M or H_R stations in the western region. In the east, a mix of hydrological regimes are seen depending on whether the basin drains a lake, plains or high-relief terrain. Higher cold-season flows are indicated in H_M basins (5) and (52) with flow regulation evident in (4). The hydrograph of (5) is highly moderated due to the presence of flow regulation and its location below Lake Athabasca. Stations with both time periods indicate generally lower peak magnitudes and earlier pulse dates in t_2.

Average hydrographs for stations in the Ob basin, 1962 – 2000 and 1980 – 2000, are given in Figure 7. A nival regime is seen in all northern stations, with rainfall peaks evident in (78), a small-sized basin which drains high-relief terrain. Effects of upstream flow impoundment are minimally evident at the outlet (57). During t_2, pulse dates are generally earlier and peak magnitudes are lower, with exception of (78) whose hydrograph suggests more substantial rainfall-driven peaks during t_2. In the southern region, a hybrid regime prevails, with rainfall peaks evident in (62), (63), (66) and (68), all of which drain high-relief terrain. Minimal flow impoundment is seen in (61) from the upstream Novosibirsk dam. In the western region, extensive wetlands suppress the spring peaks seen in the nival regimes. A spring peak is still generated during the snowmelt period, when water retention capacity of the frozen wetlands is limited (French and Slaymaker, 1993). Interestingly, although there are no substantial shifts in pulse dates, the peak magnitudes of (76) and (77) are greater during t_2, possibly because of reduced water retention as a result of thawing permafrost. The effect of several large

downstream dams are evident in the moderated hydrograph of (59). In the east, a similar nival regime with wetland influence is seen with little change from t_1 to t_2.

Average hydrographs for stations in the Yenisei basin, 1962 – 2000 and 1980 – 2000, are given in Figure 8. In the northern region, hydrographs are suggestive of a distinctly nival regime with no secondary rainfall-driven peaks and some evidence of regulation in (82) and at the outlet. Peak magnitudes during t_2 are generally lower than during t_1. In the southern and western regions, the smaller basins exhibit strong influence of high-relief drainage with generally higher rainfall peaks during t_2. The Angara and Yenisei stems (84 & 85) are heavily regulated and this is evident in their hydrographs. The mountainous eastern basins above Lake Baikal follow the general pluvial pattern of high-relief drainages with more pronounced rainfall peaks and slightly subdued spring flow during t_2.

Figure 9 shows the average hydrographs for stations in the Lena basin, 1962 – 2000 and 1980 – 2000. There are no northern stations in the Lena basin. In the southern region, a pronounced spring peak indicative of a nival regime is seen in all sub-basins. Additional rainfall peaks are visible in the high-relief southern basins. In most cases, freshet magnitudes have increased during t_2 although there are no notable differences in pulse dates. Similarly, the hydrographs of the western region show a distinctly nival regime with very low or absent winter base flow and an increased peak magnitude during t_2. Minimal influence of flow regulation is noted in the Vilyuy tributary (99), located downstream of the Vilyuy reservoir. The sole eastern basin suggests an alpine flow regime with a spring peak followed by successive summer and autumn peaks. At the outlet, influence of the Vilyuy reservoir is minimal and the hydrograph indicates an Arctic nival regime.

4.4.2 Sub-basin trends

Trends in freshet pulse dates F_P are given in Figure 10 and Figure 11. During t_1, the majority of stations in all four major basins do not exhibit any change in trend slope (Figure 10, Table 4a). However, where change has occurred, trends are generally decreasing (freshet start dates happening earlier). 44% of stations have decreasing F_P at a rate of up to 0.10 - 0.49 days per year during t_1 in the Mackenzie basin, 35% in the Ob, 22% in the Lena and 18% in the Yenisei (Table 4a), although it must be noted that not all of these trends are statistically significant (see Figure 10 and Figure 11). Depending on basin, between 50 – 100% of all significant (5% level) F_P trends occur in sub-basins classified as H_U (Table 5a). There are no clear regional distinctions in trends. A higher percentage of stations indicate a decreasing trend slope in F_P during t_2, with only the Lena station not indicating decreasing trends as a majority (Table 4b). Trend slopes are generally higher during t_2, particularly in the Mackenzie basin, where pulse dates are decreasing at a rate of up to 1 or more days per year. In the Mackenzie basin, a large number of decreasing trends occur in the southern and western regions, but no significant trends exist in the southern alpine region. The Ob basin also shows a high number of decreasing, but not significant, trends in its southern region. As seen in Table 5b, nearly all trends which are considered significant (60 – 100% of total) occur in H_U basins during t_2.

Trends in freshet length F_L are given in Figure 12 and Figure 13. During t_1, increasing trends at a rate of up to 0.50 – 1.0 days per year (i.e., longer freshet duration) occur in the majority (Figure 12, Table 4a), particularly in the southern Ob and western Yenisei regions. During t_2, however, trends in freshet length are more mixed, despite a greater occurrence of decreasing pulse dates in the same time period. Only the Mackenzie and Yenisei basins depict a majority of stations having increased F_L (57% and 76%, respectively) while the Ob shows an

equal occurrence of increasing and decreasing trends (35%), and the Lena indicates more decreasing trends (44%) than increasing (33%). The southern Mackenzie displays a mix of increasing and decreasing trends, while in the west trends are mostly increasing. Trends appear to be mixed in all Eurasian regions with the exception of the high-relief eastern Yenisei region, which exclusively depicts increasing trends in freshet length. In both time periods, at least 50% and up to 100% of all significant trends occur in H_U stations (Table 5).

Trends in peak freshet magnitude F_M are depicted in Figure 14 and Figure 15. During t_1, the majority of sub-basins in the Mackenzie, Ob and Yenisei experience a decreasing trend in F_M (i.e., lower maximum peak discharge occurring during freshet), while the Lena has an equal occurrence (44%) of decreasing and increasing trends in F_M (Table 4a). Several significant decreasing trends occur in the southern Mackenzie and along the regulated Peace tributary, as well as in the southern Ob and western Yenisei. Meanwhile, during t_2, 78% of stations in the Lena represent an increasing trend in F_M while the Mackenzie, Ob and Yenisei continue to portray mostly decreasing trends (66%, 35% and 53% of sub-basins, respectively). The southern and western Mackenzie again show the highest concentration of decreasing trends, although significant (5%) trends are only found in the western region. Table 5 shows that in both time periods, the majority of significant results occur in H_U stations.

Trends in freshet volume by either definition V_1 or V_2 (Figure 16 through Figure 19) show a distinct difference between t_1 and t_2. During t_1, sub-basins in the Mackenzie basin indicated largely decreasing trends (81% of all stations, by either definition) (Table 4a), particularly in the southern alpine region. Meanwhile, the Ob and Lena basins exhibit mostly increasing V_1 and V_2 although a minor majority of stations in the Yenisei basin depict decreasing volumes. During t_2, however, the majority of stations in the Mackenzie basin now specify increasing volumes V_1 and

V_2 (57% and 59%, respectively), with the exception of a clustering of non-significant decreasing trends on the eastern side of the southern alpine region, while the Ob and Lena continue to indicate a large majority of increasing trends (96% and 78%, respectively, for V_1) (Table 4b). These tendencies agree with the findings of Chapter 3, whereby freshet volumes at the outlet stations increased during 1980 – 2000. Interestingly, during t_2 the majority of Yenisei sub-basins (53%) experience increasing freshet volume by the V_2 definition only, whereas according to the V_1 definition (April – July volume) the majority of sub-basins exhibit decreasing volume (59%). This suggests a potential shift in timing of discharge peaks (seen in monthly spring-season volume trends). In both time periods, the majority of significant results occur in H_U stations (Table 5).

Figure 20 to Figure 27 present the trends in April, May, June and July volumes for t_1 and t_2. During t_1, April trends are mostly decreasing (38% of stations) in the Mackenzie, and present no change in the Ob and Lena basins (57% and 78%, respectively) with only the Yenisei indicating a majority in increasing trends (76% of stations) (Table 4a). May volumes are again mostly decreasing in the Mackenzie (81%), while the Ob and Lena now indicate mostly increasing trends (52% and 89%, respectively) during May. Despite the large majority of Yenisei sub-basins portraying increasing April trends, in May the majority of Yenisei sub-basins are now decreasing (47%). June and July trends during t_1 are generally decreasing in all basins with the exception of an increase in June volumes in the majority of Lena sub-basins. During t_2, all basins now indicate mostly increasing trends in April volume (particularly in the eastern Ob and western Yenisei) with the exception of the Lena basin, which still shows no change (89% of stations) in a majority of sub-basins (Table 4b). May volumes are mostly increasing in all Eurasian basins, while in the Mackenzie there is a minor majority of decreasing volume in May

(50% of stations), mostly occurring in the western and southern regions. While June and July volume results show a mix of increasing and decreasing trends (generally increasing overall) in the Mackenzie, Ob and Lena basins, a large majority of stations in the Yenisei basin exhibit a decreasing trend in June and July volume (71% and 47%, respectively). This is consistent with combined April – July volume (i.e., V_1) decreases in the Yenisei as discussed earlier. The overall picture of t_2 trends is that most basins experience an overall shift to greater April or May volumes, with the exception of the Lena basin, which sees a shift to greater May and June volumes. Although there are fewer statistically significant results seen in April – July trend figures, particularly during t_2, the majority of significant results still occur in H_U stations for most basins (Table 5).

4.4.3 Flow relationships

Figure 28 through Figure 31 show the annual ranking of standardized freshet volumes and magnitudes for selected sub-basins within the Mackenzie, Ob, Yenisei and Lena basins, based on the years of the highest 25% (i.e., the highest five years) of freshet volumes or peak freshet magnitudes at the outlet stations during t_2, 1980 – 2000. For each major basin, at least one station from each region and regulation classification is chosen as a representative basin. Scaling issues that may arise from comparing sub-basins of different sizes are discussed in Section 4.3.1.

For the Mackenzie, five sub-basins are used. Station 07BE001, located on the Athabasca tributary, represents a medium-sized unregulated H_U drainage in the alpine southern region. The Peace River gauge (07HA001) also drains a large portion of the alpine south, but is a highly regulated H_R-classified station. The Liard (10ED002) is representative of the large unregulated western alpine region, while the northern Great Bear (10JC003) station is unregulated but located

at the outlet of a large water body. Lastly, the eastern Slave (07NB001) station is classified as minimally regulated HM, and is located downstream of Lake Athabasca draining a large section of interior plains and alpine south. The top five years of freshet volumes near the Mackenzie River outlet occur, in descending order, during 1997, 1988, 1992, 1986 and 1991, while the top five years of peak freshet magnitudes occur during 1992, 1985, 1988, 1993 and 1986. Note that high freshet volume on a particular year does not necessarily correspond to high peak freshet magnitude on the same year, although 1992, 1986 and 1988 are in the top 25% of both volume and peak freshet magnitude at the outlet.

As shown in Figure 28a, annual rankings of the Liard station are most similar to rankings at the outlet station for freshet volumes, with all years which correspond to high volume at the outlet also falling in the top 25% of freshet volumes at the Liard station. Rankings of the highly regulated Peace station are least similar to the outlet, with only one year also corresponding to the top 25% of freshet volumes at the Peace station. For peak freshet magnitudes (Figure 28b), the Great Bear station is most similar to the outlet, with four out of five years also landing within the top 25% of peak freshet magnitudes at that station. The Athabasca and Peace stations reveal the weakest relationships, with only one out of five years ranking in the top 25% of peak freshet magnitudes for the Athabasca and zero out of five years landing in the top 25% for the Peace.

Five sub-basins are chosen to compare rankings with the Ob outlet station. The Irtish (11048) is a highly regulated large basin located in the western plains. The Ob River at Kolpashevo (10021), also a large basin, drains the southern portion of the Ob main stem including high-relief areas, but is located downstream of the Novosibirsk Dam and is thus classified as H_M. The small Chulyshman River basin (10062) is selected to characterise an unregulated, southern alpine drainage while Vasyugan (10478) and Poluy (11558) represent

unregulated medium-sized eastern and northern plains basins, respectively. The top five years of freshet volumes near the Ob River outlet occur, in descending order, during 1999, 1997, 1986, 1994 and 1990, while the top five years of freshet magnitudes occur during 1999, 1997, 1981, 1998 and 1985.

Annual rankings of the Vasyugan station are most similar to rankings at the outlet station for freshet volumes (Figure 29a), with four out of five years also ranking within the top 25% of freshet volumes at the Vasyugan station. The Irtish and Ob River at Kolpashevo are least similar to the outlet station, with only one year also corresponding to the top 25% of freshet volumes at those stations. However, for freshet magnitudes (Figure 29b), the Ob at Kolpashevo is most similar to the outlet, with three out of five years corresponding to the top 25% of freshet magnitudes at that station. The Chulyshman station has the weakest relationship, with zero out of five years ranking in the top 25% of peak magnitudes at that station.

Five stations are used for sub-basin comparisons to the Yenisei outlet. The small, unregulated Abakan (9207) is a western alpine drainage, while the southern Yenisei main stem at Kyizyil (9002) drains a medium-sized unregulated alpine area. The Khilok (7102) is a small, unregulated high-relief eastern basin. The large, H_R-classified Angara (8091) tributary represents the general southern and eastern Yenisei basin draining mostly high-relief terrain but with four major dams located along its stem. Downstream is the Yenisei at Podkamennaya Tunguska (9092), characterizing the north-central high plateau of the Yenisei basin and incorporating the highly regulated flow of the Angara but demonstrating a diminished effect of regulation. The top five years of freshet volumes near the Yenisei River outlet occur, in descending order, during 1992, 1983, 1990, 1999 and 1991, while the top five years of peak freshet magnitudes occur during 1990, 1999, 1992, 1986 and 1998.

Figure 30a indicates that annual rankings of the Abakan basin are most similar to rankings at the outlet station for freshet volumes, despite only one out of five years corresponding to the top 25% of freshet volumes at that station. Few relationships are seen in the other stations, although only the highly regulated Angara demonstrates zero out of five years ranking in its top 25% of freshet volumes for corresponding outlet station maximums. For peak freshet magnitudes (Figure 30b), the Yenisei at Pod. Tunguska and Angara basins demonstrate the top relationships, with two out of five years falling in the top 25% of rankings for those stations. The relationship between peak magnitude and freshet volume in regulated H_R and H_M basins is discussed in Section 4.5.

Due to limited data availability, only three basins are chosen to compare annual rankings of standardized freshet volumes and peak freshet magnitudes in the Lena basin. The large, minimally regulated Vilyuy (3329) basin represents the western plains region. It is located downstream of the Vilyuy Reservoir. The medium-sized Allakh-Yun' (3277) is unregulated and located in the eastern high-relief terrain of the Verkhoyansk Mountains. Representing the high-relief southern region is the medium-sized unregulated Aldan (3219) basin. There are no H_R basins located in the Lena basin. The top five years of freshet volumes near the Lena River outlet occur, in descending order, during 1989, 2000, 1988, 1998 and 1994, while the top five years of peak freshet magnitudes occur during 1989, 1993, 1994, 1990 and 1991.

Annual rankings of the Vilyuy station are most similar to rankings at the outlet station for freshet volumes (Figure 31a), with three out of five years corresponding to the top 25% of freshet volumes at that station. The southern Aldan station has zero out of five years corresponding to its top 25% of freshet volumes, while Allakh-Yun' has two out of five years corresponding to its top 25%. For peak freshet magnitudes (Figure 31b), no stations indicate a

strong relationship with the outlet in terms of rankings, but the Vilyuy station has two out of five years corresponding to its top 25% of freshet magnitudes.

In addition to displaying annual rankings of representative sub-basins during the years of the top 25% of freshet volumes or magnitudes, Figure 32 to Figure 35 depict which sub-basin stations record a significantly higher or lower freshet volume or peak freshet magnitude, based on a t-test at a 95% confidence level, during years which correspond to the highest or lowest 25% of freshet volumes or peak freshet magnitudes at the outlet stations during t_2. Figure 32 displays the station sub-basins which indicate a significantly higher (Figure 32a) or lower (Figure 32b) freshet volume during years of the highest (lowest) 25% of freshet volumes at the Mackenzie River outlet, while Figure 33 gives the station sub-basins which demonstrate a significantly higher (Figure 33a) or lower (Figure 33b) peak freshet magnitude during years of the highest (lowest) 25% of peak freshet magnitudes at the Mackenzie River outlet. High freshet volumes at the outlet are mostly associated with high volumes at stations located near the western high-relief Liard basin, while low freshet volume associations have a wide spatial distribution throughout the Mackenzie basin. This suggests that while the Liard basin may be an important contributor to high freshet volume at the outlet, years of exceptionally low freshet volume at the outlet tend to coincide with low volumes throughout the basin. Meanwhile, high peak freshet magnitudes at the outlet are largely associated with basins located in the southern alpine region. Low peak freshet magnitudes are again associated with the Liard basin and surrounding regions. All regulation classifications H_U, H_M or H_R show some relationship to either high or low freshet magnitude or volume at the outlet.

Figure 34 gives the station sub-basins which show significantly higher (Figure 34a) or lower (Figure 34b) freshet volumes during years of the highest (lowest) 25% of freshet volumes

at Eurasian river outlets. Meanwhile, Figure 35 indicates the station sub-basins which have a significantly higher (Figure 35a) or lower (Figure 35b) peak freshet magnitude during years of the highest (lowest) 25% of peak freshet magnitudes at Eurasian river outlets.

High freshet volumes recorded at the Ob River outlet are associated with high volumes along the minimally regulated Ob main stem and Irtish tributary as well as the unregulated Vasyugan sub-basin. Low volumes are again associated with the Ob main stem. High peak freshet magnitudes do not show any associations with station sub-basins, while low peak freshet magnitudes only show associations with two small sub-basins (Balakhley and Chulyshman). In the Yenisei basin, high freshet volumes near the Yenisei River outlet do not show any associations with station sub-basins, while low volumes only show an association with the minimally regulated Yenisei main channel at Pod. Tunguska. Similarly, there are no significant relationships with high peak freshet magnitudes; however, low peak freshet magnitudes have associations with the Yenisei channel at Pod. Tunguska as well as at Yeniseysk, which has a highly regulated drainage pattern. A handful of smaller, unregulated basins also display a relationship with low peak magnitudes. Lastly, high freshet volumes at the Lena River outlet are associated only with a single small, unregulated southern basin (Bol'shoy Patom) while low freshet volumes display significant relationships three unregulated small-sized basins draining into the Lena main channel. Low peak freshet magnitudes are associated with a single, unregulated high-relief southern basin (Buotama) and there are no relations with high magnitudes.

4.5 Discussion

Elevation, latitude and flow regulation are seen to be dominant controls of hydrologic responses. Regardless of basin, northern sub-regions typically portray a nival regime while

alpine-dominated southerly regions indicate a pluvial or hybrid regime. Flow regulation in any region results in a disturbed annual runoff pattern, with higher cold-season flows and subdued peaks, similar to that of a prolacustrine hydrologic regime. Observations of average hydrographs during the periods 1962 – 2000 and 1980 – 2000 suggest a general "flattening" of hydrograph shapes in most sub-basins, as late-fall and early winter low flows rise meanwhile peak freshet magnitudes decrease and freshet durations (earlier pulse dates and later freshet end dates) increase. Secondary summer rainfall-driven peaks show an increase in many basins, particularly in pluvial-dominated regimes. This overall flattening of the seasonal runoff cycle is not universal, however, and a small number of sub-basins display an increased peak freshet magnitude and shorter freshet duration. Typically, flattening of the seasonal runoff cycle is evidence of a potential shift to a more pluvial and mixed runoff regime from a nival regime in the Arctic and sub-Arctic climates, as more precipitation begins to fall as rain versus snow (e.g., Anisimov et al., 2001). In addition, increased infiltration capacity into thawing permafrost may also contribute to changes in the annual runoff cycle seen here. However, flow regulation behaves similarly to climate-change effects, acting to increase winter low flows and decrease summer peak flows (Anisimov et al., 2007). For example, flow regulation in the Yenisei and Ob rivers has been shown to have caused seasonal discharge effects previously attributed to climate change (Yang et al., 2004a; 2004b), whereas in the Lena basin, seasonal changes have been attributed to increased winter precipitation and temperatures (Yang et al., 2002). Generally, evidence of more moderated annual hydrograph shapes in a large number of sub-basins agrees with the patterns seen in discharge recorded at the outlets, as discussed in Chapter 3.

Hydrograph characteristics are further dissected by analyzing freshet trends in sub-basins. Temporal trends show a general pattern of earlier pulse dates, longer freshet duration and

decreased peak freshet magnitude in sub-basins of the Mackenzie, Ob and Yenisei basins, particularly in the more recent 1980 – 2000 time period. The Lena basin displays the opposite tendencies to the Mackenzie, Ob and Yenisei, with the majority of sub-basins experiencing a delayed freshet onset, shorter freshet duration and increased peak freshet magnitude during 1980 – 2000, although few of these trends are statistically significant. Although the exact reasons for these discrepancies are unknown, they could be a result of differences in e.g., terrain composition and hydrologic regimes in the Lena basin, as compared to the other basins. For example, no large natural storage bodies exist in the Lena basin; and, unlike the Ob and Yenisei basins, the Lena is largely unregulated. The Lena basin also comprises the greatest proportion of continuous permafrost. Although the Lena basin contains a considerable amount of higher relief drainage area (typically between 400 – 1,500 metres a.s.l.), there is a notable lack of substantial high-elevation (e.g., above 1,500 metres a.s.l.) headwater drainage areas as found in the other three basins. Further research on the effects of elevation versus precipitation, storage and permafrost, amongst other factors, is required in order to fully evaluate the causes of this atypical behaviour in Lena sub-basins.

Freshet volumes increase in the majority of sub-basins in all four areas during 1980 – 2000, while during 1962 – 2000, most sub-basins in the Mackenzie region display decreasing freshet volume. These patterns agree with previous Chapter 3 findings, in which the Mackenzie outlet station showed decreasing freshet volume during 1973 – 2009 but significantly increasing volume during 1980 – 2009. Despite the different windows of observation, tendencies of sub-basin trends towards earlier pulse timing, increased freshet duration, decreased peak freshet magnitude and increased freshet volume match the observed trends in the outlet stations. Additionally, although Lena sub-basins display an opposite behaviour to shifts in hydrograph

shape seen in the other basins, increased peak freshet magnitudes still result in increased freshet volume at the outlet station as observed in Chapter 3. Where regional patterns in trends are notable, they usually occur in the southern and western high-relief areas of the Mackenzie, as well as in the southern Ob and western Yenisei, which also drain higher-relief terrain. Effects of changing climatic conditions may be more notable in these higher-relief sub-basins due to increased orographic precipitation and more pronounced melt cycles (compared to low-relief counterparts) resulting from the largely mechanical spring break-up mechanism controlling freshet generation.

Sub-basins are also compared to outlets in terms of volume and magnitude. Freshet volume at the Mackenzie River outlet is largely influenced by high-relief H_U basins in the western region and Liard tributary. Low peak freshet magnitudes are also associated with this region. However, high peak magnitudes at the outlet are strongly associated with the southern high-relief alpine region and regulated Peace tributary. These magnitude relationships propagate downstream along the minimally-affected main channel. This suggests that, while flow regulation acts to moderate the hydrograph, it doesn't necessarily override the short-term peaks generated by the surrounding high-relief terrain. This is further supported by the fact that no volume relationships are seen in H_R stations, either with high or low volumes at the outlet, implying that while impoundment does not negate the high peaks, it does affect overall freshet volume contribution.

Regional patterns in Eurasian basins are less distinct. High-relief drainage areas are typically located in the southern portions of the Eurasian basins. Due to the high flow rates generated by this type of terrain, flow regulation tends to be substantial and likely obscures many of the natural relationships that would otherwise be observed. In the Ob basin, similar to the

Mackenzie, a likely effect of regulation is that no volume relationships with the outlet are observed in the lower Irtish (H_R) or Ob at Kolpashevo (H_M) representing western and southern basins, respectively, and both draining some high-relief area. However, a relationship with high peak freshet magnitudes at the outlet is seen at the Ob at Kolpashevo, a station that incorporates a substantial region of high-relief terrain. This again suggests that the single dam located along this tributary does not effectively suppress all short-term peak flows. Likewise, there are no volume relationships with the outlet observed in the highly regulated and steep drainage areas of the southern and western Yenisei regions. Unlike the Mackenzie and Ob basins, however, no relationships are seen with peak freshet magnitudes at the outlet, likely owing to the multiple dams located along each tributary which successively do negate the highest peaks. The Yenisei at Pod. Tunguska (representing the northern plateau region) tends to indicate significantly lower values during years of low volume and low magnitude at the outlet, likely owing to its proximity to the outlet station. Following the same overall pattern, no significant difference is seen in freshet volumes along the minimally regulated Vilyuy tributary during years of the top 25% of freshet volumes at the outlet. Despite this, the Vilyuy station still shows a similarity to the outlet in terms of ranking amongst other representative stations, owing to its large drainage area and closeness to the outlet. High and low volumes at the outlet tend to be associated with unregulated basins draining into the southern main Lena channel.

4.6 Conclusion

Overall, sub-basin trends during 1980 – 2000 project a shift towards earlier pulse dates and longer freshet durations, with lower peak freshet magnitudes and increased freshet volumes. This suggests shifting seasonality of flow in many sub-basins, which is reflected in the outlet stations. In the Mackenzie River, trends such as these are potentially a by-product of the regime

shift seen in the pan-Pacific region during which the PDO shifted to a predominantly positive phase in 1976 – 1977 (Hartmann and Wendler, 2005; Mantua et al., 1997). Notably, unregulated stations, regardless of region, have observed similarities with freshet volumes at the outlets, although those relationships can be negated in the larger encompassing basins if there is upstream regulation. High peak freshet magnitudes in regulated stations can still relate to high peak magnitudes at the outlets, particularly if there is only one dam impounding flow.

Since the majority of all significant trends occur in H_U stations, flow regulation may be moderating the effects of climatic drivers such as temperature and precipitation on H_R and H_M basins. For example, during a period of drought an operator may still release impounded storage, affecting discharge recorded at the outlet. Thus, it is important to separate the effects of flow regulation and climate by determining the relationships with hydro-climatic conditions not only with H_U, but also H_M and H_R-classified basins, at spatial scales that reflect differences in hydro-climatic conditions controlling freshet generation at the outlets. Although the four circumpolar rivers assessed here drain to the Arctic Ocean, they originate from basins with a diversity of hydrologic and climatic regimes. For example, 46% of their combined drainage area is located south of 55°N (Brooks, 2012), well outside the Arctic or even sub-Arctic climatic regimes, and the regions encompass a range of nival, pluvial, glacial and hybrid hydrologic regimes. It was shown that stronger trends tended to occur in higher-relief drainage areas, which are typically located in the lower latitudes of the basins. Given the southerly extent of these basins where much of the flow originates, it is necessary to determine whether regional trends can be related to the mid-latitude effects of climate and synoptic-scale atmospheric variability, and what impacts these relationships can have on changing seasonality and magnitude at the outlets. Lastly,

further investigation is required to clarify the discrepancies in Lena sub-basin hydrograph characteristics compared to the other three basins.

4.7 Acknowledgements

This work was partially supported by a Discovery Grant and ArcticNet funding from the Natural Sciences and Engineering Council of Canada (NSERC) to one of the co-authors. The authors would also like to acknowledge the Arctic Rapid Integrated Monitoring System (ArcticRIMS) and the Regional Hydrometeorological Data Network for the Pan-Arctic Region (R-ArcticNet) for freely providing data.

References

Aagaard, K., Carmack, E.C., 1989. The role of fresh water in ocean circulation and climate. J. Geophys. Res. 94, 14,485–14,498.

ACIA, 2005. Arctic Climate Impact Assessment - Scientific Report. Cambridge University Press, New York.

Ahmed, R., Prowse, T.D., Dibike, Y.B., Bonsal, B.R., 2012. Temporal sequencing of annual spring runoff in major Arctic-draining rivers. In: Poster Session Presented at: American Geophysical Union Fall Meeting 2012. Dec. 3-7, 2012. San Francisco, CA.

Anisimov, O., Fitzharris, B., Hagen, J.O., Jefferies, R., Marchant, H., Nelson, F., Prowse, T.D., Vaughan, D.G., 2001. Polar regions (Arctic and Antarctic). In: McCarthy, J.J., Canziani, O.F., Leary, N.A., Dokken, D.J., White, K.S. (Eds.), Climate Change 2001: Impacts, Adaptation and Vulnerability. Contribution of Working Group II to the Third Assessment Report of the Intergovernmental Panel on Climate Change. Cambridge University Press, Cambridge, pp. 803–841.

Anisimov, O., Vaughan, D.G., Callaghan, T., Furgal, C., Marchant, H., Prowse, T.D., Vilhjalmsson, H., Walsh, J.E., 2007. Polar regions (Arctic and Antarctic). In: Parry, M.L., Canziani, O.F., Palutikof, J.P., van der Linden, P.J., Hanson, C.E. (Eds.), Climate Change 2007: Impacts, Adaptation and Vulnerability. Contribution of Working Group II to the Fourth Assessment Report of the Intergovernmental Panel on Climate Change. Cambridge University Press, Cambridge, pp. 653–685.

Beltaos, S., 2011. Developing winter flow rating relationships using slope- • area hydraulics. River Res. Appl. 27, 1076–1089.

Brooks, R., 2012. Contributing river basin area by latitude, unpublished work. University of Victoria, Department of Geography.

Burn, D.H., Cunderlik, J.M., 2004. Hydrological trends and variability in the Liard River basin. Hydrol. Sci. 49, 53–67.

Carmack, E.C., 2000. The freshwater budget of the Arctic Ocean: Sources, storage and sinks. In: Lewis, E.L. (Ed.), The Freshwater Budget of the Arctic Ocean. Kluwer, Dordrecht, Netherlands, pp. 91–126.

Carmack, E.C., Mclaughlin, F.A., Yamamoto-Kawai, M., Itoh, M., Shimada, K., Krishfield, R., Proshutinsky, A., 2008. Freshwater storage in the Northern Ocean and the special role of

the Beaufort Gyre. In: Dickson, R.R. et al. (Ed.), Arctic-Subarctic Ocean Fluxes: Defining the Role of the Northern Seas in Climate. Springer, New York, pp. 145–169.

Cayan, D.R., Kammerdiener, S.A., Dettinger, M.D., Caprio, J.M., Peterson, D.H., 2001. Changes in the Onset of Spring in the Western United States. Bull. Am. Meteorol. Soc. 82, 399–415.

Déry, S.J., 2005. Decreasing river discharge in northern Canada. Geophys. Res. Lett. 32, L10401.

Déry, S.J., Stieglitz, M., McKenna, E.C., Wood, E.F., 2005. Characteristics and trends of river discharge into Hudson, James, and Ungava Bays, 1964-2000. J. Clim. 18, 2540–2557.

Dickson, B., Osborn, T.J., Hurrell, J.W., Meincke, J., Blindheim, J., Adlandsvik, B., Vinje, T., Alekseev, G., Maslowski, W., 2000. The Arctic Ocean response to the North Atlantic Oscillation. J. Clim. 13, 2671–2696.

Dickson, B., Yashayaev, I., Meincke, J., Turrell, B., Dye, S., Holfort, J., 2002. Rapid freshening of the deep North Atlantic Ocean over the past four decades. Nature 416, 832–7.

Dyurgerov, M.B., Carter, C.L., 2004. Observational Evidence of Increases in Freshwater Inflow to the Arctic Ocean. Arctic, Antarct. Alp. Res. 36, 117–122.

Finnis, J., Cassano, J., Holland, M.M., Uotila, P., 2009. Synoptically forced hydroclimatology of major Arctic watersheds in general circulation models, Part 1 : the Mackenzie River Basin. Int. J. Climatol. 29, 1226–1243.

French, H.M., Slaymaker, O., 1993. Canada's cold environments, Vol. 1. ed. McGill-Queen's Press-MQUP.

Gibson, J.J., Prowse, T.D., Peters, D.L., 2006. Hydroclimatic controls on water balance and water level variability in Great Slave Lake 4172, 4155–4172.

Grabs, W.E., Portmann, F., De Couet, T., 2000. Discharge observation networks in Arctic regions: Computation of the river runoff into the Arctic Ocean, its seasonality and variability. In: Lewis, E.L. (Ed.), The Freshwater Budget of the Arctic Ocean. Kluwer, Dordrecht, Netherlands, pp. 249–267.

Hartmann, B., Wendler, G., 2005. The significance of the 1976 Pacific climate shift in the climatology of Alaska. J. Clim. 18, 4824–4839.

Hirsch, R.M., Slack, J.R., 1984. A non-parametric trend test for seasonal data with serial dependence. Water Resour. Res. 20, 727–732.

Jasek, M., 2003. Ice jam release surges, ice runs, and breaking fronts: field measurements, physical descriptions, and research needs. Can. J. Civ. Eng. 30, 113–127.

Kääb, A., Prowse, T.D., 2011. Cold-regions river flow observed from space. Geophys. Res. Lett. 38, L08403.

Kattsov, V.M., Walsh, J.E., Chapman, W.L., Govorkova, V.A., Pavlova, T. V., Zhang, X., 2007. Simulation and Projection of Arctic Freshwater Budget Components by the IPCC AR4 Global Climate Models. J. Hydrometeorol. 8, 571–589.

Kendall, M., 1975. Rank Correlation Measures. Charles Griffin, London, UK.

Lammers, R.B., Shiklomanov, A.I., 2013. A Regional, Hydrometeorological Data Network for Russia. Available online at http://www.r-arcticnet.sr.unh.edu/v4.0/index.html.

Lammers, R.B., Shiklomanov, A.I., Vörösmarty, C.J., Fekete, B.M., Peterson, B.J., 2001. Assessment of contemporary Arctic river runoff based on observational discharge records. J. Geophys. Res. 106, 3321–3334.

Loeng, H., Brander, K., Carmack, E.C., Denisenko, S., Drinkwater, K., Hansen, B., Kovacs, K., Livingston, P., Mclaughlin, F.A., Bellerby, R., Browman, H., Furevik, T., Grebmeier, J.M., Jansen, E., Jónsson, S., Jørgensen, L.L., 2005. Ch. 9: Marine Systems. In: Symon, C., Arris, L., Heal, B. (Eds.), Arctic Climate Impact Assessment. Cambridge University Press, New York, pp. 453–538.

Mann, H.B., 1945. Nonparametric tests against trend. Econom. J. Econom. Soc. 13, 245–259.

Mantua, N.J., Hare, S.R., Zhang, Y., Wallace, J.M., Francis, R.C., 1997. A Pacific interdecadal climate oscillation with impacts on salmon production. Bull. Am. Meteorol. Soc. 78, 1069–1079.

Marsh, P., Hey, M., 1989. The Flooding Hydrology of Mackenzie Delta Lakes. Arctic 42, 41–49.

Massey, F.J., 1951. The Kolmogorov-Smirnov test for goodness of fit. J. Am. Stat. Assoc. 46, 68–78.

McClelland, J.W., Holmes, R.M., Dunton, K.H., Macdonald, R.W., 2011. The Arctic Ocean Estuary. Estuaries and Coasts 35, 353–368.

Nghiem, S. V., Hall, D.K., Rigor, I.G., 2014. Effects of Mackenzie River discharge and bathymetry on sea ice in the Beaufort Sea. Geophys. Res. Lett. 873–879.

Peterson, B.J., Holmes, R.M., McClelland, J.W., Vörösmarty, C.J., Lammers, R.B., Shiklomanov, A.I., Shiklomanov, I.A., Rahmstorf, S., 2002. Increasing river discharge to the Arctic Ocean. Science (80-.). 298, 2171–2173.

Polyakov, I. V., Alekseev, G., Bekryaev, R., Bhatt, U., Colony, R., Johnson, M., Karklin, V., Makshtas, A., Walsh, D., Yulin, A., 2002. Observationally based assessment of polar amplification of global warming. Geophys. Res. Lett. 29, 1878.

Proshutinsky, A., Bourke, R.H., McLaughlin, F.A., 2002. The role of the Beaufort Gyre in Arctic climate variability: Seasonal to decadal climate scales. Geophys. Res. Lett. 29, 15–1– 15–4.

Prowse, T.D., Conly, F.M., 1998. Effects of climatic variability and flow regulation on ice-jam flooding of a northern delta. Hydrol. Process. 12, 1589–1610.

Prowse, T.D., Flegg, P.O., 2000. Arctic river flow: A review of contributing areas. In: Lewis, E.L. (Ed.), The Freshwater Budget of the Arctic Ocean. Kluwer, Dordrecht, Netherlands, pp. 269–280.

Rawlins, M.A., Steele, M., Holland, M.M., Adam, J.C., Cherry, J.E., Francis, J.A., Groisman, P.Y., Hinzman, L.D., Huntington, T.G., Kane, D.L., Kimball, J.S., Kwok, R., Lammers, R.B., Lee, C.M., Lettenmaier, D.P., McDonald, K.C., Podest, E., Pundsack, J.W., Rudels, B., Serreze, M.C., Shiklomanov, A.I., Skagseth, Ø., Troy, T.J., Vörösmarty, C.J., Wensnahan, M., Wood, E.F., Woodgate, R., Yang, D., Zhang, K., Zhang, T., 2010. Analysis of the Arctic System for Freshwater Cycle Intensification: Observations and Expectations. J. Clim. 23, 5715–5737.

Serreze, M.C., Barrett, A.P., Slater, A.G., Woodgate, R.A., Aagaard, K., Lammers, R.B., Steele, M., Moritz, R., Meredith, M., Lee, C.M., 2006. The large-scale freshwater cycle of the Arctic. J. Geophys. Res. 111, C11010.

Serreze, M.C., Francis, J.A., 2006. The Arctic Amplification Debate. Clim. Change 76, 241–264.

Shiklomanov, A.I., Lammers, R.B., Rawlins, M.A., Smith, L.C., Pavelsky, T.M., 2007. Temporal and spatial variations in maximum river discharge from a new Russian data set. J. Geophys. Res. 112, G04S53.

Shiklomanov, A.I., Yakovleva, T.I., Lammers, R.B., Karasev, I.P., Vörösmarty, C.J., Linder, E., 2006. Cold region river discharge uncertainty—estimates from large Russian rivers. J. Hydrol. 326, 231–256.

Shiklomanov, I.A., 1998. Comprehensive assessment of the freshwater resources of the world: assessment of water resources and water availability in the world. World Meteorological Organization, Geneva.

Smith, L.C., Pavelsky, T.M., MacDonald, G.M., Shiklomanov, A.I., Lammers, R.B., 2007. Rising minimum daily flows in northern Eurasian rivers: A growing influence of groundwater in the high-latitude hydrologic cycle. J. Geophys. Res. 112, G04S47.

Steele, M., Boyd, T., 1998. Retreat of the cold halocline layer in the Arctic Ocean. J. Geophys. Res. 103, 10419–10435.

Stewart, I.T., Cayan, D.R., Dettinger, M.D., 2005. Changes toward earlier streamflow timing across western North America. J. Clim. 18, 1136–1155.

Stuefer, S., Yang, D., Shiklomanov, A.I., 2011. Effect of streamflow regulation on mean annual discharge variability of the Yenisei River. In: Cold Region Hydrology in a Changing Climate (Proceedings of Symposium H02 Held during IUGG2011 in Melbourne, Australia, July 2011). IAHS Publ. 346, pp. 27–32.

Tank, S.E., Manizza, M., Holmes, R.M., McClelland, J.W., Peterson, B.J., 2011. The processing and impact of dissolved riverine nitrogen in the Arctic Ocean. Estuaries and Coasts 35, 401–415.

Toggweiler, J.R., Key, R.M., 2001. Ocean Circulation: Thermohaline Circulation. In: Encyclopedia of Atmospheric Sciences, Vol. 4. Academic Press, San Diego, CA, pp. 1549–1555.

White, D., Hinzman, L., Alessa, L., Cassano, J., Chambers, M., Falkner, K., Francis, J., Gutowski, W.J., Holland, M., Holmes, R.M., Huntington, H., Kane, D., Kliskey, A., Lee, C., McClelland, J.W., Peterson, B.J., Rupp, T.S., Straneo, F., Steele, M., Woodgate, R., Yang, D., Yoshikawa, K., Zhang, T., 2007. The Arctic freshwater system: changes and impacts. J. Geophys. Res. 112, G04S54.

Woo, M.K., Thorne, R., 2003. Streamflow in the Mackenzie basin, Canada. Arctic 56, 328–340.

Wu, P., Wood, R., Stott, P., 2005. Human influence on increasing Arctic river discharges. Geophys. Res. Lett. 32, L02703.

Yang, D., Kane, D.L., Hinzman, L.D., Zhang, X., Zhang, T., Ye, H., 2002. Siberian Lena River hydrologic regime and recent change. J. Geophys. Res. 107, 4694.

Yang, D., Ye, B., Kane, D.L., 2004a. Streamflow changes over Siberian Yenisei River Basin. J. Hydrol. 296, 59–80.

Yang, D., Ye, B., Shiklomanov, A., 2004b. Discharge characteristics and changes over the Ob River watershed in Siberia. J. Hydrometeorol. 5, 595–610.

Yue, S., Pilon, P.J., Phinney, B., Cavadias, G., 2002. The influence of autocorrelation on the ability to detect trend in hydrological series. Hydrol. Process. 16, 1807–1829.

Zhang, X., Ikeda, M., Walsh, J.E., 2003. Arctic sea ice and freshwater changes driven by the atmospheric leading mode in a coupled sea ice-ocean model. J. Clim. 16, 2159–2177.

List of Tables

Table 1. Characteristics of major hydroelectric dams/reservoirs located in the study regions.

Reservoir/Dam Name	Latitude (°N)	Longitude (°E)	Basin	River	Capacity (MW)	Commissioned	Maximum Capacity (km^3)	Reservoir Catchment Area (km^2)
W.A.C. Bennett	56.0	-122.2	Mackenzie	Peace	2730	1968	74	70275
Shul'binsk	50.4	81.1	Ob	Irtysh	702	1989	2.4	131598
Bukhtarma	49.7	83.3	Ob	Irtysh	750	1960	49.8	103923
Ust-Kamenogorsk	49.9	82.7	Ob	Irtysh	331.2	1952	0.6	107636
Novosibirsk	54.8	83.0	Ob	Ob	455	1957	8.8	212076
Boguchany	58.4	97.4	Yenisei	Angara	3000	2011	58.2	845694
Ust-Ilimsk	58.0	102.7	Yenisei	Angara	4320	1974	59.3	767413
Bratsk	56.3	101.8	Yenisei	Angara	4500	1967	169	714017
Irkutsk	52.2	104.3	Yenisei	Angara	662.4	1958	46	572704
Sayano-Shushenskoe	52.8	91.4	Yenisei	Yenisei	6400	1978	31.3	172529
Krasnoyarskoye More	55.9	92.3	Yenisei	Yenisei	6000	1972	73.3	276174
Kurejka	66.94	88.34	Yenisei	Kurejka	600	1987	--	65974
Vilyuy	63.0	112.5	Lena	Viluy	680	1967	35.9	104566

Table 2. Characteristics of drainage sub-basins as labeled in Figures 2 and 3. Note: M = Mackenzie, O = Ob, L = Lena, Y = Yenisei; D.A. = Drainage Area. Stations IDs in *italic* have data during t_2 only. Labels are colour-coded according to regulation classification (red = regulated; orange = minimally regulated; green = unregulated).

Label	Basin	ID	Lat. (°N)	Long. (°E)	D.A. (km^2)	% Infilled	Classification	Region
1	M	07AD002	53.42	-117.57	9765	--	H_U	South
2	M	*07DA001*	56.78	-111.4	132585	--	H_U	East
3	M	07GJ001	55.71	-117.62	50300	--	H_U	South
4	M	07KC001	59.11	-112.43	293000	--	H_R	East
5	M	07NB001	59.87	-111.58	606000	--	H_M	East
6	M	*10BE001*	59.41	-126.1	104000	--	H_U	West
7	M	*10CD001*	58.79	-122.66	20300	--	H_U	West
8	M	*10ED002*	61.75	-121.22	275000	--	H_U	West
9	M	*10JC003*	65.13	-123.55	146400	15.60%	H_U	North
10	M	*10FA002*	61.14	-119.84	9270	--	H_U	East
11	M	*10FB005*	61.45	-121.24	1310	--	H_U	West
12	M	*10GC003*	61.9	-121.61	2050	--	H_U	North
13	M	*10KA001*	65.27	-126.84	1594500	11.80%	H_M	North
14	M	*07OB001*	60.74	-115.86	51700	--	H_U	East
15	M	*07TA001*	63.11	-116.97	13900	--	H_U	East
16	M	*07AA001*	52.86	-118.11	629	--	H_U	South
17	M	*07AA002*	52.91	-118.06	3872	--	H_U	South
18	M	07AF002	53.47	-116.63	2562	--	H_U	South
19	M	07AG003	53.6	-116.27	826	--	H_U	South
20	M	07BB002	53.6	-115	4402	--	H_U	South
21	M	07BC002	54.45	-113.99	13014	--	H_U	South
22	M	07BE001	54.72	-113.29	74602	--	H_U	South
23	M	*07BF002*	55.45	-116.49	1152	--	H_U	South
24	M	*07BJ001*	55.32	-115.42	1900	--	H_U	South
25	M	*07BK007*	55.26	-114.23	2100	--	H_U	East
26	M	07CD001	56.69	-111.26	30792	--	H_U	East
27	M	*07EC002*	55.92	-124.57	5560	--	H_U	South
28	M	*07EE007*	55.08	-122.9	4930	--	H_U	South
29	M	07FB001	55.72	-121.21	12100	--	H_U	South
30	M	*07FC001*	56.28	-120.7	15600	--	H_U	South
31	M	*07FC003*	56.68	-121.22	1770	--	H_U	South
32	M	*07FD001*	55.96	-120.56	3630	--	H_U	South
33	M	*07FD007*	55.86	-120.03	2860	14.00%	H_U	South
34	M	07GE001	55.07	-118.8	11300	--	H_U	South
35	M	*07GG001*	54.75	-117.21	1040	--	H_U	South
36	M	07GH002	55.46	-117.16	11100	--	H_U	South
37	M	07HA001	56.24	-117.31	194374	--	H_R	South

Table 2 cont'd…

Label	Basin	ID	Lat. (°N)	Long. (°E)	D.A. (km²)	% Infilled	Classification	Region
38	M	*07HA003*	56.06	-117.13	1968	--	H_U	South
39	M	07HC001	56.92	-117.62	4679	--	H_U	East
40	M	*07JD002*	57.87	-115.39	35800	--	H_U	East
41	M	07LE002	59.15	-105.54	50700	4.80%	H_U	East
42	M	*07MB001*	58.97	-108.18	9120	--	H_U	East
43	M	*07OC001*	58.6	-118.33	10370	1.30%	H_U	East
44	M	*10AB001*	60.47	-129.12	12800	--	H_U	West
45	M	*10AC005*	59.12	-129.82	882	--	H_U	West
46	M	*10BE004*	58.85	-125.38	2540	--	H_U	West
47	M	*10BE007*	59.34	-125.94	1170	--	H_U	West
48	M	*10CB001*	57.23	-122.69	2180	--	H_U	South
49	M	*10EA003*	61.53	-125.41	8560	0.30%	H_U	West
50	M	*10EB001*	61.64	-125.8	14500	--	H_U	West
51	M	*10ED001*	60.24	-123.48	222000	2.50%	H_U	West
52	M	*10GC001*	61.87	-121.36	127000	--	H_M	East
53	M	*10LA002*	66.79	-133.09	18750	1.10%	H_U	North
54	M	*10LC014*	67.456	-133.75	1679100	2.00%	H_M	Outlet
55	M	*10MC002*	67.26	-134.89	70600	6.30%	H_U	North
56	M	*10ED003*	61.33	-122.09	542	--	H_U	West
57	O	11801	66.63	66.6	2950000	2.60%	H_M	Outlet
58	O	11056	58.2	68.23	1500000	0.80%	H_M	West
59	O	11048	55.02	73.3	769000	--	H_R	West
60	O	10031	61.07	68.9	2690000	5.60%	H_M	East
61	O	10021	58.3	82.88	486000	--	H_M	South
62	O	10062	51.28	87.72	16600	9.90%	H_U	South
63	O	10126	51.02	84.32	3480	5.60%	H_U	South
64	O	10176	53.73	84.95	15900	5.10%	H_U	South
65	O	10219	55.32	84.1	15700	5.10%	H_U	South
66	O	10277	53.33	87.23	7080	5.10%	H_U	South
67	O	10317	55.38	91.62	14700	12.20%	H_U	South
68	O	10387	56.2	87.78	9820	5.10%	H_U	South
69	O	10407	56.18	86.4	3460	7.70%	H_U	South
70	O	10428	57.78	82.63	25000	5.10%	H_U	South
71	O	10444	56.85	83.07	2560	5.10%	H_U	South
72	O	10466	59.37	82.83	6500	5.10%	H_U	East
73	O	10478	59.22	78.22	31700	9.40%	H_U	East
74	O	10489	59.85	81.95	24500	5.10%	H_U	East
75	O	11309	55.45	78.32	12200	5.10%	H_U	West
76	O	11353	56.38	75.25	16400	--	H_U	West

Table 2 cont'd…

Label	Basin	ID	Lat. (°N)	Long. (°E)	D.A. (km²)	% Infilled	Classification	Region
77	O	11496	57.13	69.22	2140	2.60%	H_U	West
78	O	11556	66.87	65.78	1240	0.60%	H_U	North
79	O	11558	66.03	68.73	15100	2.90%	H_U	North
80	O	11574	64.93	77.8	31400	0.20%	H_U	North
81	Y	9803	67.43	86.48	2440000	--	H_M	Outlet
82	Y	9092	61.1	90.08	1760000	--	H_M	North
83	Y	9002	51.72	94.4	115000	--	H_U	South
84	Y	8091	58.35	93.55	1040000	--	H_R	South
85	Y	9079	58.45	92.15	1400000	--	H_R	West
86	Y	7156	51.95	106.35	565	--	H_U	East
87	Y	7172	51.53	104.07	959	--	H_U	South
88	Y	7015	55.85	110.15	20600	--	H_U	East
89	Y	7024	53.6	109.6	19800	--	H_U	East
90	Y	7036	52.92	108.73	5050	--	H_U	East
91	Y	7072	50.3	108.63	15600	--	H_U	East
92	Y	7102	51.2	106.97	38300	--	H_U	East
93	Y	9207	52.65	90.1	14400	--	H_U	West
94	Y	9252	53.8	92.87	31800	--	H_U	West
95	Y	9372	59.12	93.48	15100	--	H_U	North
96	Y	9422	65.65	90.12	9100	--	H_U	North
97	Y	9425	65.98	84.27	10100	5.10%	H_U	North
98	L	3821	70.68	127.39	2430000	--	H_M	Outlet
99	L	3329	63.95	124.83	452000	2.00%	H_M	West
100	L	3156	60.98	115.5	32600	2.60%	H_U	West
101	L	3157	60.17	116.8	27600	0.30%	H_U	South
102	L	3277	60.68	135.03	24200	2.60%	H_U	East
103	L	3291	59.67	127.05	23900	2.60%	H_U	South
104	L	3202	60.9	120.8	16600	10.30%	H_U	West
105	L	3210	61.05	128.65	12200	10.30%	H_U	South
106	L	3219	58.97	126.27	49500	10.30%	H_U	South

Table 3. Metrics utilized to describe freshet characteristics.

Symbol	Description
F_P	Freshet pulse date
F_L	Freshet length
F_M	Peak freshet magnitude
V_1	April – July volume
V_2	Freshet volume
V_{APR}	April volume
V_{MAY}	May volume
V_{JUN}	June volume
V_{JUL}	July volume

Table 4a. Percentage of total stations in each basin exhibiting various trends, 1962 - 2000. Significant trends are indicated in corresponding figures for each freshet measure.

	%	F_P	F_L	F_M	V_2	V_1	V_{APR}	V_{MAY}	V_{JUN}	V_{JUL}
	Decreasing	44	6	69	81	81	38	81	69	50
Mackenzie	Increasing	6	50	13	6	13	31	6	6	44
	No Change	50	44	19	13	6	31	13	25	6
	Decreasing	35	0	48	35	39	9	35	43	30
Ob	Increasing	4	57	22	52	43	35	52	22	22
	No Change	61	43	30	13	17	57	13	35	48
	Decreasing	22	11	44	22	22	0	11	22	33
Lena	Increasing	0	78	44	56	67	22	89	56	22
	No Change	78	11	11	22	11	78	0	22	44
	Decreasing	18	6	47	41	53	0	47	65	53
Yenisei	Increasing	18	71	18	29	24	76	35	12	24
	No Change	65	24	35	29	24	24	18	24	24

Table 4b. Percentage of total stations in each basin exhibiting various trends, 1980 - 2000. Significant trends are indicated in corresponding figures for each freshet measure.

	%	F_P	F_L	F_M	V_2	V_1	V_{APR}	V_{MAY}	V_{JUN}	V_{JUL}
	Decreasing	61	23	66	32	32	5	50	29	16
Mackenzie	Increasing	13	57	23	59	57	75	36	46	71
	No Change	27	20	11	9	11	20	14	25	13
	Decreasing	61	35	35	4	4	13	9	35	22
Ob	Increasing	4	35	30	87	96	57	87	26	43
	No Change	35	30	35	9	0	30	4	39	35
	Decreasing	22	44	11	11	11	0	11	22	44
Lena	Increasing	33	33	78	78	78	11	89	78	33
	No Change	44	22	11	11	11	89	0	0	22
	Decreasing	65	12	53	35	59	0	29	71	47
Yenisei	Increasing	18	76	35	53	24	88	65	6	24
	No Change	18	12	12	12	18	12	6	24	29

Table 5a. Percentage of total significant trends (5% level) that occur in unregulated (H_U) stations, 1962 – 2000. Items marked by *N/A* indicate that there were no significant trends for the corresponding freshet measure.

	F_P	F_L	F_M	V_2	V_1	V_{APR}	V_{MAY}	V_{JUN}	V_{JUL}
Mackenzie	75	50	67	75	80	75	88	50	0
Ob	100	83	86	100	100	86	75	100	N/A
Lena	N/A	50	100	100	100	33	50	100	N/A
Yenisei	50	67	100	100	N/A	64	67	33	0

Table 5b. Percentage of total significant trends (5% level) that occur in unregulated (H_U) stations, 1980 – 2000. Items marked by *N/A* indicate that there were no significant trends for the corresponding freshet measure.

	F_P	F_L	F_M	V_2	V_1	V_{APR}	V_{MAY}	V_{JUN}	V_{JUL}
Mackenzie	60	67	100	100	100	75	100	100	100
Ob	100	100	100	0	50	100	100	N/A	N/A
Lena	100	N/A	N/A	N/A	N/A	0	N/A	0	N/A
Yenisei	100	100	100	50	100	100	100	N/A	N/A

List of Figures

c) western and d) eastern regions. Dashed vertical blue line pairs denote freshet start and end dates for 1962 – 2000 respectively, while dashed vertical red line pairs denote freshest start and end dates for 1980 – 2000 respectively. Stations which exclusively show red series have data for 1980 – 2000 only. Additionally, stations are grouped according to regulation classification H_R, H_M or H_U.

Figure 8. Average annual hydrographs (discharge [m^3s^{-1}] versus Julian day) of Yenisei station sub-basins for 1962 – 2000 (blue line) and 1980 – 2000 (red line), grouped by a) northern b) southern c) western and d) eastern regions. Dashed vertical blue line pairs denote freshet start and end dates for 1962 – 2000 respectively, while dashed vertical red line pairs denote freshest start and end dates for 1980 – 2000 respectively. Stations which exclusively show red series have data for 1980 – 2000 only. Additionally, stations are grouped according to regulation classification H_R, H_M or H_U.

Figure 9. Average annual hydrographs (discharge [m^3s^{-1}] versus Julian day) of Lena station sub-basins for 1962 – 2000 (blue line) and 1980 – 2000 (red line), grouped by a) southern b) western and c) eastern regions. There are no northern sub-basin stations in the Lena basin. Dashed vertical blue line pairs denote freshet start and end dates for 1962 – 2000 respectively, while dashed vertical red line pairs denote freshest start and end dates for 1980 – 2000 respectively. Stations which exclusively show red series have data for 1980 – 2000 only. Additionally, stations are grouped according to regulation classification H_R, H_M or H_U.

Figure 10. Trends in freshet pulse dates during the period 1962 – 2000 for a) Mackenzie and b) Eurasian stations.

Figure 11. Trends in freshet pulse dates during the period 1980 – 2000 for a) Mackenzie and b) Eurasian stations.

Figure 12. Trends in freshet length during the period 1962 – 2000 for a) Mackenzie and b) Eurasian stations.

Figure 13. Trends in freshet length during the period 1980 – 2000 for a) Mackenzie and b) Eurasian stations.

Figure 14. Trends in peak freshet magnitude during the period 1962 – 2000 for a) Mackenzie and b) Eurasian stations.

Figure 15. Trends in peak freshet magnitude during the period 1980 – 2000 for a) Mackenzie and b) Eurasian stations.

Figure 16. Trends in freshet volume during the period 1962 – 2000 for a) Mackenzie and b) Eurasian stations.

Figure 17. Trends in freshet volume during the period 1980 – 2000 for a) Mackenzie and b) Eurasian stations.

Figure 18. Trends in April through July volume during the period 1962 – 2000 for a) Mackenzie and b) Eurasian stations.

Figure 19. Trends in April through July volume during the period 1980 – 2000 for a) Mackenzie and b) Eurasian stations.

Figure 20. Trends in April volume during the period 1962 – 2000 for a) Mackenzie and b) Eurasian stations.

Figure 21. Trends in April volume during the period 1980 – 2000 for a) Mackenzie and b) Eurasian stations.

Figure 22. Trends in May volume during the period 1962 – 2000 for a) Mackenzie and b) Eurasian stations.

Figure 23. Trends in May volume during the period 1980 – 2000 for a) Mackenzie and b) Eurasian stations.

Figure 24. Trends in June volume during the period 1962 – 2000 for a) Mackenzie and b) Eurasian stations.

Figure 25. Trends in June volume during the period 1980 – 2000 for a) Mackenzie and b) Eurasian stations.

Figure 26. Trends in July volume during the period 1962 – 2000 for a) Mackenzie and b) Eurasian stations.

Figure 27. Trends in July volume during the period 1980 – 2000 for a) Mackenzie and b) Eurasian stations.

Figure 28. Annual rank of standardized freshet a) volumes and b) magnitudes for major Mackenzie sub-basin stations, based on the top 25% of standardized freshet volumes (magnitudes) at Mackenzie River outlet station during the period 1980 - 2000.

Figure 29. Annual rank of standardized freshet a) volumes and b) magnitudes for major Ob sub-basin stations, based on the top 25% of standardized freshet volumes (magnitudes) at Ob River outlet station during the period 1980 - 2000.

Figure 30. Annual rank of standardized freshet a) volumes and b) magnitudes for major Yenisei sub-basin stations, based on the top 25% of standardized freshet volumes (magnitudes) at Yenisei River outlet station during the period 1980 - 2000.

Figure 31. Annual rank of standardized freshet a) volumes and b) magnitudes for major Lena sub-basin stations, based on the top 25% of standardized freshet volumes (magnitudes) at Lena River outlet station during the period 1980 - 2000.

Figure 32. Station sub-basins that display a) a high freshet volume and b) a low freshet volume during corresponding years of the top (bottom) 25% of freshet volumes at the Mackenzie River outlet station 10LC014 during the period 1980 - 2000. Stations shown are significantly different from their periodic mean based on a t test at a 95% confidence level.

Figure 33. Station sub-basins that display a) a high freshet magnitude and b) a low freshet magnitude during corresponding years of the top (bottom) 25% of freshet magnitudes at the Mackenzie River outlet station 10LC014 during the period 1980 - 2000. Stations shown are significantly different from their periodic mean based on a t test at a 95% confidence level.

Figure 34. Station sub-basins that display a) a high freshet volume and b) a low freshet volume during corresponding years of the top (bottom) 25% of freshet volumes at Eurasian outlet

stations during the period 1980 - 2000. Stations shown are significantly different from their periodic mean based on a t test at a 95% confidence level.

Figure 35. Station sub-basins that display a) a high freshet magnitude and b) a low freshet magnitude during corresponding years of the top (bottom) 25% of freshet magnitudes at Eurasian outlet stations during the period 1980 - 2000. Stations shown are significantly different from their periodic mean based on a t test at a 95% confidence level.

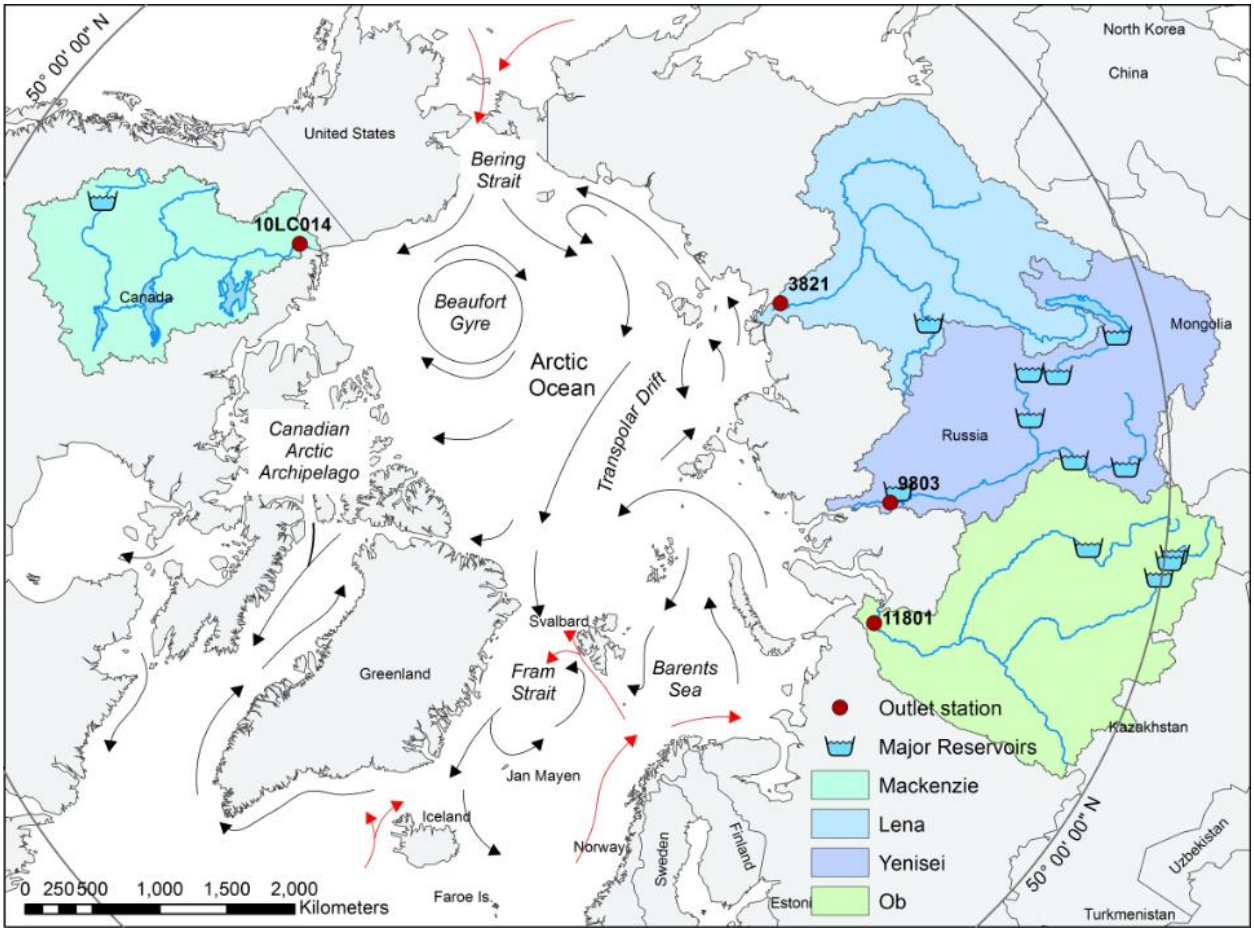

Figure 1. Map showing the Arctic Ocean, ocean features, major surface currents, major reservoirs and drainage basins and outlet stations of the Mackenzie, Ob, Yenisei and Lena rivers. Red arrows denote warmer currents, while black arrows denote colder currents. Adapted from Figure 6 in McClelland et al. (2011).

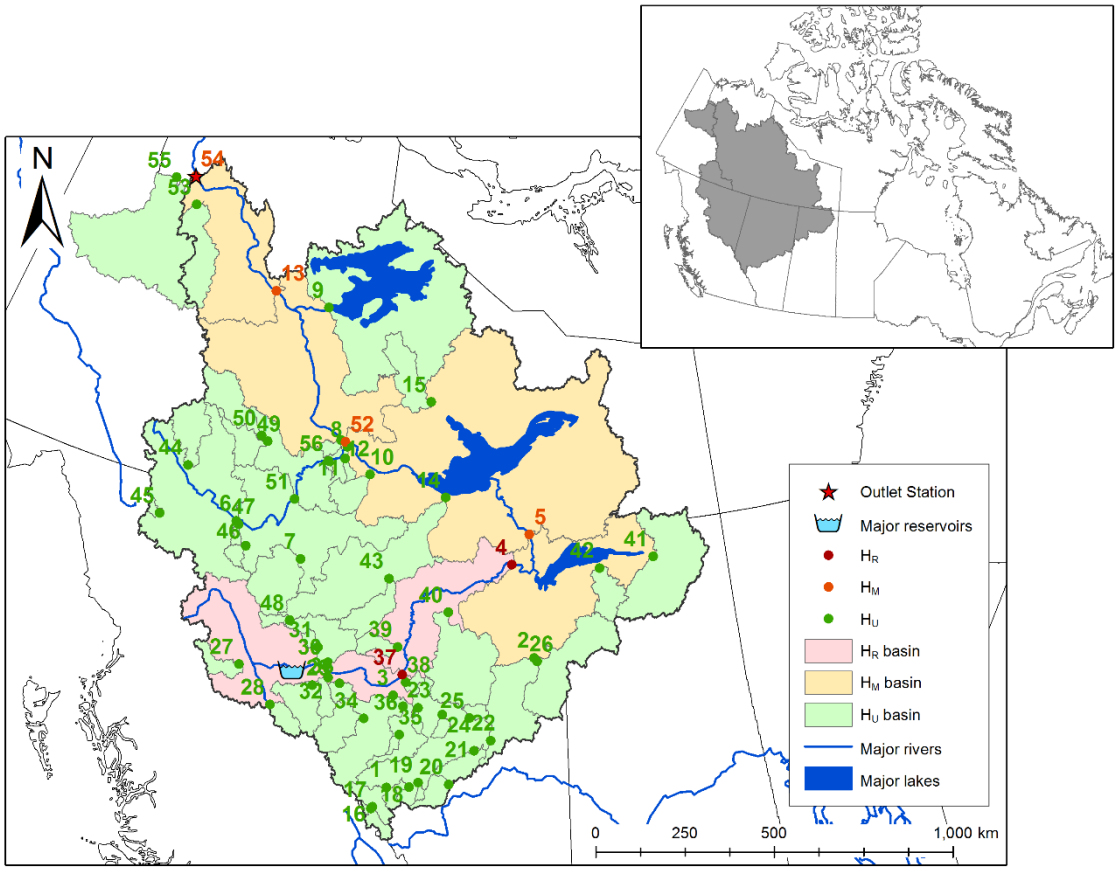

Figure 2. Study area of the Mackenzie basin showing station locations labeled with a unique identifier and station sub-basin drainage areas. Stations and basins are colour-coded and classified as regulated (H_R), minimally regulated (H_M) or unregulated (H_U). Station descriptions are provided in Table 2.

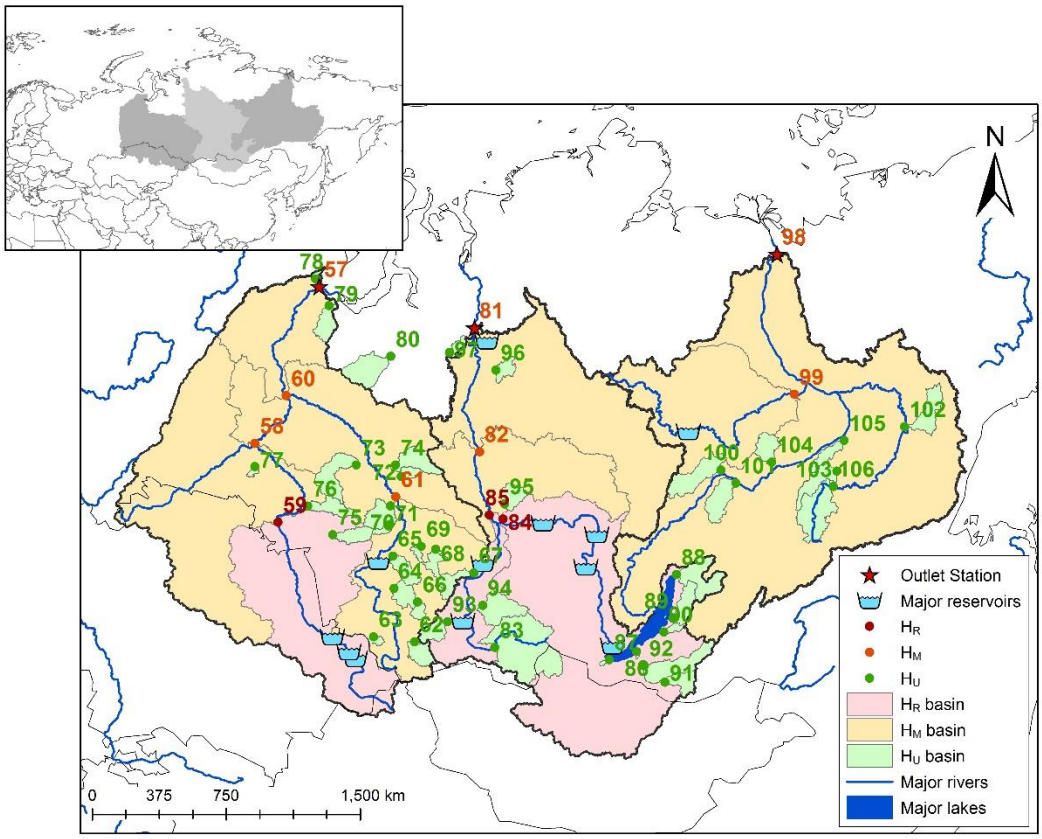

Figure 3. Study area of the (left to right in inset map) Ob, Yenisei and Lena basins showing station locations labeled with a unique identifier and station sub-basin drainage areas. Stations and basins are colour-coded and classified as regulated (H_R), minimally regulated (H_M) or unregulated (H_U). Station descriptions are provided in Table 2.

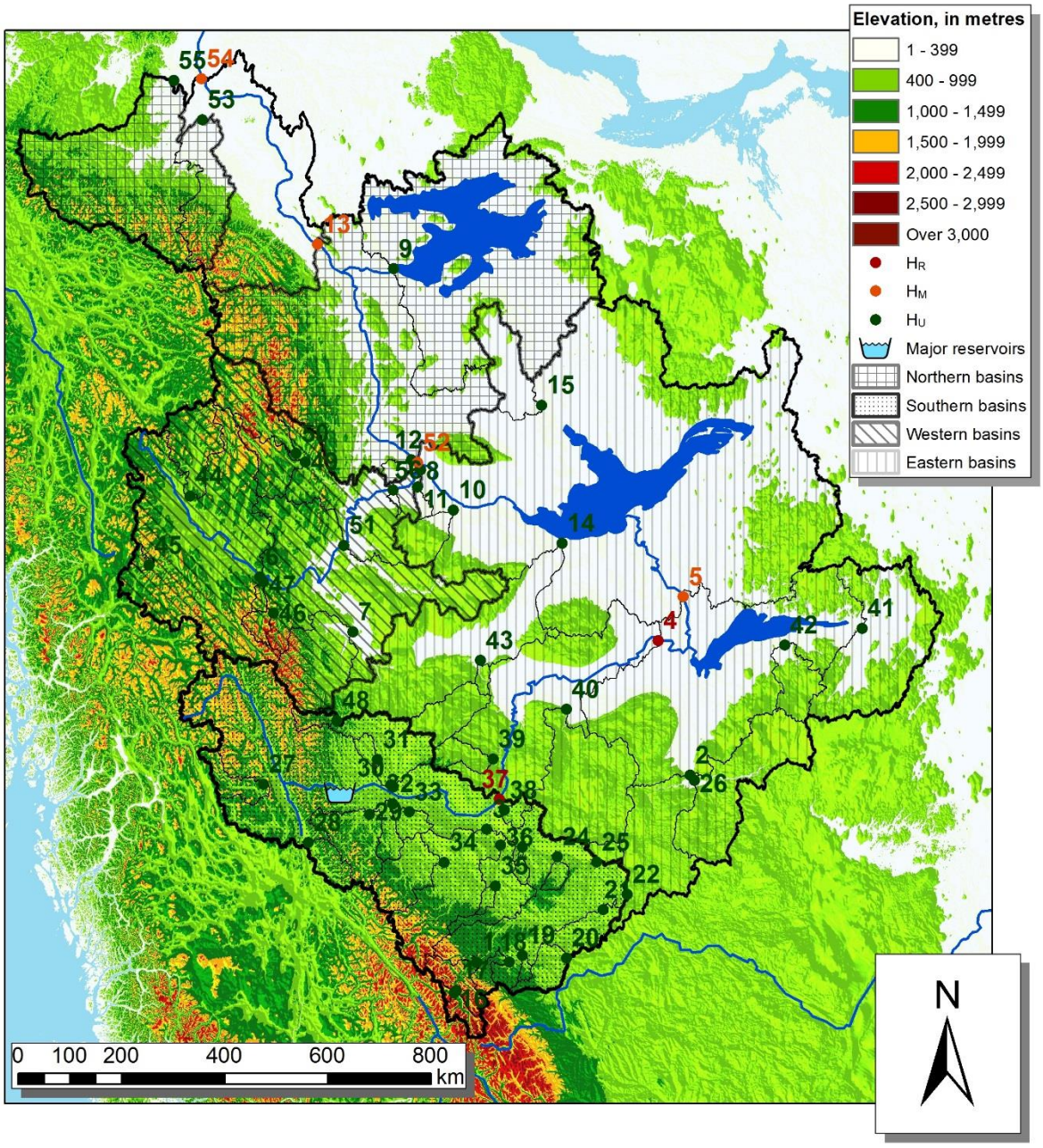

Figure 4. Topographical map of the Mackenzie basin showing regional classification of sub-basins into Northern, Southern, Western and Eastern regions. Outlet stations are not included in the classification.

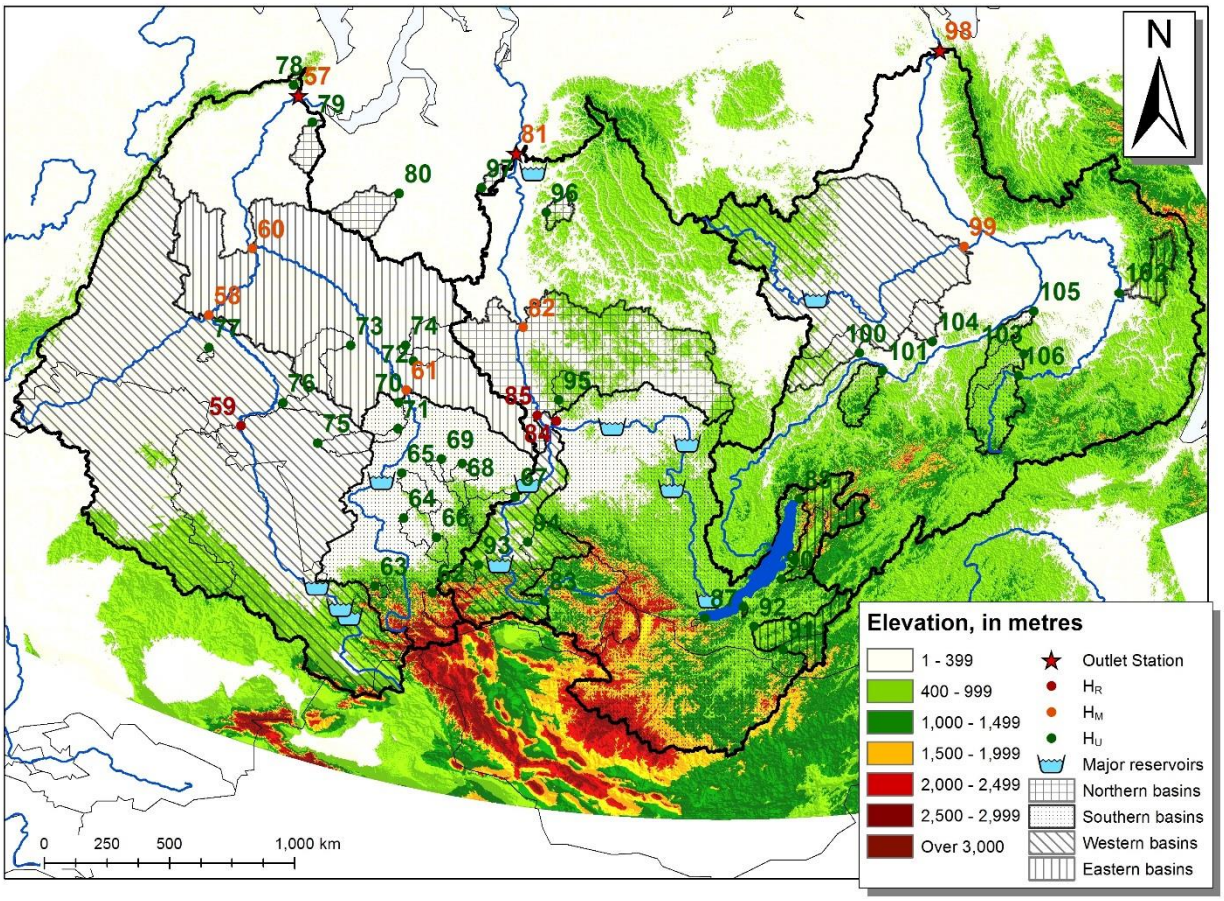

Figure 5. Topographical map of the Eurasian basins showing regional classification of sub-basins into Northern, Southern, Western and Eastern regions. Outlet stations are not included in the classification.

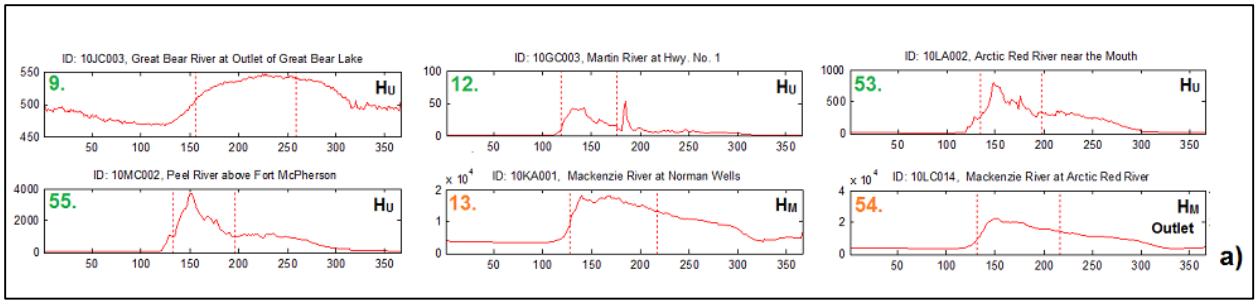

Figure 6a. Average annual hydrographs (discharge [m^3s^{-1}] versus Julian day) of Mackenzie station sub-basins for 1962 – 2000 (blue line) and 1980 – 2000 (red line), grouped by northern regions. Stations which exclusively show red series have data for 1980 – 2000 only. Dashed vertical red line pairs denote freshest start and end dates for 1980 – 2000.

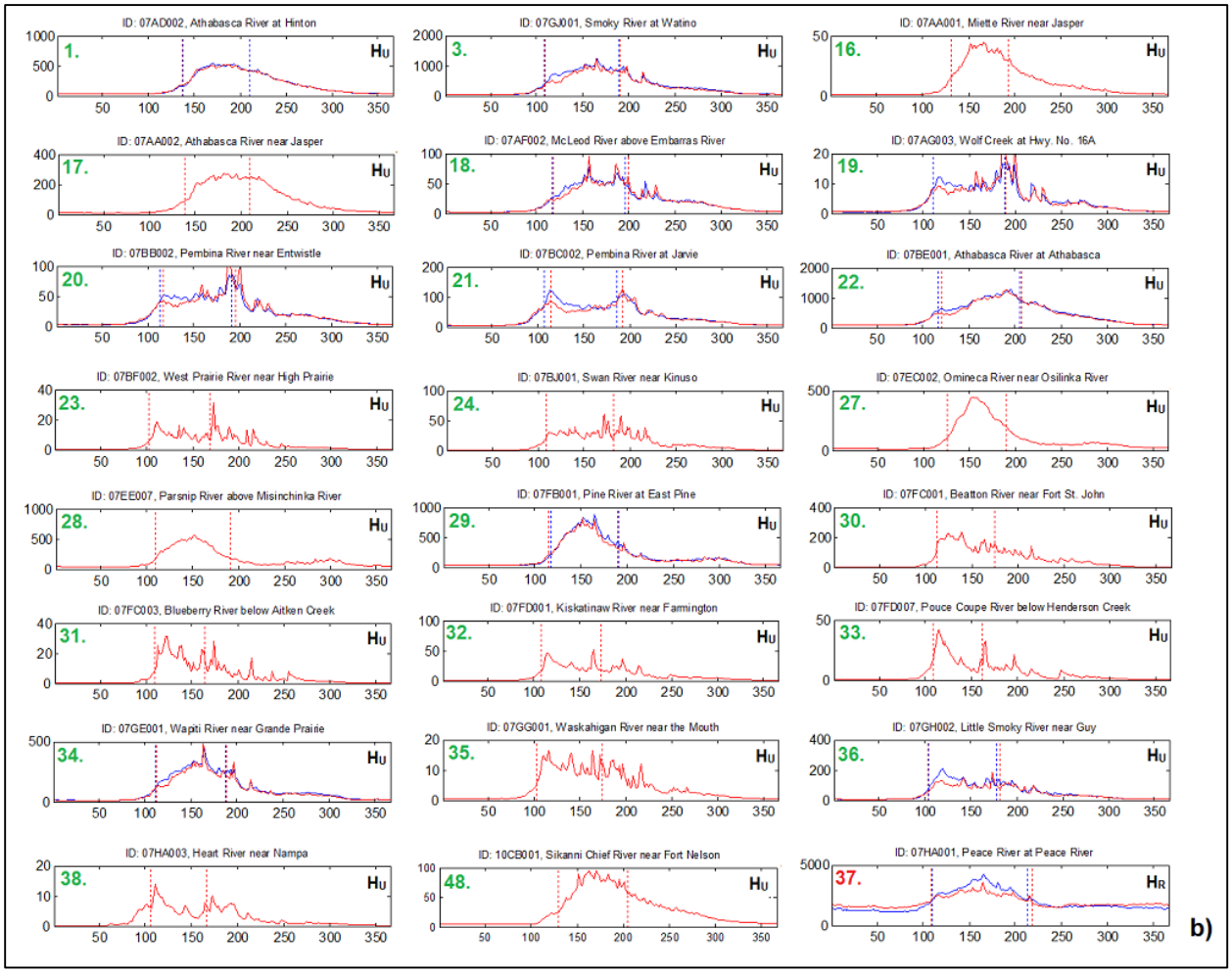

Figure 6b. Average annual hydrographs (discharge [m^3s^{-1}] versus Julian day) of Mackenzie station sub-basins for 1962 – 2000 (blue line) and 1980 – 2000 (red line), grouped by southern regions. Stations which exclusively show red series have data for 1980 – 2000 only. Dashed vertical blue line pairs denote freshet start and end dates for 1962 – 2000 respectively, while dashed vertical red line pairs denote freshest start and end dates for 1980 – 2000 respectively.

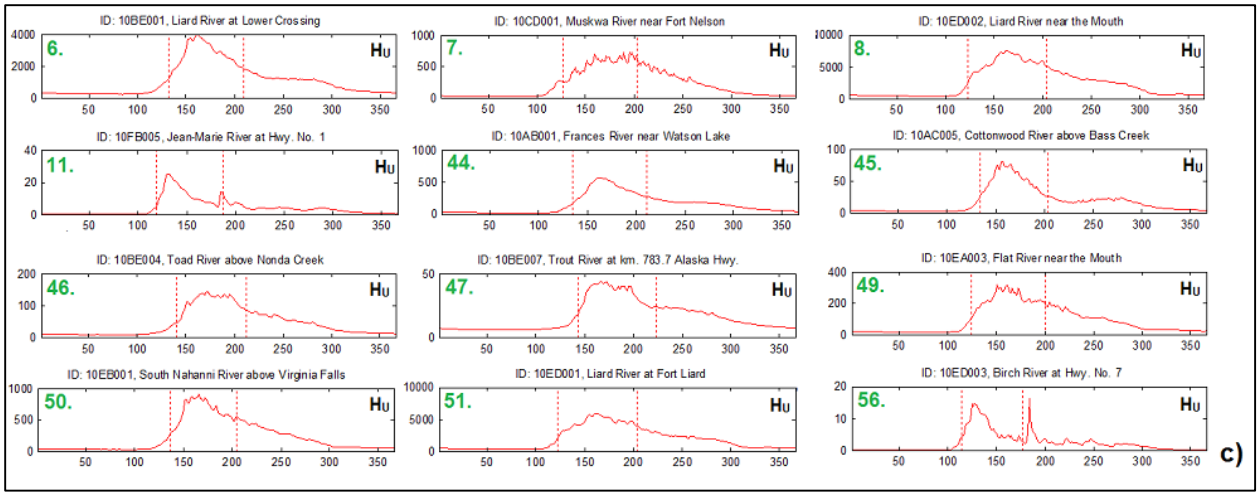

Figure 6c. Average annual hydrographs (discharge [m^3s^{-1}] versus Julian day) of Mackenzie station sub-basins for 1962 – 2000 (blue line) and 1980 – 2000 (red line), grouped by western regions. Stations which exclusively show red series have data for 1980 – 2000 only. Dashed vertical red line pairs denote freshest start and end dates for 1980 – 2000.

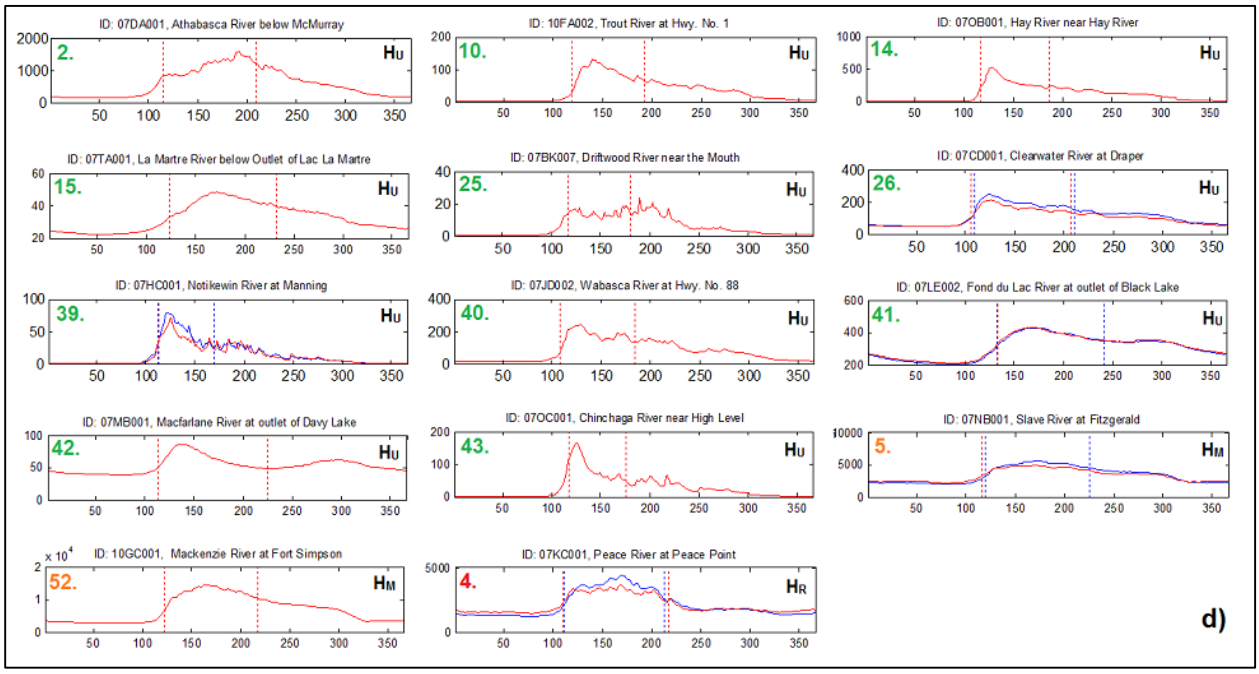

Figure 6d. Average annual hydrographs (discharge [m^3s^{-1}] versus Julian day) of Mackenzie station sub-basins for 1962 – 2000 (blue line) and 1980 – 2000 (red line), grouped by eastern regions. Stations which exclusively show red series have data for 1980 – 2000 only. Dashed vertical blue line pairs denote freshet start and end dates for 1962 – 2000 respectively, while dashed vertical red line pairs denote freshest start and end dates for 1980 – 2000 respectively.

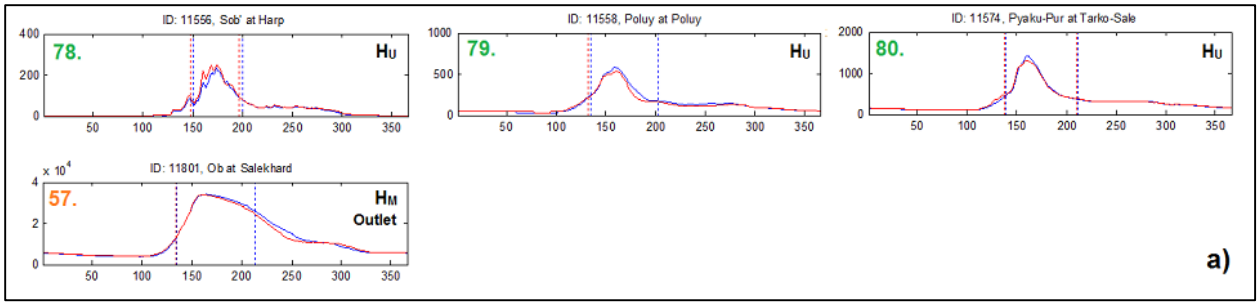

Figure 7a. Average annual hydrographs (discharge [m^3s^{-1}] versus Julian day) of Ob station sub-basins for 1962 – 2000 (blue line) and 1980 – 2000 (red line), grouped by northern regions. Stations which exclusively show red series have data for 1980 – 2000 only. Dashed vertical blue line pairs denote freshet start and end dates for 1962 – 2000 respectively, while dashed vertical red line pairs denote freshest start and end dates for 1980 – 2000 respectively.

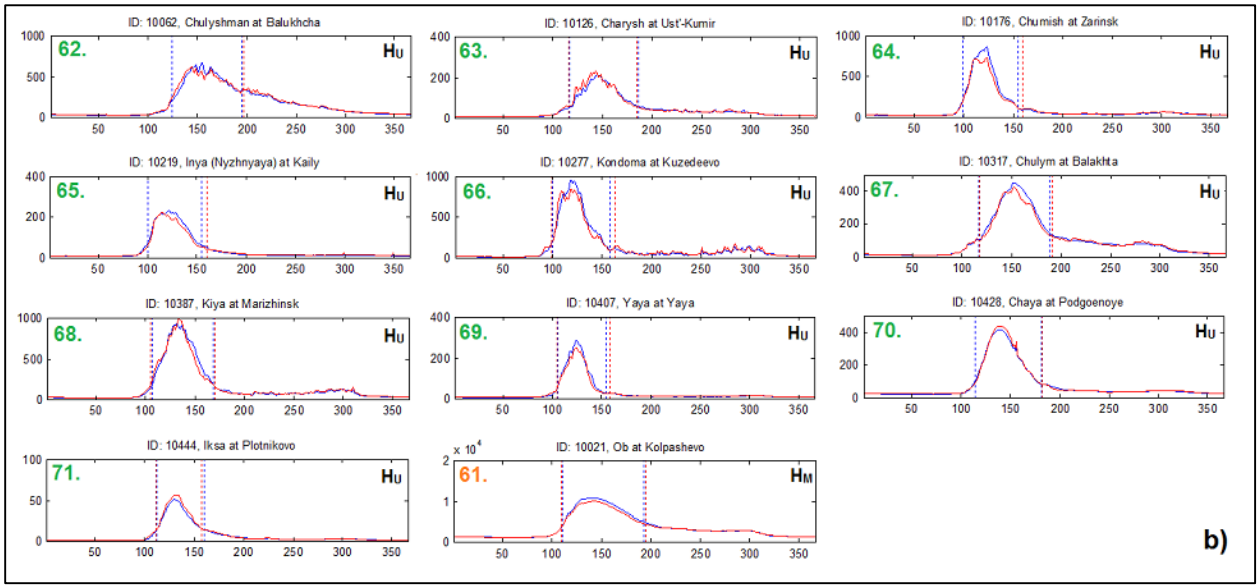

Figure 7b. Average annual hydrographs (discharge [m^3s^{-1}] versus Julian day) of Ob station sub-basins for 1962 – 2000 (blue line) and 1980 – 2000 (red line), grouped by southern regions. Stations which exclusively show red series have data for 1980 – 2000 only. Dashed vertical blue line pairs denote freshet start and end dates for 1962 – 2000 respectively, while dashed vertical red line pairs denote freshest start and end dates for 1980 – 2000 respectively.

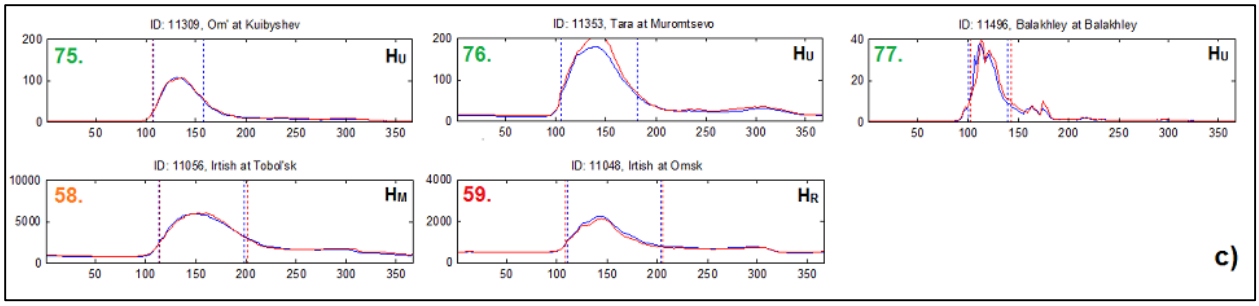

Figure 7c. Average annual hydrographs (discharge [m^3s^{-1}] versus Julian day) of Ob station sub-basins for 1962 – 2000 (blue line) and 1980 – 2000 (red line), grouped by western regions. Stations which exclusively show red series have data for 1980 – 2000 only. Dashed vertical blue line pairs denote freshet start and end dates for 1962 – 2000 respectively, while dashed vertical red line pairs denote freshest start and end dates for 1980 – 2000 respectively.

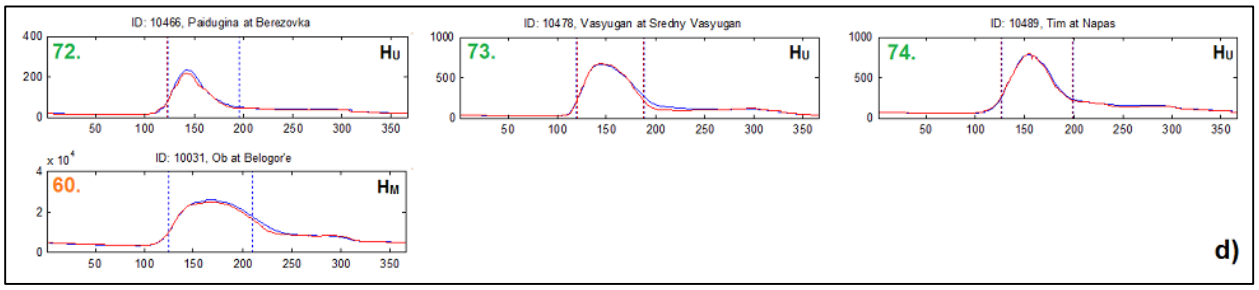

Figure 7d. Average annual hydrographs (discharge [m^3s^{-1}] versus Julian day) of Ob station sub-basins for 1962 – 2000 (blue line) and 1980 – 2000 (red line), grouped by eastern regions. Stations which exclusively show red series have data for 1980 – 2000 only. Dashed vertical blue line pairs denote freshet start and end dates for 1962 – 2000 respectively, while dashed vertical red line pairs denote freshest start and end dates for 1980 – 2000 respectively.

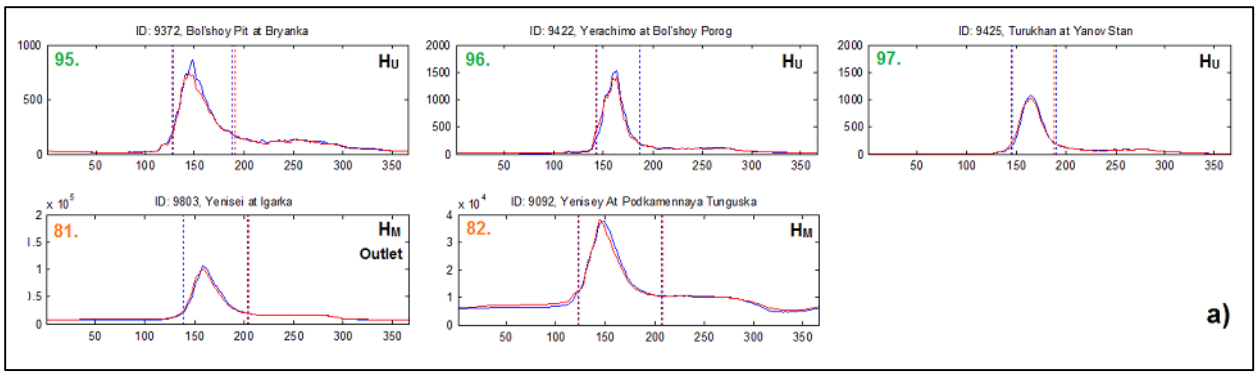

Figure 8a. Average annual hydrographs (discharge [m^3s^{-1}] versus Julian day) of Yenisei station sub-basins for 1962 – 2000 (blue line) and 1980 – 2000 (red line), grouped by northern regions. Stations which exclusively show red series have data for 1980 – 2000 only. Dashed vertical blue line pairs denote freshet start and end dates for 1962 – 2000 respectively, while dashed vertical red line pairs denote freshest start and end dates for 1980 – 2000 respectively.

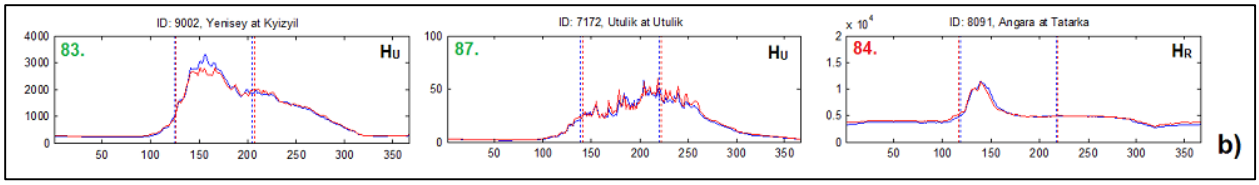

Figure 8b. Average annual hydrographs (discharge [m^3s^{-1}] versus Julian day) of Yenisei station sub-basins for 1962 – 2000 (blue line) and 1980 – 2000 (red line), grouped by southern regions. Stations which exclusively show red series have data for 1980 – 2000 only. Dashed vertical blue line pairs denote freshet start and end dates for 1962 – 2000 respectively, while dashed vertical red line pairs denote freshest start and end dates for 1980 – 2000 respectively.

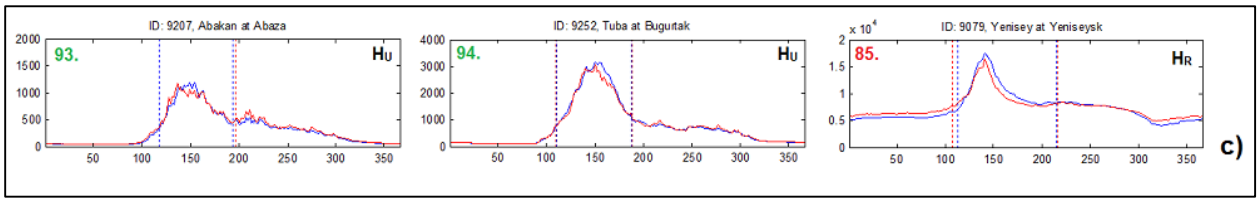

Figure 8c. Average annual hydrographs (discharge [m^3s^{-1}] versus Julian day) of Yenisei station sub-basins for 1962 – 2000 (blue line) and 1980 – 2000 (red line), grouped by western regions. Stations which exclusively show red series have data for 1980 – 2000 only. Dashed vertical blue line pairs denote freshet start and end dates for 1962 – 2000 respectively, while dashed vertical red line pairs denote freshest start and end dates for 1980 – 2000 respectively.

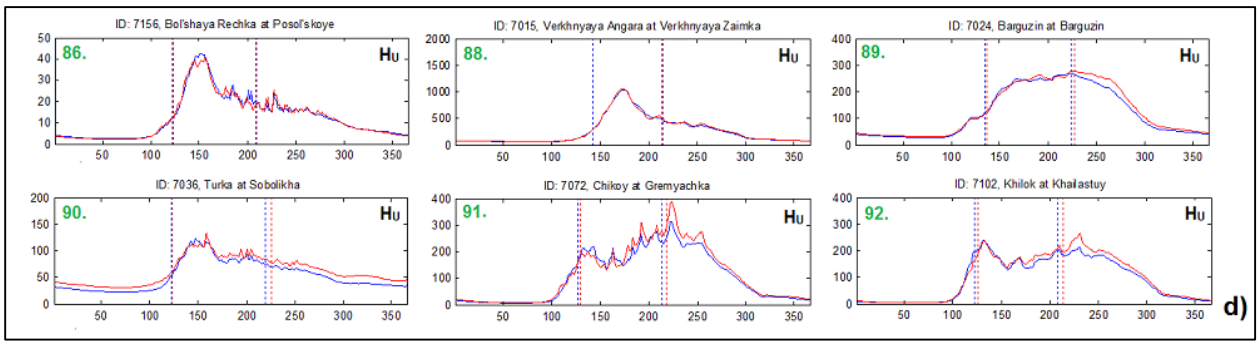

Figure 8d. Average annual hydrographs (discharge [m^3s^{-1}] versus Julian day) of Yenisei station sub-basins for 1962 – 2000 (blue line) and 1980 – 2000 (red line), grouped by eastern regions. Stations which exclusively show red series have data for 1980 – 2000 only. Dashed vertical blue line pairs denote freshet start and end dates for 1962 – 2000 respectively, while dashed vertical red line pairs denote freshest start and end dates for 1980 – 2000 respectively.

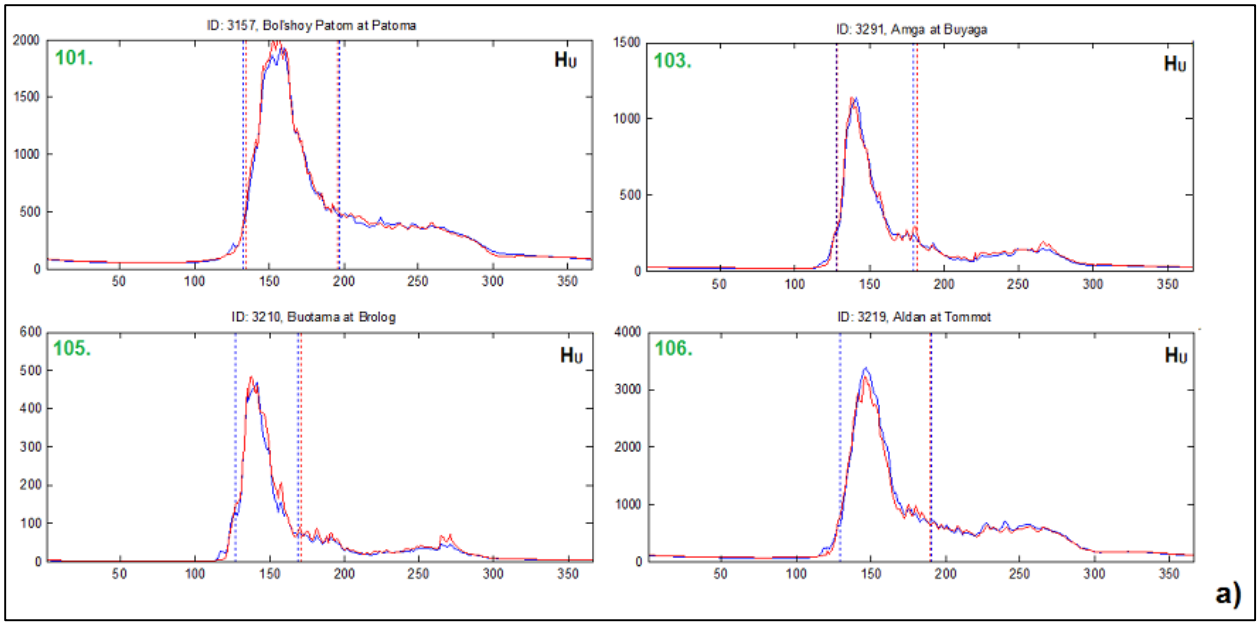

Figure 9a. Average annual hydrographs (discharge [m^3s^{-1}] versus Julian day) of Lena station sub-basins for 1962 – 2000 (blue line) and 1980 – 2000 (red line), grouped by southern regions. Stations which exclusively show red series have data for 1980 – 2000 only. Dashed vertical blue line pairs denote freshet start and end dates for 1962 – 2000 respectively, while dashed vertical red line pairs denote freshest start and end dates for 1980 – 2000 respectively.

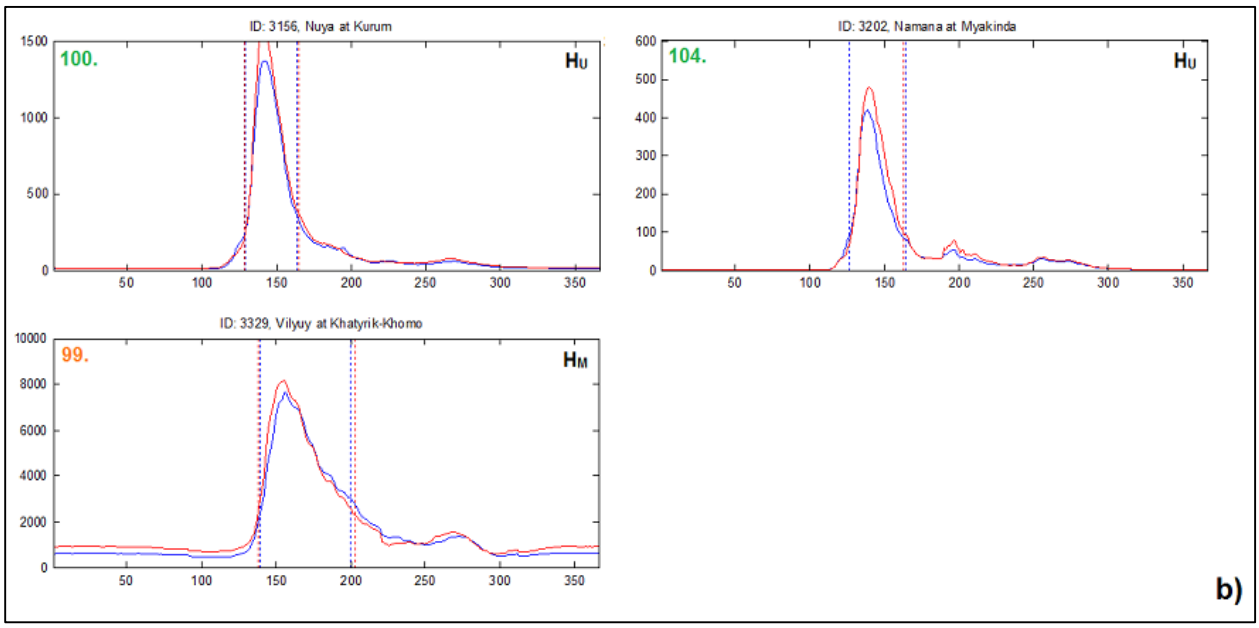

Figure 9b. Average annual hydrographs (discharge [m^3s^{-1}] versus Julian day) of Lena station sub-basins for 1962 – 2000 (blue line) and 1980 – 2000 (red line), grouped by western regions. Stations which exclusively show red series have data for 1980 – 2000 only. Dashed vertical blue line pairs denote freshet start and end dates for 1962 – 2000 respectively, while dashed vertical red line pairs denote freshest start and end dates for 1980 – 2000 respectively.

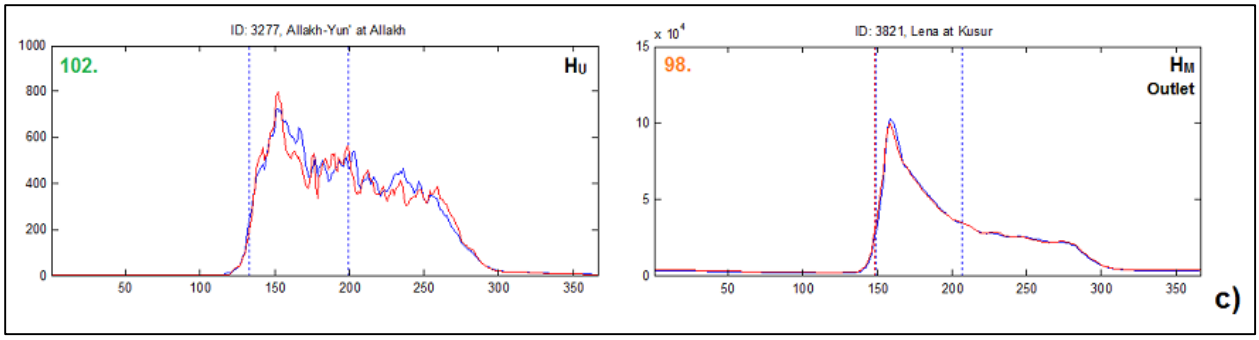

Figure 9c. Average annual hydrographs (discharge [m^3s^{-1}] versus Julian day) of Lena station sub-basins for 1962 – 2000 (blue line) and 1980 – 2000 (red line), grouped by eastern regions. Stations which exclusively show red series have data for 1980 – 2000 only. Dashed vertical blue line pairs denote freshet start and end dates for 1962 – 2000 respectively, while dashed vertical red line pairs denote freshest start and end dates for 1980 – 2000 respectively.

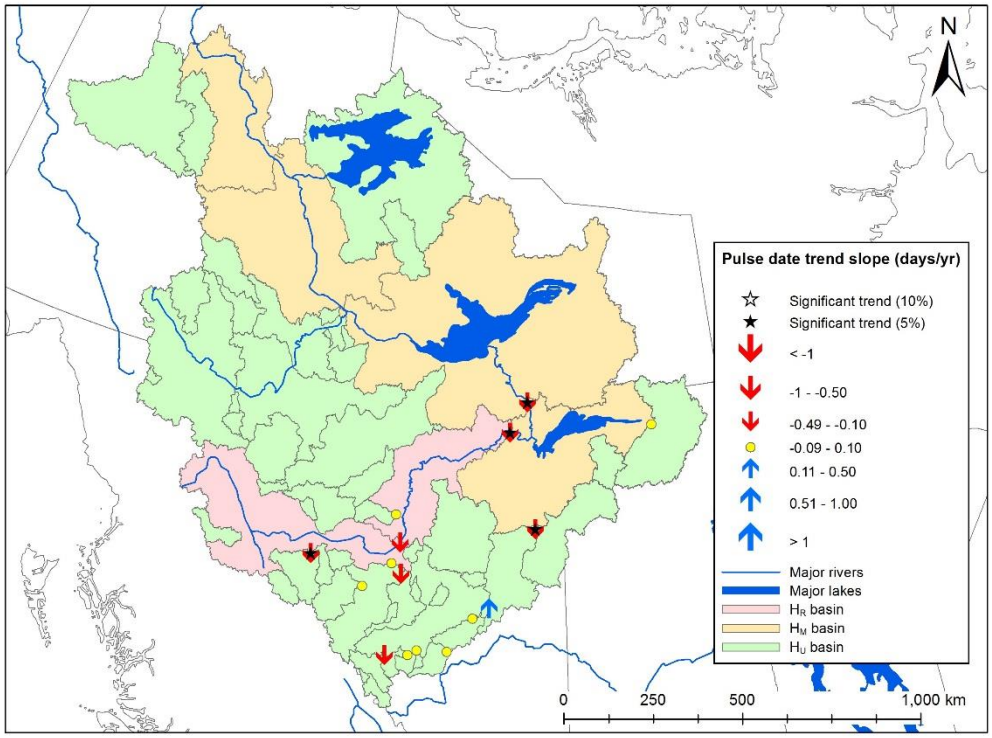

Figure 10a. Trends in freshet pulse dates during the period 1962 – 2000 for Mackenzie stations.

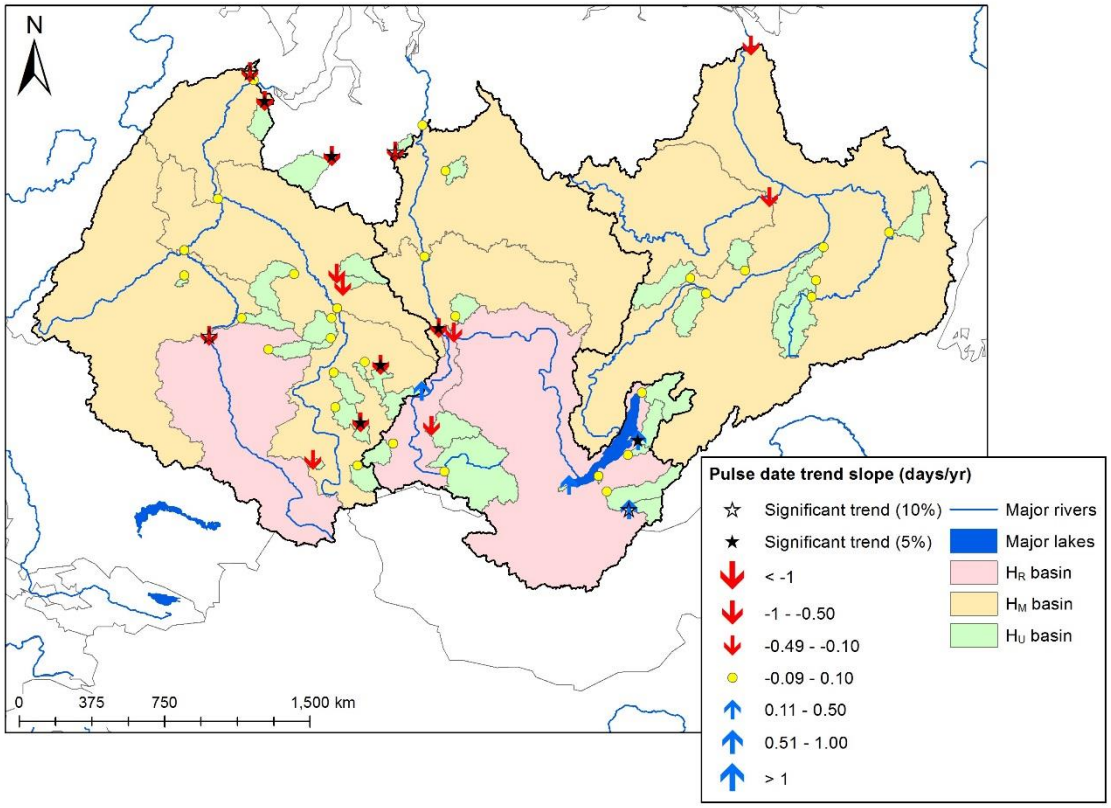

Figure 10b. Trends in freshet pulse dates during the period 1962 – 2000 for Eurasian stations.

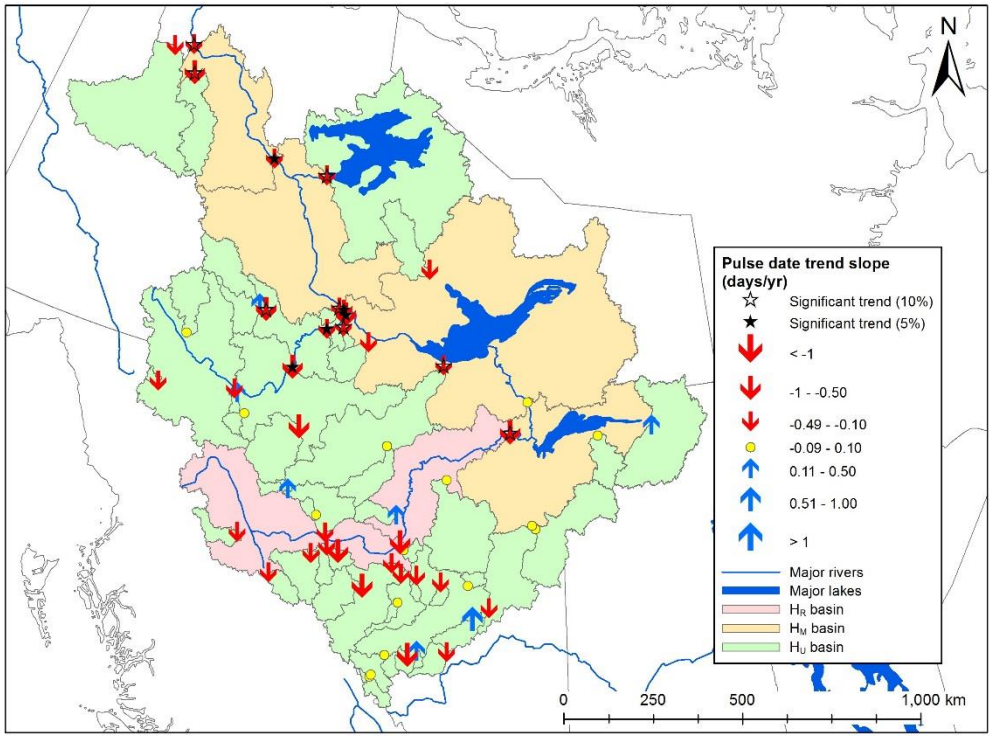

Figure 11a. Trends in freshet pulse dates during the period 1980 – 2000 for Mackenzie stations.

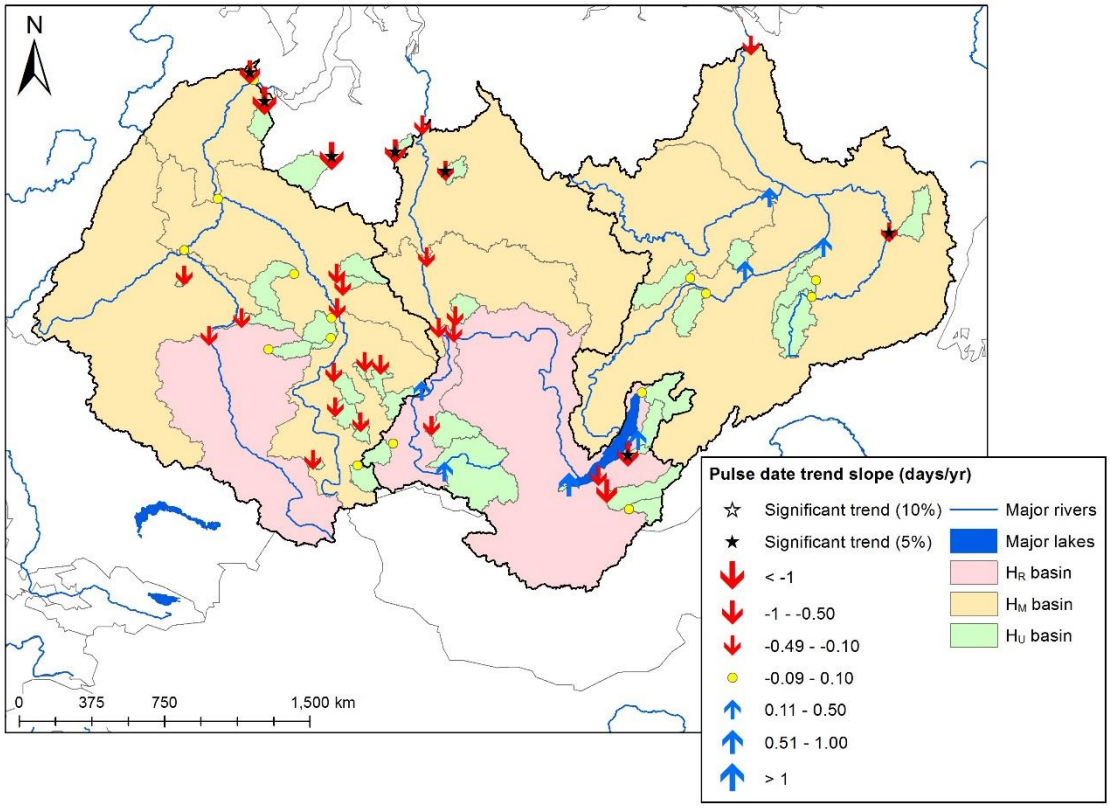

Figure 11b. Trends in freshet pulse dates during the period 1980 – 2000 for Eurasian stations.

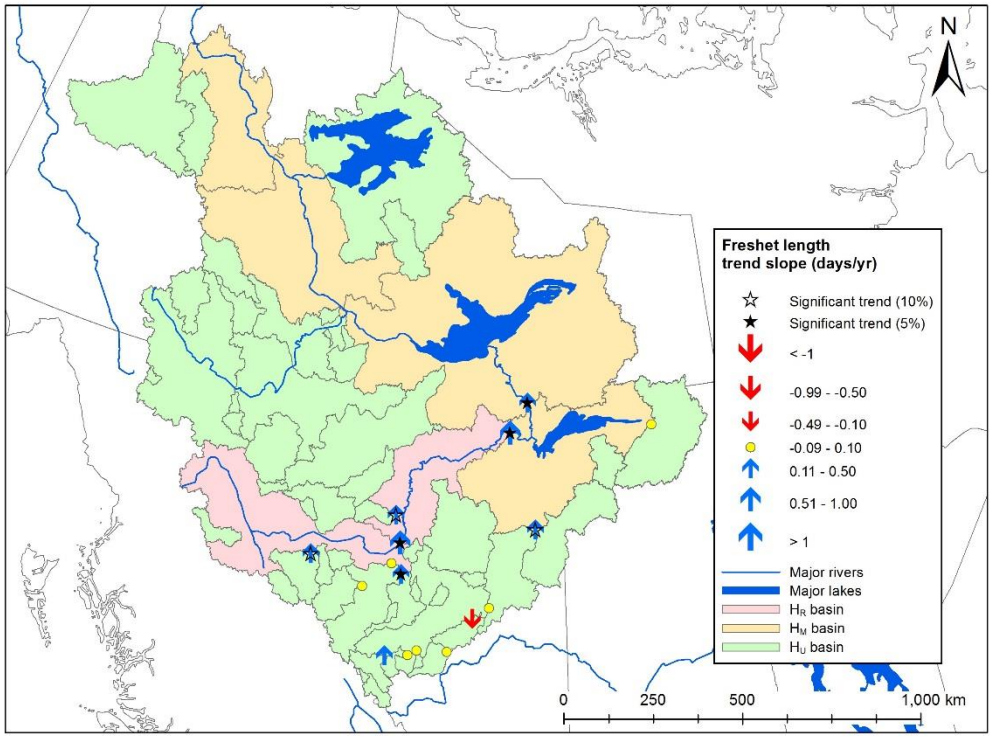

Figure 12a. Trends in freshet length during the period 1962 – 2000 for Mackenzie stations.

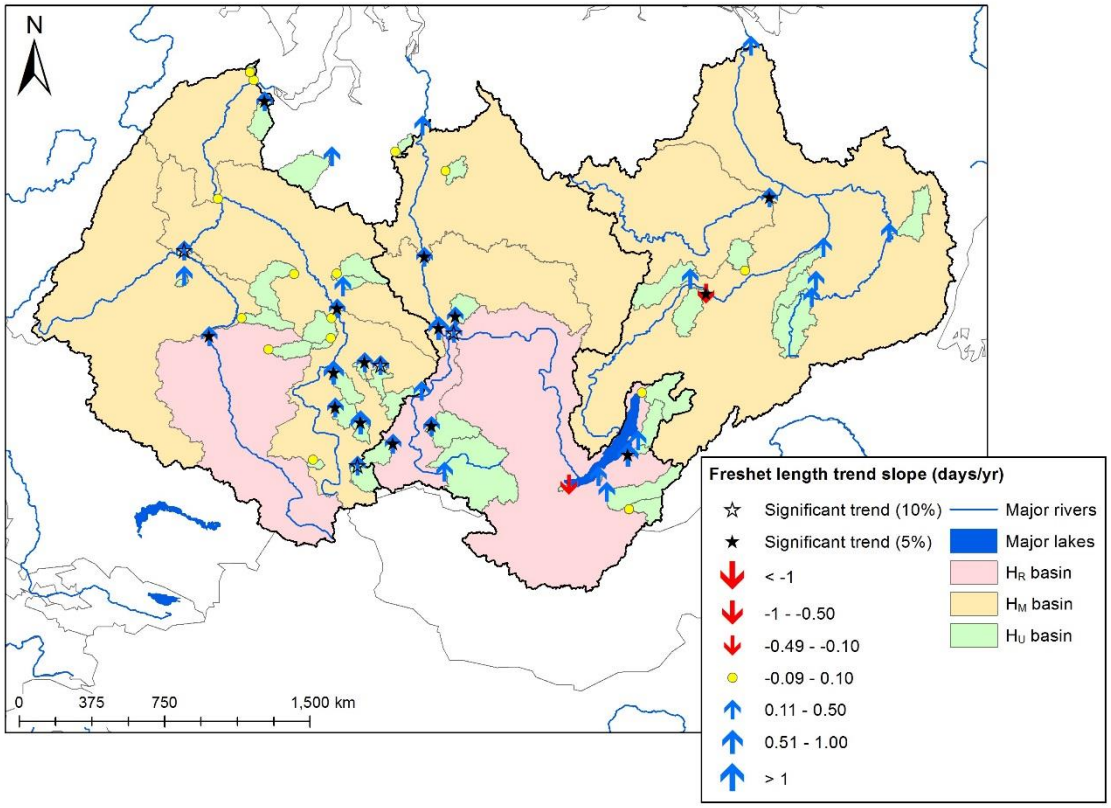

Figure 12b. Trends in freshet length during the period 1962 – 2000 for Eurasian stations.

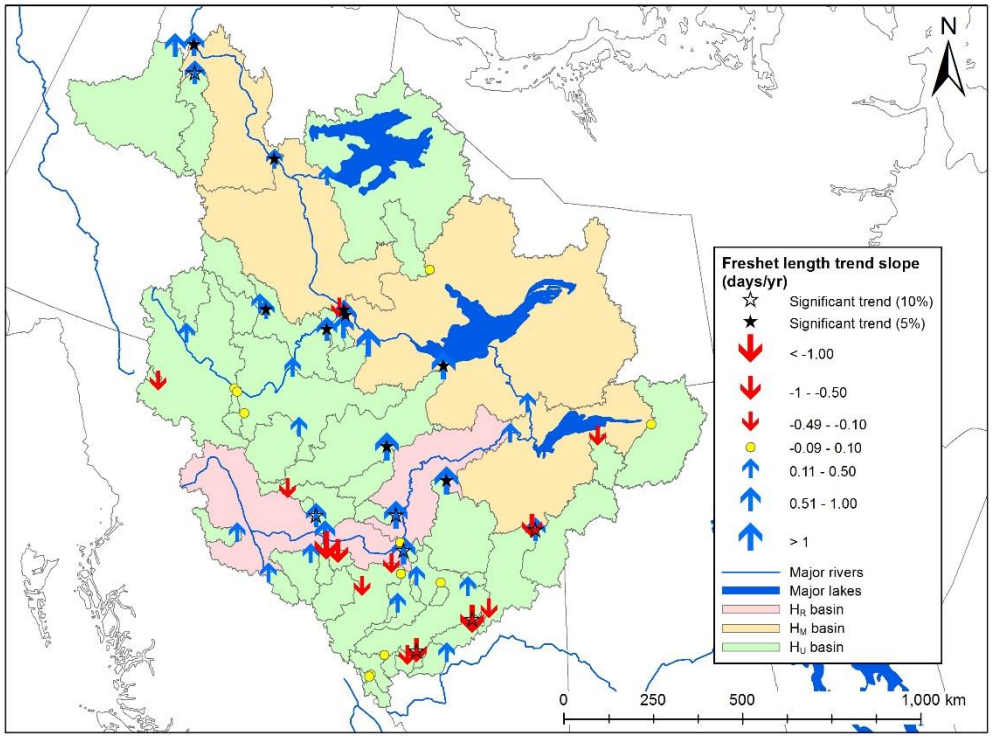

Figure 13a. Trends in freshet length during the period 1980 – 2000 for Mackenzie stations.

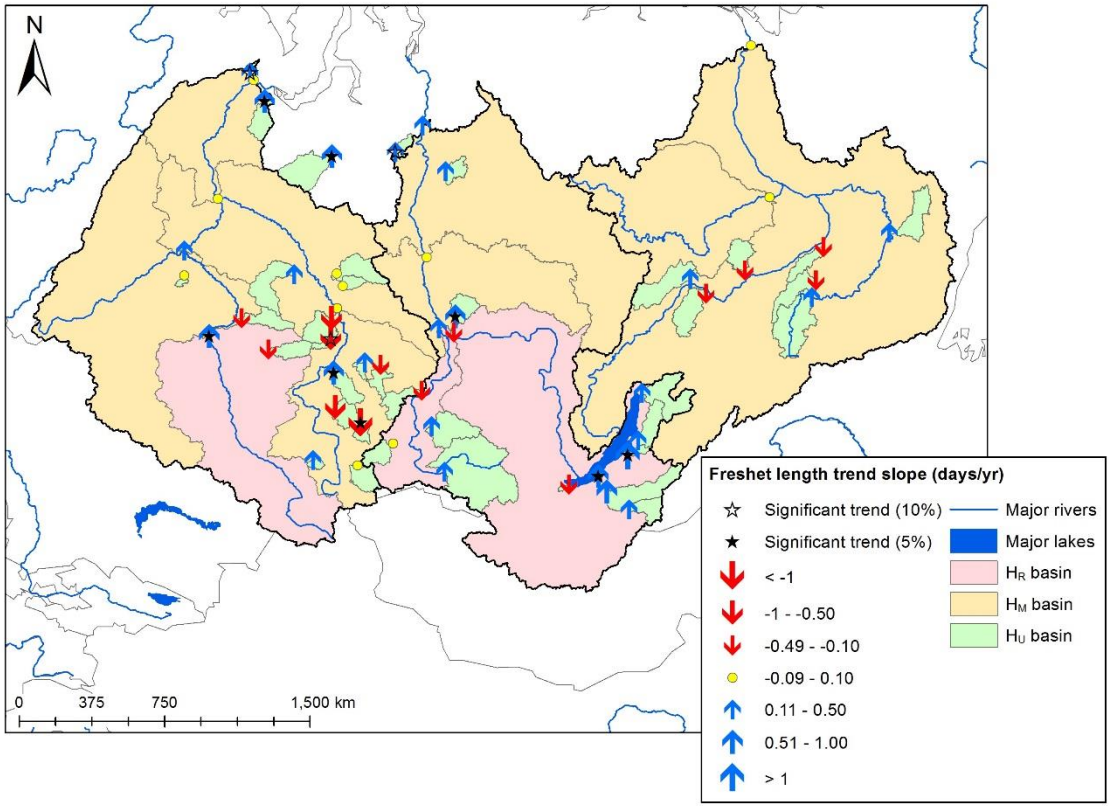

Figure 13b. Trends in freshet length during the period 1980 – 2000 for Eurasian stations.

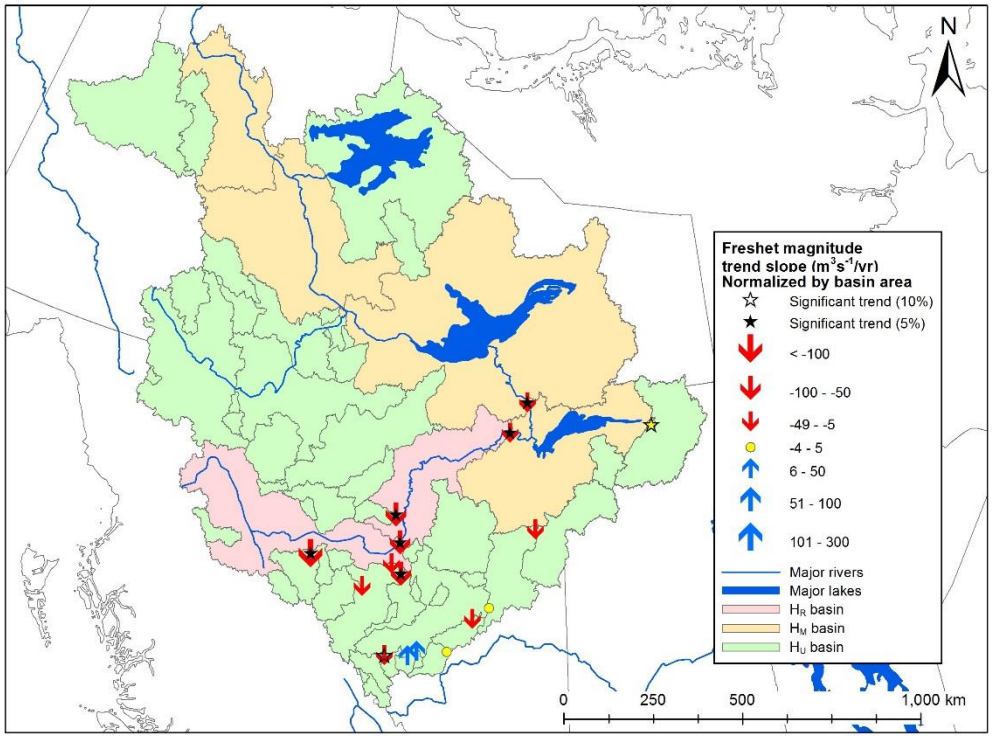

Figure 14a. Trends in freshet magnitude during the period 1962 – 2000 for Mackenzie stations.

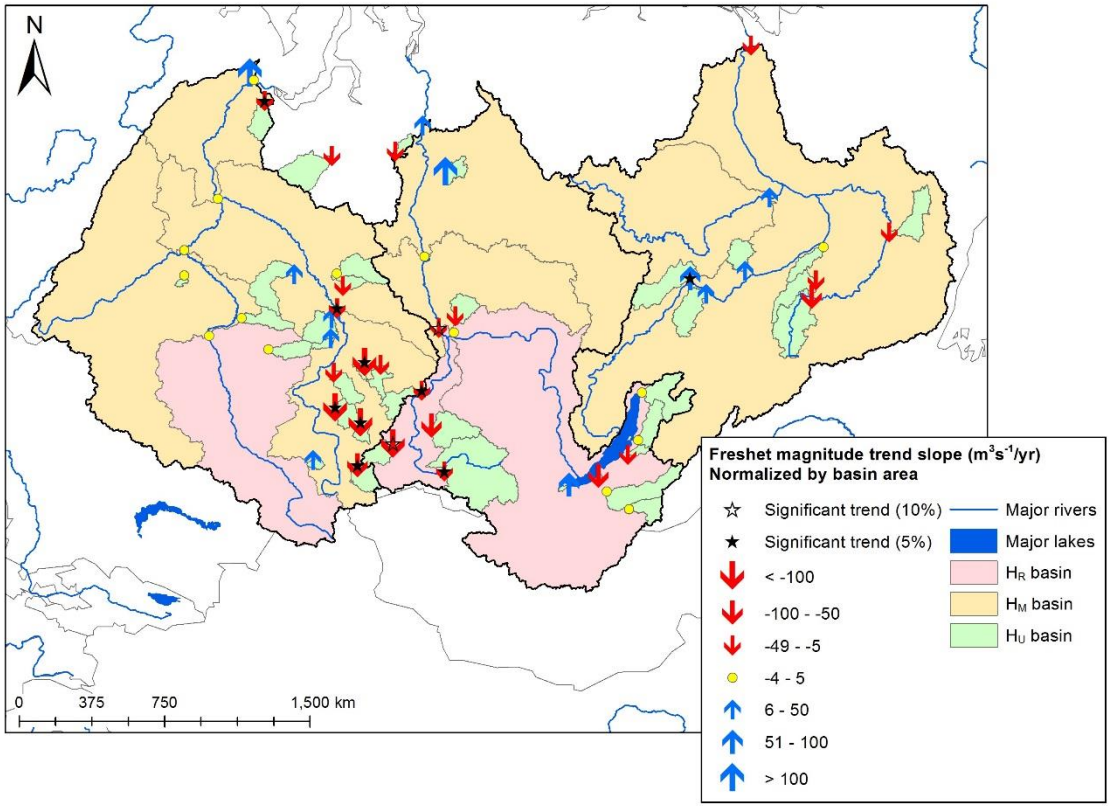

Figure 14b. Trends in freshet magnitude during the period 1962 – 2000 for Eurasian stations.

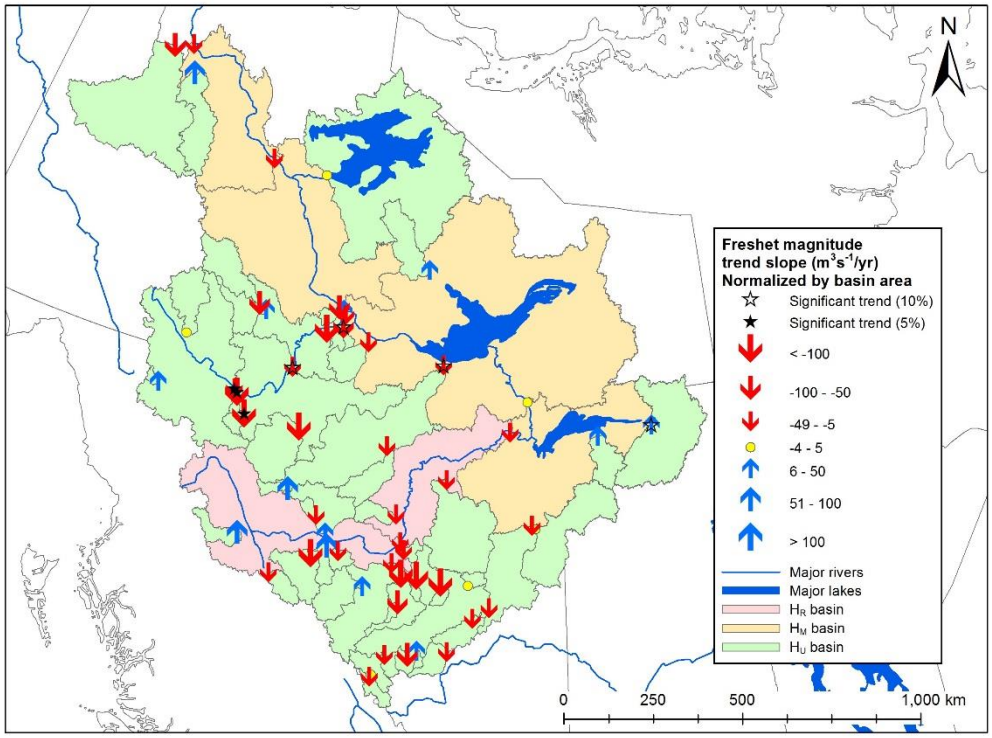

Figure 15a. Trends in freshet magnitude during the period 1980 – 2000 for Mackenzie stations.

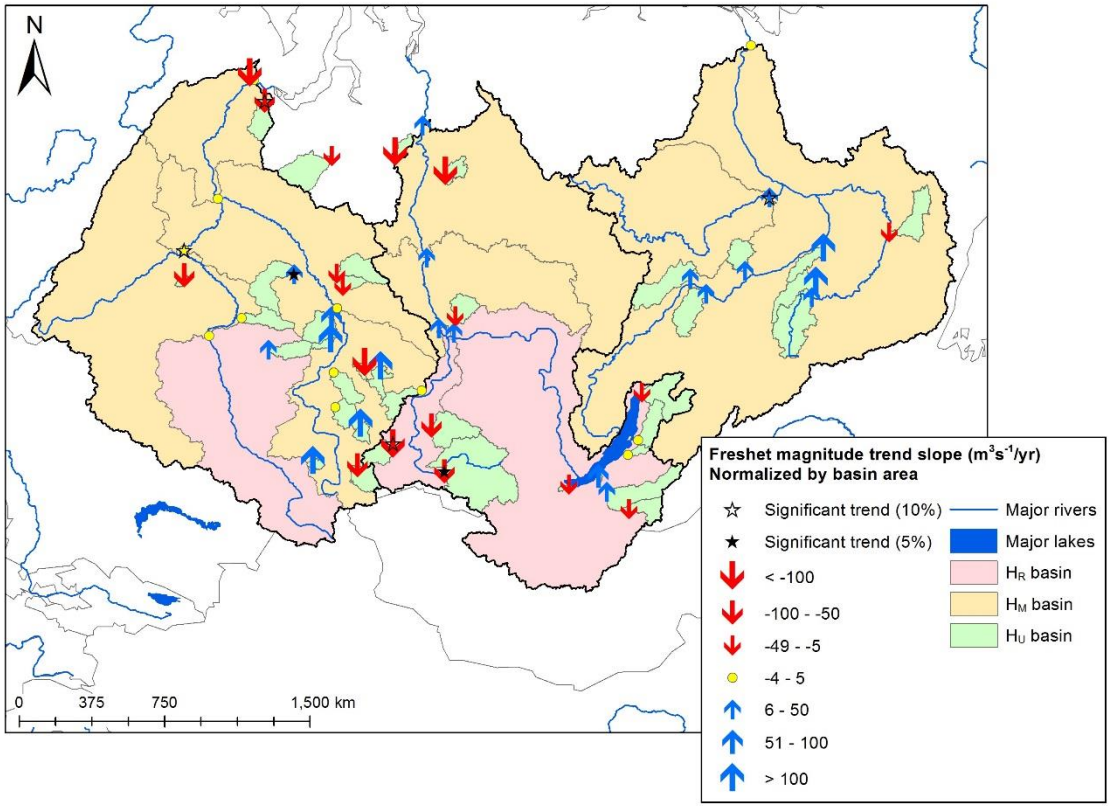

Figure 15b. Trends in freshet magnitude during the period 1980 – 2000 for Eurasian stations.

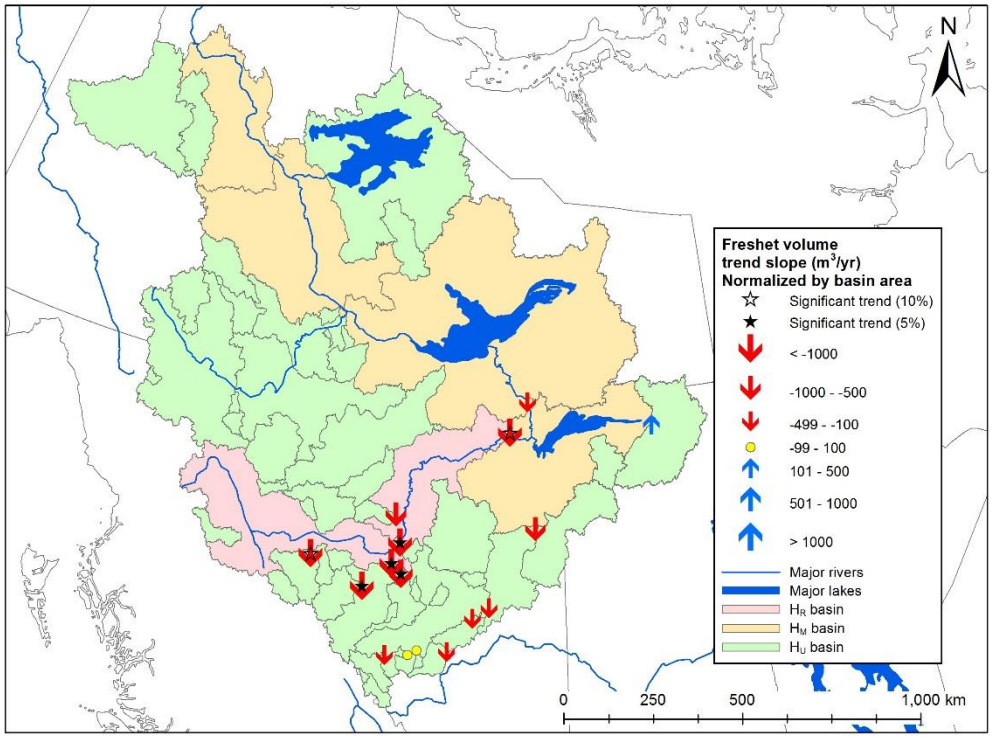

Figure 16a. Trends in freshet volume during the period 1962 – 2000 for Mackenzie stations.

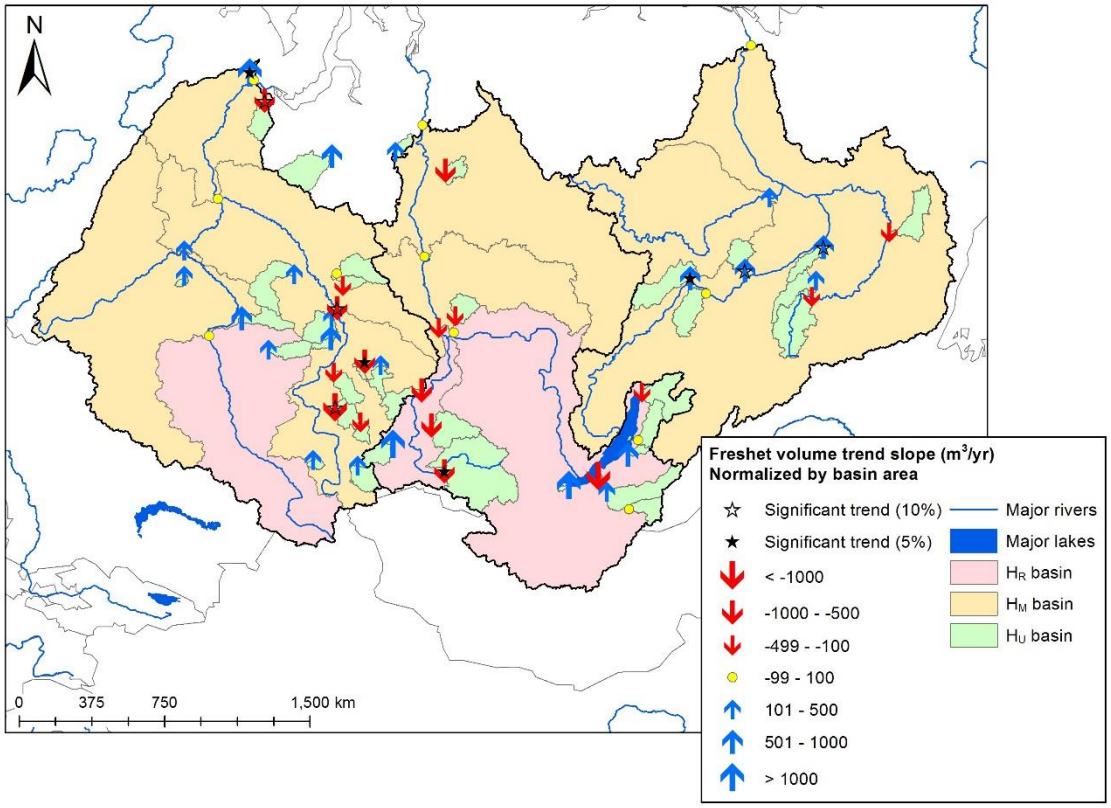

Figure 16b. Trends in freshet volume during the period 1962 – 2000 for Eurasian stations.

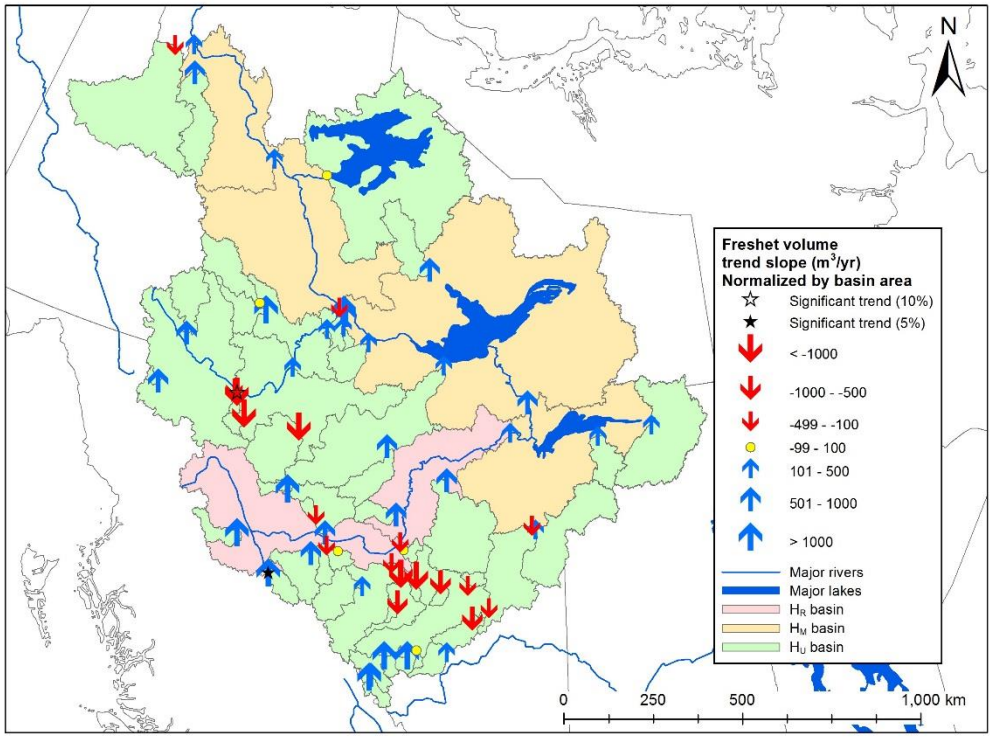

Figure 17a. Trends in freshet volume during the period 1980 – 2000 for Mackenzie stations.

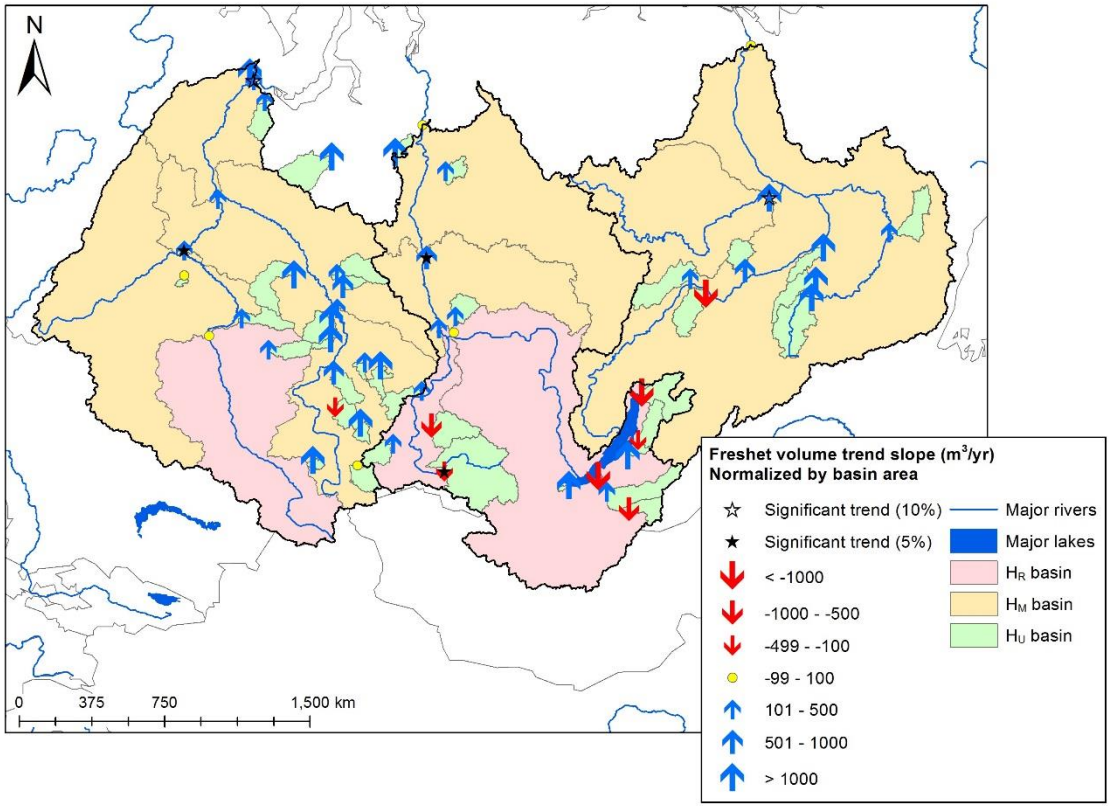

Figure 17b. Trends in freshet volume during the period 1980 – 2000 for Eurasian stations.

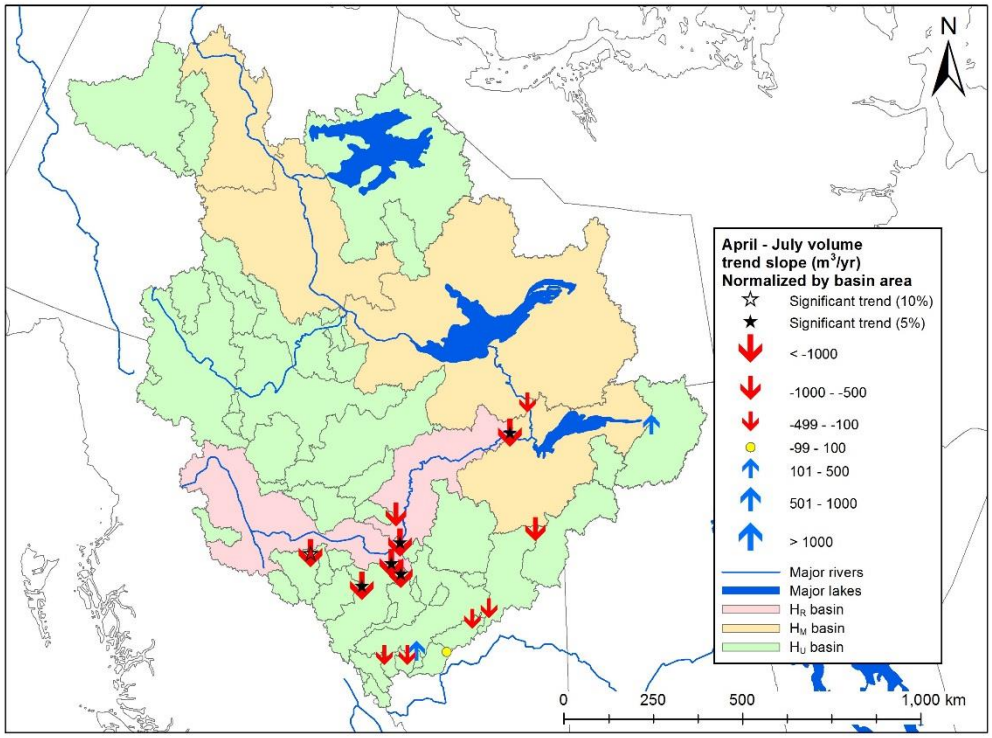

Figure 18a. Trends in April through July volume during the period 1962 – 2000 for Mackenzie stations.

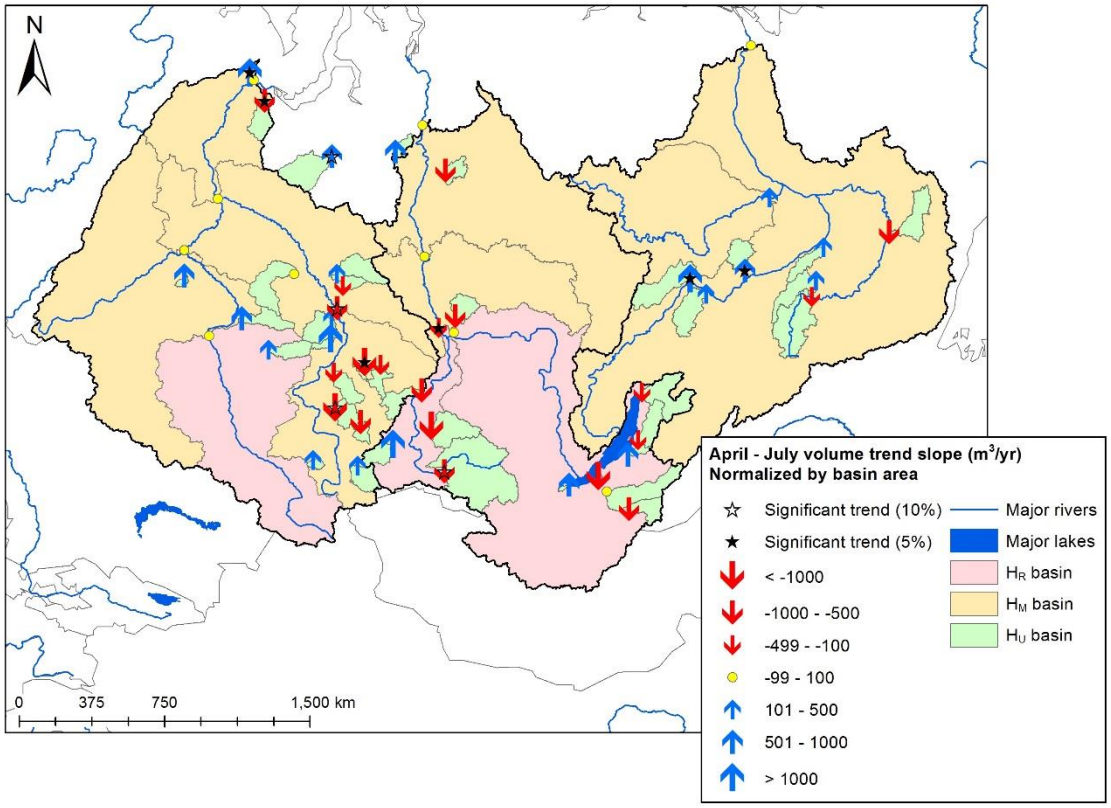

Figure 18b. Trends in April through July volume during the period 1962 – 2000 for Eurasian stations.

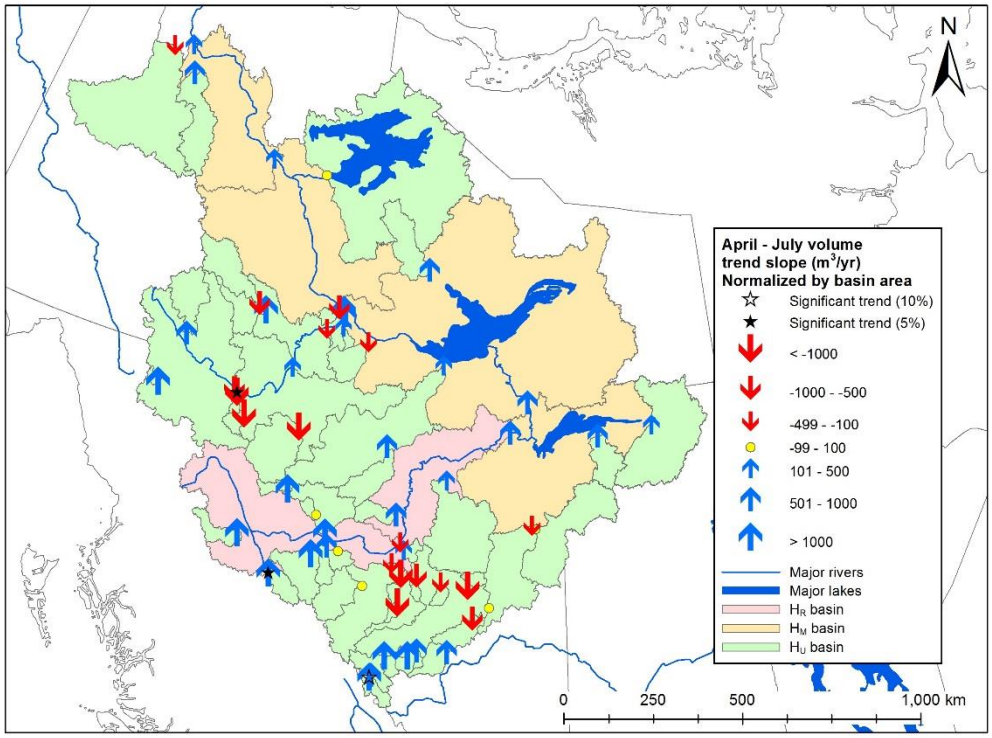

Figure 19a. Trends in April through July volume during the period 1980 – 2000 for Mackenzie stations.

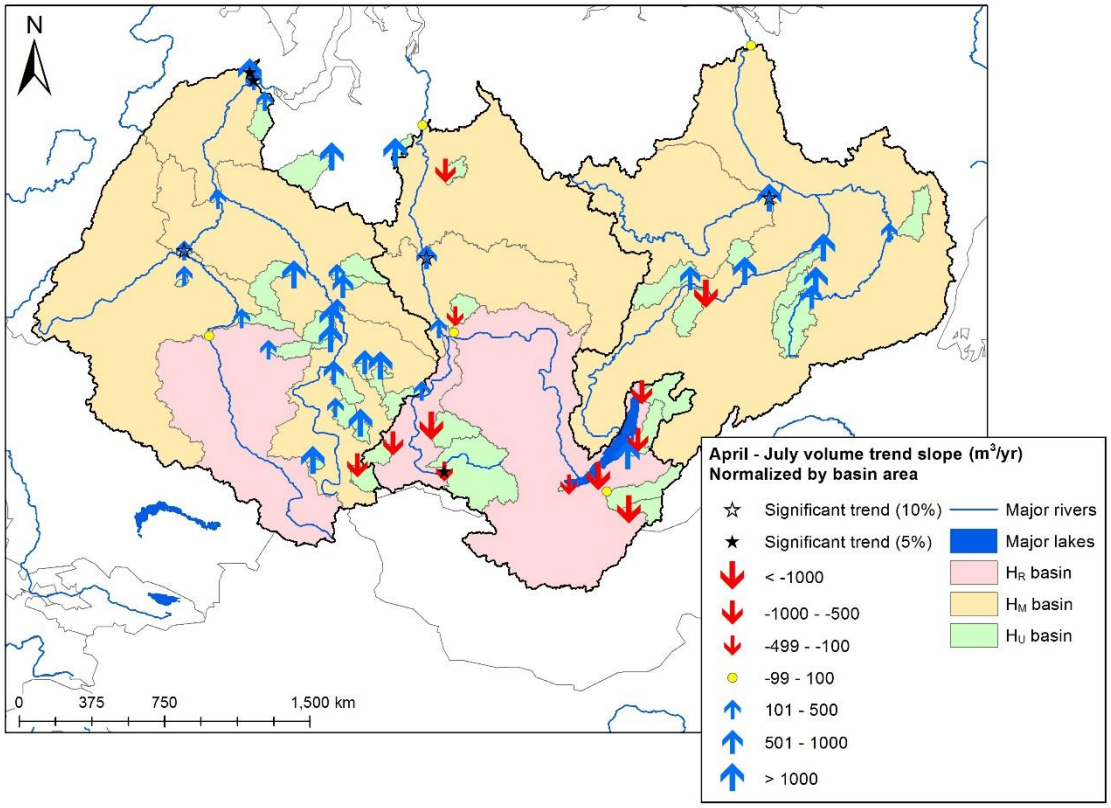

Figure 19b. Trends in April through July volume during the period 1980 – 2000 for Eurasian stations.

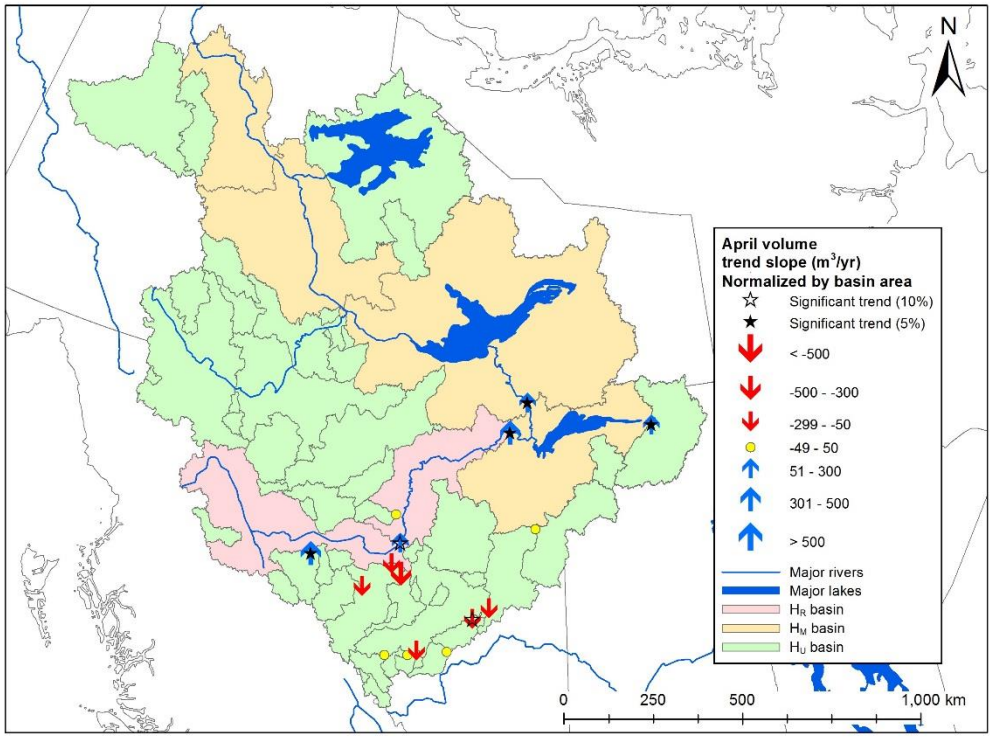

Figure 20a. Trends in April volume during the period 1962 – 2000 for Mackenzie stations.

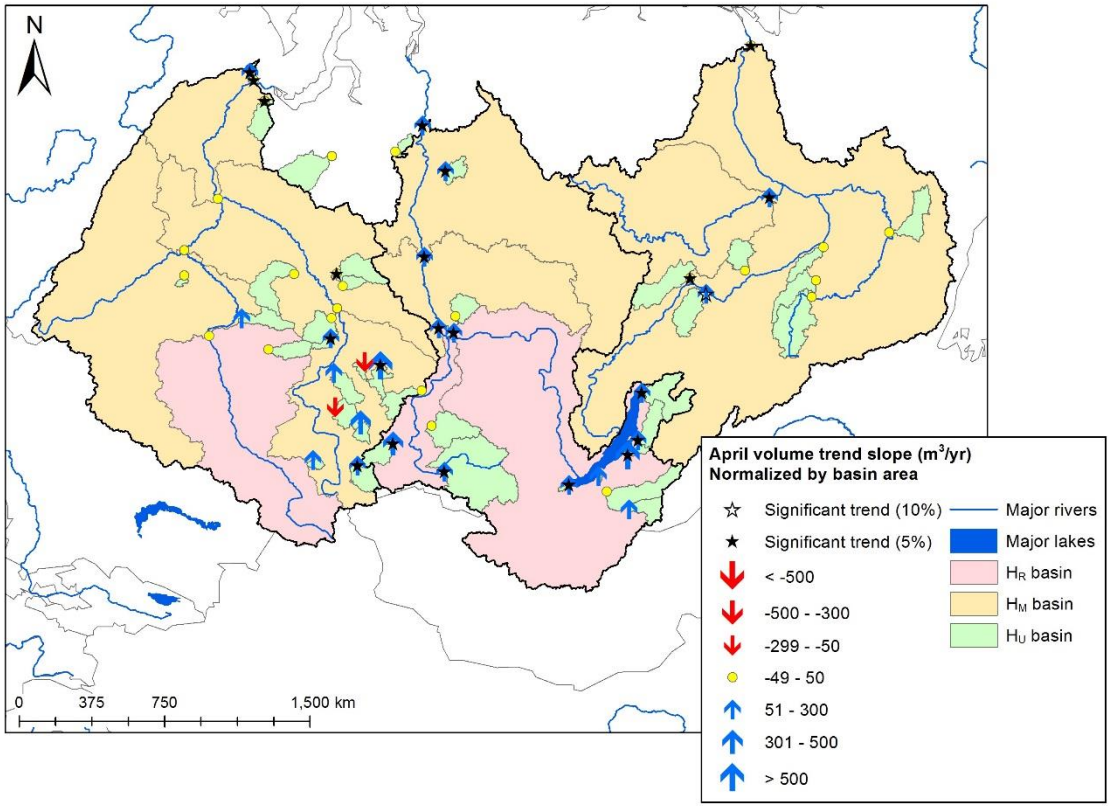

Figure 20b. Trends in April volume during the period 1962 – 2000 for Eurasian stations.

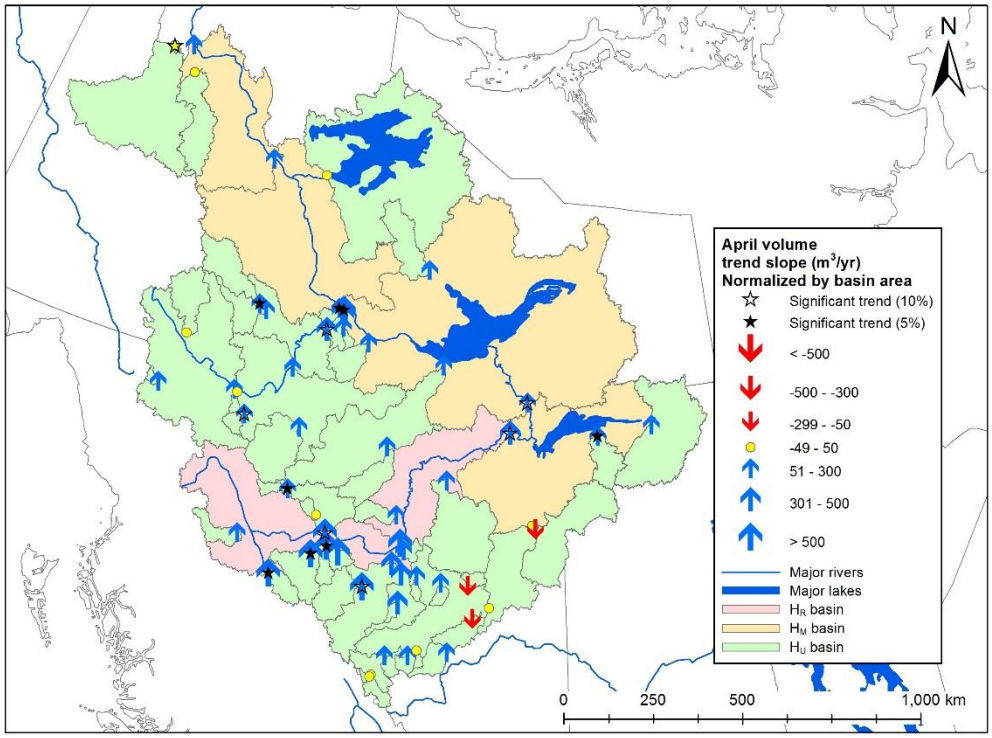

Figure 21a. Trends in April volume during the period 1980 – 2000 for Mackenzie stations.

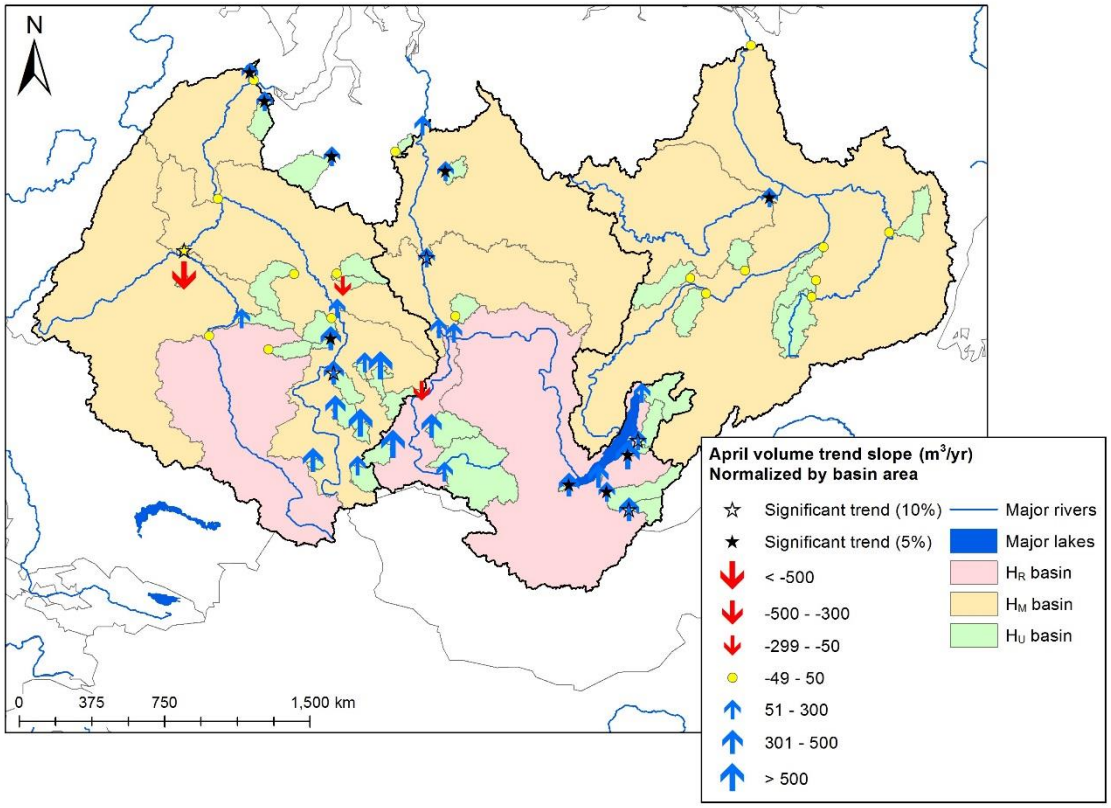

Figure 21b. Trends in April volume during the period 1980 – 2000 for Eurasian stations.

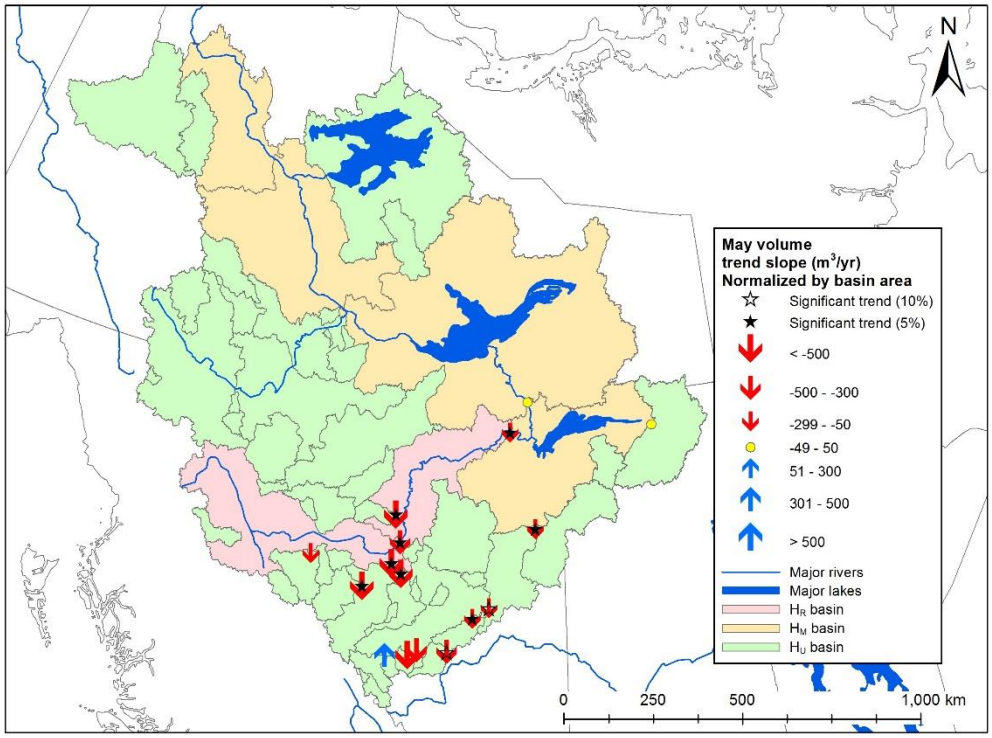

Figure 22a. Trends in May volume during the period 1962 – 2000 for Mackenzie stations.

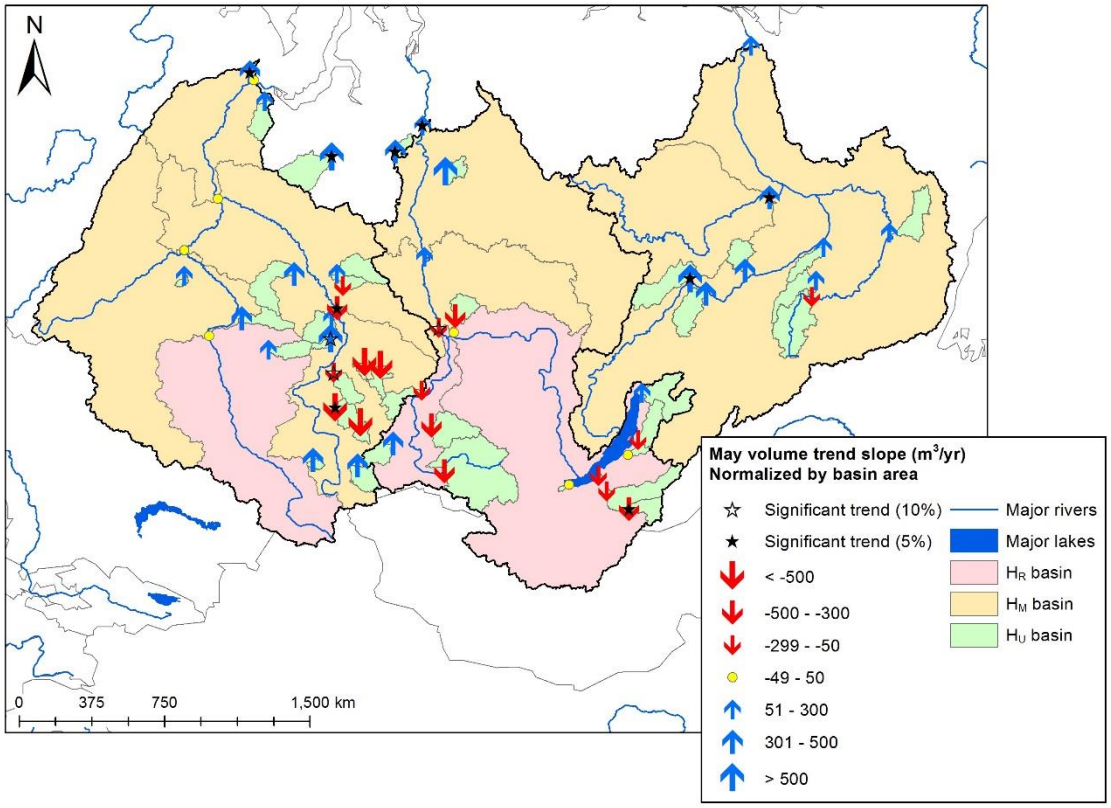

Figure 22b. Trends in May volume during the period 1962 – 2000 for Eurasian stations.

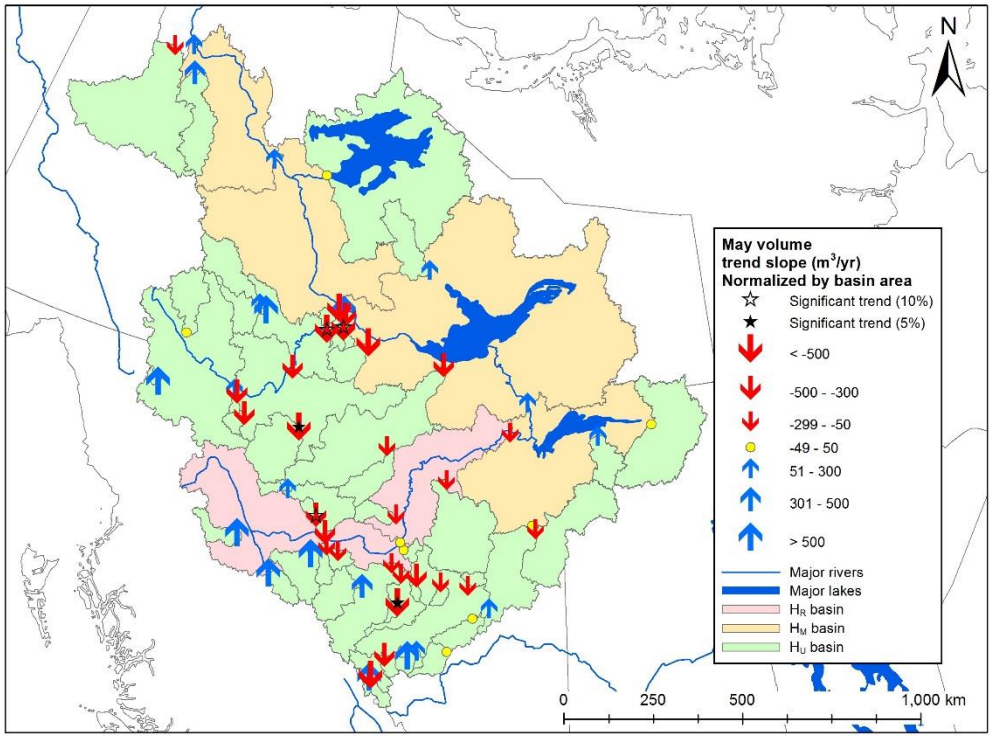

Figure 23a. Trends in May volume during the period 1980 – 2000 for Mackenzie stations.

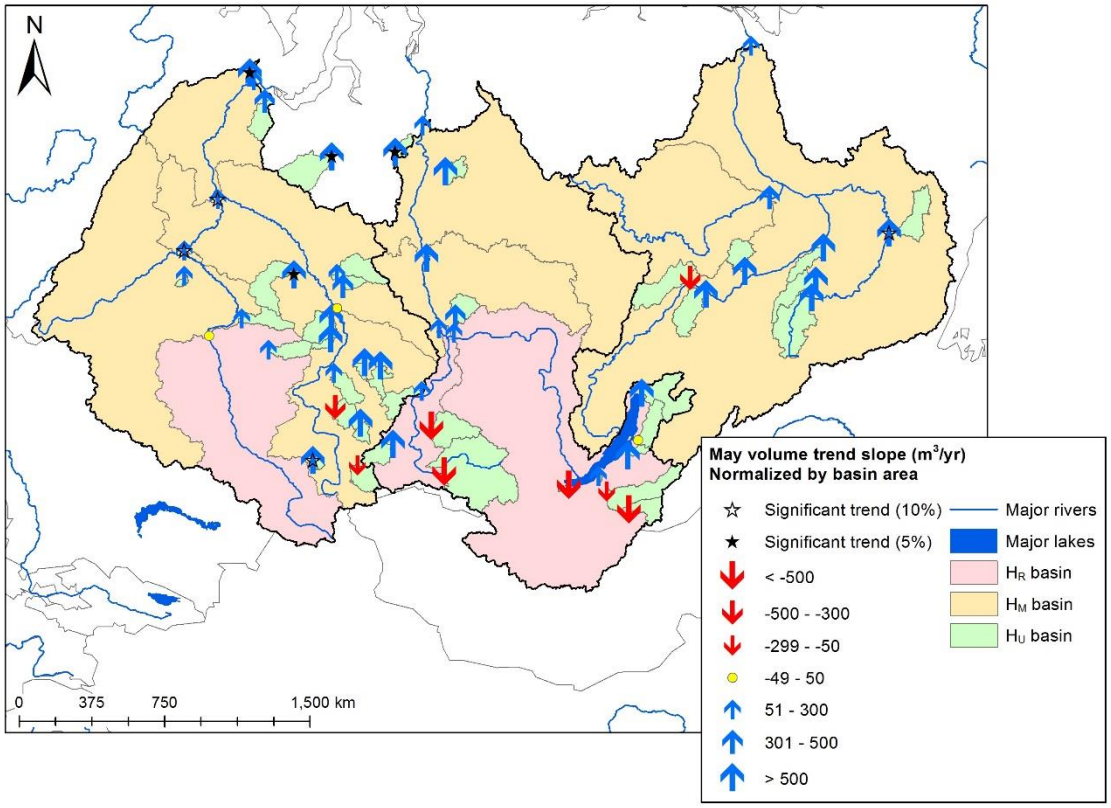

Figure 23b. Trends in May volume during the period 1980 – 2000 for Eurasian stations.

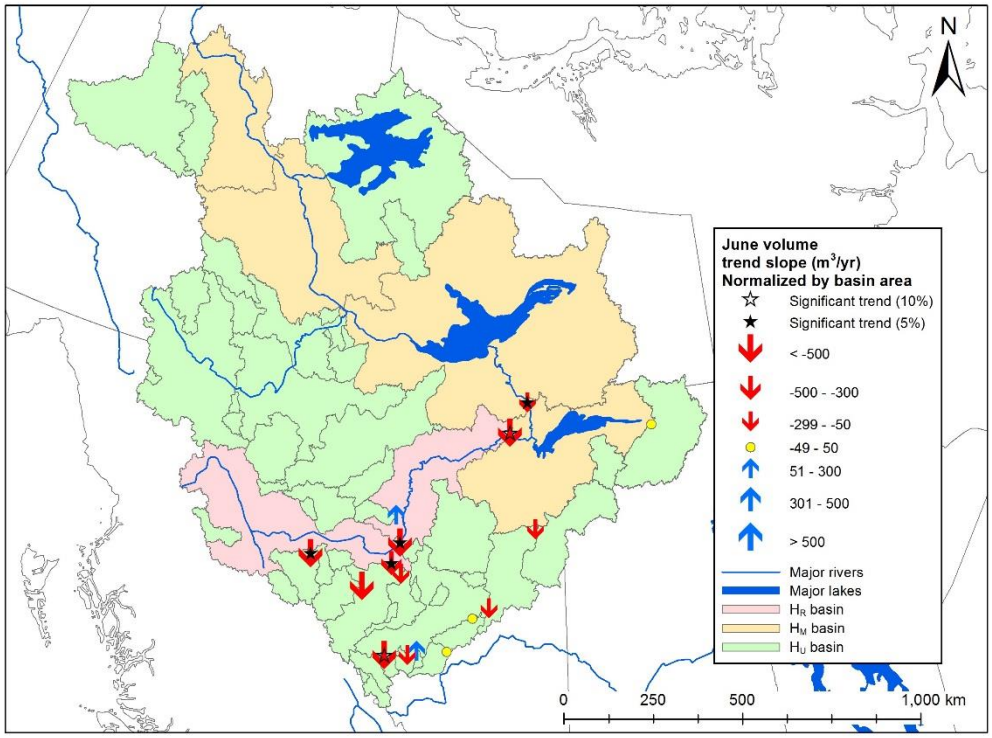

Figure 24a. Trends in June volume during the period 1962 – 2000 for Mackenzie stations.

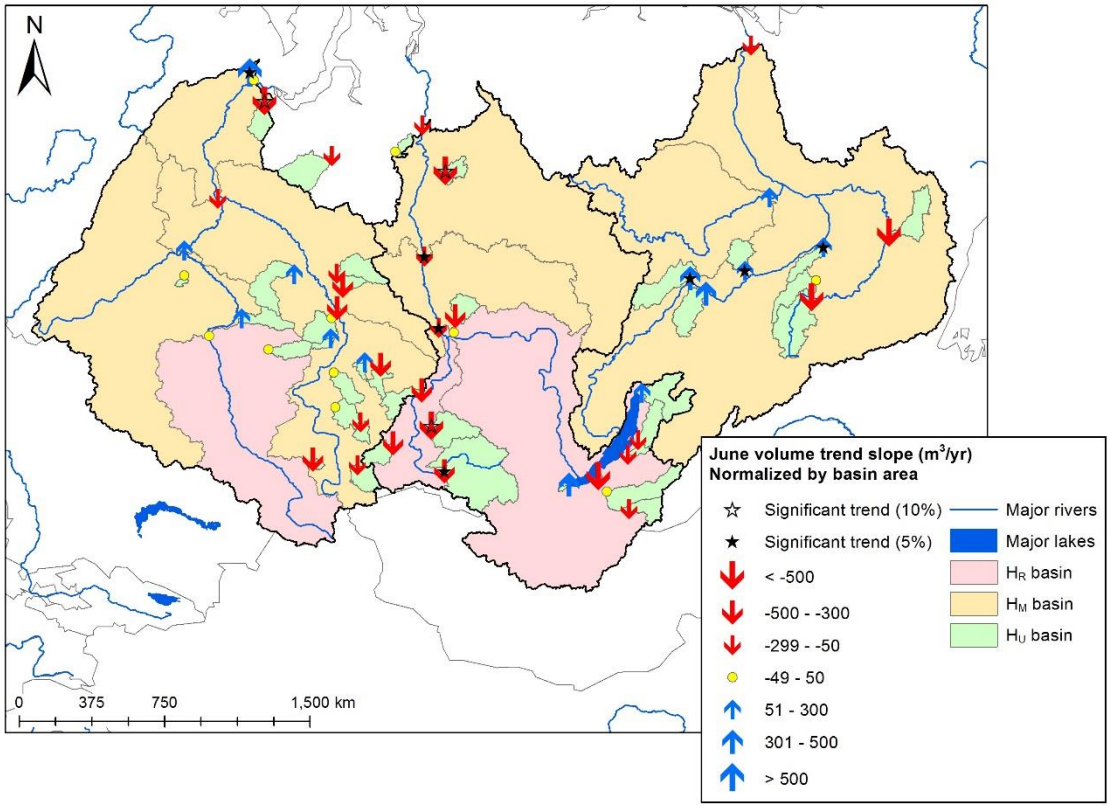

Figure 24b. Trends in June volume during the period 1962 – 2000 for Eurasian stations.

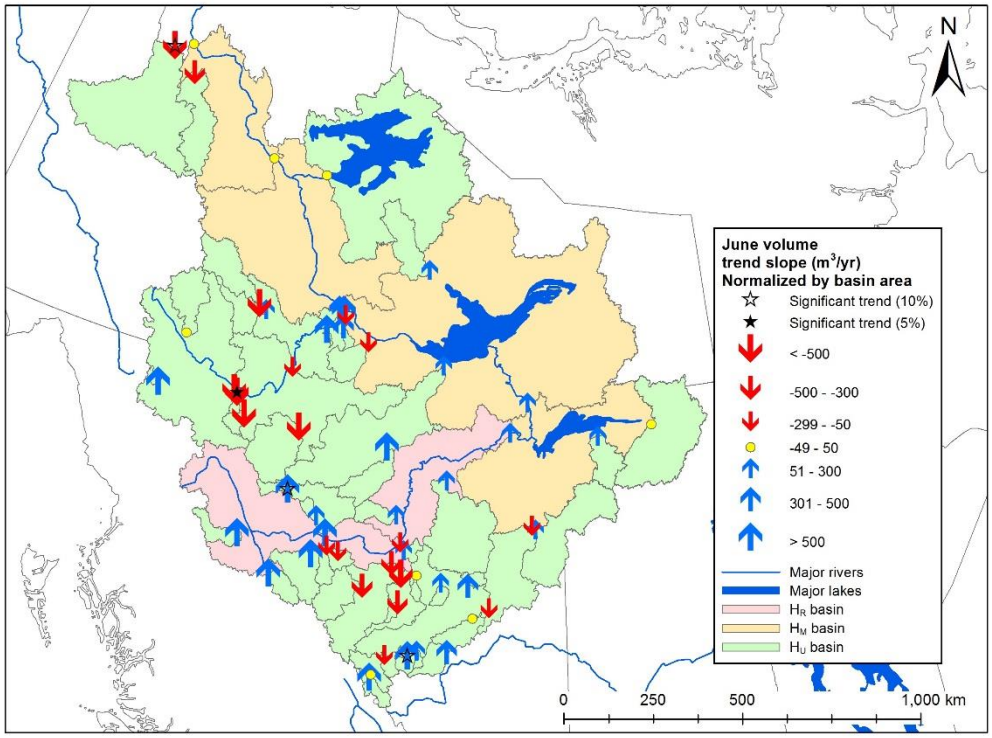

Figure 25a. Trends in June volume during the period 1980 – 2000 for Mackenzie stations.

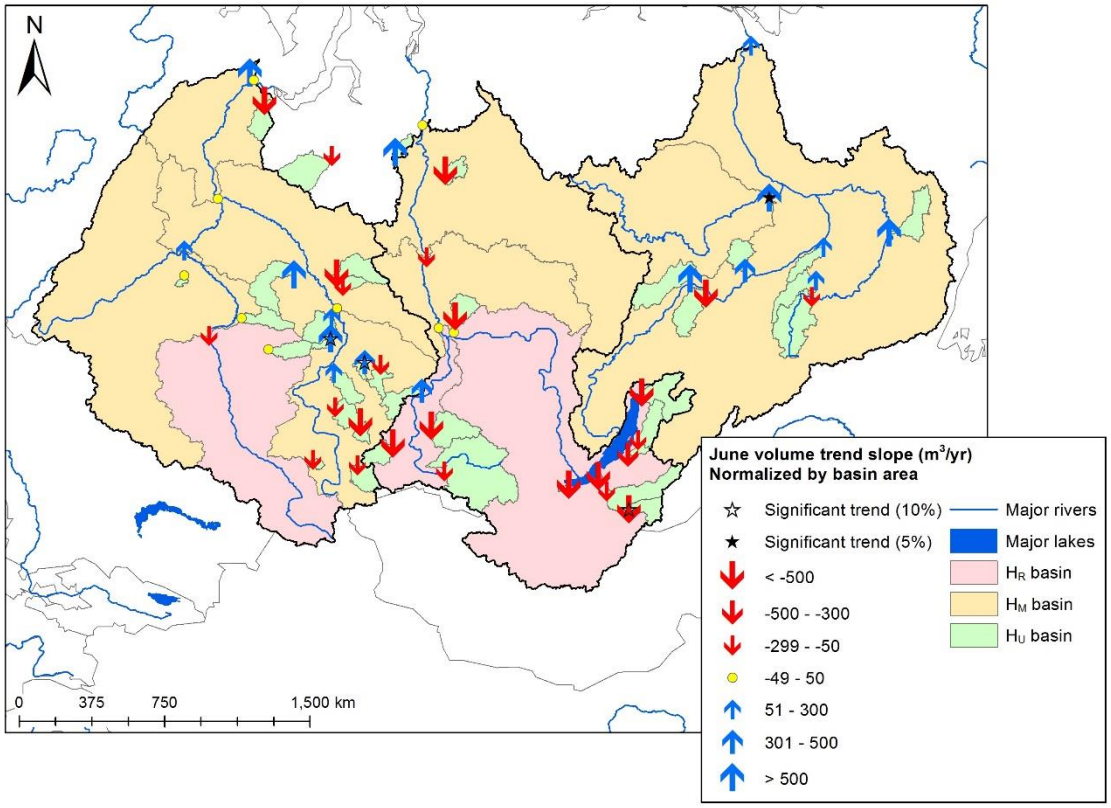

Figure 25b. Trends in June volume during the period 1980 – 2000 for Eurasian stations.

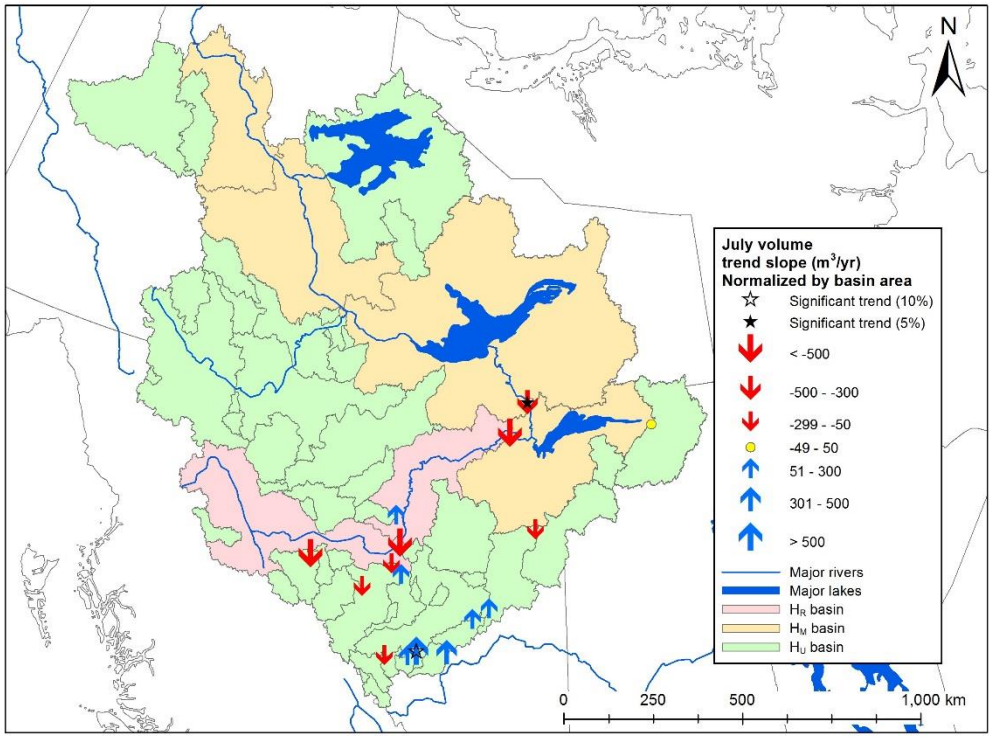

Figure 26a. Trends in July volume during the period 1962 – 2000 for Mackenzie stations.

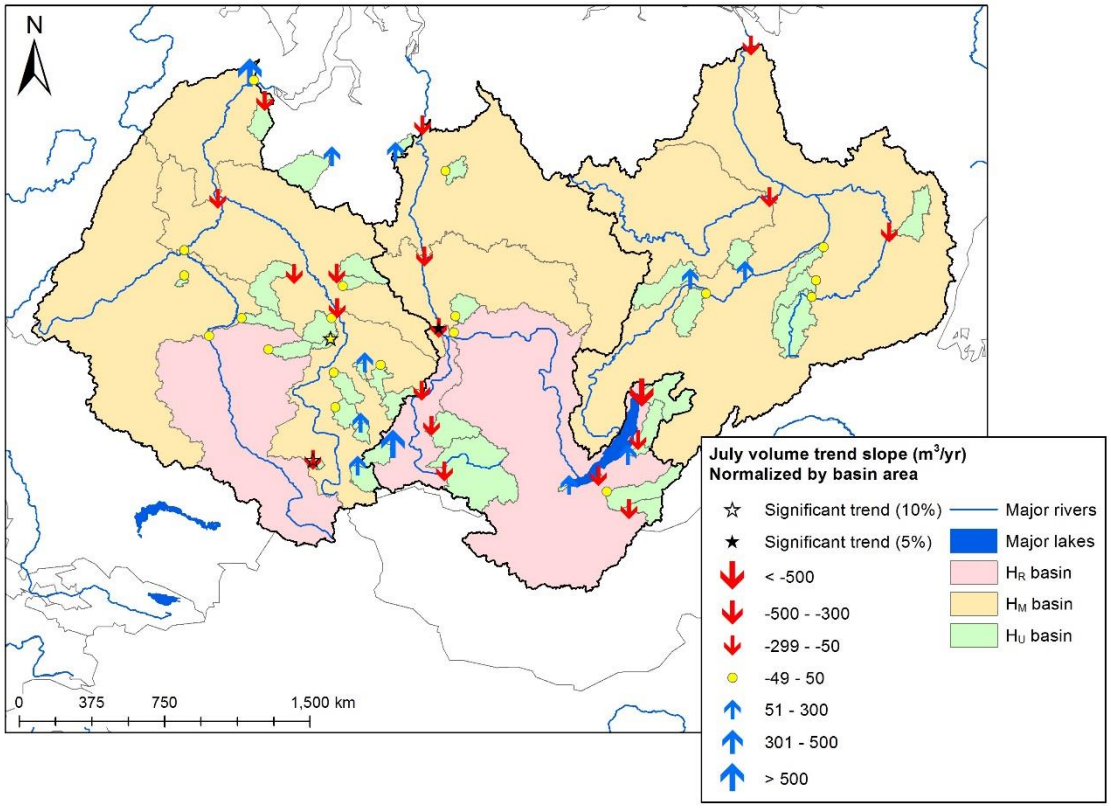

Figure 26b. Trends in July volume during the period 1962 – 2000 for Eurasian stations.

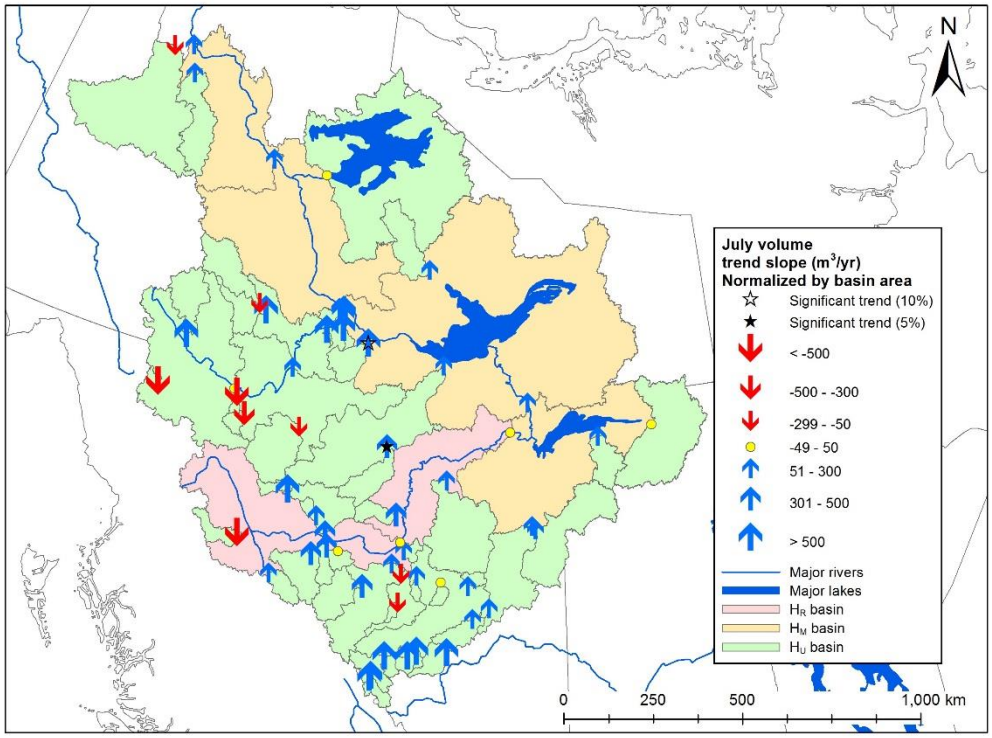

Figure 27a. Trends in July volume during the period 1980 – 2000 for Mackenzie stations.

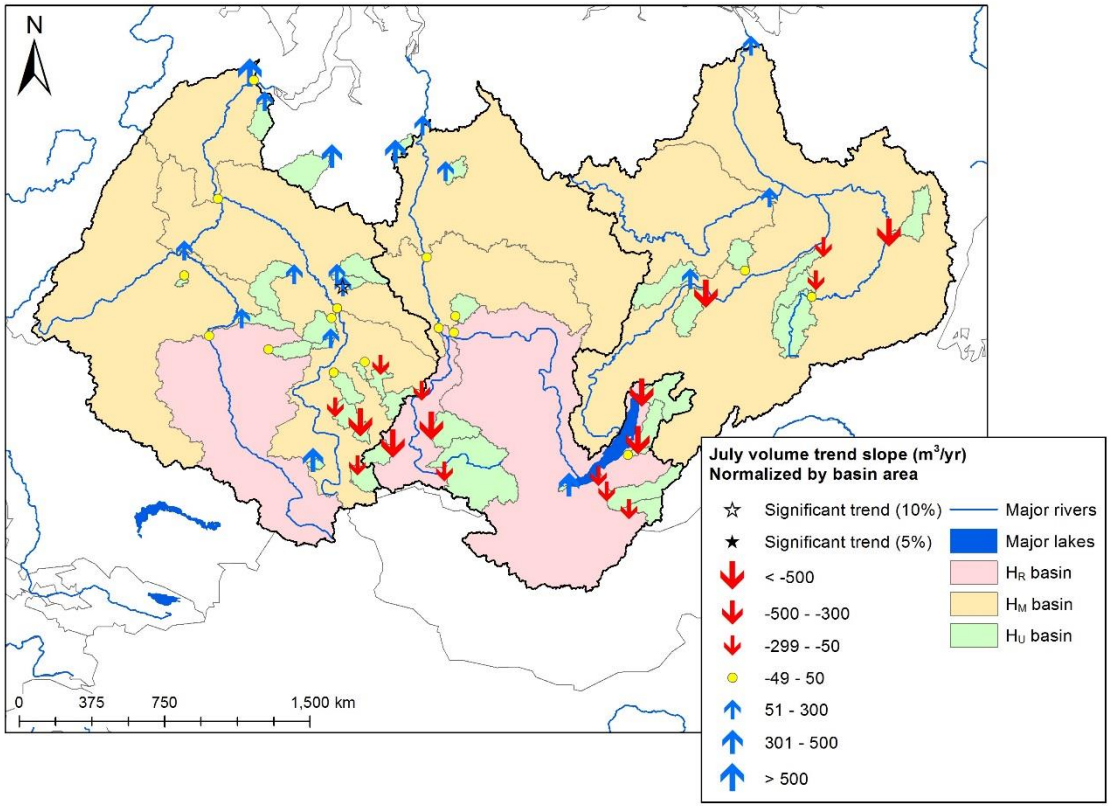

Figure 27b. Trends in July volume during the period 1980 – 2000 for Eurasian stations.

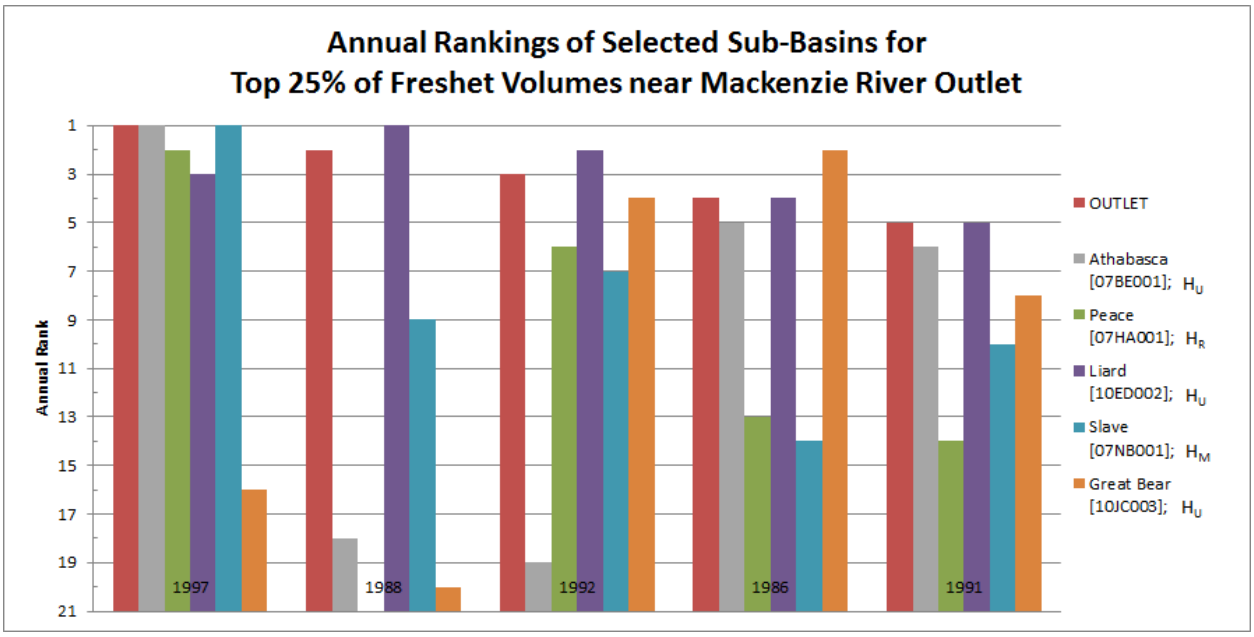

Figure 28a. Annual rank of standardized freshet volumes for representative Mackenzie sub-basin stations, based on the top 25% of standardized freshet volumes at Mackenzie River outlet station during the period 1980 - 2000.

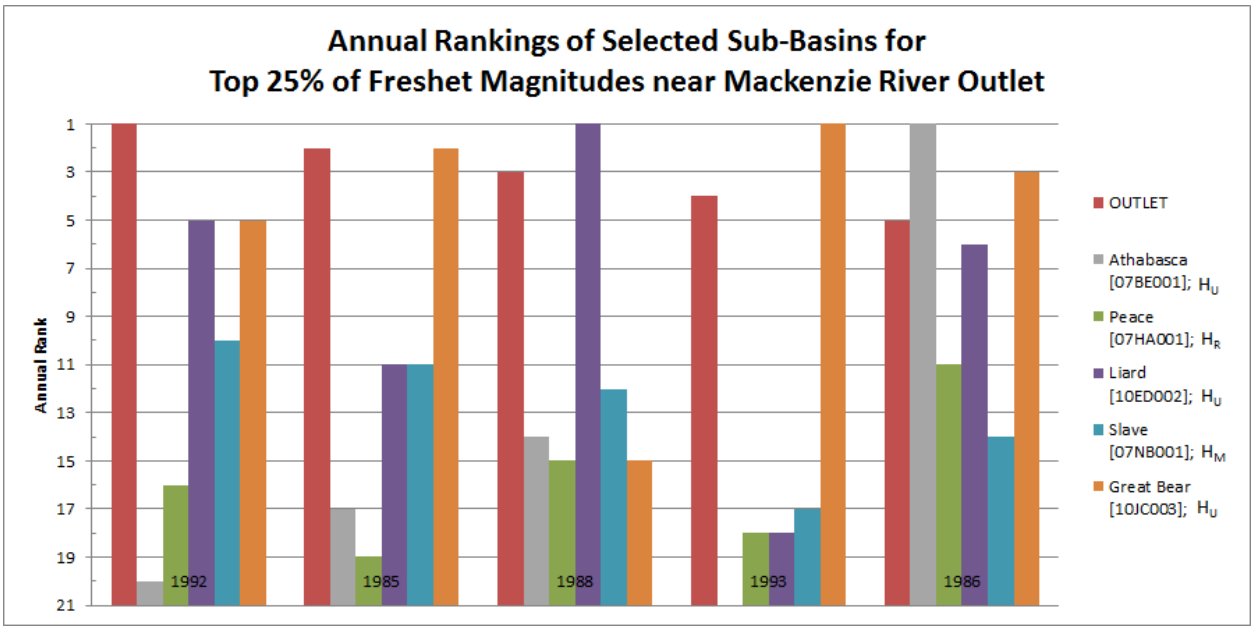

Figure 28b. Annual rank of standardized freshet magnitudes for representative Mackenzie sub-basin stations, based on the top 25% of standardized freshet magnitudes at Mackenzie River outlet station during the period 1980 - 2000.

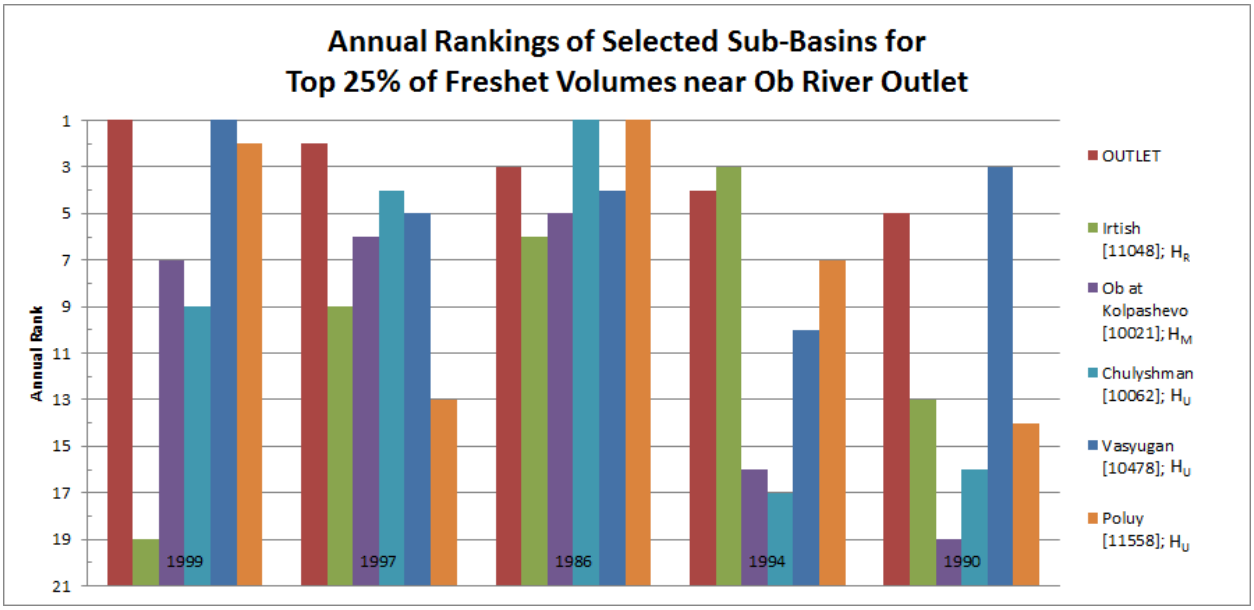

Figure 29a. Annual rank of standardized freshet volumes for representative Ob sub-basin stations, based on the top 25% of standardized freshet volumes at Ob River outlet station during the period 1980 - 2000.

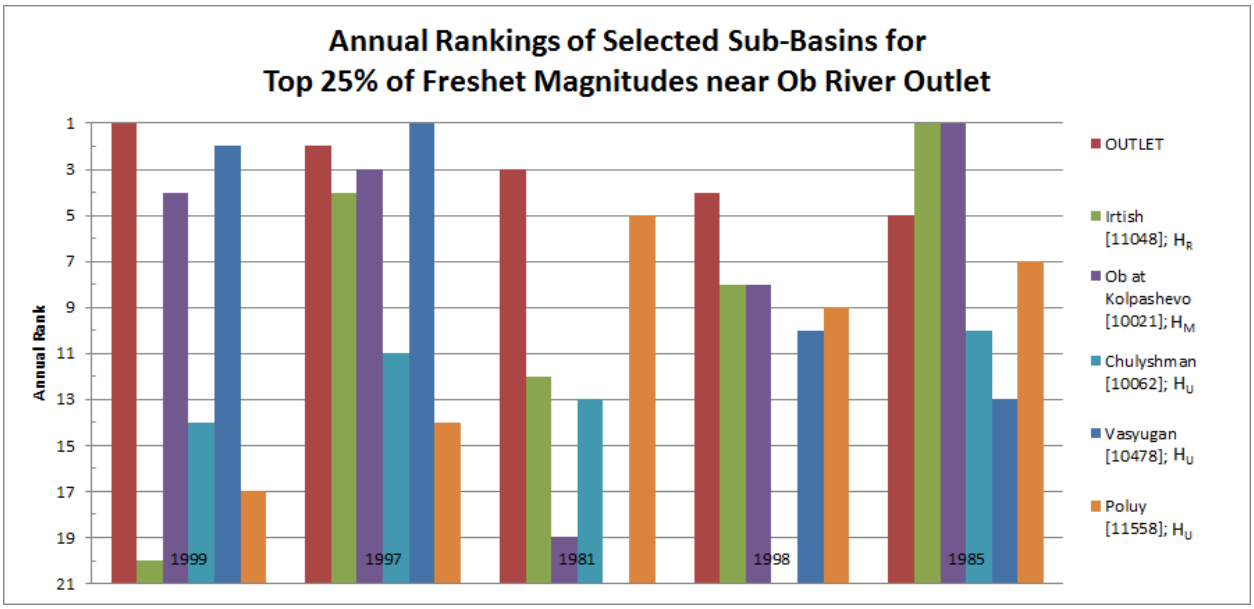

Figure 29b. Annual rank of standardized freshet magnitudes for representative Ob sub-basin stations, based on the top 25% of standardized freshet magnitudes at Ob River outlet station during the period 1980 - 2000.

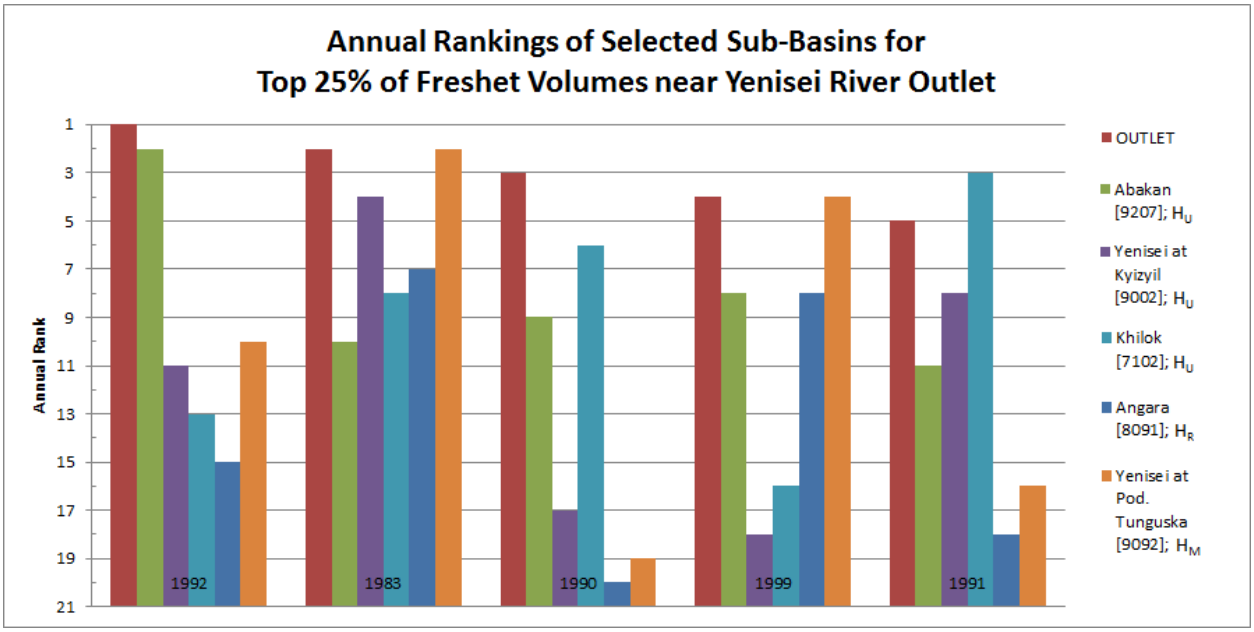

Figure 30a. Annual rank of standardized freshet volumes for representative Yenisei sub-basin stations, based on the top 25% of standardized freshet volumes at Yenisei River outlet station during the period 1980 - 2000.

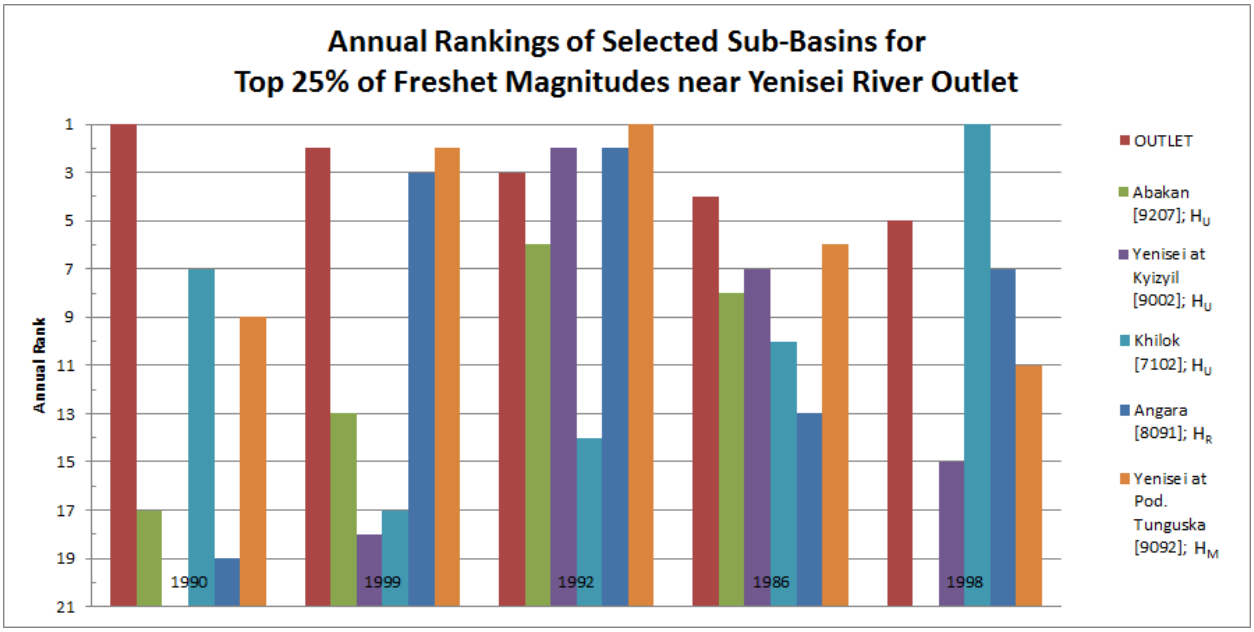

Figure 30b. Annual rank of standardized freshet magnitudes for representative Yenisei sub-basin stations, based on the top 25% of standardized freshet magnitudes at Yenisei River outlet station during the period 1980 - 2000.

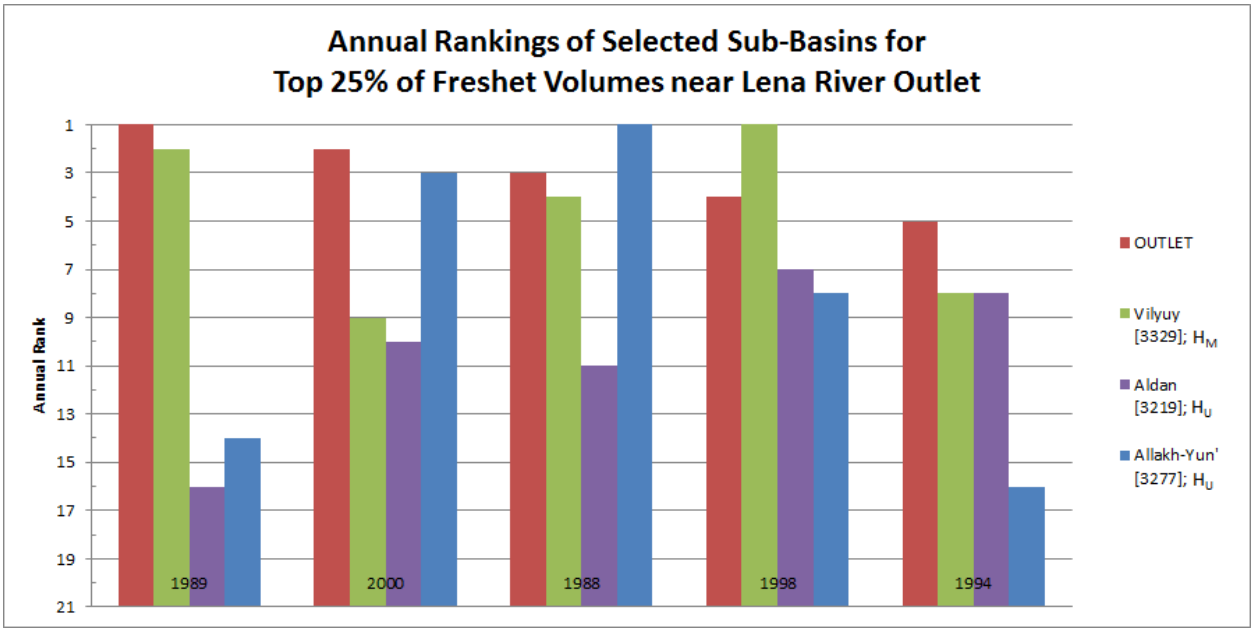

Figure 31a. Annual rank of standardized freshet volumes for representative Lena sub-basin stations, based on the top 25% of standardized freshet volumes at Lena River outlet station during the period 1980 - 2000.

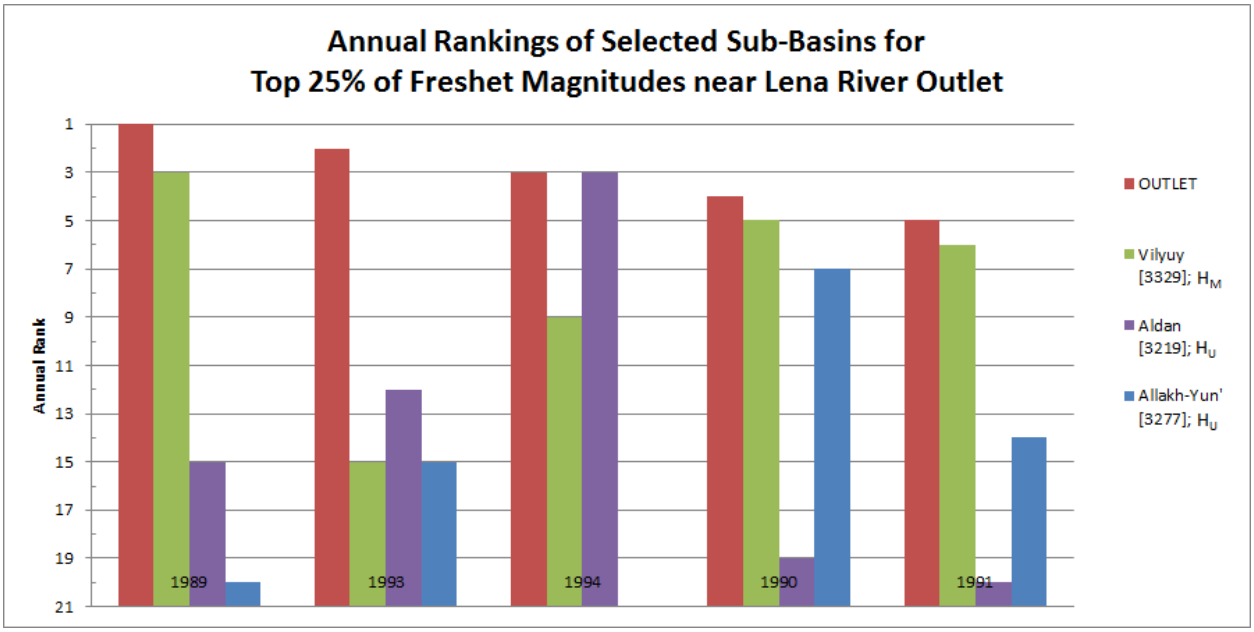

Figure 31b. Annual rank of standardized freshet magnitudes for representative Lena sub-basin stations, based on the top 25% of standardized freshet magnitudes at Lena River outlet station during the period 1980 - 2000.

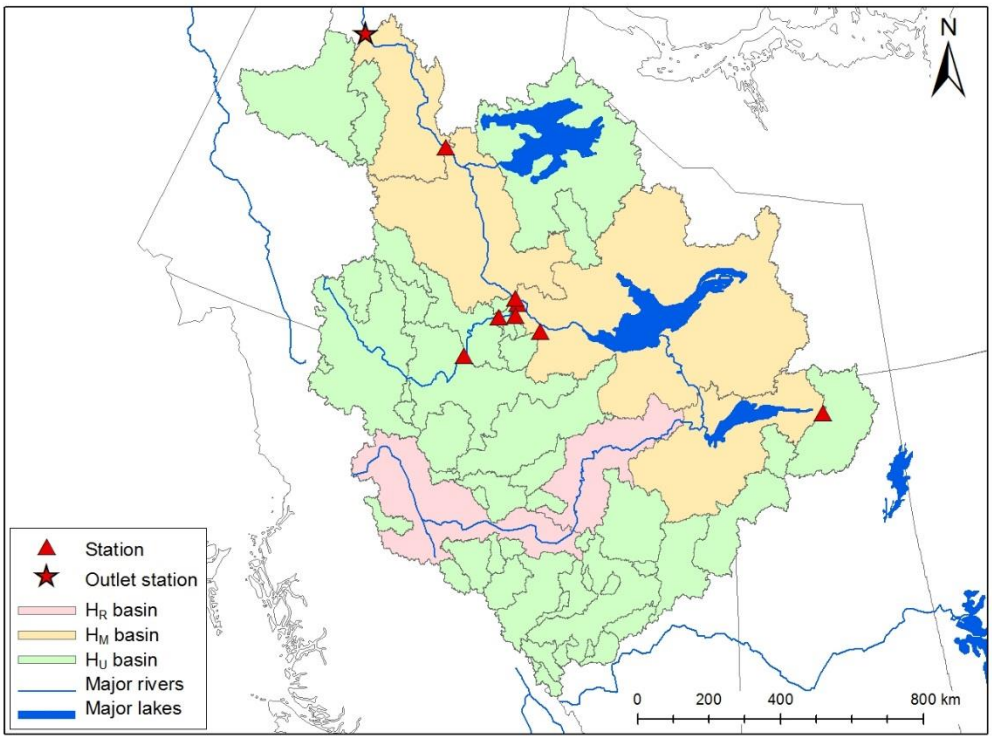

Figure 32a. Station sub-basins that display high freshet volumes during corresponding years of the top 25% of freshet volumes at the Mackenzie River outlet station 10LC014 during the period 1980 - 2000. Stations shown are significantly different from their periodic mean based on a t test at a 95% confidence level.

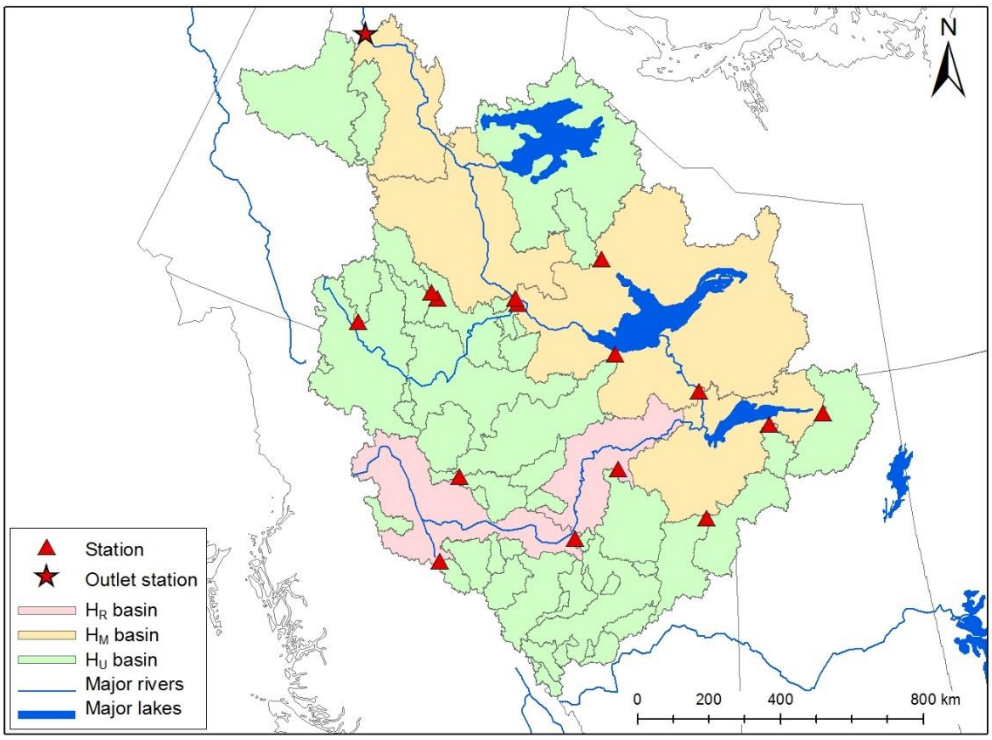

Figure 32b. Station sub-basins that display low freshet volumes during corresponding years of the bottom 25% of freshet volumes at the Mackenzie River outlet station 10LC014 during the period 1980 - 2000. Stations shown are significantly different from their periodic mean based on a t test at a 95% confidence level.

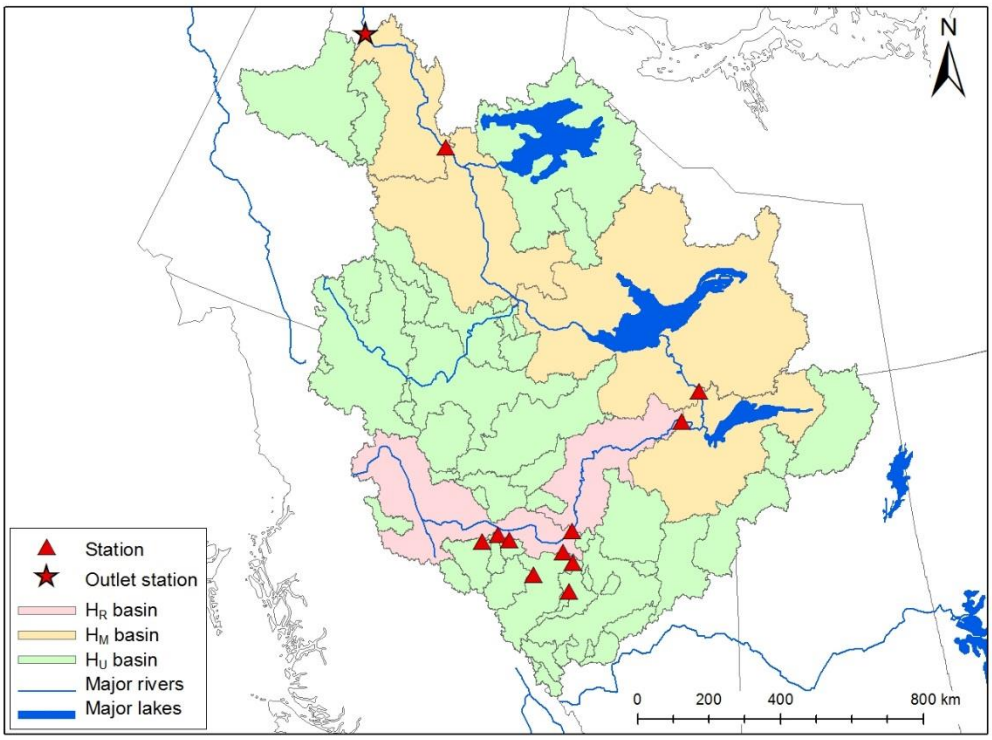

Figure 33a. Station sub-basins that display high freshet magnitudes during corresponding years of the top 25% of freshet magnitudes at the Mackenzie River outlet station 10LC014 during the period 1980 - 2000. Stations shown are significantly different from their periodic mean based on a t test at a 95% confidence level.

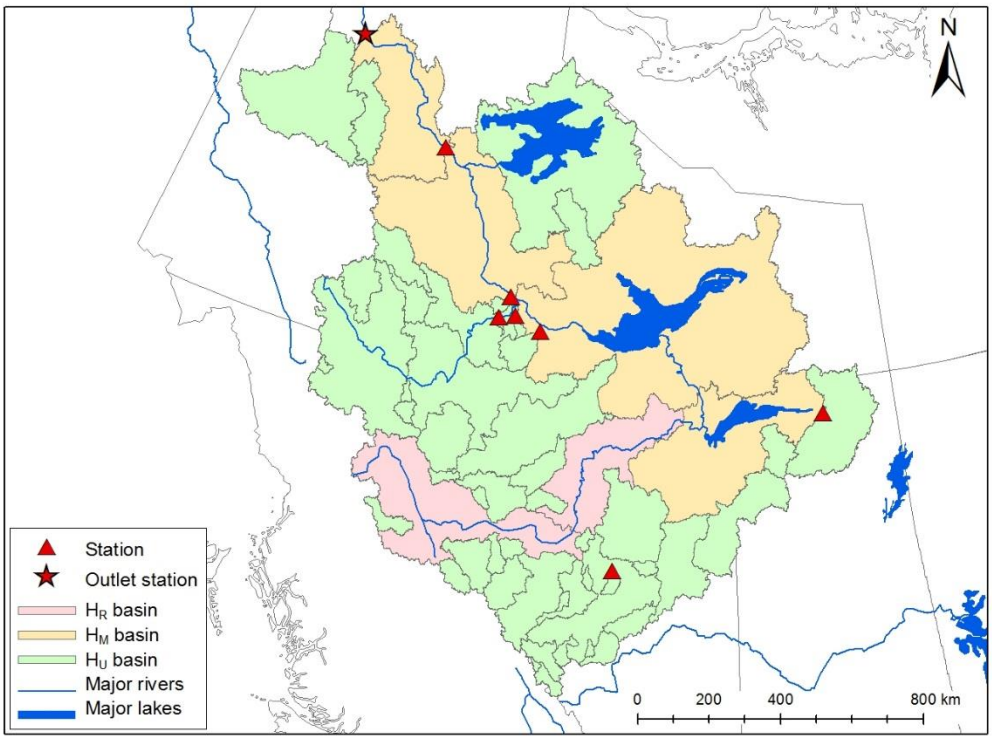

Figure 33b. Station sub-basins that display low freshet magnitudes during corresponding years of the bottom 25% of freshet magnitudes at the Mackenzie River outlet station 10LC014 during the period 1980 - 2000. Stations shown are significantly different from their periodic mean based on a t test at a 95% confidence level.

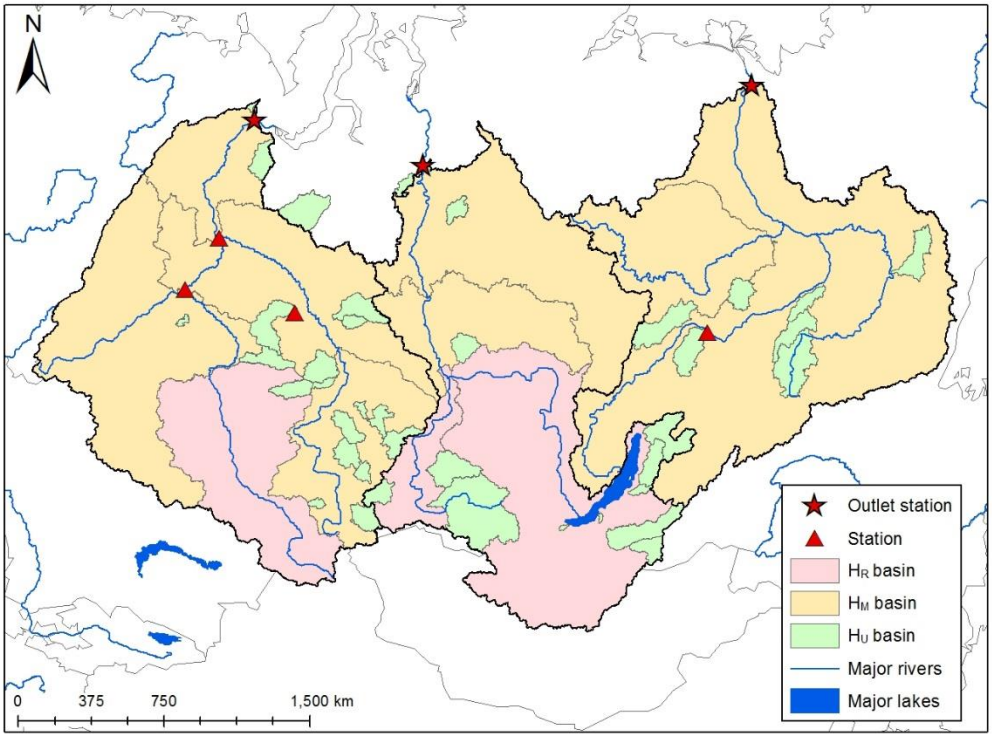

Figure 34a. Station sub-basins that display high freshet volumes during corresponding years of the top 25% of freshet volumes at Eurasian outlet stations during the period 1980 - 2000. Stations shown are significantly different from their periodic mean based on a t test at a 95% confidence level.

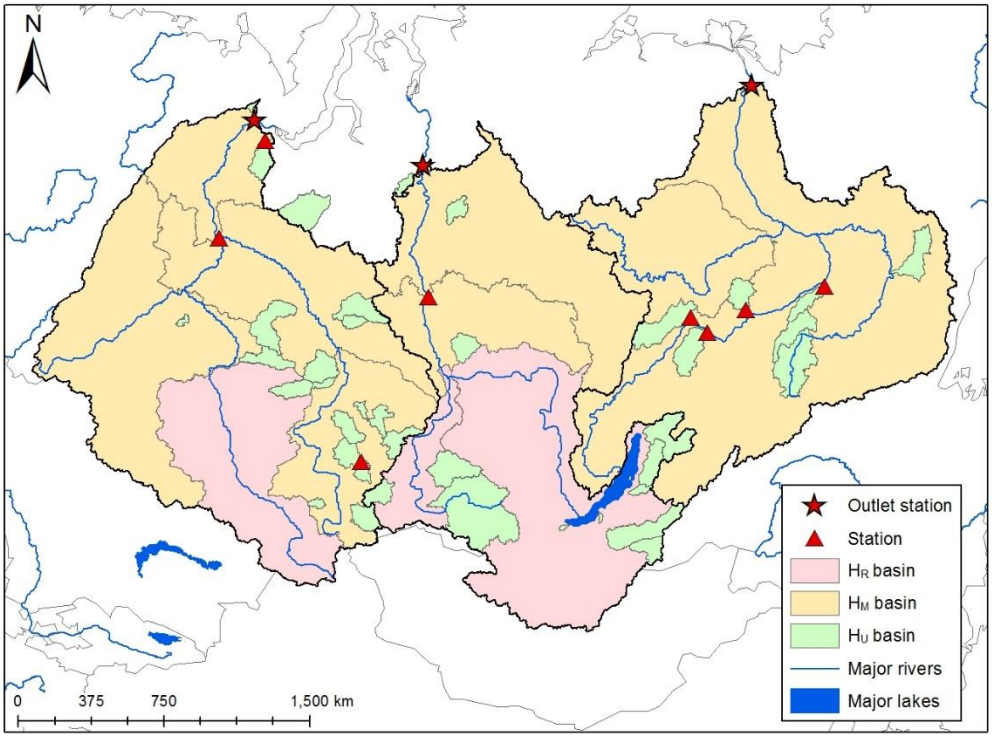

Figure 34b. Station sub-basins that display low freshet volumes during corresponding years of the bottom 25% of freshet volumes at Eurasian outlet stations during the period 1980 - 2000. Stations shown are significantly different from their periodic mean based on a t test at a 95% confidence level.

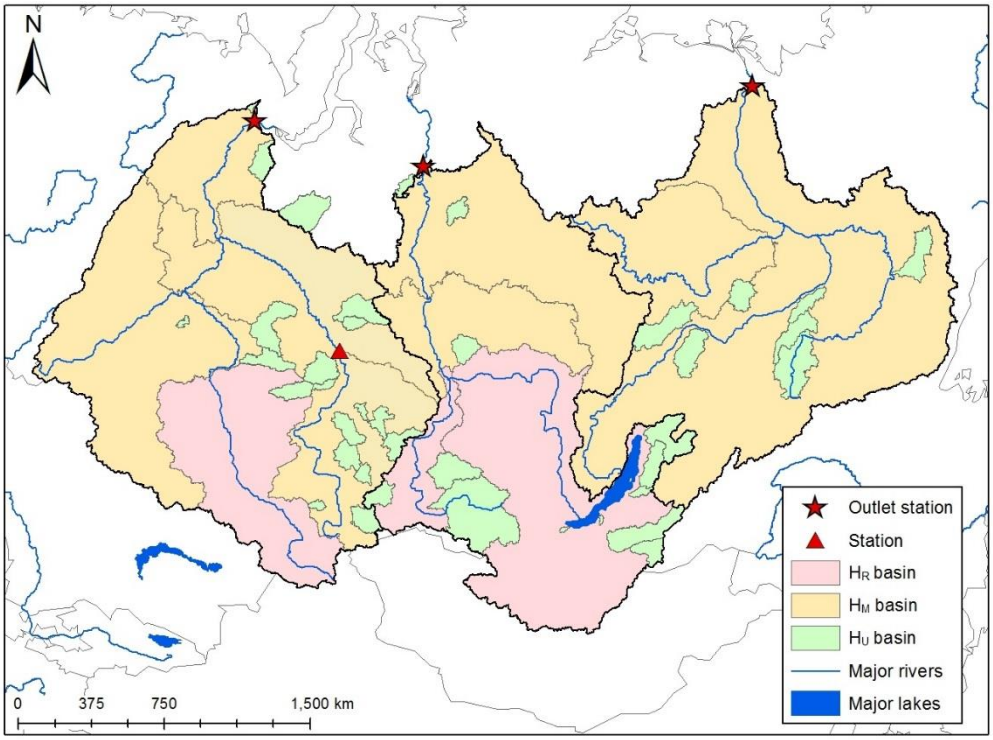

Figure 35a. Station sub-basins that display high freshet magnitudes during corresponding years of the top 25% of freshet magnitudes at Eurasian outlet stations during the period 1980 - 2000. Stations shown are significantly different from their periodic mean based on a t test at a 95% confidence level.

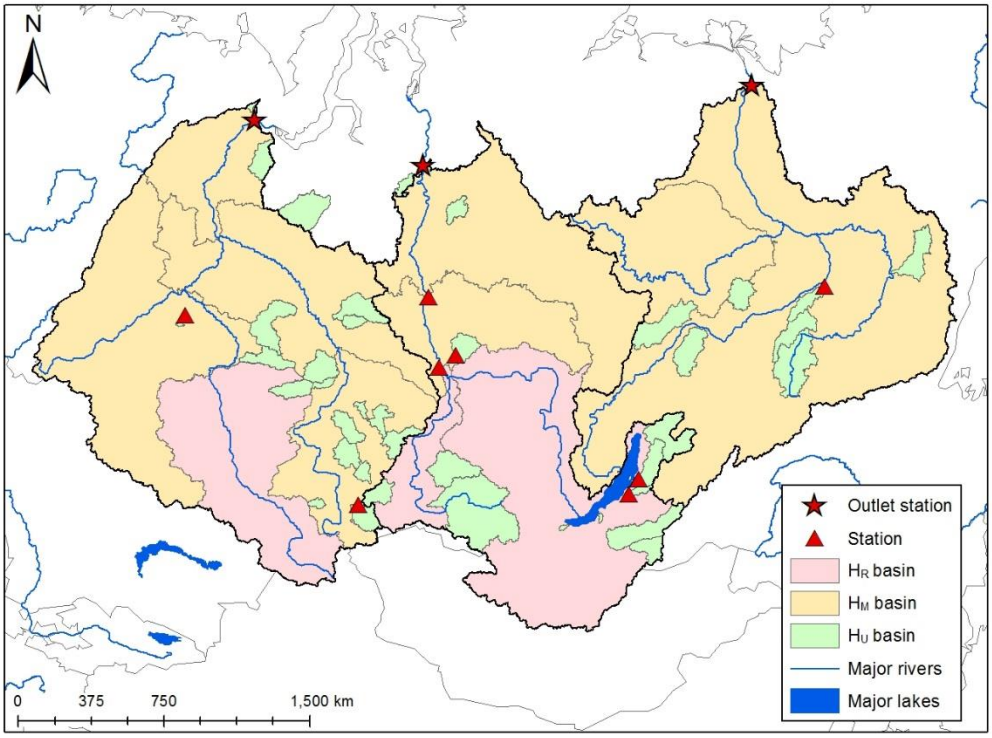

Figure 35b. Station sub-basins that display low freshet magnitudes during corresponding years of the bottom 25% of freshet magnitudes at Eurasian outlet stations during the period 1980 - 2000. Stations shown are significantly different from their periodic mean based on a t test at a 95% confidence level.

CHAPTER 5: CLIMATIC DRIVERS OF TRENDS IN THE SPRING FRESHET OF FOUR MAJOR ARCTIC RIVER SYSTEMS

Abstract

For northern Arctic-draining rivers, the spring freshet is the dominant annual discharge event producing freshwater inflow to the Arctic Ocean. Freshwater storage and circulation within the ocean are affected by seasonality of the spring freshet, which can also have impacts on the Arctic cryosphere, biota and linkages to global climate through thermohaline circulation. At the same time, rate of change in the Arctic climate is significantly higher than other parts of the globe.

This study evaluates the large-scale atmospheric and surface climatic conditions affecting the magnitude, timing and regional variability of the spring freshets by analyzing historic daily discharge data from sub-basins within the four largest Arctic-draining watersheds (Mackenzie, Ob, Lena and Yenisei). Previous research indicated that an observed change in discharge seasonality at the outlets of these rivers was marked by increasing cold-season flows, earlier pulse dates and a lower fraction of flow released during the spring freshet; those trends were generally reproduced on a sub-basin level. This study reveals that climatic relationships closely match the observed regional trends, whilst flow regulation appears to suppress the climatic drivers of freshet volume but does not have a significant impact on peak freshet magnitude or timing measures. Spring freshet characteristics are influenced by El Niño-Southern Oscillation (ENSO), Pacific Decadal Oscillation (PDO), Arctic Oscillation (AO) and North Atlantic Oscillation (NAO), particularly in their warm phases. The majority of significant relationships are seen in unregulated stations. This study provides key insight on the climatic drivers of previously observed trends in freshet characteristics, whilst clarifying the effects of regulation versus climate on the sub-basins.

Keywords: Arctic, spring freshet, hydro-climatology, teleconnections, atmospheric circulation

5.1 Introduction

The Arctic Ocean plays a critical role in the global hydrological cycle through import, export, storage and transformation of freshwater (Carmack et al., 2008). Amongst other implications, Arctic Ocean freshwater may have impacts on the global climate system through thermohaline circulation, which is affected by movement of lower-salinity waters within the ocean (Loeng et al., 2005). Export of relatively fresh water from the ocean southwards into the northern North Atlantic Ocean through Fram Strait and the Canadian Arctic Archipelago couples the Arctic hydrological system with global thermohaline circulation, with subsequent effects on oceanic heat transport to northern latitudes (e.g., Aagard and Carmack 1989; Carmack 2000; Peterson et al. 2002; Arnell 2005).

Unlike temperate seas, the cold upper Arctic ocean is predominantly stratified by salinity, rather than temperature (Carmack et al., 2008). Freshwater is delivered mainly through direct precipitation on the ocean surface, import of lower-salinity Pacific waters through Bering Strait, and terrestrial river runoff (e.g., Aagaard and Carmack, 1989; Carmack, 2000; Serreze et al., 2006). Since it is largely an enclosed system, the Arctic Ocean is particularly sensitive to river discharge from northward-flowing Arctic rivers. In fact, river runoff provides as much as 50% of the freshwater influx or greater compared to other sources (Prowse and Flegg, 2000). A change in the current freshwater budget of the Arctic Ocean can alter the mechanisms of freshwater export and deep oceanic convection in the North Atlantic, with resulting impacts to the thermohaline circulation (Kattsov et al., 2007; McClelland et al., 2011).

In Arctic-draining rivers, as much as 60% of total annual flow volume is released during the spring freshet (Lammers et al., 2001); this annual event follows the spring snowmelt and river ice breakup period and is the major hydrologic event occurring on largely nival Arctic river

systems. Since the Arctic Ocean receives a significant proportion of its freshwater influx through riverine input, it can be deduced that there is a potential link between the spring freshet of major Arctic-draining rivers and oceanic heat transport to northern latitudes through global thermohaline circulation.

Meanwhile, climate change is occurring more rapidly in Arctic regions than other parts of the globe. A warming Arctic climate corresponds to an earlier freshet onset and higher winter flow from greater subsurface infiltration into thawing permafrost. Additionally, northward redistribution of precipitation, increased sea ice melting, glacial wastage, permafrost degradation and an expected increase in river discharge may result in an intensification of the arctic hydrologic cycle. A growing number of studies point to changes in Arctic Ocean freshwater influx and distribution over recent time periods. For example, Peterson et al. (2002) found that Eurasian river discharge had increased by approximately 7% over the period 1936-1999. This amounted to a volumetric increase of 128 km^3 of freshwater annually by the end of the study period, or an increase of 2.0 ± 0.7 km^3/year, and was correlated with trends in global surface air temperature and the North Atlantic Oscillation (NAO). Polyakov et al. (2008) found that over the last century, central Arctic Ocean salinity increased while Siberian shelf regions showed a freshening trend, largely due to variations in large-scale atmospheric circulation processes. McPhee et al. (2009) described a rapid change in the freshwater content in the western portion of the Arctic Ocean; freshwater had increased by 8,500 km^3, or 26%, compared to winter climatological values. River runoff and increased precipitation were amongst the dominant sources of the increase.

In the current state of changing Arctic climate, there is a need to better understand climate-discharge relationships in Arctic river systems, particularly in the four largest Arctic-

draining rivers: the Mackenzie River in Canada, and the Ob, Lena and Yenisei rivers in Eurasia, hence referred to as MOLY. Combined, these four rivers contribute almost 1900 km^3 of freshwater to the Arctic Ocean per year, or about 60% of annual flow volume from all Arctic contributing areas (Grabs et al., 2000; Prowse and Flegg, 2000). In Chapter 3, seasonality of discharge was found to have had shifted; although combined MOLY freshet flow had increased, the percentage of discharge released as a fraction of annual flow actually decreased by 1.7% during the period 1980 – 2009, while winter, spring and fall all increased (1.3%, 2.5% and 2.5% respectively). Meanwhile, summer flows reduced by 5.8%, indicating a shift toward earlier peak discharges. Annually, combined flow was found to have increased by 8.9 km^3yr^{-1} during the period 1980 – 2009. While this increase seems proportionally larger than the earlier study incorporating only major Eurasian basins, it was noted in Chapter 3 that observed trends varied substantially depending on the analysis window utilized.

In Chapter 4, it was revealed that trends on a sub-basin level generally matched the overall outlet pattern of shifting seasonality discovered in Chapter 3. Moreover, the majority of statistically significant trends occurred in unregulated sub-basins. This signified that flow regulation may have removed the effects of climatic drivers of trends in affected sub-basins. Further to this, despite regulated sub-basins often having vast drainage areas, no significant relationships with high freshet volumes recorded at the outlets were found in any regulated sub-basin. Meanwhile, several unregulated sub-basins, even smaller ones, displayed significant relationships with high freshet volumes at the outlets. However, high peak freshet magnitudes in regulated stations still related to high peak magnitudes at the outlets, particularly if there was only one dam impounding flow. This suggested that while regulation seemed to suppress the overall pulse of freshet flow, short-term high peaks could still affect flow at the outlet.

In order to link changing seasonality and magnitude of outlet discharge to key hydro-climatic regions, the effects of flow regulation must be separated from climate. To help achieve this goal, this study analyzes correlations of climatic and atmospheric patterns to the spring freshet for 106 sub-basins located within the MOLY basins, which are classified based on regulation status and regional topography. This will identify whether significant hydro-climatic relationships over regions unaffected by flow regulation have the potential to be major drivers of changes observed at the outlets, and whether climatic conditions leading to increased peak freshet magnitudes in regulated basins are also an important control.

5.2 Background

5.2.1 Basin physiography

The pan-Arctic drainage basins of the Mackenzie, Ob, Yenisei and Lena rivers are shown in Figure 1, with detailed study areas of the Mackenzie and Eurasian basins shown in Figure 2 and Figure 3, respectively. Total contributing areas of the four major river systems, including ungauged drainage areas, are as follows: Mackenzie 1,800,000 km^2 (Finnis et al., 2009); Ob 2,975,000 km^2 (Yang et al., 2004b); Lena 2,488,000 km^2 (Yang et al., 2002); and Yenisei 2,554,482 km^2 (Zhang et al., 2003). The pan-Arctic region contains nearly half of the global alpine and sub-polar glacial area (Dyurgerov and Carter, 2004). Meanwhile, some major Eurasian Arctic basins have a catchment area extending below 50°N, further south than what is traditionally considered the Arctic region (Loeng et al., 2005) (see Figure 1 and Figure 4). As a result, discharge behaviour at each of the four major drainage outlets is influenced along its course by sub-basin tributaries which may adhere to variety of hydrological regimes such as nival, pluvial, wetland, proglacial, prolacustrine, regulated, hybrid or other. For example, hydrologic retention due to extensive wetland coverage or large lakes within a catchment, such

as found in the Ob or Mackenzie basins, will lead to a more moderated seasonal discharge characteristic than basins without such retention (Carmack, 2000). In fact, spring floods in the Ob Basin may persist for up to 100 days (Nuttall, 2005).

Basin topography is shown in Figure 5 for the Mackenzie and Figure 6 for the Ob, Yenisei and Lena basins. Hypsometric curves for individual sub-basins are given in Appendix A. The Mackenzie Basin encompasses topography typical of the North American Cordillera in the western sub-basins, interior plains along the central Mackenzie corridor, and Precambrian Canadian Shield in the eastern portion of the basin (e.g., Woo and Thorne, 2003). The Ob Basin covers a portion of the Altai Mountains, where its headwaters originate, although up to 85% of the basin is situated in the Western Siberian lowlands (Nuttall, 2005). Central portions of the lowlands consist of taiga with extensive expanses of wetlands (Lydolph et al., 1977). By contrast, the Yenisei comprises a greater proportion of mountainous terrain. Southern portions of the Yenisei Basin encompass the Western and Eastern Sayan mountain ranges as well as Lake Baikal, and up to 80% of the basin is located in the Central Siberian Plateau, with elevations ranging from 500-700 metres a.s.l. The basin is bordered by the Yenisei Ridge in the west and the Putorana Mountains in the northeast (Lydolph et al., 1977). The Lena Basin includes the Baikal Mountains in the south, Yakut Lowlands below the mouth of the Aldan tributary and Verkhoyansk Mountains to the east (Lydolph et al., 1977).

5.2.2 Climate

The Mackenzie Basin covers several climatic regions, including cold temperate, mountain, subarctic and arctic zones (Woo and Thorne, 2003). Mean surface air temperature (SAT) averaged over the entire basin is -25°C in January and 13.8°C in July (Serreze, 2003). Precipitation ranges from greater than 1000 mm in the southwest of the basin to only 200 mm in

the delta region (Woo and Thorne, 2003). Climate in the Ob Basin is characterized by a cold continental and subarctic to arctic climate. It is the warmest of the four basins, with a mean SAT of -18.7°C in January and 18.1°C in July. However, summer maximum temperatures in the arid south can reach 40°C while winter temperatures in the Altai Mountains can fall as low as -60°C. Precipitation, which falls mainly as rain during the summer, can reach up to 1,575 mm annually in the Altai Mountains while much of the rest of the basin receives 300 – 600 mm annually (Serreze, 2003). Climate in the Yenisei Basin ranges from continental in the southern and central portions to subarctic in the north. Average winter temperatures range from -20°C in the southern regions to -32°C in the northern regions, while summer average temperatures range from 20°C in the south to 12°C in the north. Mean SAT is -26.5°C in January and 15.2°C in July. Precipitation, which falls chiefly as rain during the warmer months, ranges from 400 – 500 mm annually in the north, 500 – 750 mm in the central regions, and up to 1200 mm annually in the south (Serreze, 2003). Similarly, climate in the Lena Basin ranges from continental to subarctic and arctic. The Lena Basin is the coldest of the four basins. Winters are cold, clear and calm, with temperatures falling as low as -70°C. Summer temperatures range from 10 to 20°C. Mean SAT in January is -35°C and 14.7°C in July. The southern mountain ranges receive up to 600-700 mm of precipitation annually, while the central basin receives 200 – 400 mm and 100 mm falls annually in the delta regions. Like the other basins, most precipitation falls as rain during the summer (Lydolph et al., 1977; Serreze, 2003).

5.2.3 Climate Indices

Relationships between various large-scale oceanic and atmospheric oscillations and freshet characteristics are explored with focus on four climate indices that have previously been shown to affect climate in the areas of interest: Arctic Oscillation (AO), North Atlantic

Oscillation (NAO), Pacific Decadal Oscillation (PDO), and El Niño-Southern Oscillation (ENSO). ENSO is the leading pattern of interannual climate variability in the Pacific (Trenberth, 1997). The PDO index is derived as the leading principal component of monthly SST anomalies in the Pacific Ocean north of 20°N, separated from global SST anomalies to distinguish the pattern from any climate warming signal (Mantua et al., 1997). The AO is defined as the leading principal component of sea level pressure (SLP) anomalies north of 20°N and varies considerably in intra-seasonal time scales in mid- to high-latitudes (Thompson and Wallace, 1998). The NAO is the normalized difference in surface pressure (SP) between stations in Azores and Iceland (Hurrell, 1995).

In Canada, freshwater trends and variability have been linked to phases of the AO, ENSO and PDO (Bonsal et al., 2006). For example, stronger positive phases of the PDO and ENSO have been shown to be a factor in decreased precipitation and subsequently, decreased river discharge in northern Canada (Déry, 2005) while PDO in particular has been shown to affect hydrologic variability in western North American regions which may be encompassed by the Mackenzie basin (e.g., Hamlet and Lettenmaier, 1999; Neal et al., 2002). El Niño conditions and positive phases of PDO are representative of a deeper Aleutian Low, which has been linked to warmer winter and spring temperatures and subsequently, earlier snowmelt and freshwater ice break-up events in Western Canada (Bonsal et al., 2006). The opposite tendencies are associated with La Niña/negative phases of PDO.

Meanwhile, spring river discharge in the three Siberian basins has been positively correlated with winter and spring AO, an effect likely due to a high correlation of spring air temperature with the AO (Ye et al., 2004). The AO has a strong center of action over the central Arctic Ocean, but displays weaker centers of opposing sign over the northern Atlantic and

northern Pacific oceans (Serreze et al., 2002), thus exhibiting a weaker influence on climatic conditions over those regions. The positive phase of the AO results in anomalously high sea-level pressure in the mid-latitudes and lower pressure in the Arctic, causing confinement of cold air to the Arctic and resulting in warmer Northern Hemisphere winters (Stoner et al., 2009). Positive indices of NAO are representative of a stronger Icelandic Low, leading to colder winters and springs (and hence later freshwater break-up dates) over western Atlantic regions and vice versa (e.g., Hurrell, 1995; Bonsal et al., 2006) . Like the AO, the NAO is most active in winter months, bringing cold, dry Arctic air over northern Canada during its positive phase (Kingston et al., 2006). Although the NAO and AO are highly correlated and nearly identical in the temporal domain, with both demonstrating similar structures (Thompson and Wallace, 1998), there is evidence of distinct regional differences (e.g., Rogers et al., 2001). For example, effects of the NAO tend to be regionalized while AO effects are on a more global scale (Sveinsson *et al*., 2008), with the NAO in particular being shown to affect variability in temperature and precipitation over the Northern Hemisphere (Hurrell, 1995). Thus, both indices are included in this study to assess any potential regional differences.

Descriptive plots of surface air temperature (SAT) and precipitation anomalies regressed onto normalized anomalies of November through April AO, ENSO and PDO may be obtained from the Joint Institute for the Study of the Atmosphere and Ocean (JISAO), available at http://jisao.washington.edu/analyses0500/#details, and aid in interpretation of teleconnections results. These plots show that during 1950 – 1996, the positive phase of AO was associated with positive SAT anomalies and positive precipitation anomalies over most parts of the Mackenzie and Eurasian basins during the cold season. The warm phase of ENSO (El Niño) was associated with positive SAT and precipitation anomalies over the Mackenzie while Eurasian basins

showed mostly negative SAT with some positive SAT anomalies in the southern portions of the basins. Precipitation anomalies were mostly negative over Eurasian basins, with some regional indications of positive anomalies. PDO in its warm phase was associated with positive SAT anomalies in the Mackenzie and Eurasian basins, with very high anomalies over the Mackenzie. Distribution of precipitation anomalies varied, with mostly positive anomalies in the Mackenzie and Ob basins, and a mix of positive and negative precipitation anomalies in the Yenisei and Lena basins.

5.2.4 Flow regulation

Each of the MOLY watersheds experiences some degree of flow regulation within their catchments. The Yenisei basin is the most substantially regulated of the four basins, with at least six major reservoirs having a capacity greater than 25 km^3 located along the Yenisei and Angara stems (Yang et al., 2004a; Stuefer et al., 2011). The next most regulated is the Ob basin, containing one major reservoir with capacity greater than 25 km^3 and three midsize dams (Yang et al., 2004b). Of the Eurasian basins, the Lena is least affected by flow regulation, with only one major reservoir located along the Vilyuy tributary. The Mackenzie basin is also considered moderately affected, despite only one major reservoir located along the Peace tributary. Large lakes in the Mackenzie basin (e.g., Great Slave L. and Great Bear L.) provide substantial storage capacity, acting to reduce high spring peaks and sustain lower flows resulting in a more consistent runoff pattern throughout the year, similar to the effect of flow regulation (Woo and Thorne, 2003). Percentage of area in each basin directly upstream of a major reservoir, obtained by delineating the drainage area of each major reservoir, is as follows: Mackenzie 3.9%; Ob 11.6%; Yenisei 46.5% and Lena 4.2%. See Table 1 for characteristics of major reservoirs and

Figure 1 for locations of major reservoirs. Flow regulation on a sub-basin level is discussed in Section 5.3.1.

5.3 Data and Analysis

5.3.1 Data sources

Daily discharge data are obtained from the Environment Canada Hydrometric Database (HYDAT) for stations in the Mackenzie basin and from the Regional, Hydrometeorological Data Network for Russia (R-ArcticNET Russia v4.0) (Lammers and Shiklomanov, cited 2012) for the Ob, Lena and Yenisei basins. R-ArcticNET Russia (v4.0) contains information from 139 Russian Arctic gauges compiled from original archives of the State Hydrological Institute (SHI) and the Arctic and Antarctic Research Institute (AARI), St. Petersburg, Russia.

Climatic relationships over all basins are assessed using the CRU TS3.21: Climatic Research Unit (CRU) Time-Series (TS) Version 3.21 of High Resolution Gridded Data of Month-by-month Variation in Climate (Jan. 1901 – Dec. 2012), a dataset made publicly available through the British Atmospheric Data Centre (BADC) (see http://badc.nerc.ac.uk/data/cru/) at a spatial resolution of 0.5 x 0.5 degrees covering all global land areas, excluding Antarctica. Correlations are computed using the spatial average of the climatic variable over the respective basin. CRU TS3.21 is a gridded climatic dataset constructed from monthly observations of global meteorological stations. Mean, minimum and maximum temperature and total precipitation time series of an earlier predecessor of the dataset, CRU TS3.10, were found to compare favourably to other gridded datasets with the only exceptions occurring in regions or temporal periods with sparser observational data (Harris et al., 2014).

For comparison purposes, Appendix C provides the climatic relationships utilizing other available climatic datasets. For the Mackenzie basin, climatic relationships were also analyzed using a 10x10 km resolution, spline-interpolated dataset of daily precipitation and maximum and minimum daily temperature covering the period 1950 – 2010, referred to as NRCAN (2012) (Hutchinson et al., 2009; McKenney et al., 2011). The ERA-40 dataset was utilized for the Eurasian basins. ERA-40 is a re-analysis product of meteorological observations covering the period September 1957 to August 2002, produced by the European Centre for Medium-Range Weather Forcasts (ECMWF) (Uppala et al., 2005). Resolution is based on the T159 Gaussian grid, corresponding to a spatial resolution of approximately 1.125° x 1.125°. Bengtsson et al. (2004) noted that care must be taken when using re-analysis data such as ERA-40 in longer-term climate analyses due to inhomogeneities inherent in the available observational data. Because of the limited spatial resolution of the ERA-40 re-analysis dataset and limited spatial coverage of NRCAN (2012), CRU TS3.21 was chosen as the best available climatic dataset with the required spatial and temporal coverage and variables.

Climate indices for AO, NAO, PDO and ENSO are obtained from the National Oceanic and Atmospheric Administration (http://www.esrl.noaa.gov/psd/data/climateindices/list/) as monthly standardized anomalies. In this study the common Niño 3.4 index of sea surface temperature (SST) anomalies is used to classify ENSO conditions, which capture the region bounded between 5°S – 5°N and 170°W – 120°W.

Availability of hydrometric data is temporally limited, particularly in the Mackenzie region. As a result, two time periods are utilized to maximize the number of stations selected for inclusion; 1962 – 2000 and 1980 – 2000. These two periods are hence referred to as t_1 and t_2, respectively. Currently, the temporal range of Eurasian station data for most Lena, Yenisei or

Ob sub-basins obtained from R-ArcticNET Russia (v4.0) does not extend past the year 2000, whilst many stations in the Mackenzie basin have incomplete or missing data in the period 1970 – 1979. Hence, the shorter period t_2 is chosen to maximize spatial coverage of stations with available data, while the longer period t_1 is used to increase the power of significance testing and t-tests for stations that had available data. Table 2 identifies which stations in the Mackenzie region have available data throughout both time periods. All Eurasian sub-basin stations have data from 1962 or earlier. In total, there are 66 analyzed stations for t_1 and 106 analyzed stations for t_2. Relevant station information for all 106 stations is given in Table 2.

5.3.2 Sub-basin classification

Regulation is a necessary consideration when investigating trends in the magnitude and timing of the spring freshet. However, removing the effects of flow regulation by means of hydraulic modelling is not tractable within the scope of this study, nor would it be useful in determining the effects regulation may have on observed outlet discharge. To accommodate this, sub-basin stations have been classified into three categories. Unregulated stations (H_U) are not impounded in their upstream catchment areas. These catchment areas are considered regionally representative of a natural, unregulated basin with stable hydrologic conditions. Regulated stations (H_R) are located downstream of a major reservoir and have an average seasonal runoff pattern that is strongly influenced by the upstream flow impoundment. Lastly, minimally regulated stations (H_M) incorporate an upstream impounded flow signal that has been noticeably diminished by contribution from unaffected H_U basins. For example, the outlet station of the Mackenzie River, gauged near Inuvik, NT, is located approximately 3,120 km downstream of the W.A.C. Bennett Dam, gauged near Hudson's Hope, BC. Given the distance, the flow gauged

near Inuvik integrates a virtually insignificant percentage of impounded flow from the W.A.C. Bennett Dam.

Of course, there is a subjective element involved in differentiating between stations classified as H_R or H_M. Determining whether the regulation signal has been significantly diminished to classify as H_M requires comparing the station's average hydrograph to that of an H_R-classified upstream station, and also to unaffected H_U-classified upstream contributing basins. Note that H_U stations gauging the outlet of any large water body such as a natural lake will exhibit flow characteristics similar to that of an H_R station. The assigned classifications of each of the 106 analyzed stations are given in Table 2 with their associated sub-basin drainage areas are shown in Figure 2 for the Mackenzie basin and Figure 3 for the Eurasian basins. Approximately 85% of total gauged drainage area is classified as H_U in the Mackenzie. Due to limited station availability and expansive flow regulation in the Eurasian regions, only 9% of gauged area is classified as H_U in the Ob basin, 12% in the Yenisei and 8% in the Lena basin.

Sub-basins are also classified using a simple characterization based on geography and topology. Sub-basins, where available, are roughly divided into northern, southern, eastern and western regions of similar topographical composition. For example, the southern region of the Mackenzie basin incorporates largely alpine drainage areas, while the eastern region mostly consists of plains and large lakes. These regions are given in Figure 5 for the Mackenzie basin and Figure 6 for the Eurasian basins. Appendix A gives the hypsometric curves for each sub-basin separated by regional classification. These curves are useful in interpreting the effects elevation and topographic relief may have on freshet characteristics and trends.

In the Mackenzie basin, the southern region contains a high proportion of high-relief alpine drainage typical of the North American Cordillera, with one major dam in the southwest. The western region also consists of high-relief, high-elevation alpine zones including portions of the Mackenzie Mountains. The eastern region contains interior plains and Precambrian Canadian Shield while the northern region incorporates the plains surrounding Great Bear Lake and the Mackenzie Mountains to the west. In the Ob basin, the western and eastern regions consist largely of Western Siberian lowlands, although the western region covers a small section of the Altai Mountains at the headwaters of the Irtish River. Vast expanses of wetlands cover these regions. The southern region contains the largest proportion of high-relief drainage in the entire Ob basin. There are only three stations located in the Ob lowlands characterized as the northern region. In the Yenisei, the western region contains the Altai Mountains while the southern region contains the Sayan mountain ranges as well as Lake Baikal. Eastern drainages include higher-relief smaller watersheds below Lake Baikal, covering the Baikal Mountains to the east. The northern Yenisei basins include portions of the higher-elevation Central Siberian Plateau. Finally, the western regions of the Lena basin include the impounded Vilyuy River and Central Siberian Plateau. Southern basins cover some portions of the Baikal Mountains while the sole eastern basin drains a portion of the Verkhoyansk Mountains. Due to limited data availability, there are no northern-classified sub-basins in the Lena basin.

5.3.3 Flow estimation

Missing data in the hydrometric records are estimated using three different techniques. If there is an available upstream or downstream station gauging the same water course as the station with missing records, measurements from that recording gauge are used provided that it

has a complete record over the period to be estimated. To account for lesser or additional contributing area, the estimated river runoff rate is scaled such that

$$R_P = R_F A_P / A_F \qquad (1)$$

whereby R denotes the runoff rate ($m^3 s^{-1}$) over an area A (m^2) and subscripts P and F identify the partial and full records, respectively (Déry et al., 2005). Similarly, stations with partial records that have no upstream or downstream station along the same tributary are assessed for areal runoff scaling by comparing the hydrologic response to the closest available basin, provided it has a similar hydrologic response. Whenever possible, missing records are assigned values from basins with similar morphology and scaled by basin area in the same fashion as (1) (Gibson et al., 2006).

If there are no suitable stations to use for runoff scaling, then missing discharge values are estimated from the mean daily value of discharge over the entire evaluated time period, adjusted by the deviation in discharge from the mean of all rivers in the larger basin (evaluated over the same time period) for which data are available on the missing day (Déry et al., 2005). At least three rivers which do not have concurrent missing data are used for reconstruction in all cases. Here, data are reconstructed according to

$$R_P = \frac{R_1 + R_2 + \cdots + R_N}{\overline{R_1} + \overline{R_2} + \cdots + \overline{R_N}} \times \overline{R_P} \qquad (2)$$

whereby R_P is the station with partial records for which missing data are to be reconstructed, $\overline{R_P}$ is the mean discharge for a specific day over the remaining time period, and $R_1 \ldots R_N$ and $\overline{R_1} \ldots \overline{R_N}$ are the time series of discharge for a particular day and the daily mean of the corresponding station for the evaluated time period, respectively. In total, 46 out of 106

stations required infilling techniques to estimate missing data for one or more days throughout their records. The percentages of missing data infilled for each station, where applicable, are given in Table 2.

5.3.4 Spring freshet definition

Two methods are used to define the volume of discharge released during the spring freshet period: i) flows occurring during the period April through July (AMJJ), referred to as V_1 and ii) integrated flow from the date of the spring pulse onset to the hydrograph centre of mass calculated from pulse onset to the last day of the calendar year, referred to as V_2. July is used as the end-date of the V_1 period since some basins display high discharge rates well into the summer months. The date of the spring pulse onset is determined as the date at which cumulative departure from mean annual flow is most negative. This yields the date when flows on subsequent days are greater than the year average (Cayan et al., 2001; Stewart et al., 2005); see Appendix B for an illustration of the algorithm as well as visual indicators of the pulse onset, freshet end date, peak magnitude and V_1 and V_2 definitions of the spring freshet for a sample year of the Yenisei River outlet station.

Visual inspection of the results as shown in the example in Appendix B verified that this is a reliable method for identifying the start date of spring freshet. Choosing the freshet end date by visual means is subjective and influenced by precipitation, temperature and other factors; therefore, the hydrograph centre of mass adjusted by pulse onset as the freshet end date is used as a consistent method for determination of the freshet end date. Other metrics used to analyze freshet characteristics are given in Table 3.

5.3.5 Climatic correlations

A Pearson's *r* correlation analysis is used to examine the linear associations between climatic variables and spring freshet discharge. Significant correlations are indicated at the 5% and 10% levels. For each sub-basin, climatic correlations are obtained for pulse dates F_P, freshet lengths F_L, and peak freshet magnitudes F_M with temperature, and freshet volumes V_1 and April – July volumes V_2 with precipitation. Correlations are computed using the spatial average of the climatic variable over the respective sub-basin. Temperatures are averaged over April - June for climatic correlations with F_P, F_L and F_M since these measures may be affected by climatic conditions just prior to or during the spring break-up period. However, volume measures may be affected by previous seasonal conditions, so to accommodate for seasonal lag of accumulated precipitation, the period of November - March is chosen for climatic correlations of cumulative precipitation with V_1 and V_2.

5.3.6 Teleconnections

Climate indices are averaged into a "winter" season of December – February, and a "spring" season of March – May to accommodate for influence of both current and lagged previous-season atmospheric/oceanic conditions. In this study, the winter season is used for precipitation-related variables (i.e., volume) while the spring season is used for temperature-related variables (i.e., pulse dates and peak freshet magnitude). Several iterations of individual months and monthly combinations have been assessed; the described seasons given here are chosen since they show the greatest spatial coherence of significant results across the pan-Arctic domain. For example, fewer significant relationships were found between winter climate indices and freshet pulse dates. Similarly, few relationships were found between spring climate indices and freshet volume.

Following Maurer (2004) and Burn (2008), a composite approach is used to assess potential relationships between climate indices and freshet measures. This approach is chosen since climate signals from large-scale teleconnections are not always linearly related to the hydro-climatic variable in question; for example, a strong relationship may exist in one phase but may be non-existent or weak in the other. The scatterplot of Figure 7 illustrates an example of this, in which the ten highest and ten lowest NAO anomalies are averaged over December – February and plotted against freshet volume for station 07NB001 in the Mackenzie basin. Here, the relationship is clearly stronger for positive values of the NAO anomaly, but weaker for negative values. For this analysis, freshet statistics for years corresponding to the top/bottom 25% of climate indices for each time period are evaluated separately, using a t-test at a 5% significance level to determine if the set is significantly different from the entire series mean.

5.4 Results

5.4.1 Climatic Relationships

Strength and significance of correlations of climatic variables with freshet measures for the time periods 1962 – 2000 and 1980 – 2000 (t_1 and t_2, respectively) are shown in Figure 8 through Figure 17. Correlations significant at the 10% level are marked with an asterisk ✳ while correlations significant at the 5% level are marked with a bolded asterisk ✱.

Figure 8 displays the correlations of average April – June temperatures with freshet pulse dates F_P during t_1 for the Mackenzie and Eurasian basins, while correlations with F_P during t_2 are given in Figure 9. A negative relationship indicates that warmer April – June temperatures are correlated with earlier pulse dates, and vice versa. During both time periods, relationships are overwhelmingly moderate to strong negative and significant at the 5% level in all four basins. The most notable clustering of weak or negligible correlations reside in the southern portion of

the Mackenzie basin and eastern Yenisei, and are observed during both t_1 and t_2. Only one small-sized basin, 07AF002 located in the southern portion of the Mackenzie basin, demonstrates a significant, positive relationship of warmer April – June temperature with later pulse dates in both time periods. At least 64% and up to 100% of all significant correlations with F_P occur in H_U stations (Table 4), although significant correlations are seen in the regulated Irtish (Ob), Angara (Ob) and Yenisei stems.

Correlations of average April – June temperatures with freshet length F_L during t_1 for the Mackenzie and Eurasian basins are given in Figure 10, while Figure 11 provides the correlations with F_L during t_2. A positive relationship indicates that warmer April – June temperatures are correlated with longer freshet length as the spring melt period is extended, and vice versa. During t_1, the majority of sub-basins demonstrate weak to strong positive relationships, significant at the 5% level. No negative correlations exist although there are several negligible relationships in the southern Mackenzie and Ob basins. During t_2, relationships are generally weaker, with greater occurrence of negligible or weak positive relationships when compared to t_1. Some negative correlations are also shown in the Mackenzie and Ob basins although relationships are still dominated by positive correlations, particularly in the southern and western high-relief regions of the Mackenzie. The differences in relationships seen in t_1 and t_2 may be indicative of the changing nature of the seasonal snowpack; this is further discussed in Section 5.5. Similarly to the analysis for F_P, the majority of significant correlations typically occur in H_U basins (Table 4), with no significant (5%) correlations in H_R stations during t_2.

Correlations of average April – June temperatures with peak freshet magnitude F_M during t_1 for the Mackenzie and Eurasian basins are given in Figure 12, while Figure 13 provides the correlations with F_M during t_2. A negative relationship indicates that warmer April – June

temperatures are correlated with a lower freshet magnitude, and vice versa. This may be indicative of a more moderated annual runoff regime, in which cold season flows are increased while spring peaks are decreased in magnitude, but extended in duration. During both t_1 and t_2, negative correlations are prevalent in the Mackenzie and Ob basins, with many relationships significant at the 5% level although correlations are generally weak to moderate. The Lena and Yenisei basins exhibit very few significant correlations in either time period and most correlations are ranked negligible or weak. Relationships are strongest in the southern and western Mackenzie regions during t_2, with the regulated Peace tributary indicating a significant relationship in both time periods. However, the majority of significant correlations again occur in H_U basins, as given in Table 4. No significant trends occur in any H_R-classified Eurasian sub-basin during t_2.

Figure 14 provides the correlations of cumulative November – March precipitation with freshet volume V_2 during t_1 for the Mackenzie and Eurasian basins, while Figure 15 shows the correlations with V_2 during t_2. A positive relationship indicates that higher cumulative November – March precipitation is correlated with a higher freshet volume, and vice versa. During t_1, the southern Mackenzie basin, and northern and eastern regions of the Ob and Yenisei basins, are dominated by weak to strong positive correlations significant at the 5% level. Relationships in the southern portions of the Eurasian basins are less distinct, with the majority of basins demonstrating a negligible correlation value. During t_2, the southern Mackenzie basin and northern regions of the Eurasian basins again show a greater incidence of positive relationships, although the strength and significance of these relationships are generally weaker compared to t_1. In addition, all basins show a greater occurrence of negative relationships (particularly in the high-relief eastern Ob and western Yenisei) although none of these

correlations are significant at the 5% or 10% levels. The notable regional patterns of freshet volume correlations with winter precipitation suggest potential changes in hydrologic regime for some basins; this is further discussed in Section 5.5. Between 50 – 100% of all significant (5%) correlations occur in H_U basins during both time periods.

Similarly, Figure 16 gives the correlations of winter precipitation with freshet volume V_1 (April through July cumulative volume) for the Mackenzie and Eurasian basins during t_1, while Figure 17 displays correlations of winter precipitation with V_1 during t_2. Spatial distribution of correlations in V_1 and V_2 are very similar during their respective time periods, with significant, positive relationships more prevalent in the southern Mackenzie, and northern and eastern Yenisei and Ob basins. Significant relationships of volume V_1 or V_2 with cumulative cold season precipitation largely occur in H_U basins (Table 4). No significant results are seen in any H_R basin during t_2.

5.4.2 Teleconnections

Similarly to climatic relationships, the majority of significant teleconnections to any freshet measure are largely limited to H_U basins, with exception of a few instances of significant results in the regulated Irtish tributary and southern Yenisei main channel. Figure 18 presents the statistically significant March – May teleconnections with pulse dates F_P during t_1 while Figure 19 gives the results during t_2. During t_1, NAO and ENSO show little influence in any of the basins during either phase, although some stations exhibited later pulse dates during the negative phase of each oscillation. The negative phase of AO (associated with cooler SAT anomalies) was shown to relate to later pulse dates in some Eurasian and Mackenzie stations while the positive phase was related to earlier pulse dates in two northern Ob basin stations. Positive phase of PDO was correlated with delayed pulse dates in the northern Ob and Yenisei

regions. In the Mackenzie basin, negative PDO associated with lower SAT anomalies was correlated with later pulse dates in two stations while positive PDO was correlated with an earlier occurrence of pulse dates in one station. During t_2, there were few significant teleconnections with NAO. AO in its negative phase was largely associated with later occurrence of pulse dates (5 or more days) in northern Ob and Yenisei, although it was also related to earlier pulse dates in two eastern Yenisei basins. In the Mackenzie basin, the positive phase of AO was associated with earlier pulse dates. These results were consistent with descriptions of SAT anomalies during the positive phase of AO, discussed in Section 5.2.3. PDO was generally linked with later pulse dates in the western Mackenzie, Central Siberian Plateau and eastern Yenisei in its positive phase, while in its negative phase relationships with earlier pulse dates were mostly seen in the Ob basin. This is somewhat unexpected since PDO in its positive phase is linked with positive SAT anomalies in all basins, which would generally lead to earlier pulse dates. These results may be in part due to small sample sizes, and also due to the decadal nature of PDO. Here, the t_2 period covers an entirely positive PDO regime, which explains the high bias towards significant relationships with positive phases. El Niño conditions were connected with earlier pulse dates in the Mackenzie and later pulse dates in Eurasia, although few significant relationships were found. These results were again consistent with SAT anomalies associated with El Niño.

Figure 20 presents the March – May teleconnections with peak freshet magnitude F_M during t_1 while Figure 21 gives the results during t_2. During t_1, NAO and AO in their positive phases were associated with lower peak freshet magnitudes, particularly in Eurasian basins. NAO exhibited a strong influence in the eastern Ob and Yenisei regions while AO was mostly detectable in northern and western Ob. Similarly, PDO in its positive phase was associated with

lower F_M except most results were located in high-relief regions of the southern Mackenzie and western Yenisei. These findings were consistent with positive SAT anomalies associated with the positive phases of these indices, as discussed in Section 5.2.3. They were also consistent with positive correlations of temperature with decreased F_M, as discussed in Section 5.4.1. Meanwhile, ENSO demonstrated little effect on F_M. During t_2, positive NAO associated with higher SAT anomalies again demonstrated linkages with lower peak freshet magnitude, especially in the eastern Ob, although AO relationships did not persist in Eurasian basins; during the latter period, negative AO leading to lower Mackenzie basin winter precipitation anomalies (i.e., drier winter conditions) largely demonstrated relationships with decreased F_M in the northern and eastern Mackenzie basin. Significant relationships with PDO were limited to its negative phase during t_2, showing that for the most part, negative PDO associated with cooler winter temperatures as well as somewhat drier winter conditions (albeit with regional variation) had significant relationships with decreased freshet magnitude. ENSO revealed strong relationships in both phases in the Mackenzie sub-basins, with a distinct separation of phases visible between lower and middle latitudes. JISAO plots as discussed in Section 5.2.3 show that there is indeed a division between the north-western and south-eastern portions of the Mackenzie basin, whereby El Niño conditions lead to wetter winters in the former and drier winters in the latter, and vice versa for La Niña. Here, La Niña (cooler, drier winters in the upper region) showed strong relationships with decreased F_M in the upper Mackenzie while El Niño (warmer, drier winters in the southern region) was similarly connected to decreased F_M in the southern Mackenzie.

Distributions of December – February teleconnections with freshet volume were similar for V_1 and V_2 during their respective time periods. Figure 22 and Figure 23 present the

December – February teleconnections with freshet volume V_2 during t_1 and t_2, respectively, while Figure 24 and Figure 25 display the teleconnections with freshet volume V_1 during t_1 and t_2, respectively. Regional patterns were most pronounced during t_1, with strong influence of positive phases of PDO, AO, NAO and ENSO (El Niño) reflecting positive Central Pacific SST anomalies resulting in warmer, drier winter conditions for the southern Mackenzie basin and correspondingly decreased freshet volumes. In the Eurasian basins, negative NAO and AO were related to increased volumes in some southern Ob basins. This is likely due to regional variation in precipitation anomalies associated with these indices, where negative phases can lead to increased winter precipitation anomalies in southern portions of the Eurasian basins. PDO generally did not exhibit any significant relationships in Eurasian basins. ENSO, meanwhile, showed increased volume during El Niño (wetter winters, regionally) in two Ob sub-basins, while nearby in southern Ob and western Yenisei alpine regions, La Niña (drier winters, regionally) showed significant relationships with decreased freshet volumes. During t_2, relationships were less distinct. With exceptions in some sub-basins, positive phases of AO and NAO were generally linked with decreased freshet volumes, mostly in the eastern Yenisei. Despite positive AO and NAO typically leading to wetter winter conditions, freshet volume may be adversely affected due to higher winter temperatures resulting in lower snowpack accumulation. PDO and ENSO demonstrated the strongest relationships during t_2, particularly in the southern Mackenzie basin. Negative PDO (drier winter conditions over much of the Mackenzie basin) was associated with decreased freshet volumes, although it must again be noted that t_2 falls in a positive PDO regime, so shorter-term negative anomalies given here are relative to that period only and do not necessarily reflect the overall state of the PDO in that time period. Similarly to how positive AO and NAO resulting in warmer winter temperatures may

lead to less winter snowpack accumulation, El Niño conditions were also strongly associated with decreased volumes in the southern Mackenzie basin. In Eurasia, positive PDO (associated with generally drier winters in the Ob basin and wetter winters in the Yenisei) was related to decreased freshet volumes in several Ob sub-basins and increased volumes in one Yenisei sub-basin.

5.5 Discussion

Correlations of spring temperatures with F_P, F_L and F_M timing measures were typically stronger and had more significant results when compared to correlations of cumulative cold-season precipitation with freshet measures V_1 and V_2, particularly in the Eurasian basins where few significant precipitation-volume correlations existed. Climatic relationships are compared to regional trends as determined in Chapter 4 in order to resolve whether trends can be attributable to climate or flow regulation, and what effects climatic relationships over key regions might have on outlet flows. Trends in the Mackenzie basin were largely marked by strong regional similarities in the southern and western high-relief drainage areas, with fewer patterns evident in the low-relief northern and eastern regions. Freshet volume as well as low peak freshet magnitudes at the Mackenzie River outlet displayed significant associations with unregulated, mountainous western basins. High peak freshet magnitudes, meanwhile, were strongly associated with the southern alpine region and along the regulated Peace tributary, implying that regulation did not negate the downstream impacts of the highest peaks generated during the spring snowmelt period.

Regional patterns of trends in the Eurasian basins were less clear, with the strongest clustering appearing in the higher-relief areas of the southern Ob, and southern, western and eastern Yenisei basin. High volume at the Ob River outlet was related to the upper Ob and Irtish

stations gauging minimally regulated areas. No volume associations with the Ob outlet were recorded in the regulated lower Irtish (H_R) or Ob at Kolpashevo (H_M) stations, both draining large basins. However, a relationship with high peak freshet magnitude at the outlet was seen at the Ob at Kolpashevo station which has an upstream dam but also has a substantial high-relief headwater area. In the Yenisei, no high volume or magnitude relationships with the outlet were observed in any of the highly regulated but steep western and southern drainage regions. The multiple dams along the tributary stems likely suppressed any high peak flows that might still be evident in other sub-basins (such as the Peace or Ob at Kolpashevo) with only one dam impounding flow. Low magnitude was, however, associated with unregulated eastern stations below Lake Baikal and along the Yenisei main channel, owing to outlet proximity. The Lena basin followed the same general pattern, with no outlet flow relationships seen in the large but minimally-regulated Vilyuy tributary. High and low volumes had some associations with unregulated basins draining into the southern main Lena channel and there were no high magnitude relationships with the outlet in any sub-basin.

Pulse dates were strong negatively correlated with April – June temperature in most sub-basins, with the majority of those correlations statistically significant. This indicated that warmer spring temperatures resulted in an earlier freshet onset in those basins. Meanwhile, sub-basin trends revealed pulse dates were, for the most part, decreasing in the same sub-basins. Pulse date correlations in the Mackenzie basin were exclusively limited to H_M and H_U sub-basins. In the Eurasian basins, significant correlations and trends were also found in H_R sub-basins, suggesting that flow regulation does not have a substantial impact on pulse timing in those regions. Freshet length showed mostly positive correlations throughout all basins during 1962 – 2000, indicating that warmer April – June temperatures were correlated with sustained

snow melt and a longer freshet period. However, during 1980 – 2000, relationships were generally weaker, with some sub-basins showing negative correlations with freshet length. Many of those mixed results occurred in lowland regions with limited topographical relief, suggesting that basins with less high-elevation snow storage were more susceptible to decreased freshet duration with warmer spring temperatures. Warmer spring temperatures may also have enhanced infiltration into a thawing active layer, resulting in a reduction of the spring flood duration. Significant correlations as well as trends were found in H_R sub-basins, suggesting again that flow regulation does not strongly affect the natural relationship of temperature with timing measures.

Peak freshet magnitude displayed mostly negative correlations in the Mackenzie basin and in the Ob and Yenisei basins during both time periods. This revealed that warmer spring temperatures resulted in decreased peak freshet magnitudes in those regions. Again, correlation patterns were consistent with previously observed decreasing trends in peak freshet magnitude, with some notable exceptions particularly in the Lena basin during t_2 where peak freshet magnitudes were shown to be largely increasing. The trend and hydrograph analysis of Chapter 4 revealed that the combination of generally more persistent freshet durations and lower freshet magnitudes resulted in an overall flattening of the annual hydrograph shape in many sub-basins. This may also have been indicative of a potential shift from a distinctly nival hydrological regime to a more pluvial or hybrid regime in some basins. Notably, as discussed in the recap of Chapter 4, low peak freshet magnitudes at the Mackenzie outlet during 1980 – 2000 were found to have a relationship with the unregulated western region, while high outlet magnitudes were strongly associated with the southern alpine region and along the regulated Peace tributary. Here, negative correlations are indicated in the same regions, signifying that the climatic drivers

influenced flow at the outlet regardless of regulation. In the Eurasian basins, magnitude correlations again agree with outlet and sub-basin relationships, showing a significant correlation in the minimally-regulated Ob at Kolpashevo station that was related to high peak magnitudes at the outlet. No high peak magnitude relationships with the outlet were discovered in the Yenisei and Lena basins, and similarly, there are few significant climatic correlations in those regions.

Freshet volume correlations by either definition showed distinct regional variability in all basins, where higher winter precipitation in the southern alpine region of the Mackenzie and northern regions of the Eurasian basins were positively correlated with freshet volumes and increasing trends in those basins. However, in the southern Ob and western Yenisei basins, higher cumulative winter precipitation did not necessarily result in greater freshet volumes. This was evidenced by weaker or even negative correlations (not statistically significant) of freshet volume to winter precipitation, possibly due to susceptibility to a warming climate causing a shift to a more rainfall-driven hydrologic regime, whereby the integrated effects of increased temperature and precipitation may have resulted in less winter snowpack precipitation accumulation and correspondingly lower freshet volumes. Interestingly, volume correlations with winter precipitation were strongest in the southern Mackenzie region, although no significant relationships were found in any southern sub-basin with outlet volume, likely as a result of upstream regulation along the Peace River tributary whose drainage area encompasses these smaller regions. In Eurasian basins, no strong correlations were found in any H_R basin during 1980 – 2000, while few sub-basins displayed any relationship with volume at the outlet. Those that did were either H_U or H_M-classified. This suggests that extensive regulation in the Eurasian basins may be obscuring the impact of climatic controls on those regions.

Relationships between freshet measures and a variety of teleconnections indices averaged over different seasons revealed that regional patterns were generally less consistent during the shorter period of t_2 compared to t_1, most likely due to smaller sample sizes. Where statistically significant relationships existed, only one phase of a particular climate signal was typically associated with the relationship although there were a limited number of occasions where significant results in both phases resulted in an opposite response. Positive AO and NAO leading to warmer winters and springs were typically associated with earlier pulse dates, decreased peak freshet magnitude and lower freshet volume although there were some regional exceptions. Positive ENSO (El Niño), associated with positive SAT and precipitation anomalies over the Mackenzie and negative SAT and precipitation anomalies over the Eurasian basins (with some regional variability), demonstrated relationships with earlier Mackenzie and later Eurasian pulse dates, and decreased peak freshet magnitude in the southern Mackenzie basin. El Niño had strong associations with decreased freshet volume in the southern Mackenzie but had little effect on Eurasian volumes. Meanwhile, positive PDO, associated with positive SAT anomalies and mixed, mostly positive precipitation anomalies in all basins, tended to coincide with later pulse dates and lower freshet magnitudes in all basins. These unexpected relationships of PDO with delayed pulse onset may be due to the long-term decadal variation of this index, particularly during t_2 which occurs entirely in a warm PDO phase. Similarly, warm phase PDO was associated with decreased freshet volume in the Mackenzie basin during t_1 but not during t_2. Further research is suggested to obtain more insight into these PDO interactions, as well as potential integrated effects of multiple climate indices.

Finally, it is important to note which teleconnections indices influenced regions which presented a significant association with high or low peak freshet magnitudes or volumes at the

outlet. In the Mackenzie basin, low magnitude at the outlet, associated with the western region, showed a strong connection to negative ENSO affecting peak freshet magnitudes. High outlet magnitude, meanwhile, was linked with the southern region, which indicated strong positive ENSO influence. High outlet volume was related to the western region, which displayed some negative PDO volume relationships, while scattered low volume relationships were linked with both negative PDO and positive ENSO. In Eurasia, high magnitude at the outlet was only connected with one Ob sub-basin, corresponding to negative NAO in that region. Low magnitudes at the outlet were associated with several scattered basins, but indicated little influence of any teleconnections indices. Similarly, high and low volumes at the outlet were linked with several sub-basins, although none of these displayed any significant influence of NAO, AO, PDO or ENSO.

5.6 Conclusions

In summary, the effects of regulation versus climate on the hydrologic response of sub-basins, and their corresponding relationship to outlet flow, were clarified by comparing regional variations in climatic correlations with sub-basin trends that were obtained in Chapter 4. Here, timing and peak magnitude (F_P, F_L and F_M) of the freshets within sub-basins were found to be strongly linked to spring temperatures. Moreover, regulation did not appear to completely suppress these climatic relationships, since significant trends were found where significant climatic correlations existed, regardless of regulation status.

Regulation did, however, appear to limit climatic relationships of cold season precipitation accumulation with freshet volume V_1 and V_2, since few significant correlations with volume were found in regulated stations. This reinforces the notion that flow impoundment does act to suppress some natural climatic drivers of freshet generation, with potential impact to seasonal

runoff regimes. However, volume relationships with cold season precipitation were not as distinct as temperature linkages with freshet timing. This suggests that an integrated multi-variable approach incorporating both temperature and precipitation is needed to further clarify these freshet volume relationships. Furthermore, although the correlation analysis reveals some climatic relations with freshet measures, it doesn't account for all climatic interactions with trends. It is therefore recommended to analyze climatic trends in temperature and precipitation for side-by-side comparison to freshet trends, and to perform this comparison using a suite of re-analysis and observed climatic data sets.

Sub-basin freshet measures were significantly related to several large-scale climate indices. Some climate indices were linked with regions that had previously been shown to impact freshet measures at the outlets. This knowledge is valuable in determining potential predictors controlling freshet generation. Additionally, atmospheric variability has been shown not only to affect runoff generation within basins but also to affect terrestrial runoff trajectory upon entering the Arctic Ocean. For example, the state of the AO was noted to affect the way runoff enters the interior ocean waters, whereby a positive AO forces Eurasian runoff eastward into the Beaufort Gyre and a negative AO forces runoff directly towards the Transpolar Drift (Johnson and Polyakov, 2001).

Since there were significant differences in climatic and large-scale atmospheric variability relationships with unregulated stations versus those stations incorporating an upstream regulation signal, the effects of flow regulation on the timing and magnitude of freshet response need to be more fully evaluated. It is recommended to approach this via hydraulic flow modelling that can remove the effect of regulation and thereby permit the controlling signals of climate to be better identified. Likewise, flow modelling can be used to determine whether regulation can actually

mitigate the effects of climatic variation on discharge seasonality and magnitude at the outlets. Lastly, it is recommended to undertake a travel-time analysis utilizing a hydrologic flow-routing model to determine the proportional contribution of the given sub-basins to flow recorded at the outlet. This will allow for further discussion on the regional impacts of climatic influences to overall circumpolar freshet freshwater contribution to the Arctic Ocean. This discussion is especially important since climate change, resulting in an increase in precipitation and air temperature over Arctic basins, as well as a potential increase in extreme climatic events such as stronger El Niños, will continue to alter the nature of terrestrial freshwater contribution to the Arctic Ocean.

5.7 Acknowledgements

This work was partially supported by a Discovery Grant and ArcticNet funding from the Natural Sciences and Engineering Council of Canada (NSERC). The authors would also like to acknowledge the Arctic Rapid Integrated Monitoring System (ArcticRIMS), the Regional Hydrometeorological Data Network for the Pan-Arctic Region (R-ArcticNet), the European Centre for Medium-Range Weather Forecasts, and the National Oceanic and Atmospheric Administration for freely providing data.

References

Aagaard, K., Carmack, E.C., 1989. The role of fresh water in ocean circulation and climate. J. Geophys. Res. 94, 14,485–14,498.

Ahmed, R., Prowse, T.D., Bonsal, B.R., Dibike, Y.B., 2014a. Seasonal runoff characteristics of four major Arctic-draining rivers. Unpubl. thesis results.

Ahmed, R., Prowse, T.D., Bonsal, B.R., Dibike, Y.B., 2014b. Trends in the spring freshet of four major Arctic-draining rivers. Unpubl. thesis results.

Ahmed, R., Prowse, T.D., Dibike, Y.B., Bonsal, B.R., 2012. Temporal sequencing of annual spring runoff in major Arctic-draining rivers. In: Poster Session Presented at: American Geophysical Union Fall Meeting 2012. Dec. 3-7, 2012. San Francisco, CA.

Arnell, N.W., 2005. Implications of climate change for freshwater inflows to the Arctic Ocean. J. Geophys. Res. 110, D07105.

Bengtsson, L., Hodges, K.I., Hagemann, S., 2004. Sensitivity of the ERA40 reanalysis to the observing system: determination of the global atmospheric circulation from reduced observations. Tellus A 56, 456–471.

Bonsal, B.R., Prowse, T.D., Duguay, C.R., Lacroix, M.P., 2006. Impacts of large-scale teleconnections on freshwater-ice break/freeze-up dates over Canada. J. Hydrol. 330, 340–353.

Burn, D.H., 2008. Climatic influences on streamflow timing in the headwaters of the Mackenzie River Basin. J. Hydrol. 352, 225–238.

Carmack, E., Mclaughlin, F., Yamamoto-Kawai, M., Itoh, M., Shimada, K., Krishfield, R., Proshutinsky, A., 2008. Freshwater storage in the Northern Ocean and the special role of the Beaufort Gyre. In: Dickson, R.R. et al. (Ed.), Arctic-Subarctic Ocean Fluxes: Defining the Role of the Northern Seas in Climate. Springer, New York, pp. 145–169.

Carmack, E.C., 2000. The freshwater budget of the Arctic Ocean: Sources, storage and sinks. In: Lewis, E.L. (Ed.), The Freshwater Budget of the Arctic Ocean. Kluwer, Dordrecht, Netherlands, pp. 91–126.

Cayan, D.R., Kammerdiener, S.A., Dettinger, M.D., Caprio, J.M., Peterson, D.H., 2001. Changes in the Onset of Spring in the Western United States. Bull. Am. Meteorol. Soc. 82, 399–415.

Déry, S., Stieglitz, M., McKenna, E., Wood, E.F., 2005. Characteristics and trends of river discharge into Hudson, James, and Ungava Bays, 1964-2000. J. Clim. 18, 2540–2557.

Déry, S.J., 2005. Decreasing river discharge in northern Canada. Geophys. Res. Lett. 32, L10401.

Dyurgerov, M.B., Carter, C.L., 2004. Observational Evidence of Increases in Freshwater Inflow to the Arctic Ocean. Arctic, Antarct. Alp. Res. 36, 117–122.

Finnis, J., Cassano, J., Holland, M., Uotila, P., 2009. Synoptically forced hydroclimatology of major Arctic watersheds in general circulation models, Part 1 : the Mackenzie River Basin. Int. J. Climatol. 29, 1226–1243.

Gibson, J.J., Prowse, T.D., Peters, D.L., 2006. Hydroclimatic controls on water balance and water level variability in Great Slave Lake 4172, 4155–4172.

Grabs, W.E., Portmann, F., De Couet, T., 2000. Discharge observation networks in Arctic regions: Computation of the river runoff into the Arctic Ocean, its seasonality and variability. In: Lewis, E.L. (Ed.), The Freshwater Budget of the Arctic Ocean. Kluwer, Dordrecht, Netherlands, pp. 249–267.

Hamlet, A.F., Lettenmaier, D.P., 1999. Columbia River streamflow forecasting based on ENSO and PDO climate signals. J. Water Resour. Plan. Manag. 125, 333–341.

Harris, I., Jones, P.D., Osborn, T.J., Lister, D.H., 2014. Updated high-resolution grids of monthly climatic observations - the CRU TS3.10 Dataset. Int. J. Climatol. 34, 623–642.

Hurrell, J.W., 1995. Decadal Trends in the North Atlantic Oscillation: Regional Temperatures and Precipitation. Science (80-.). 269, 676–679.

Hutchinson, M.F., McKenney, D.W., Lawrence, K., Pedlar, J.H., Hopkinson, R.F., Milewska, E., Papadopol, P., 2009. Development and testing of Canada-wide interpolated spatial models of daily minimum–maximum temperature and precipitation for 1961–2003. J. Appl. Meteorol. Climatol. 48, 725–741.

Johnson, M.A., Polyakov, I. V, 2001. The Laptev Sea as a source for recent Arctic Ocean salinity changes. Geophys. Res. Lett. 28, 2017–2020.

Kattsov, V.M., Walsh, J.E., Chapman, W.L., Govorkova, V. a., Pavlova, T. V., Zhang, X., 2007. Simulation and Projection of Arctic Freshwater Budget Components by the IPCC AR4 Global Climate Models. J. Hydrometeorol. 8, 571–589.

Kingston, D.G., Lawler, D.M., McGregor, G.R., 2006. Linkages between atmospheric circulation, climate and streamflow in the northern North Atlantic: research prospects. Prog. Phys. Geogr. 30, 143–174.

Lammers, R.B., Shiklomanov, A.I., 2013. A Regional, Hydrometeorological Data Network for Russia. Available online at http://www.r-arcticnet.sr.unh.edu/v4.0/index.html.

Lammers, R.B., Shiklomanov, A.I., Vörösmarty, C.J., Fekete, B.M., Peterson, B.J., 2001. Assessment of contemporary Arctic river runoff based on observational discharge records. J. Geophys. Res. 106, 3321–3334.

Loeng, H., Brander, K., Carmack, E., Denisenko, S., Drinkwater, K., Hansen, B., Kovacs, K., Livingston, P., Mclaughlin, F., Bellerby, R., Browman, H., Furevik, T., Grebmeier, J.M., Jansen, E., Jónsson, S., Jørgensen, L.L., 2005. Ch. 9: Marine Systems. In: Symon, C., Arris, L., Heal, B. (Eds.), Arctic Climate Impact Assessment. Cambridge University Press, New York, pp. 453–538.

Lydolph, P.E., Temple, D., Temple, D., 1977. Geograhpy of the U.S.S.R. Wiley, New York.

Mantua, N.J., Hare, S.R., Zhang, Y., Wallace, J.M., Francis, R.C., 1997. A Pacific interdecadal climate oscillation with impacts on salmon production. Bull. Am. Meteorol. Soc. 78, 1069–1079.

Maurer, E.P., Lettenmaier, D.P., Mantua, N.J., 2004. Variability and potential sources of predictability of North American runoff. Water Resour. Res. 40, W09306.

McClelland, J.W., Holmes, R.M., Dunton, K.H., Macdonald, R.W., 2011. The Arctic Ocean Estuary. Estuaries and Coasts 35, 353–368.

McKenney, D.W., Hutchinson, M.F., Papadopol, P., Lawrence, K., Pedlar, J.H., Campbell, K., Milewska, E., Hopkinson, R.F., Price, D., Owen, T., 2011. Customized spatial climate models for North America. Bull. Am. Meteorol. Soc. 92, 1611–1622.

McPhee, M.G., Proshutinsky, A., Morison, J.H., Steele, M., Alkire, M.B., 2009. Rapid change in freshwater content of the Arctic Ocean. Geophys. Res. Lett. 36, L10602.

Neal, E.G., Walter, M.T., Coffeen, C., 2002. Linking the Pacific Decadal Oscillation to seasonal stream discharge patterns in Southeast Alaska. J. Hydrol. 188–197.

Nuttall, M., 2005. Encyclopedia of the Arctic. Routledge.

Peterson, B.J., Holmes, R.M., McClelland, J.W., Vörösmarty, C.J., Lammers, R.B., Shiklomanov, A.I., Shiklomanov, I.A., Rahmstorf, S., 2002. Increasing river discharge to the Arctic Ocean. Science (80-.). 298, 2171–2173.

Polyakov, I. V., Alexeev, V.A., Belchansky, G.I., Dmitrenko, I.A., Ivanov, V. V., Kirillov, S.A., Korablev, A.A., Steele, M., Timokhov, L.A., Yashayaev, I., 2008. Arctic Ocean Freshwater Changes over the Past 100 Years and Their Causes. J. Clim. 21, 364–384.

Prowse, T.D., Flegg, P.O., 2000. Arctic river flow: A review of contributing areas. In: Lewis, E.L. (Ed.), The Freshwater Budget of the Arctic Ocean. Kluwer, Dordrecht, Netherlands, pp. 269–280.

Rogers, A.N., Bromwich, D.H., Sinclair, E.N., Cullather, R.I., 2001. The atmospheric hydrologic cycle over the Arctic basin from reanalyses, Part 2. J. Clim. 14, 2414–2429.

Serreze, M.C., 2003. Arctic Climate. In: Holton, J.R., Curry, J.A., Pyle, J.A. (Eds.), Encyclopedia of Atmospheric Sciences. Academic Press, p. 171.

Serreze, M.C., Barrett, A.P., Slater, A.G., Woodgate, R.A., Aagaard, K., Lammers, R.B., Steele, M., Moritz, R., Meredith, M., Lee, C.M., 2006. The large-scale freshwater cycle of the Arctic. J. Geophys. Res. 111, C11010.

Serreze, M.C., Bromwich, D.H., Clark, M.P., Etringer, A.J., Zhang, T., Lammers, R., 2002. Large-scale hydro-climatology of the terrestrial Arctic drainage system. J. Geophys. Res. 108, 8160.

Stewart, I., Cayan, D., Dettinger, M., 2005. Changes toward earlier streamflow timing across western North America. J. Clim. 18, 1136–1155.

Stoner, A.M.K., Hayhoe, K., Wuebbles, D.J., 2009. Assessing General Circulation Model Simulations of Atmospheric Teleconnection Patterns. J. Clim. 22, 4348–4372.

Stuefer, S., Yang, D., Shiklomanov, A., 2011. Effect of streamflow regulation on mean annual discharge variability of the Yenisei River. In: Cold Region Hydrology in a Changing Climate (Proceedings of Symposium H02 Held during IUGG2011 in Melbourne, Australia, July 2011). IAHS Publ. 346, pp. 27–32.

Thompson, D.W.J., Wallace, J.M., 1998. The Arctic Oscillation signature in the wintertime geopotential height and temperature fields. Geophys. Res. Lett. 25, 1297–1300.

Trenberth, K., 1997. The definition of El Nino. Bull. Am. Meteorol. Soc. 78, 2771–2777.

Uppala, S.M., Kallberg, P.W., Simmons, A.J., Andrae, U., Bechtold, V.D.C., Fiorino, M., Gibson, J.K., Haseler, J., Hernandez, A., Kelly, G.A., Li, X., Onogi, K., Saarinen, S., Sokka, N., Allan, R.P., Andersson, E., Arpe, K., Balmaseda, M.A., Beljaars, A.C.M., Berg, L. Van De, Bidlot, J., Bormann, N., Caires, S., Chevallier, F., Dethof, A., Dragosavac, M.,

Fisher, M., Fuentes, M., Hagemann, S., Hólm, E., Hoskins, B.J., Isaksen, L., Janssen, P.A.E.M., Jenne, R., Mcnally, A.P., Mahfouf, J.-F., Morcrette, J.-J., Rayner, N.A., Saunders, R.W., Simon, P., Sterl, A., Trenberth, K.E., Untch, A., Vasiljevic, D., Viterbo, P., Woollen, J., 2005. The ERA-40 re-analysis. Q. J. R. Meteorol. Soc. 131, 2961–3012.

Woo, M., Thorne, R., 2003. Streamflow in the Mackenzie basin, Canada. Arctic 56, 328–340.

Yang, D., Kane, D.L., Hinzman, L.D., Zhang, X., Zhang, T., Ye, H., 2002. Siberian Lena River hydrologic regime and recent change. J. Geophys. Res. 107, 4694.

Yang, D., Ye, B., Kane, D.L., 2004a. Streamflow changes over Siberian Yenisei River Basin. J. Hydrol. 296, 59–80.

Yang, D., Ye, B., Shiklomanov, A., 2004b. Discharge characteristics and changes over the Ob River watershed in Siberia. J. Hydrometeorol. 5, 595–610.

Ye, H., Yang, D., Zhang, T., Zhang, X., Ladochy, S., Ellison, M., 2004. The impact of climatic conditions on seasonal river discharges in Siberia. J. Hydrometeorol. 5, 286–295.

Zhang, X., Ikeda, M., Walsh, J., 2003. Arctic sea ice and freshwater changes driven by the atmospheric leading mode in a coupled sea ice-ocean model. J. Clim. 16, 2159–2177.

List of Tables

Table 1. Characteristics of major hydroelectric dams/reservoirs located in the study regions.

Reservoir/Dam Name	Latitude (°N)	Longitude (°E)	Basin	River	Capacity (MW)	Commissioned	Maximum Capacity (km^3)	Reservoir Catchment Area (km^2)
W.A.C. Bennett	56.0	-122.2	Mackenzie	Peace	2730	1968	74	70275
Shul'binsk	50.4	81.1	Ob	Irtysh	702	1989	2.4	131598
Bukhtarma	49.7	83.3	Ob	Irtysh	750	1960	49.8	103923
Ust-Kamenogorsk	49.9	82.7	Ob	Irtysh	331.2	1952	0.6	107636
Novosibirsk	54.8	83.0	Ob	Ob	455	1957	8.8	212076
Boguchany	58.4	97.4	Yenisei	Angara	3000	2011	58.2	845694
Ust-Ilimsk	58.0	102.7	Yenisei	Angara	4320	1974	59.3	767413
Bratsk	56.3	101.8	Yenisei	Angara	4500	1967	169	714017
Irkutsk	52.2	104.3	Yenisei	Angara	662.4	1958	46	572704
Sayano-Shushenskoe	52.8	91.4	Yenisei	Yenisei	6400	1978	31.3	172529
Krasnoyarskoye More	55.9	92.3	Yenisei	Yenisei	6000	1972	73.3	276174
Kurejka	66.94	88.34	Yenisei	Kurejka	600	1987	--	65974
Vilyuy	63.0	112.5	Lena	Viluy	680	1967	35.9	104566

Table 2. Characteristics of drainage sub-basins as labeled in Figure 2 and Figure 3. An asterisk * beside the station ID denotes an "index" station with no upstream flow regulation. Note: M = Mackenzie, O = Ob, L = Lena, Y = Yenisei. Stations IDs in *italic* have data during t_2 only.

Label	Basin	ID	Lat. (°N)	Long. (°E)	D.A. (km²)	% Infilled	Classification	Region
1	M	07AD002	53.42	-117.57	9765	--	H_U	South
2	M	*07DA001*	56.78	-111.4	132585	--	H_U	East
3	M	07GJ001	55.71	-117.62	50300	--	H_U	South
4	M	07KC001	59.11	-112.43	293000	--	H_R	East
5	M	07NB001	59.87	-111.58	606000	--	H_M	East
6	M	*10BE001*	59.41	-126.1	104000	--	H_U	West
7	M	*10CD001*	58.79	-122.66	20300	--	H_U	West
8	M	*10ED002*	61.75	-121.22	275000	--	H_U	West
9	M	*10JC003*	65.13	-123.55	146400	15.60%	H_U	North
10	M	*10FA002*	61.14	-119.84	9270	--	H_U	East
11	M	*10FB005*	61.45	-121.24	1310	--	H_U	West
12	M	*10GC003*	61.9	-121.61	2050	--	H_U	North
13	M	*10KA001*	65.27	-126.84	1594500	11.80%	H_M	North
14	M	*07OB001*	60.74	-115.86	51700	--	H_U	East
15	M	*07TA001*	63.11	-116.97	13900	--	H_U	East
16	M	*07AA001*	52.86	-118.11	629	--	H_U	South
17	M	*07AA002*	52.91	-118.06	3872	--	H_U	South
18	M	07AF002	53.47	-116.63	2562	--	H_U	South
19	M	07AG003	53.6	-116.27	826	--	H_U	South
20	M	07BB002	53.6	-115	4402	--	H_U	South
21	M	07BC002	54.45	-113.99	13014	--	H_U	South
22	M	07BE001	54.72	-113.29	74602	--	H_U	South
23	M	*07BF002*	55.45	-116.49	1152	--	H_U	South
24	M	*07BJ001*	55.32	-115.42	1900	--	H_U	South
25	M	*07BK007*	55.26	-114.23	2100	--	H_U	East
26	M	07CD001	56.69	-111.26	30792	--	H_U	East
27	M	*07EC002*	55.92	-124.57	5560	--	H_U	South
28	M	*07EE007*	55.08	-122.9	4930	--	H_U	South
29	M	07FB001	55.72	-121.21	12100	--	H_U	South
30	M	*07FC001*	56.28	-120.7	15600	--	H_U	South
31	M	*07FC003*	56.68	-121.22	1770	--	H_U	South
32	M	*07FD001*	55.96	-120.56	3630	--	H_U	South
33	M	*07FD007*	55.86	-120.03	2860	14.00%	H_U	South
34	M	07GE001	55.07	-118.8	11300	--	H_U	South
35	M	*07GG001*	54.75	-117.21	1040	--	H_U	South
36	M	07GH002	55.46	-117.16	11100	--	H_U	South
37	M	07HA001	56.24	-117.31	194374	--	H_R	South

Table 2 cont'd…

Label	Basin	ID	Lat. (°N)	Long. (°E)	D.A. (km^2)	% Infilled	Classification	Region
38	M	*07HA003*	56.06	-117.13	1968	--	H_U	South
39	M	07HC001	56.92	-117.62	4679	--	H_U	East
40	M	*07JD002*	57.87	-115.39	35800	--	H_U	East
41	M	07LE002	59.15	-105.54	50700	4.80%	H_U	East
42	M	*07MB001*	58.97	-108.18	9120	--	H_U	East
43	M	*07OC001*	58.6	-118.33	10370	1.30%	H_U	East
44	M	*10AB001*	60.47	-129.12	12800	--	H_U	West
45	M	*10AC005*	59.12	-129.82	882	--	H_U	West
46	M	*10BE004*	58.85	-125.38	2540	--	H_U	West
47	M	*10BE007*	59.34	-125.94	1170	--	H_U	West
48	M	*10CB001*	57.23	-122.69	2180	--	H_U	South
49	M	*10EA003*	61.53	-125.41	8560	0.30%	H_U	West
50	M	*10EB001*	61.64	-125.8	14500	--	H_U	West
51	M	*10ED001*	60.24	-123.48	222000	2.50%	H_U	West
52	M	*10GC001*	61.87	-121.36	127000	--	H_M	East
53	M	*10LA002*	66.79	-133.09	18750	1.10%	H_U	North
54	M	*10LC014*	67.456	-133.75	1679100	2.00%	H_M	Outlet
55	M	*10MC002*	67.26	-134.89	70600	6.30%	H_U	North
56	M	*10ED003*	61.33	-122.09	542	--	H_U	West
57	O	11801	66.63	66.6	2950000	2.60%	H_M	Outlet
58	O	11056	58.2	68.23	1500000	0.80%	H_M	West
59	O	11048	55.02	73.3	769000	--	H_R	West
60	O	10031	61.07	68.9	2690000	5.60%	H_M	East
61	O	10021	58.3	82.88	486000	--	H_M	South
62	O	10062	51.28	87.72	16600	9.90%	H_U	South
63	O	10126	51.02	84.32	3480	5.60%	H_U	South
64	O	10176	53.73	84.95	15900	5.10%	H_U	South
65	O	10219	55.32	84.1	15700	5.10%	H_U	South
66	O	10277	53.33	87.23	7080	5.10%	H_U	South
67	O	10317	55.38	91.62	14700	12.20%	H_U	South
68	O	10387	56.2	87.78	9820	5.10%	H_U	South
69	O	10407	56.18	86.4	3460	7.70%	H_U	South
70	O	10428	57.78	82.63	25000	5.10%	H_U	South
71	O	10444	56.85	83.07	2560	5.10%	H_U	South
72	O	10466	59.37	82.83	6500	5.10%	H_U	East
73	O	10478	59.22	78.22	31700	9.40%	H_U	East
74	O	10489	59.85	81.95	24500	5.10%	H_U	East
75	O	11309	55.45	78.32	12200	5.10%	H_U	West
76	O	11353	56.38	75.25	16400	--	H_U	West

Table 2 cont'd…

Label	Basin	ID	Lat. (°N)	Long. (°E)	D.A. (km^2)	% Infilled	Classification	Region
77	O	11496	57.13	69.22	2140	2.60%	H_U	West
78	O	11556	66.87	65.78	1240	0.60%	H_U	North
79	O	11558	66.03	68.73	15100	2.90%	H_U	North
80	O	11574	64.93	77.8	31400	0.20%	H_U	North
81	Y	9803	67.43	86.48	2440000	--	H_M	Outlet
82	Y	9092	61.1	90.08	1760000	--	H_M	North
83	Y	9002	51.72	94.4	115000	--	H_U	South
84	Y	8091	58.35	93.55	1040000	--	H_R	South
85	Y	9079	58.45	92.15	1400000	--	H_R	West
86	Y	7156	51.95	106.35	565	--	H_U	East
87	Y	7172	51.53	104.07	959	--	H_U	South
88	Y	7015	55.85	110.15	20600	--	H_U	East
89	Y	7024	53.6	109.6	19800	--	H_U	East
90	Y	7036	52.92	108.73	5050	--	H_U	East
91	Y	7072	50.3	108.63	15600	--	H_U	East
92	Y	7102	51.2	106.97	38300	--	H_U	East
93	Y	9207	52.65	90.1	14400	--	H_U	West
94	Y	9252	53.8	92.87	31800	--	H_U	West
95	Y	9372	59.12	93.48	15100	--	H_U	North
96	Y	9422	65.65	90.12	9100	--	H_U	North
97	Y	9425	65.98	84.27	10100	5.10%	H_U	North
98	L	3821	70.68	127.39	2430000	--	H_M	Outlet
99	L	3329	63.95	124.83	452000	2.00%	H_M	West
100	L	3156	60.98	115.5	32600	2.60%	H_U	West
101	L	3157	60.17	116.8	27600	0.30%	H_U	South
102	L	3277	60.68	135.03	24200	2.60%	H_U	East
103	L	3291	59.67	127.05	23900	2.60%	H_U	South
104	L	3202	60.9	120.8	16600	10.30%	H_U	West
105	L	3210	61.05	128.65	12200	10.30%	H_U	South
106	L	3219	58.97	126.27	49500	10.30%	H_U	South

Table 3. Metrics used to describe freshet characteristics.

Symbol	Description
F_P	Freshet pulse date
F_L	Freshet length
F_M	Peak freshet magnitude
V_1	April – July volume
V_2	Freshet volume

Table 4a. Percentage of total significant correlations (5% level) occurring in unregulated (H_U) stations, 1962 – 2000. Items marked by *N/A* indicate that there were no significant correlations for the corresponding freshet measure.

	F_P	F_L	F_M	V_2	V_1
Mackenzie	100	88	80	92	86
Ob	78	57	63	75	100
Lena	75	50	100	100	100
Yenisei	64	50	50	50	50

Table 4b. Percentage of total significant correlations (5% level) occurring in unregulated (H_U) stations, 1980 – 2000. Items marked by *N/A* indicate that there were no significant correlations for the corresponding freshet measure.

	F_P	F_L	F_M	V_2	V_1
Mackenzie	88	91	100	83	71
Ob	76	100	100	N/A	100
Lena	71	0	N/A	N/A	N/A
Yenisei	67	67	100	N/A	100

List of Figures

Figure 9. Pulse date correlations with April through June average temperature during the period 1980 – 2000 for a) Mackenzie and b) Eurasian stations.

Figure 10. Freshet length correlations with April through June average temperature during the period 1962 – 2000 for a) Mackenzie and b) Eurasian stations.

Figure 11. Freshet length correlations with April through June average temperature during the period 1980 – 2000 for a) Mackenzie and b) Eurasian stations.

Figure 12. Peak freshet magnitude correlations with April through June average temperature during the period 1962 – 2000 for a) Mackenzie and b) Eurasian stations.

Figure 13. Peak freshet magnitude correlations with April through June average temperature during the period 1980 – 2000 for a) Mackenzie and b) Eurasian stations.

Figure 14. Freshet volume correlations with November through March cumulative precipitation during the period 1962 – 2000 for a) Mackenzie and b) Eurasian stations.

Figure 15. Freshet volume correlations with November through March cumulative precipitation during the period 1980 – 2000 for a) Mackenzie and b) Eurasian stations.

Figure 16. April through July volume correlations with November through March cumulative precipitation during the period 1962 – 2000 for a) Mackenzie and b) Eurasian stations.

Figure 17. April through July volume correlations with November through March cumulative precipitation during the period 1980 – 2000 for a) Mackenzie and b) Eurasian stations.

Figure 18. Climate signals (March through May) for a) NAO b) AO c) PDO and d) ENSO exhibiting 95% significant teleconnections to pulse dates during the period 1962 – 2000.

Figure 19. Climate signals (March through May) for a) NAO b) AO c) PDO and d) ENSO exhibiting 95% significant teleconnections to pulse dates during the period 1980 – 2000.

Figure 20. Climate signals (March through May) for a) NAO b) AO c) PDO and d) ENSO exhibiting 95% significant teleconnections to freshet magnitude during the period 1962 – 2000.

Figure 21. Climate signals (March through May) for a) NAO b) AO c) PDO and d) ENSO exhibiting 95% significant teleconnections to freshet magnitude during the period 1980 – 2000.

Figure 22. Climate signals (December through February) for a) NAO b) AO c) PDO and d) ENSO exhibiting 95% significant teleconnections to freshet volume during the period 1962 – 2000.

Figure 23. Climate signals (December through February) for a) NAO b) AO c) PDO and d) ENSO exhibiting 95% significant teleconnections to freshet volume during the period 1980 – 2000.

Figure 24. Climate signals (December through February) for a) NAO b) AO c) PDO and d) ENSO exhibiting 95% significant teleconnections to April through July volume during the period 1962 – 2000.

Figure 25. Climate signals (December through February) for a) NAO b) AO c) PDO and d) ENSO exhibiting 95% significant teleconnections to April through July volume during the period 1980 – 2000.

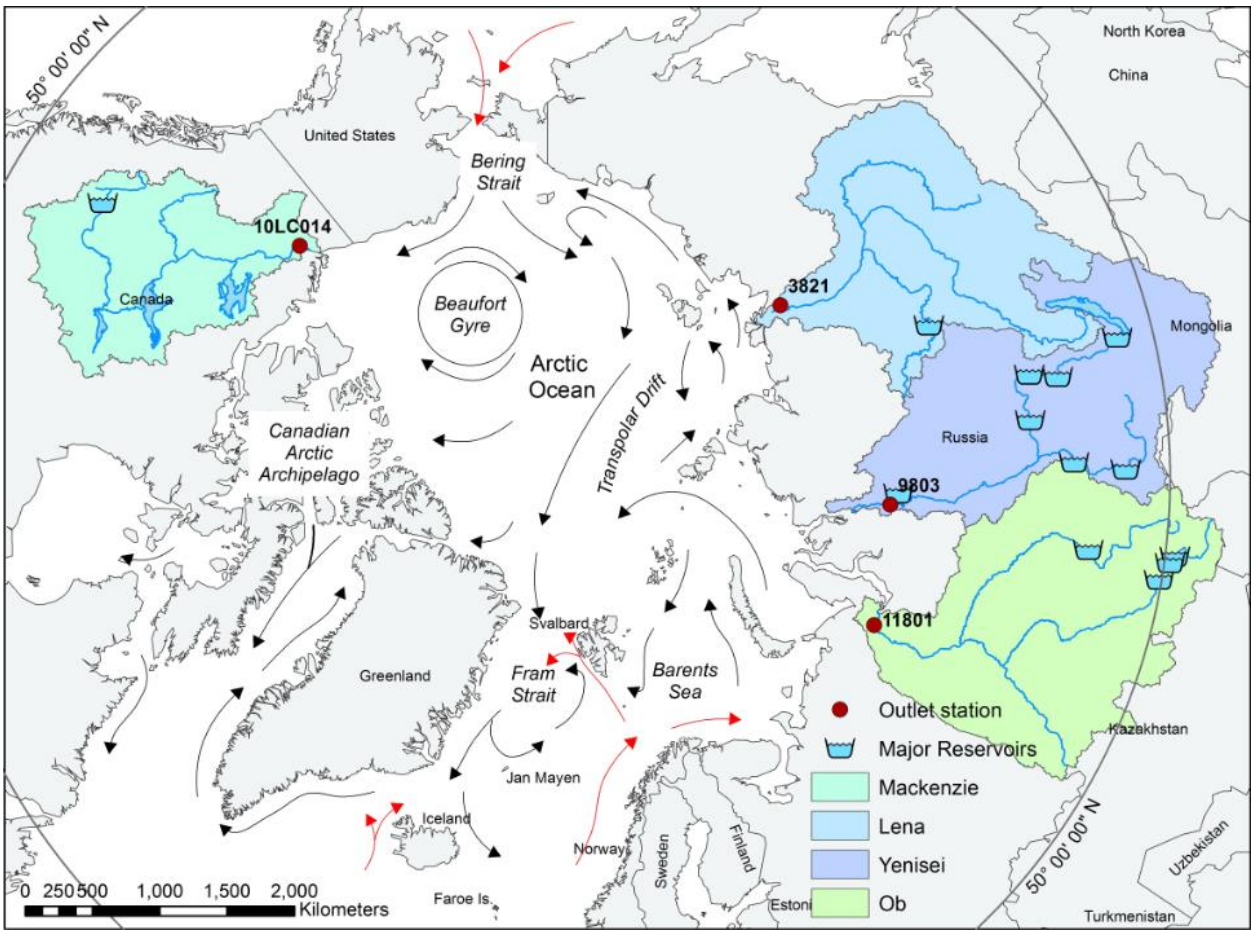

Figure 1. Map showing the Arctic Ocean, ocean features, major surface currents, and drainage basins and outlet stations of the Mackenzie, Ob, Yenisei and Lena rivers. Red arrows denote warmer currents, while black arrows denote colder currents. Figure adapted from Figure 6 in McClelland et al. (2011).

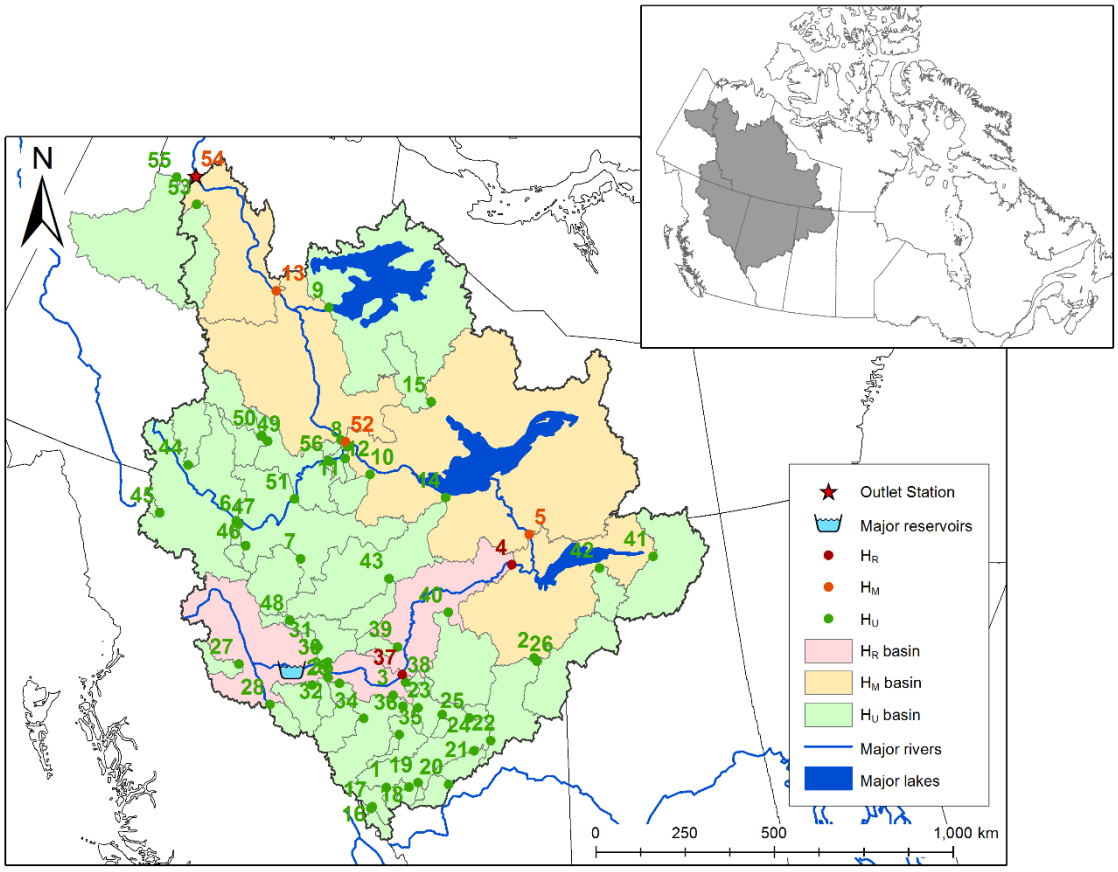

Figure 2. Study area of the Mackenzie basin showing station locations labeled with a unique identifier and station sub-basin drainage areas. Stations and basins are colour-coded and classified as regulated (H_R), minimally regulated (H_M) or unregulated (H_U). Station descriptions are provided in Table 2.

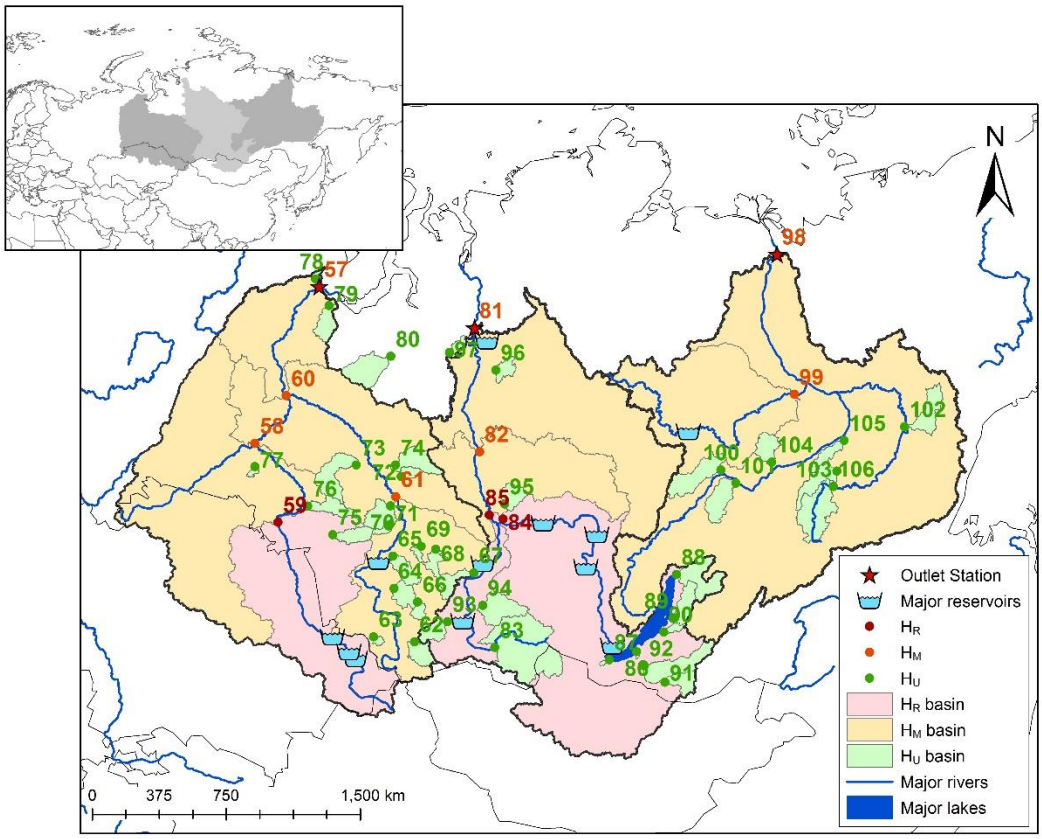

Figure 3. Study area of the (left to right in inset map) Ob, Yenisei and Lena basins showing station locations labeled with a unique identifier and station sub-basin drainage areas. Stations and basins are colour-coded and classified as regulated (H_R), minimally regulated (H_M) or unregulated (H_U). Station descriptions are provided in Table 2.

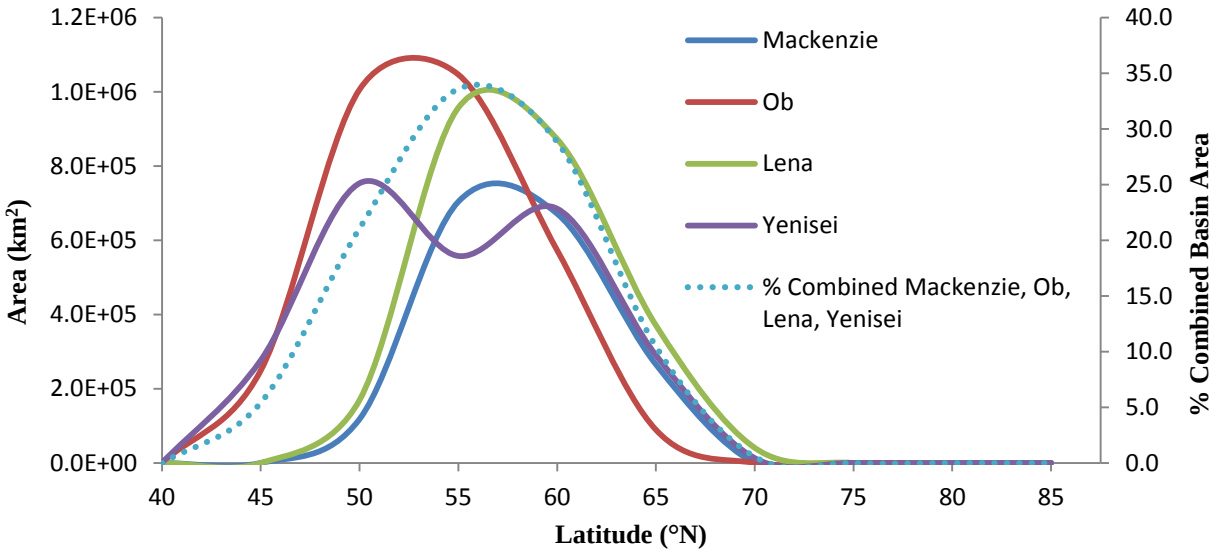

Figure 4. Hypsometric curves (area versus degrees latitude) of Mackenzie, Ob, Lena and Yenisei basins showing basin area per increment of latitude as well as percentage of combined basin area by latitude.

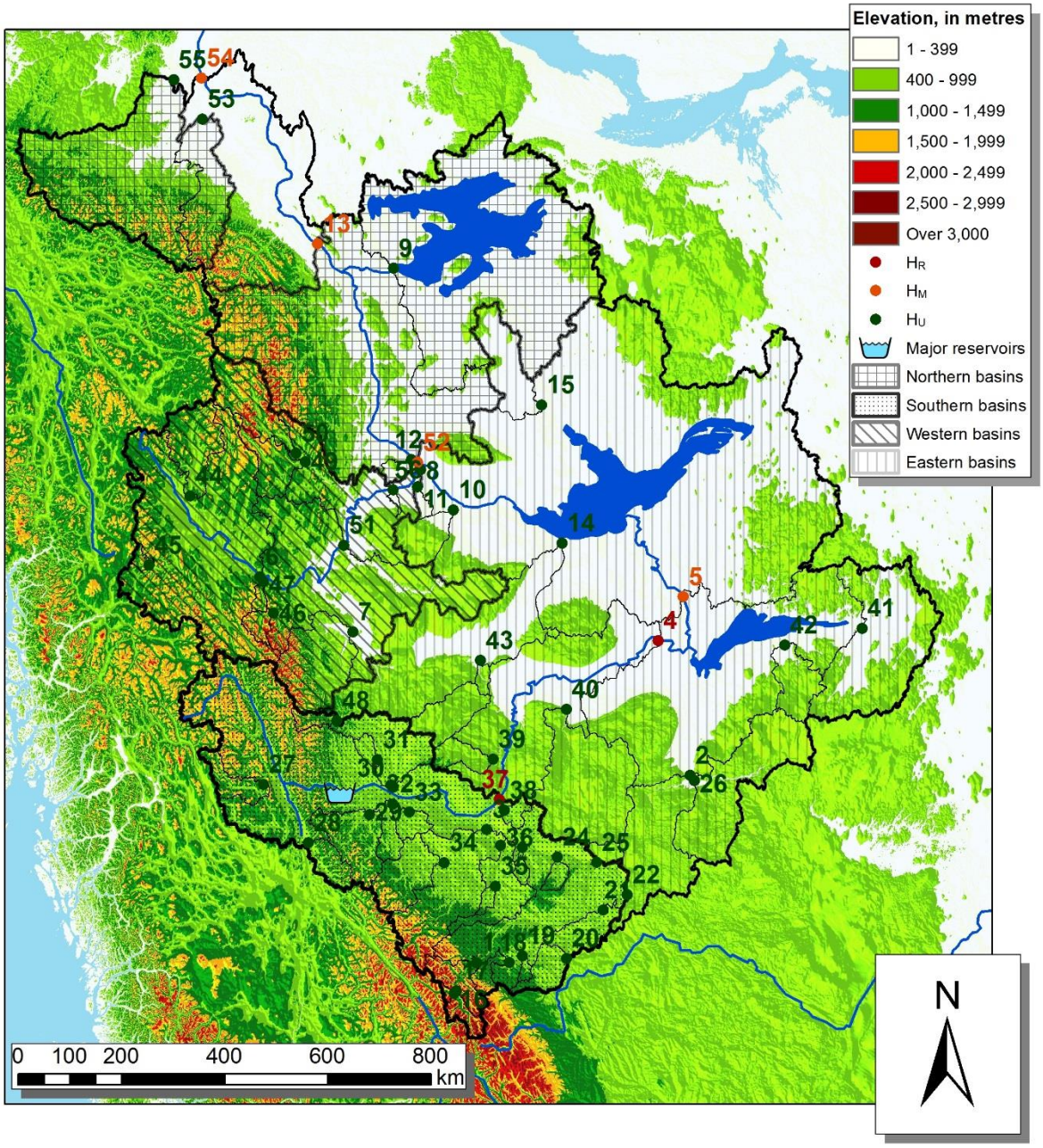

Figure 5. Topographical map of the Mackenzie basin showing regional classification of sub-basins into Northern, Southern, Western and Eastern regions. Outlet stations are not included in the classification.

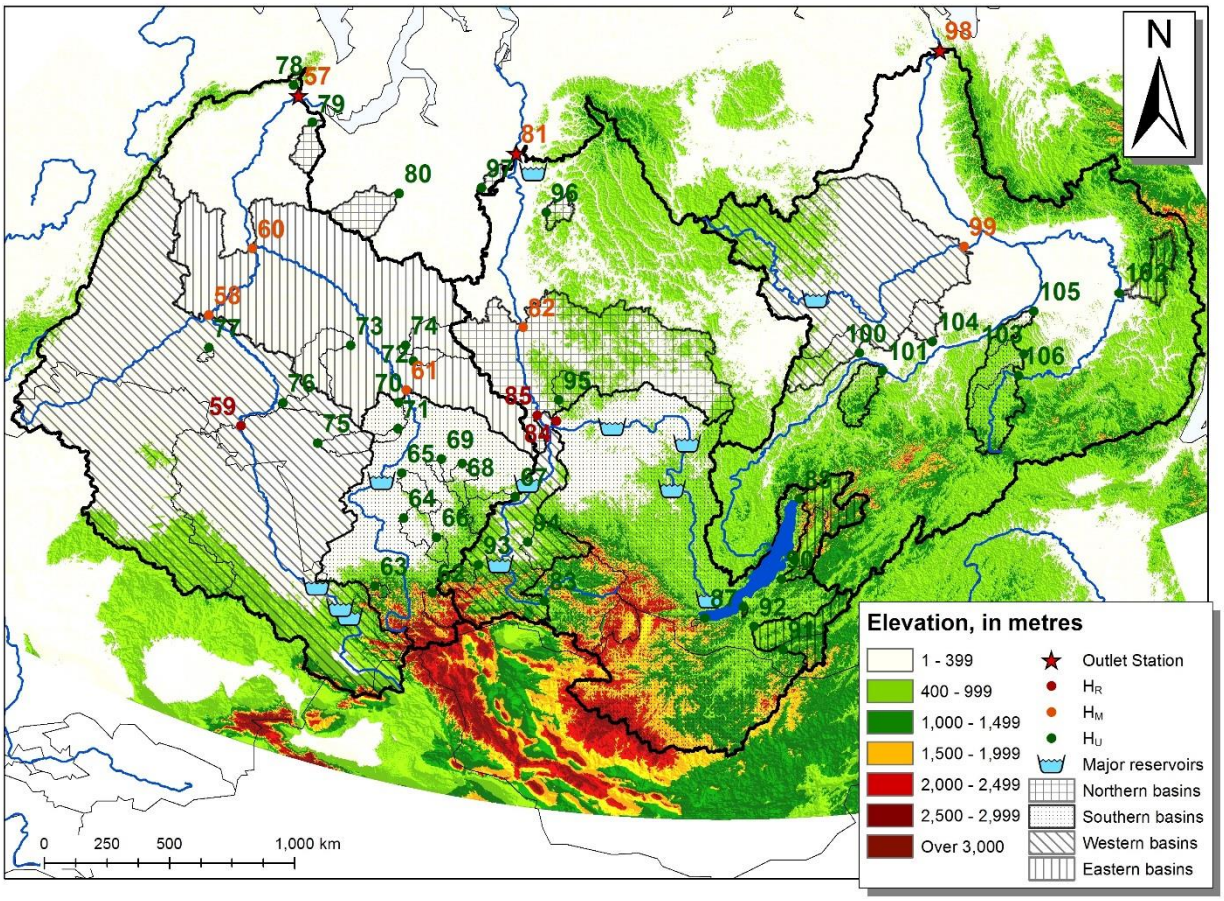

Figure 6. Topographical map of the Eurasian basins showing regional classification of sub-basins into Northern, Southern, Western and Eastern regions. Outlet stations are not included in the classification.

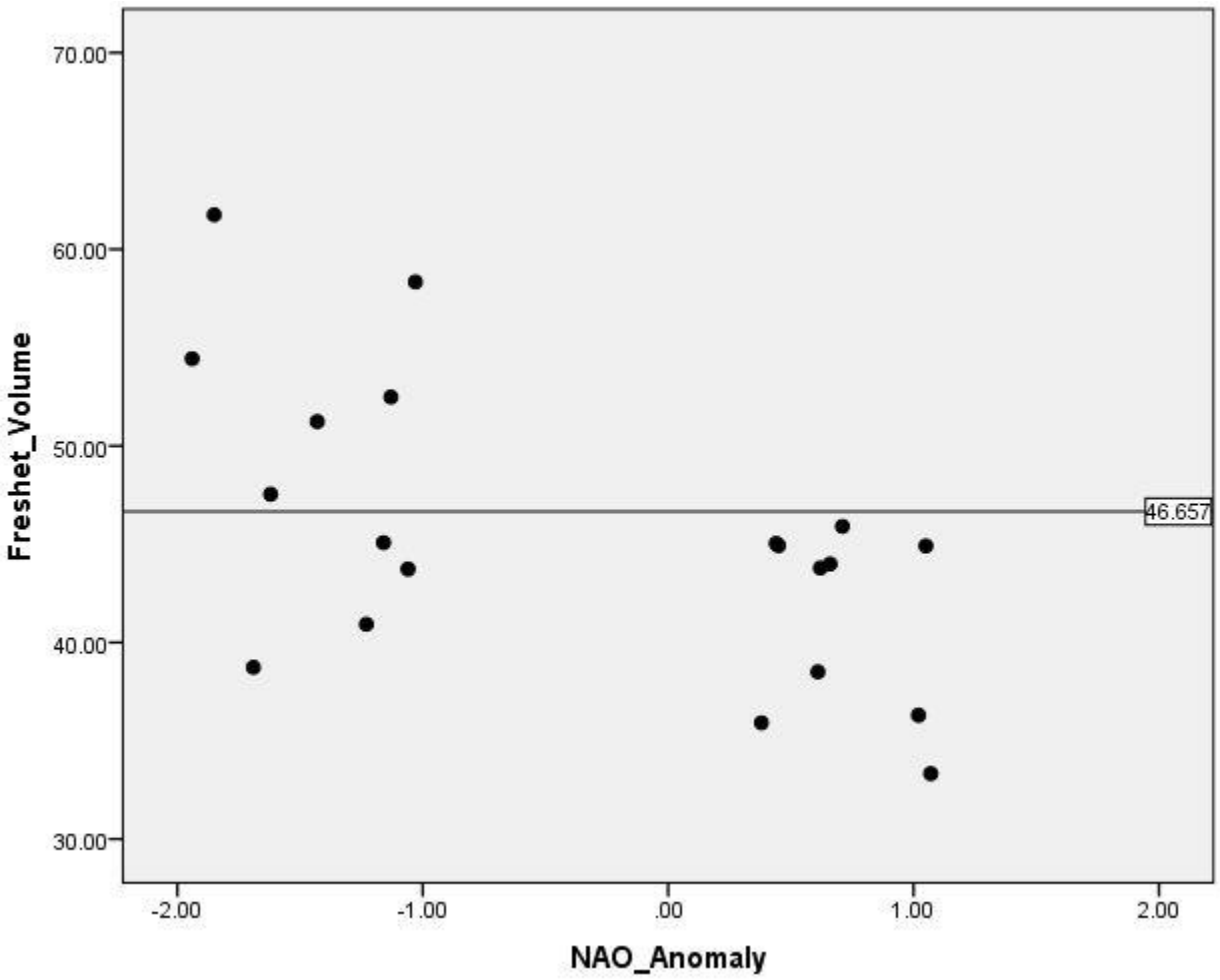

Figure 7. Scatterplot of the ten highest and ten lowest NAO average December – February values against freshet volume for station 07NB001 during the period 1962 - 2000. Horizontal line denotes mean freshet volume for the period.

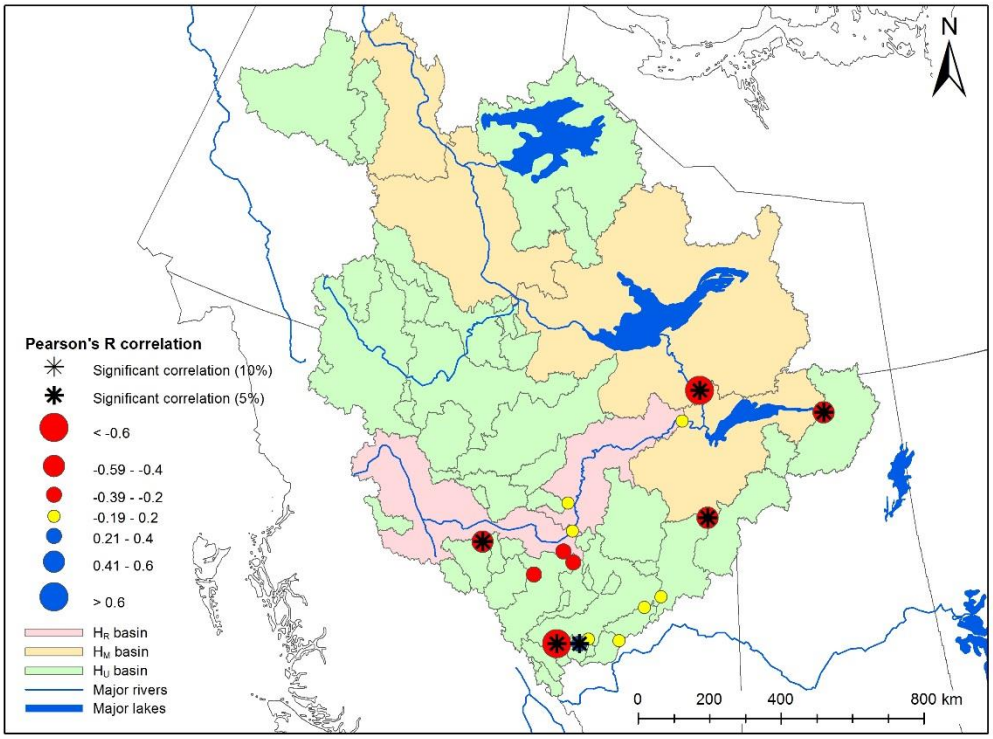

Figure 8a. Pulse date correlations with April through June average temperature during the period 1962 – 2000 for Mackenzie stations. A negative (red) correlation indicates a relationship with earlier pulse dates, while a positive (blue) correlation indicates later pulse dates.

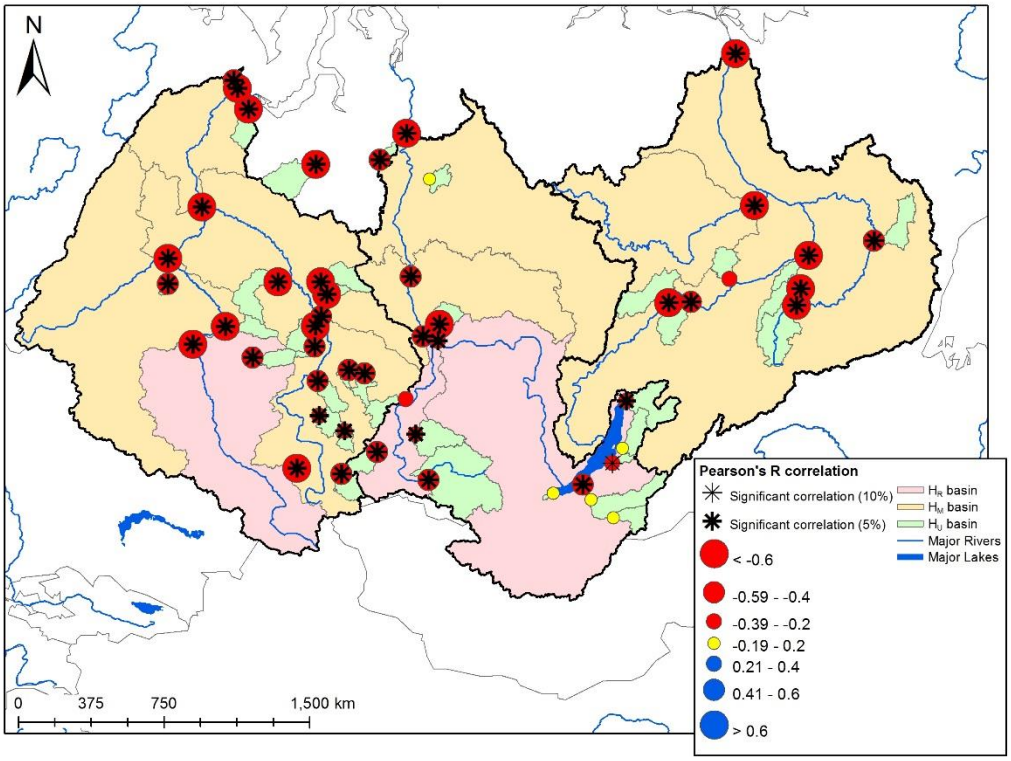

Figure 8b. Pulse date correlations with April through June average temperature during the period 1962 – 2000 for Eurasian stations. A negative (red) correlation indicates a relationship with earlier pulse dates, while a positive (blue) correlation indicates later pulse dates.

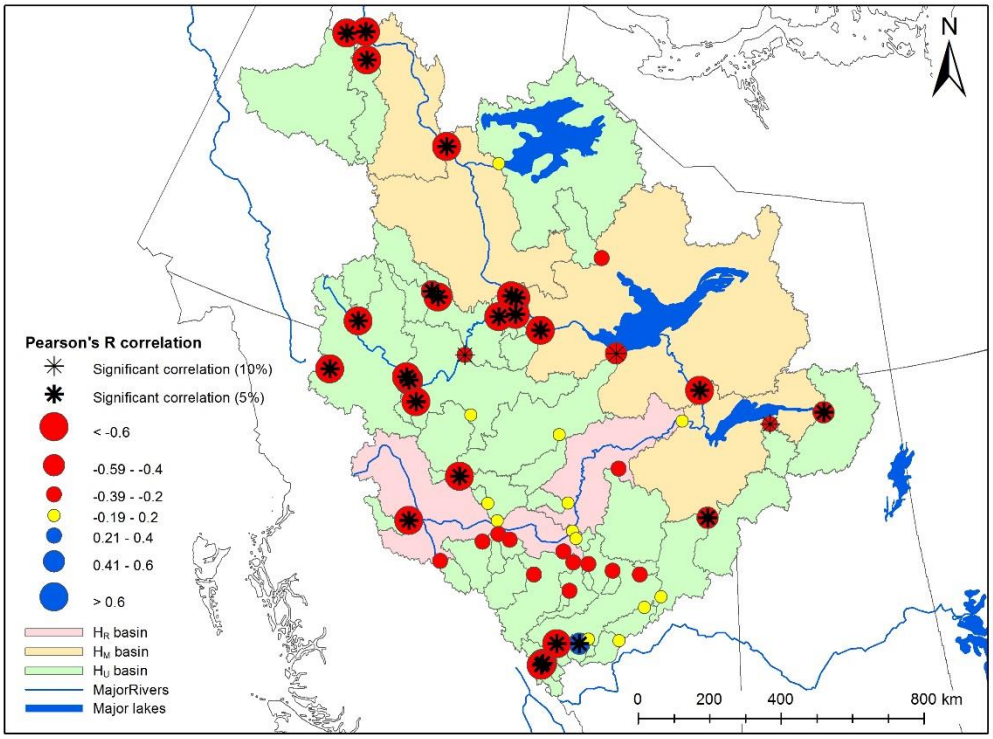

Figure 9a. Pulse date correlations with April through June average temperature during the period 1980 – 2000 for Mackenzie stations. A negative (red) correlation indicates a relationship with earlier pulse dates, while a positive (blue) correlation indicates later pulse dates.

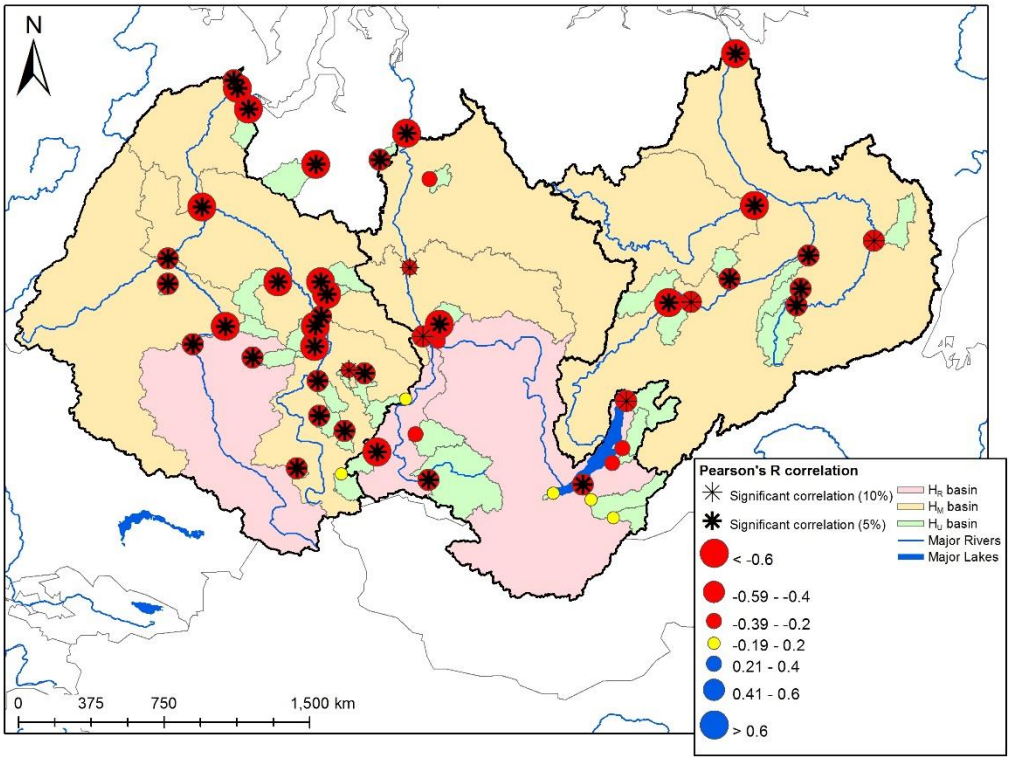

Figure 9b. Pulse date correlations with April through June average temperature during the period 1980 – 2000 for Eurasian stations. A negative (red) correlation indicates a relationship with earlier pulse dates, while a positive (blue) correlation indicates later pulse dates.

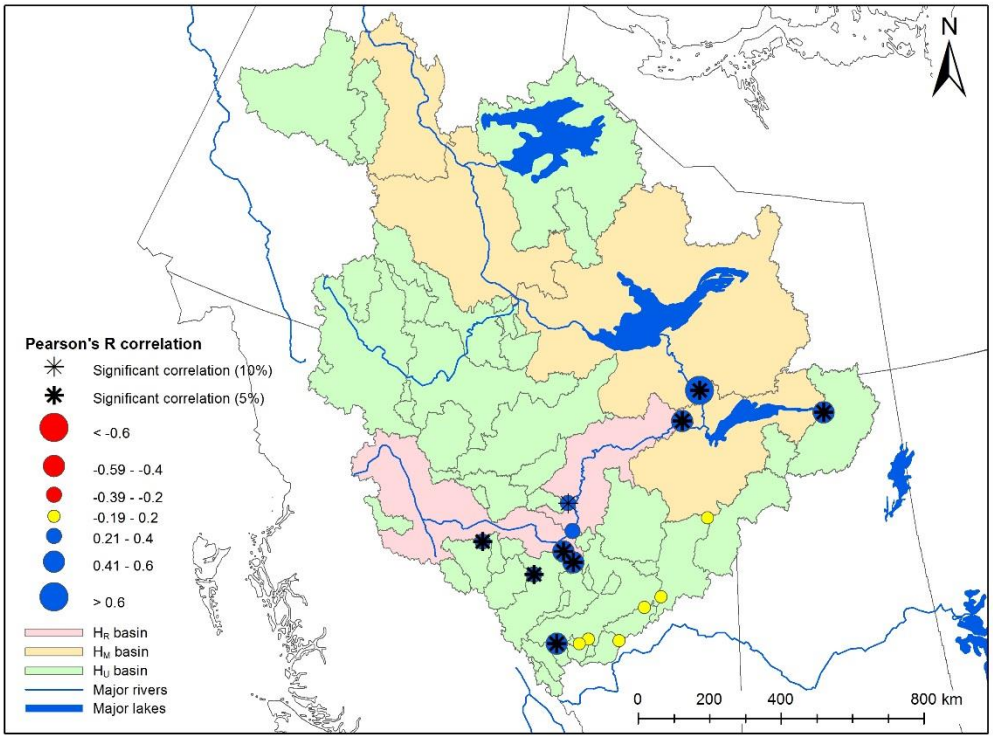

Figure 10a. Freshet length correlations with April through June average temperature during the period 1962 – 2000 for Mackenzie stations. A negative (red) correlation indicates a relationship with shorter freshet length, while a positive (blue) correlation indicates longer freshet length.

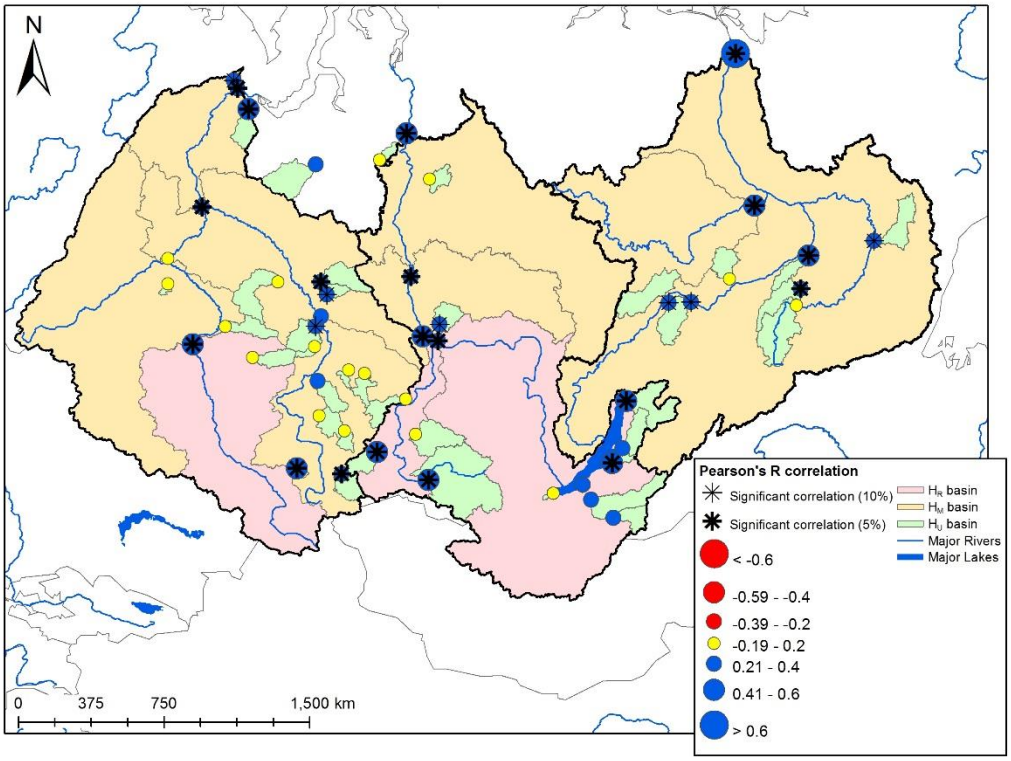

Figure 10b. Freshet length correlations with April through June average temperature during the period 1962 – 2000 for Eurasian stations. A negative (red) correlation indicates a relationship with shorter freshet length, while a positive (blue) correlation indicates longer freshet length.

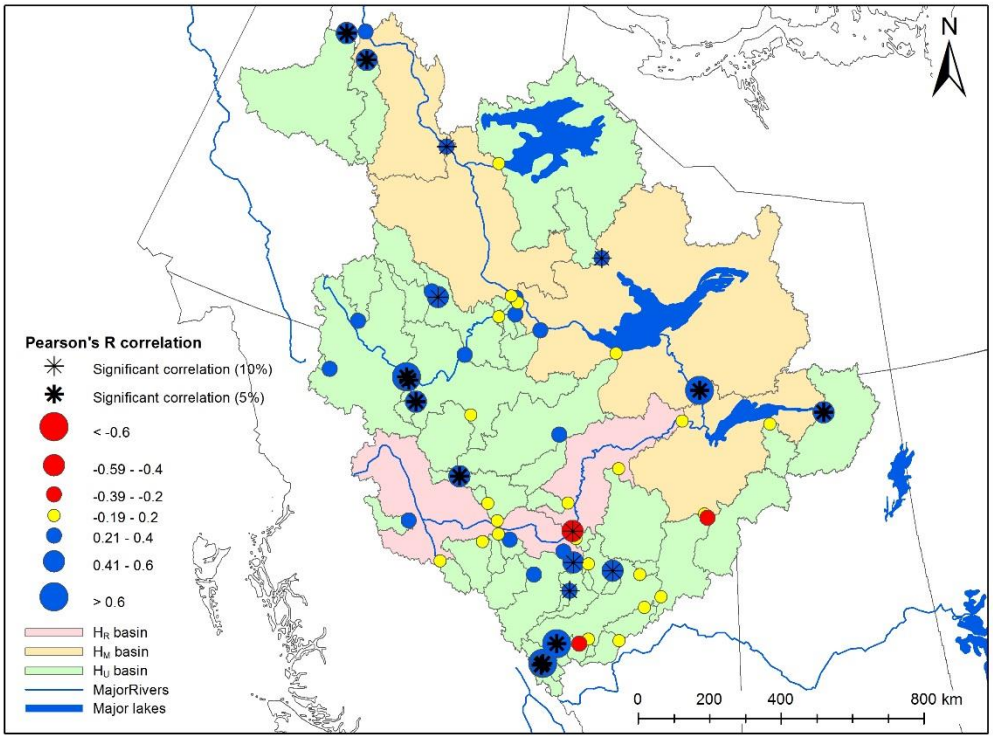

Figure 11a. Freshet length correlations with April through June average temperature during the period 1980 – 2000 for Mackenzie stations. A negative (red) correlation indicates a relationship with shorter freshet length, while a positive (blue) correlation indicates longer freshet length.

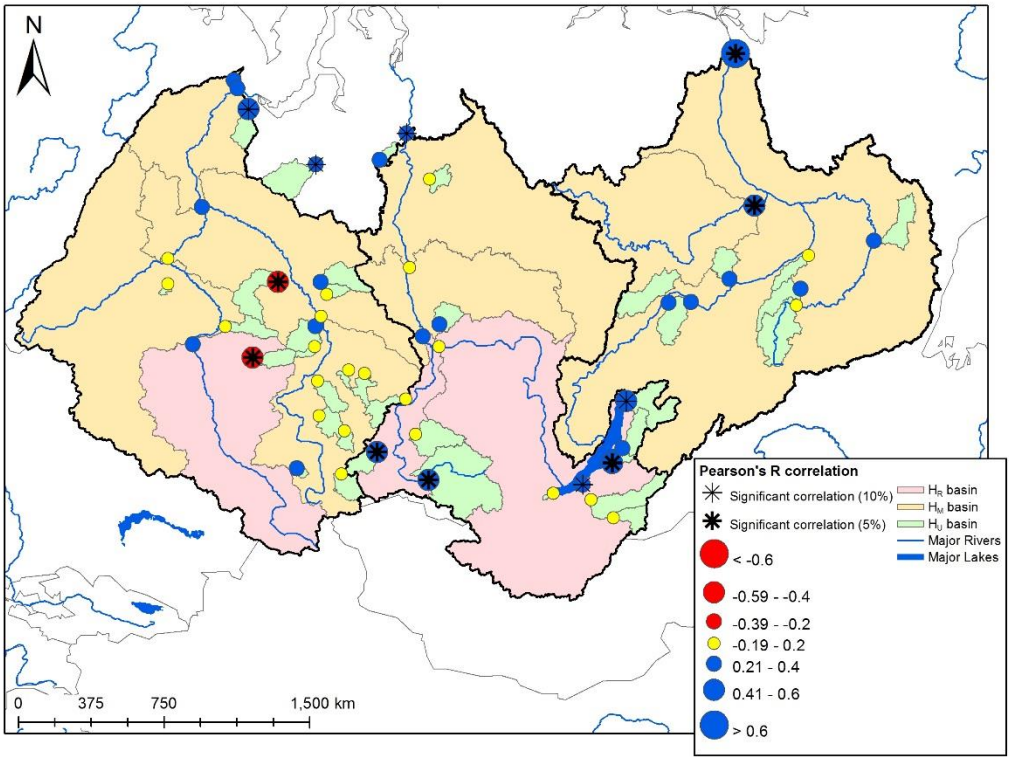

Figure 11b. Freshet length correlations with April through June average temperature during the period 1980 – 2000 for Eurasian stations. A negative (red) correlation indicates a relationship with shorter freshet length, while a positive (blue) correlation indicates longer freshet length.

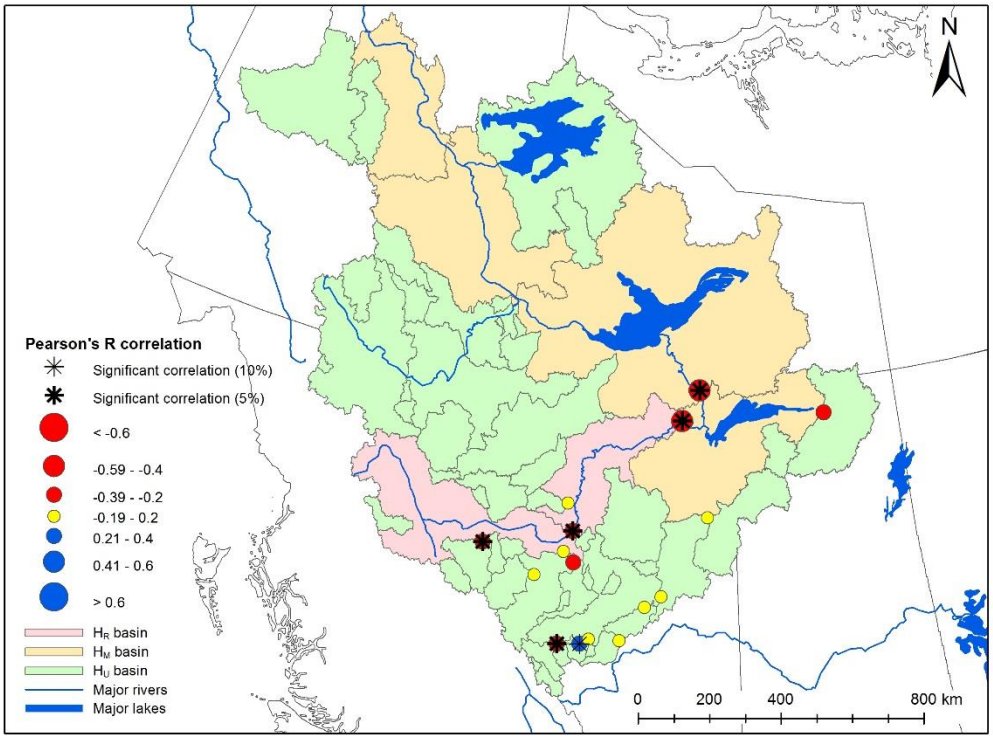

Figure 12a. Peak freshet magnitude correlations with April through June average temperature during the period 1962 – 2000 for Mackenzie stations. A negative (red) correlation indicates a relationship with lower peak freshet magnitude, while a positive (blue) correlation indicates higher peak freshet magnitude.

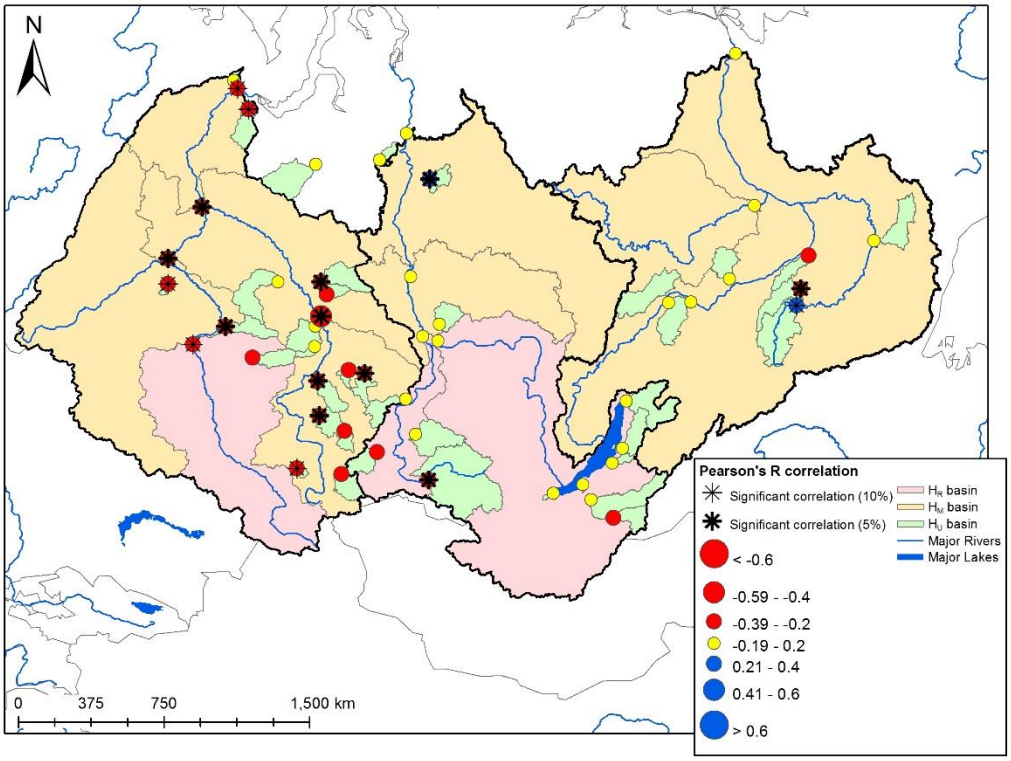

Figure 12b. Peak freshet magnitude correlations with April through June average temperature during the period 1962 – 2000 for Eurasian stations. A negative (red) correlation indicates a relationship with lower peak freshet magnitude, while a positive (blue) correlation indicates higher peak freshet magnitude.

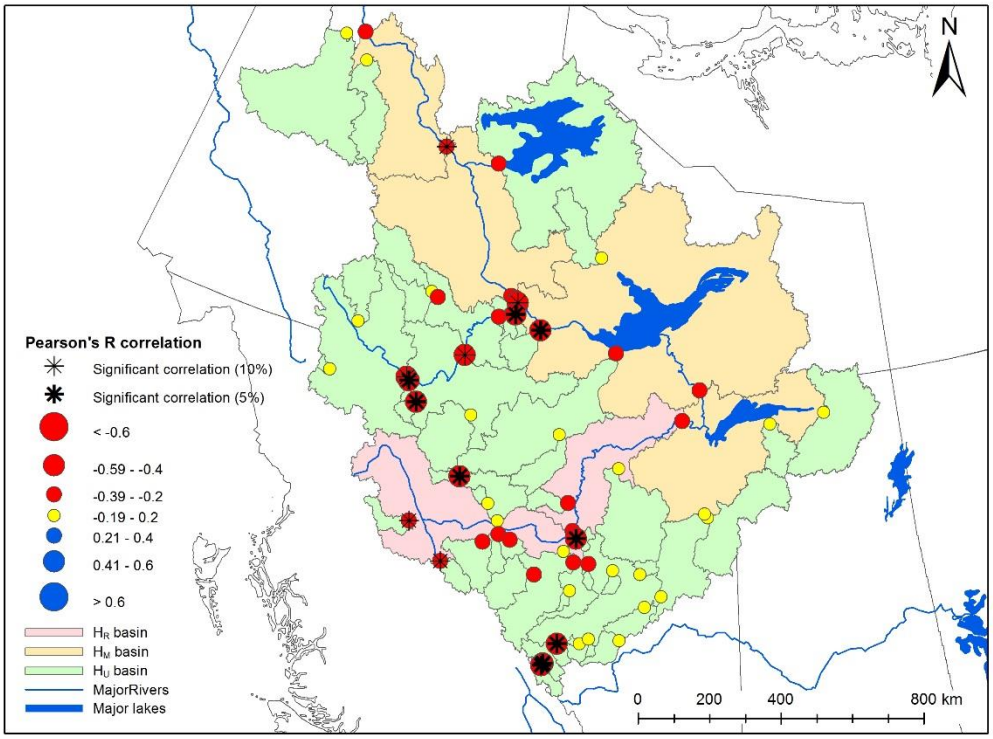

Figure 13a. Peak freshet magnitude correlations with April through June average temperature during the period 1980 – 2000 for Mackenzie stations. A negative (red) correlation indicates a relationship with lower peak freshet magnitude, while a positive (blue) correlation indicates higher peak freshet magnitude.

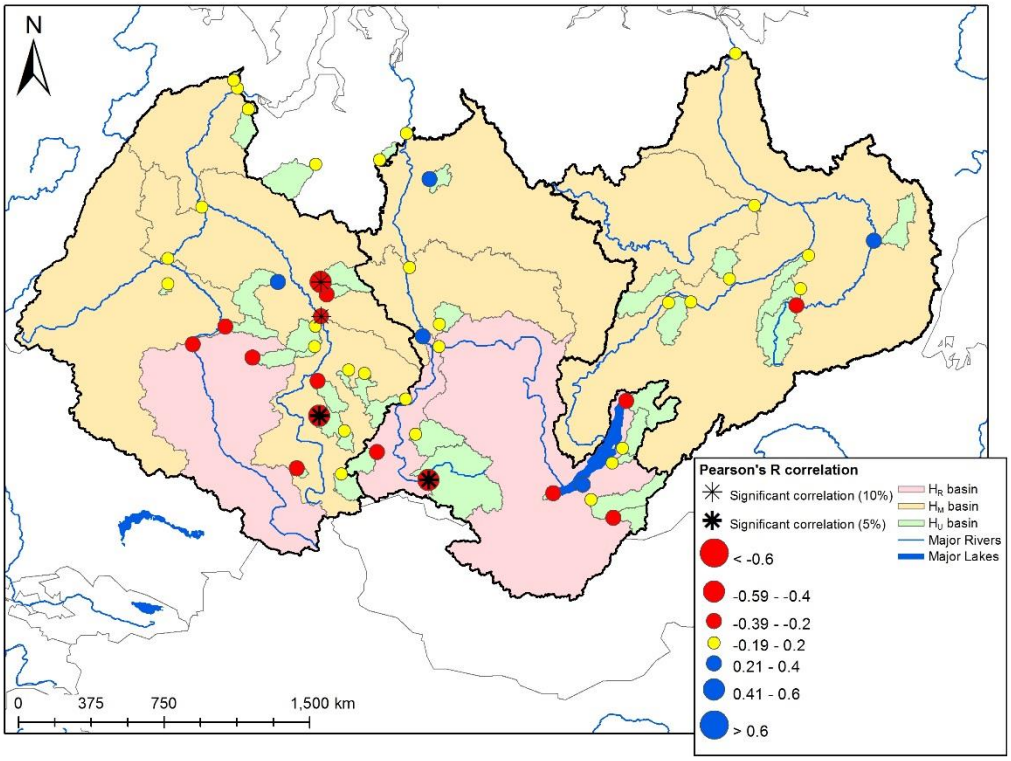

Figure 13b. Peak freshet magnitude correlations with April through June average temperature during the period 1980 – 2000 for Eurasian stations. A negative (red) correlation indicates a relationship with lower peak freshet magnitude, while a positive (blue) correlation indicates higher peak freshet magnitude.

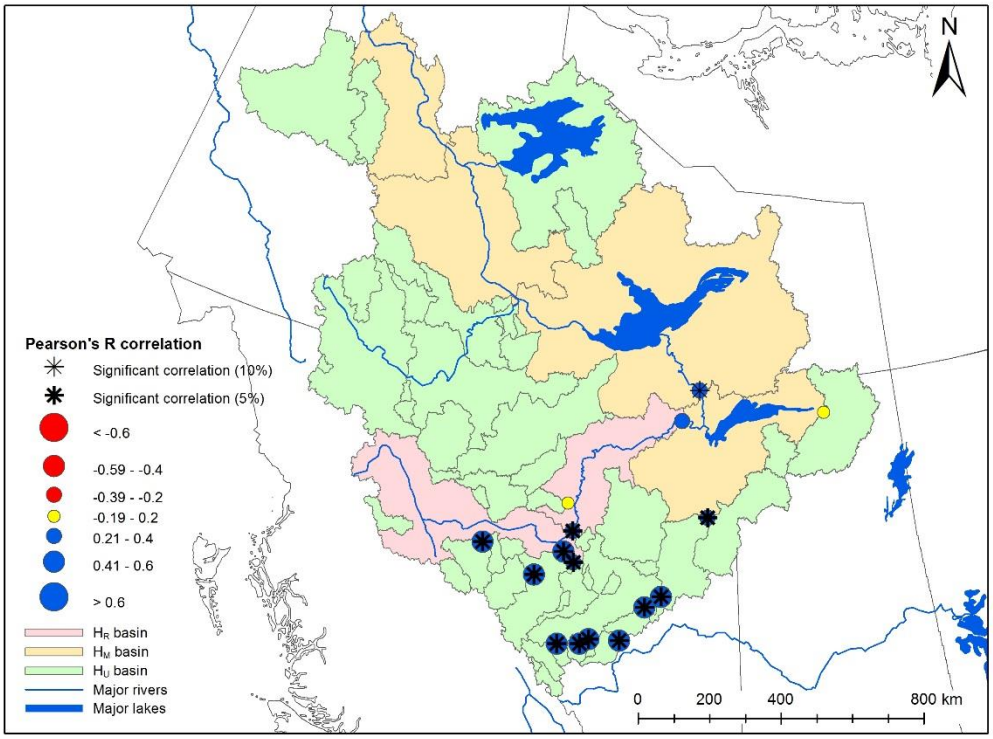

Figure 14a. Freshet volume correlations with November through March cumulative precipitation during the period 1962 – 2000 for Mackenzie stations. A negative (red) correlation indicates a relationship with lower freshet volume, while a positive (blue) correlation indicates higher freshet volume.

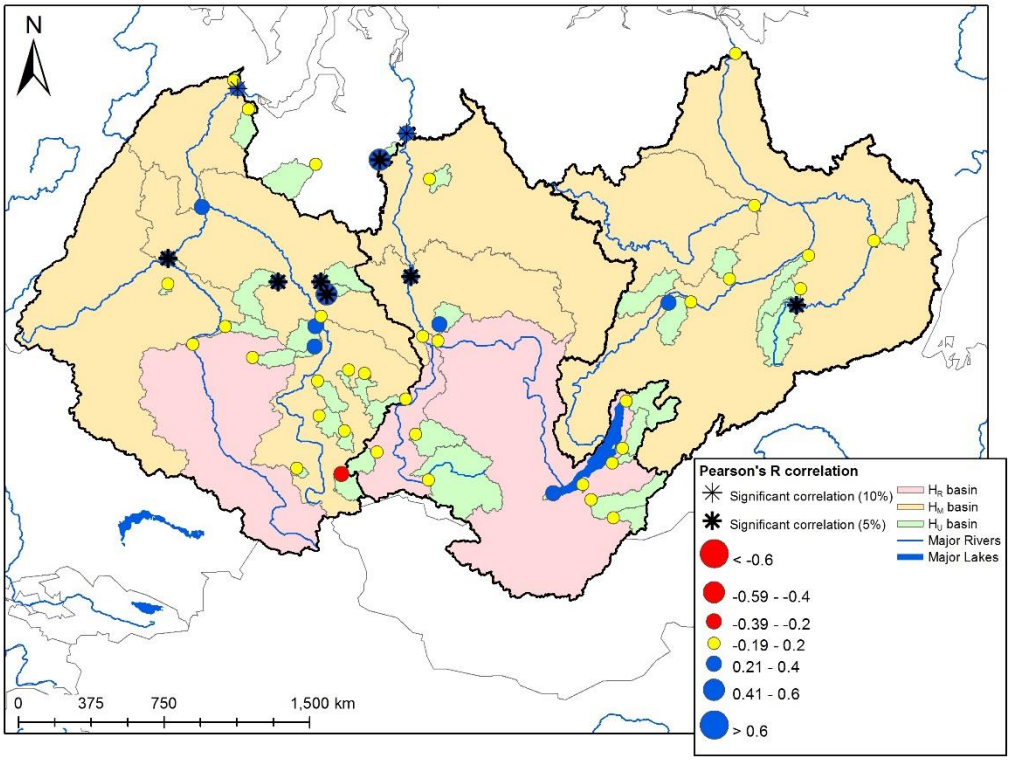

Figure 14b. Freshet volume correlations with November through March cumulative precipitation during the period 1962 – 2000 for Eurasian stations. A negative (red) correlation indicates a relationship with lower freshet volume, while a positive (blue) correlation indicates higher freshet volume.

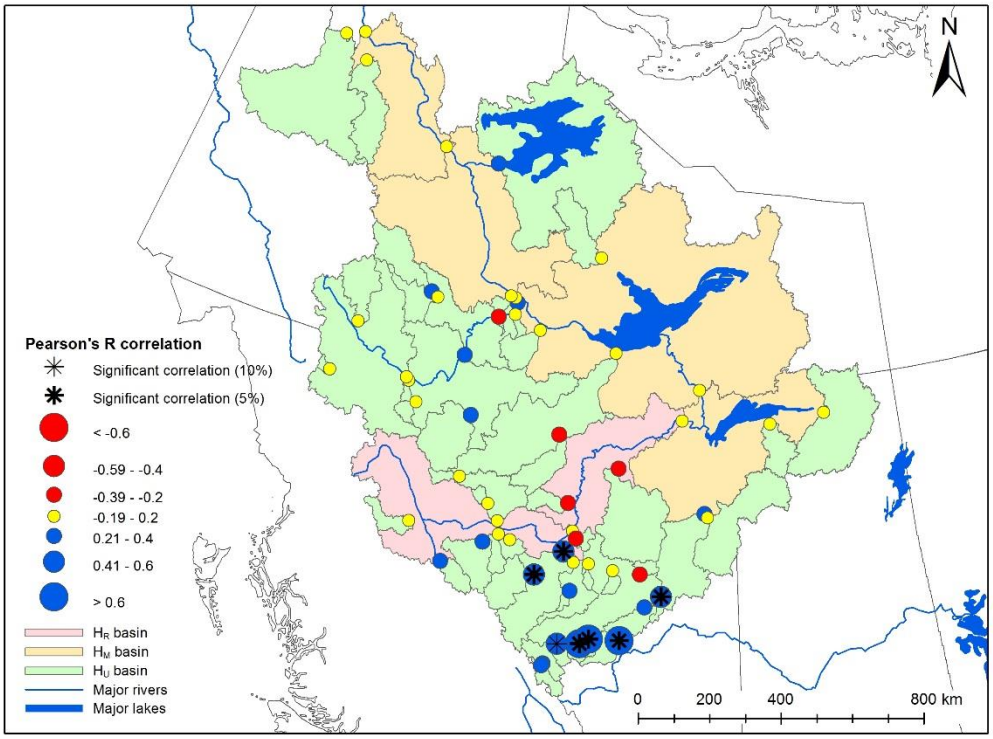

Figure 15a. Freshet volume correlations with November through March cumulative precipitation during the period 1980 – 2000 for Mackenzie stations. A negative (red) correlation indicates a relationship with lower freshet volume, while a positive (blue) correlation indicates higher freshet volume.

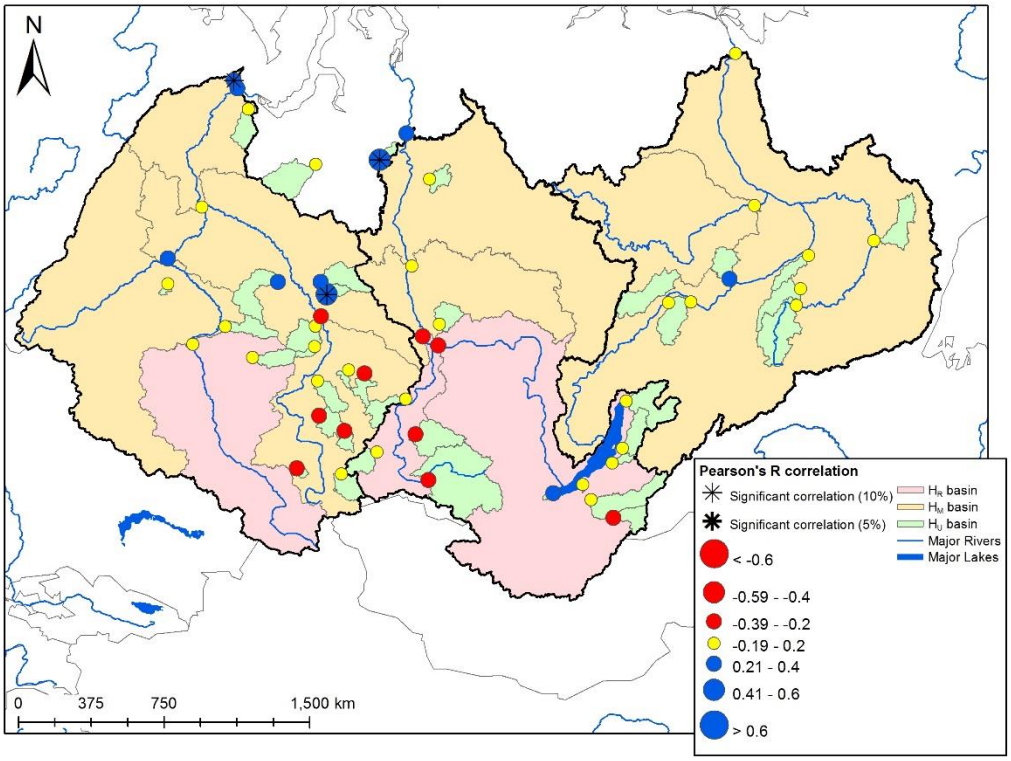

Figure 15b. Freshet volume correlations with November through March cumulative precipitation during the period 1980 – 2000 for Eurasian stations. A negative (red) correlation indicates a relationship with lower freshet volume, while a positive (blue) correlation indicates higher freshet volume.

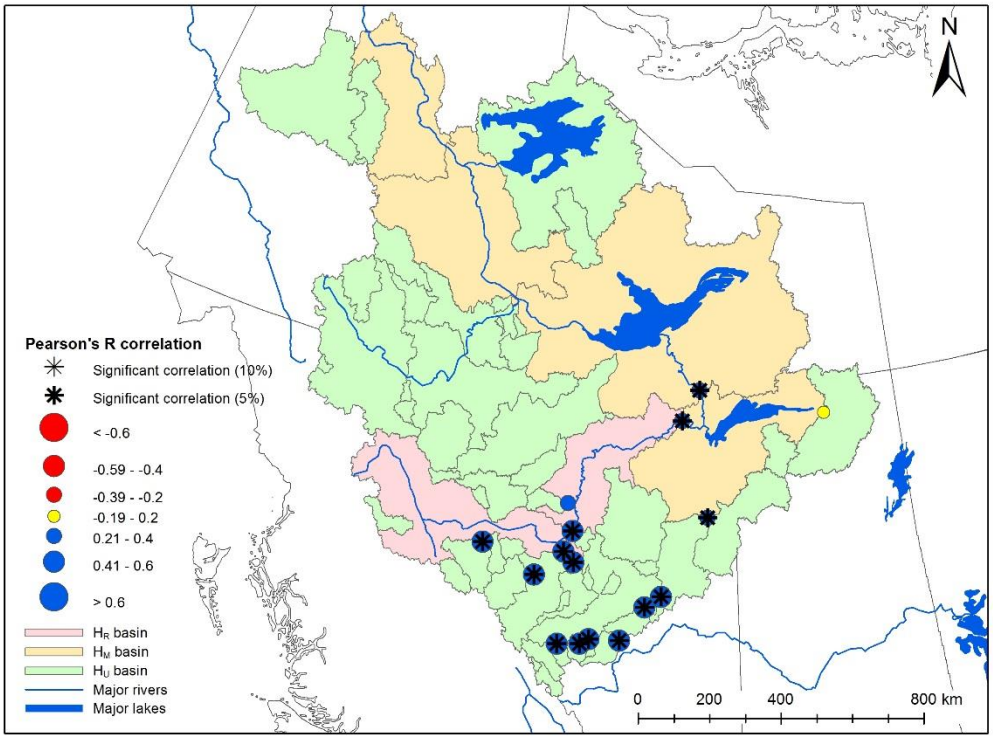

Figure 16a. April through July volume correlations with November through March cumulative precipitation during the period 1962 – 2000 for Mackenzie stations. A negative (red) correlation indicates a relationship with lower freshet volume, while a positive (blue) correlation indicates higher freshet volume.

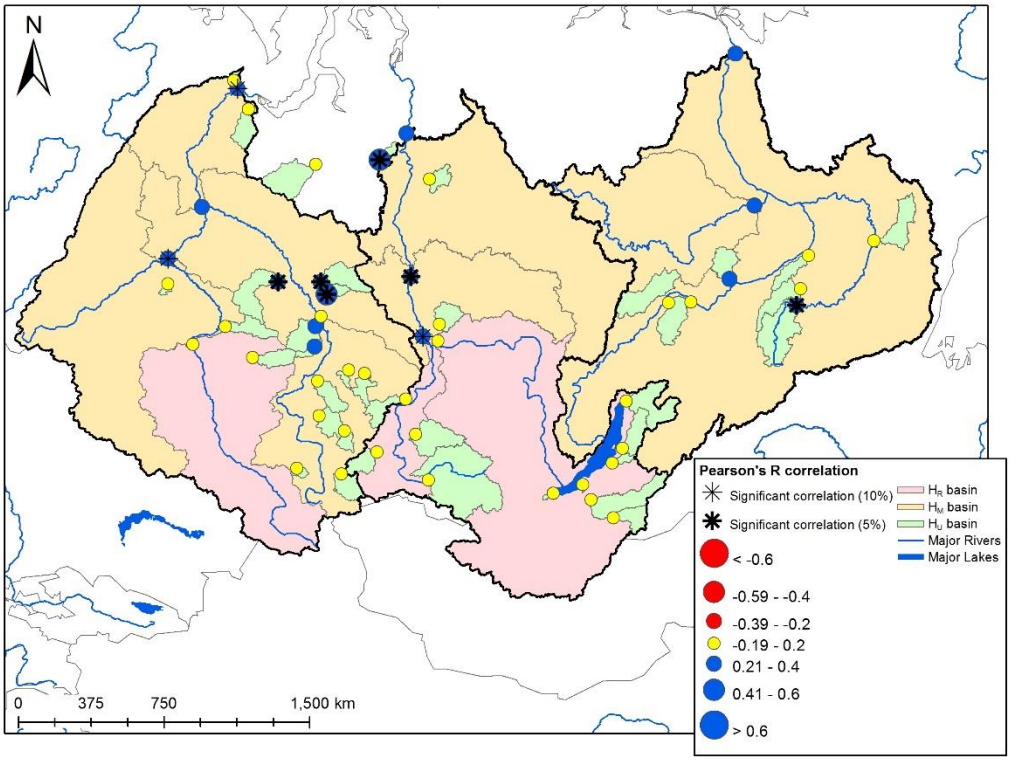

Figure 16b. April through July volume correlations with November through March cumulative precipitation during the period 1962 – 2000 for Eurasian stations. A negative (red) correlation indicates a relationship with lower freshet volume, while a positive (blue) correlation indicates higher freshet volume.

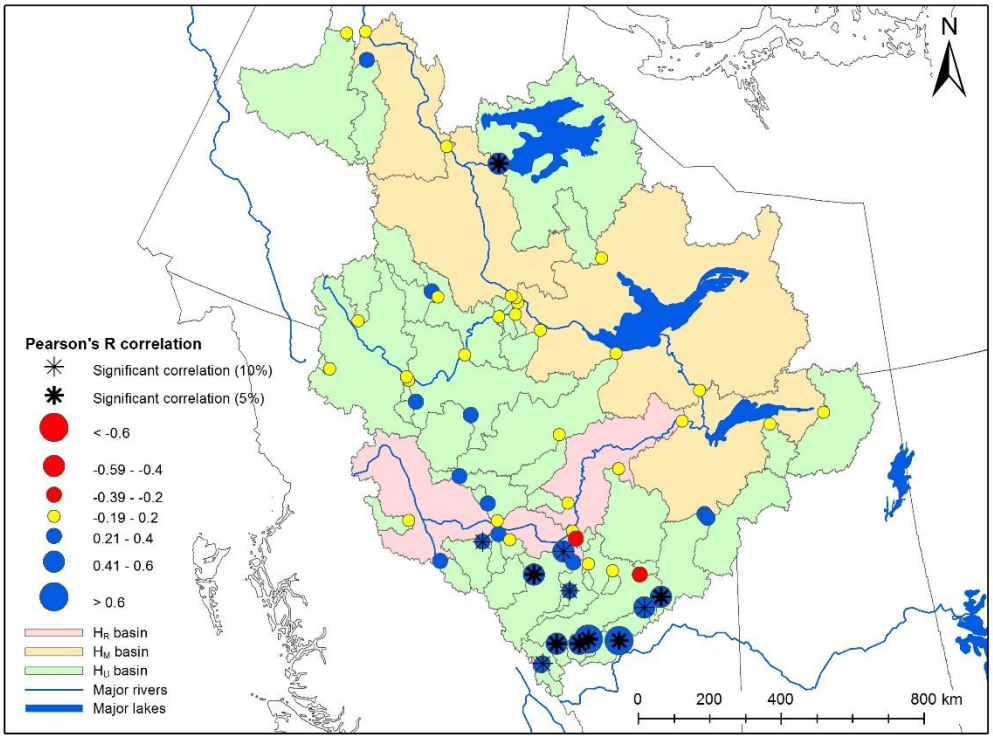

Figure 17a. April through July volume correlations with November through March cumulative precipitation during the period 1980 – 2000 for Mackenzie stations. A negative (red) correlation indicates a relationship with lower freshet volume, while a positive (blue) correlation indicates higher freshet volume.

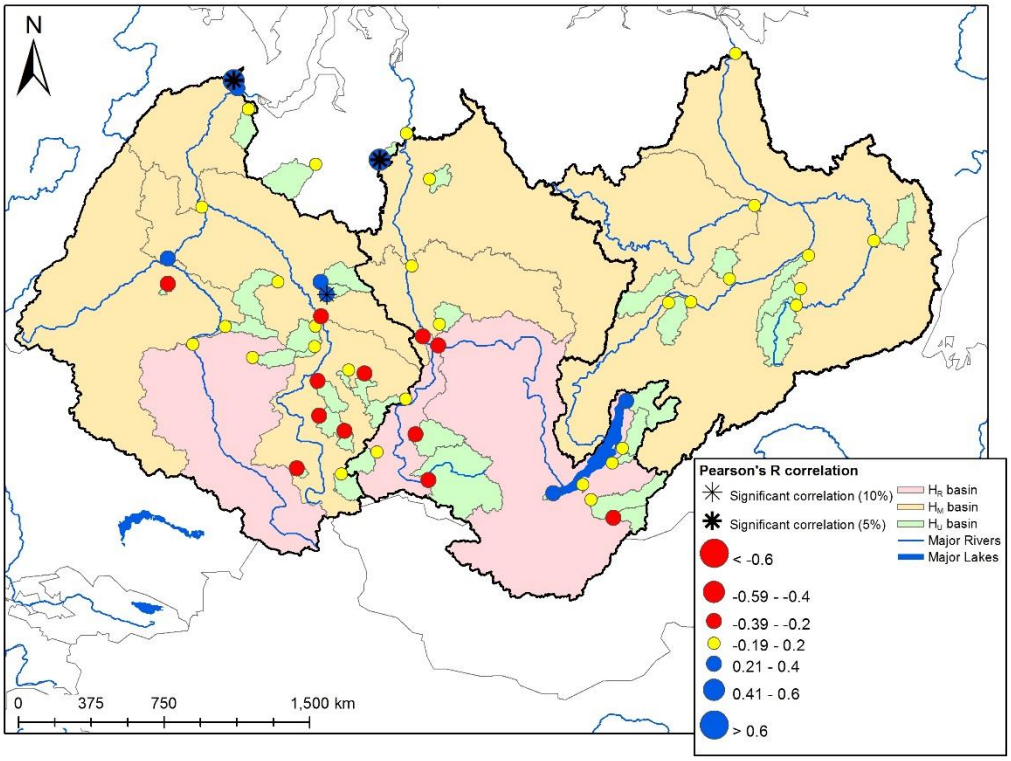

Figure 17b. April through July volume correlations with November through March cumulative precipitation during the period 1980 – 2000 for Eurasian stations. A negative (red) correlation indicates a relationship with lower freshet volume, while a positive (blue) correlation indicates higher freshet volume.

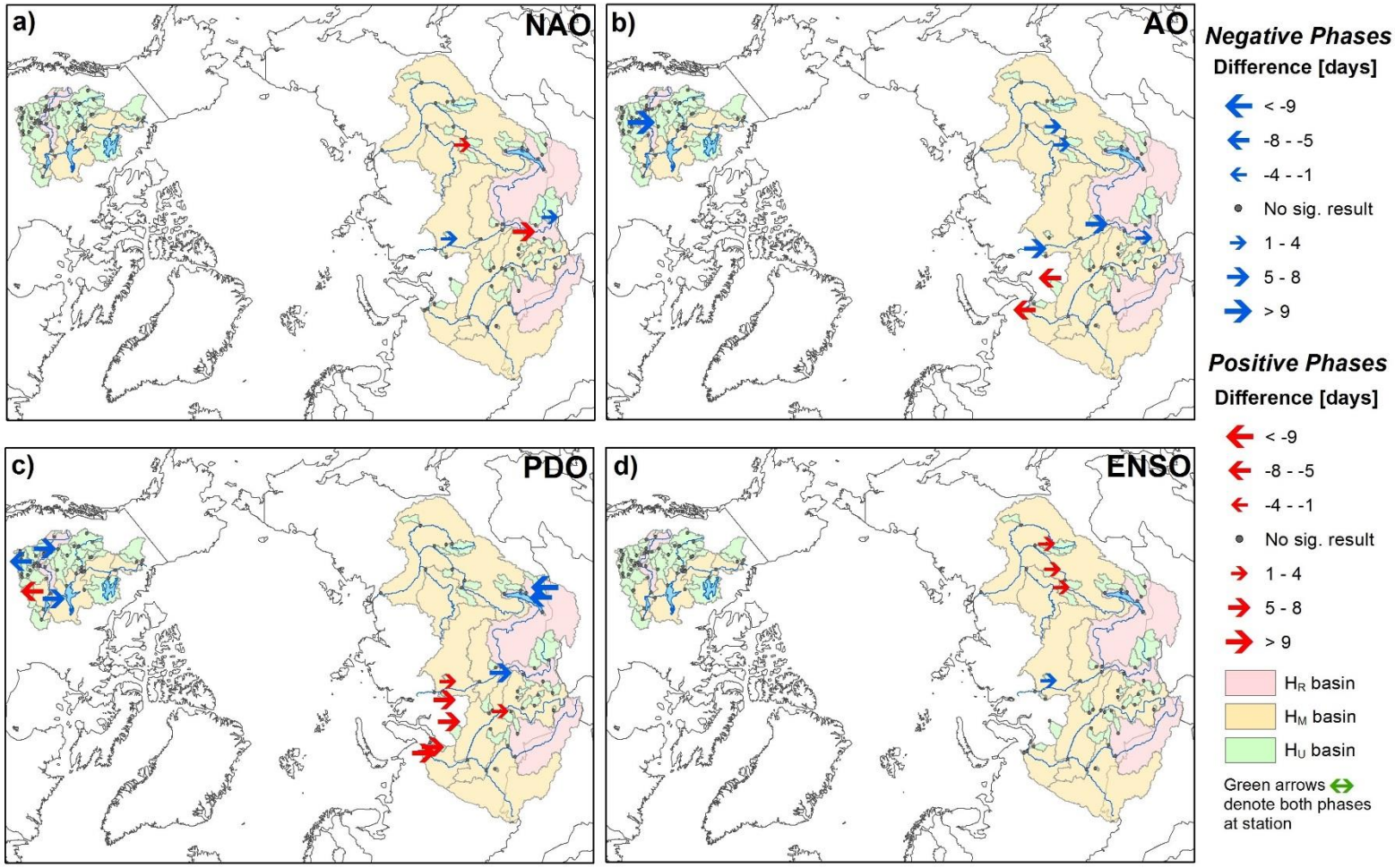

Figure 18. Climate signals (March through May) for a) NAO b) AO c) PDO and d) ENSO exhibiting 95% significant teleconnections to pulse dates during the period 1962 – 2000.

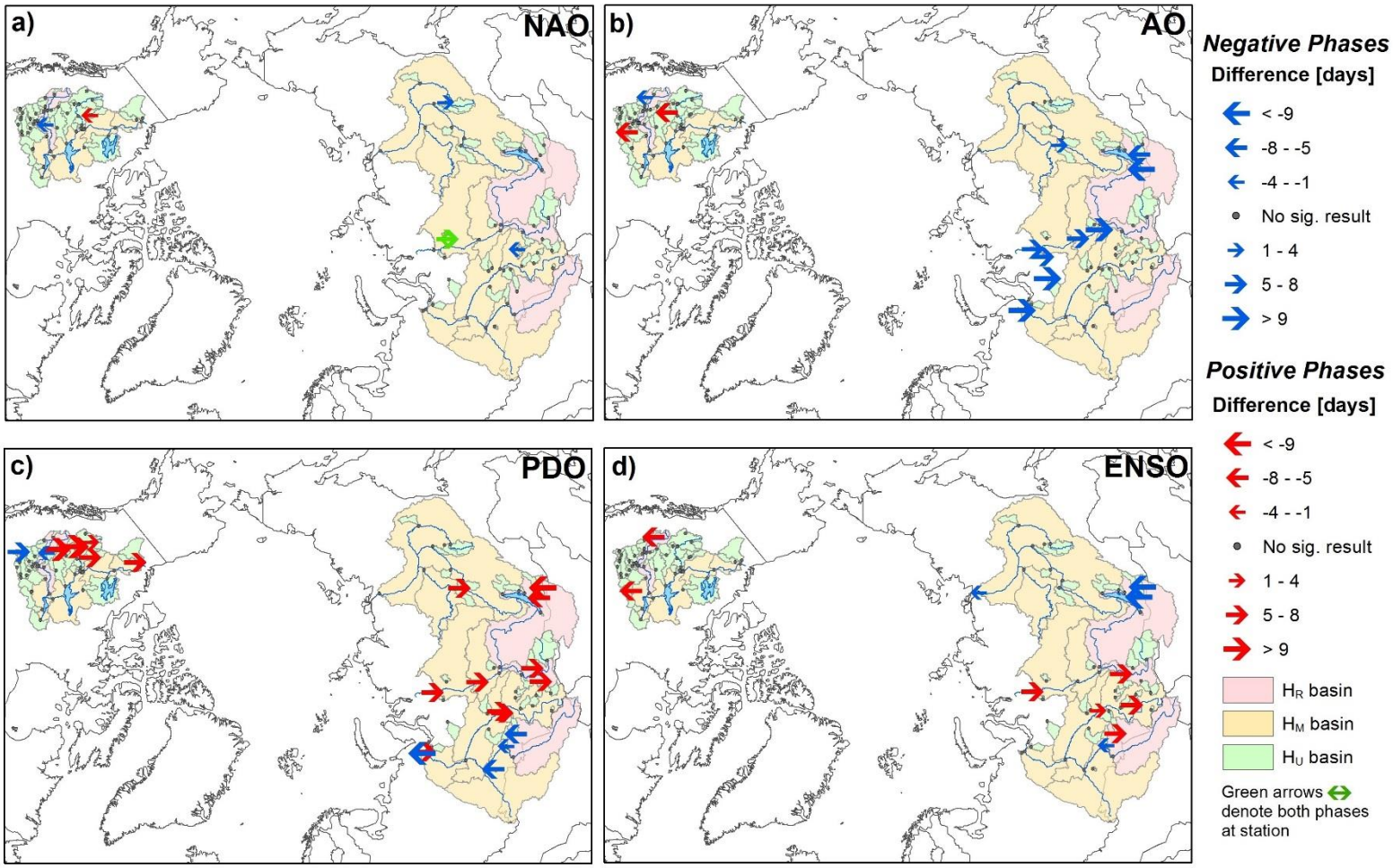

Figure 19. Climate signals (March through May) for a) NAO b) AO c) PDO and d) ENSO exhibiting 95% significant teleconnections to pulse dates during the period 1980 – 2000.

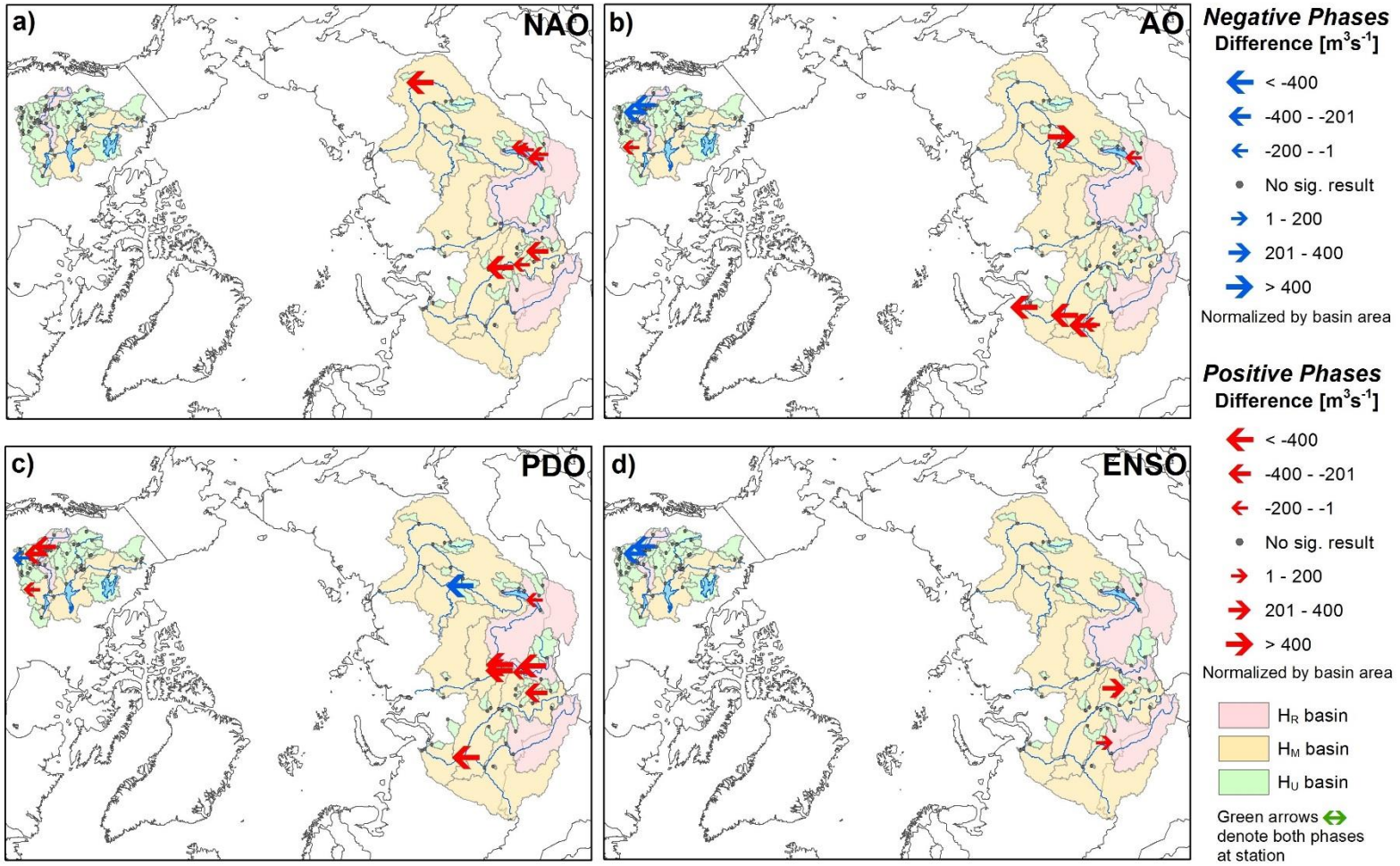

Figure 20. Climate signals (March through May) for a) NAO b) AO c) PDO and d) ENSO exhibiting 95% significant teleconnections to freshet magnitude during the period 1962 – 2000.

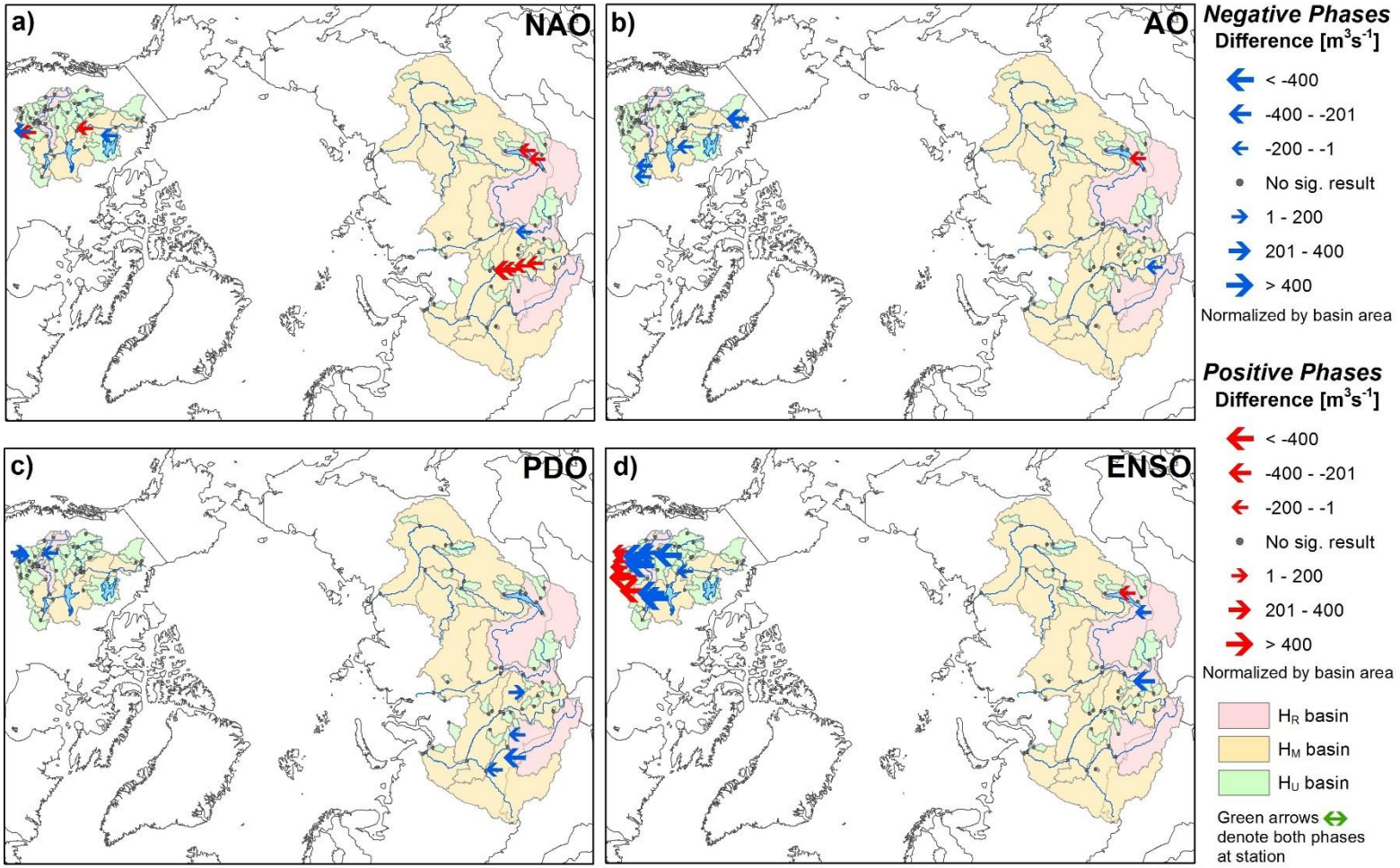

Figure 21. Climate signals (March through May) for a) NAO b) AO c) PDO and d) ENSO exhibiting 95% significant teleconnections to freshet magnitude during the period 1980 – 2000.

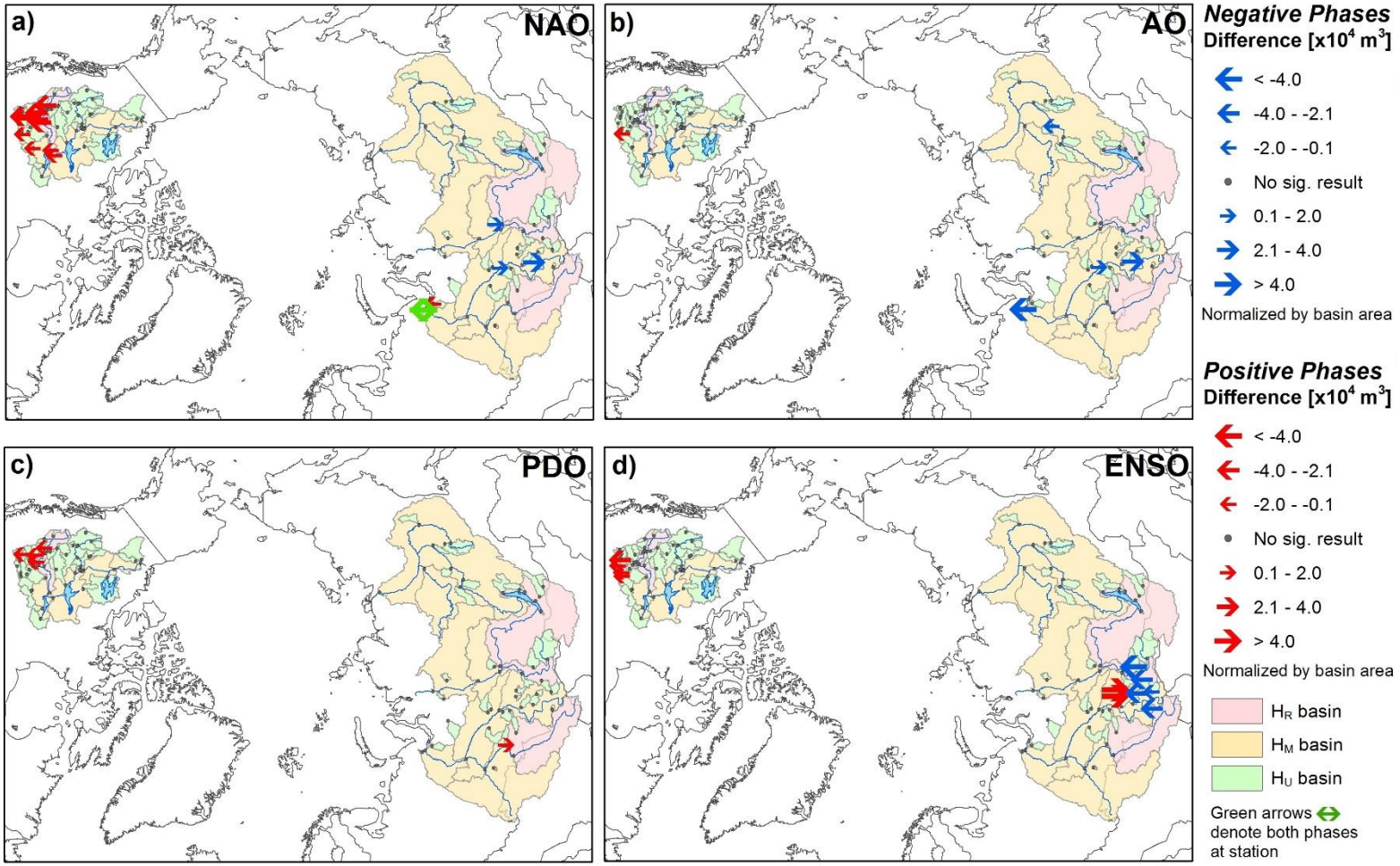

Figure 22. Climate signals (December through February) for a) NAO b) AO c) PDO and d) ENSO exhibiting 95% significant teleconnections to freshet volume during the period 1962 – 2000.

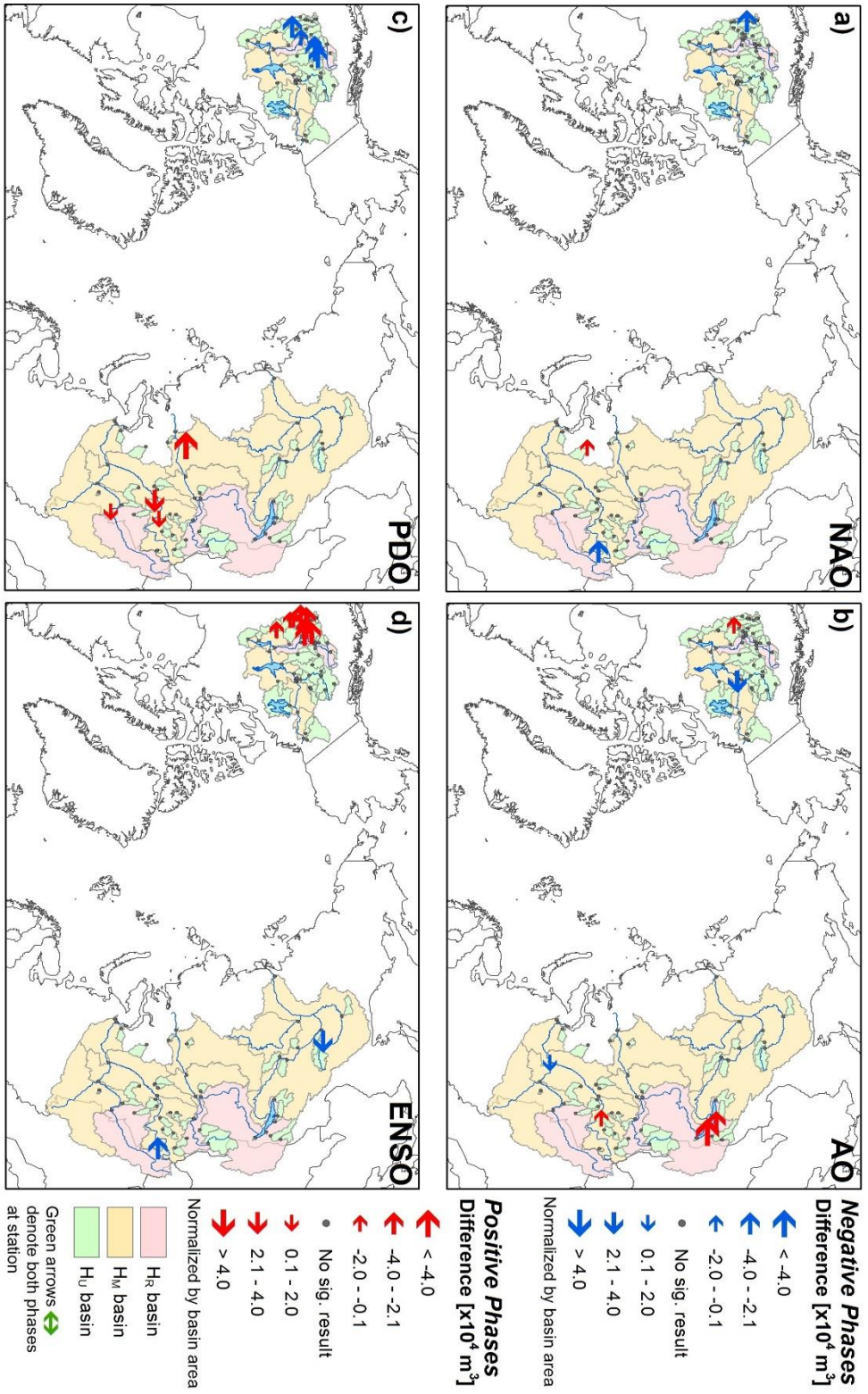

Figure 23. Climate signals (December through February) for a) NAO b) AO c) PDO and d) ENSO exhibiting 95% significant teleconnections to freshet volume during the period 1980 – 2000.

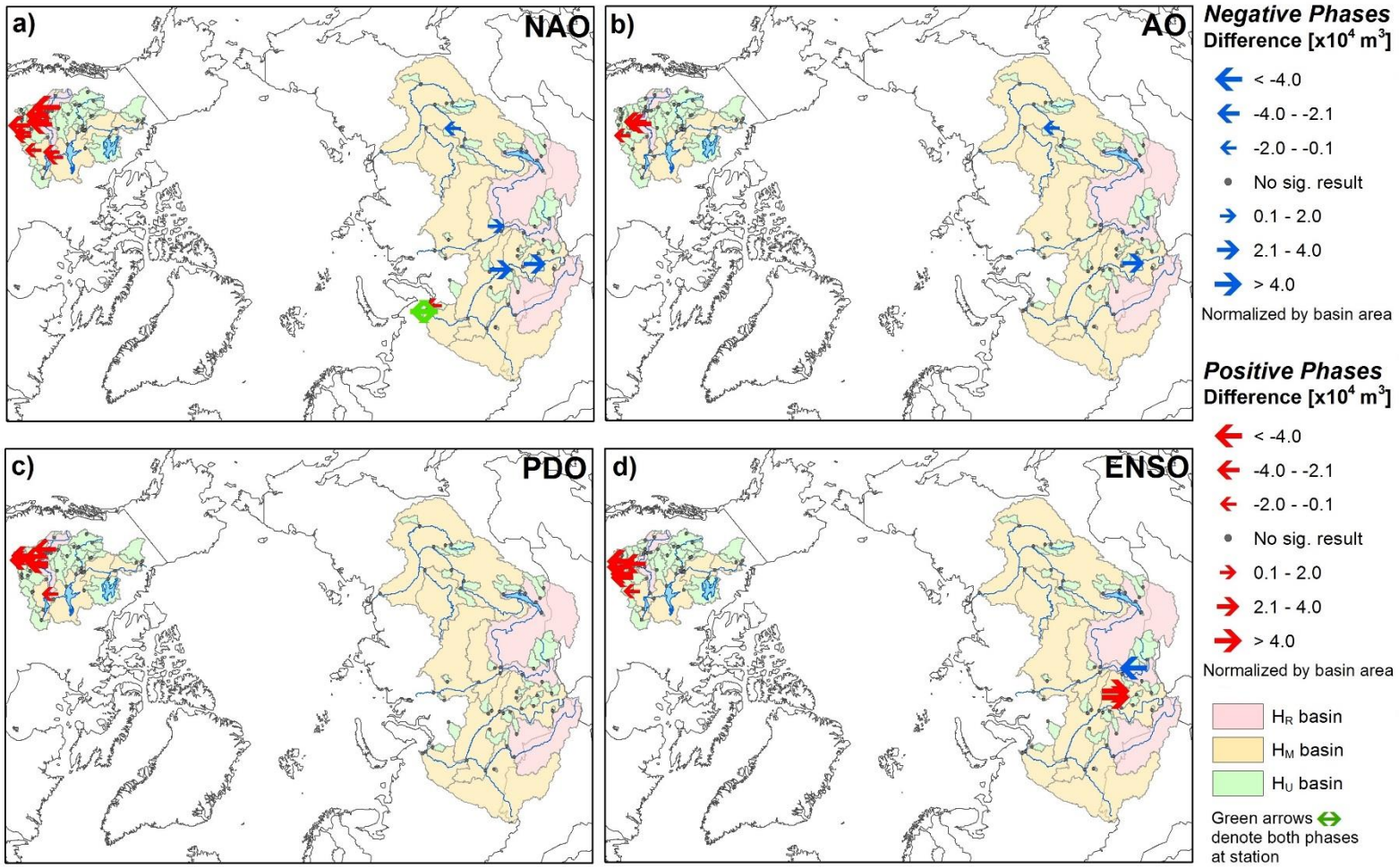

Figure 24. Climate signals (December through February) for a) NAO b) AO c) PDO and d) ENSO exhibiting 95% significant teleconnections to April through July volume during the period 1962 – 2000.

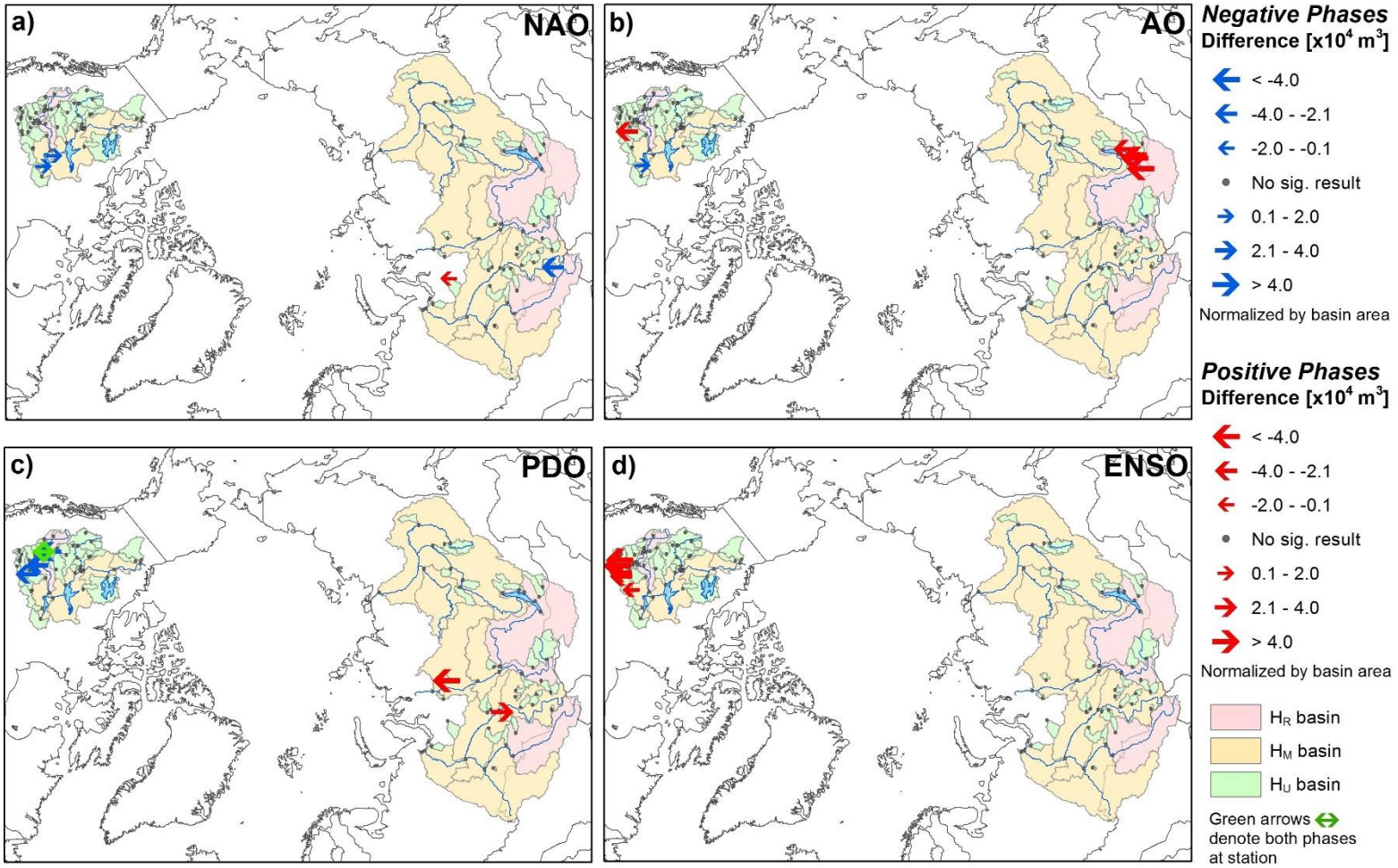

Figure 25. Climate signals (December through February) for a) NAO b) AO c) PDO and d) ENSO exhibiting 95% significant teleconnections to April through July volume during the period 1980 – 2000.

CHAPTER 6: SUMMARY & CONCLUSION

Daily discharge data from the Environment Canada Hydrometric Database (HYDAT) for 56 sub-basin stations in the Mackenzie Basin and from the Regional, Hydrometeorological Data Network (R-ArcticNET v4.0) for 50 sub-basin stations in the Ob, Yenisei and Lena basins were analyzed for the periods 1962 – 2000 and 1980 – 2000, while data for the MOLY outlet stations were analyzed for the period 1980 – 2009. From these data, information describing the spring freshet such as pulse onset, freshet end date and duration, peak freshet magnitude, freshet volume, April – July volume, and April, May, June and July volume were extracted for each time period. These freshet indices were then analyzed to address a series of new, previously unaddressed research goals outlined in Chapter 1. The goals were as follows:

(I) Quantify the trends in freshet timing and magnitude in outlet stations of the four major river basins (MOLY) around the circumpolar Arctic. This primary goal will determine whether there were any changes (e.g., increasing or decreasing annual or seasonal flows) and, importantly, whether a shift in seasonality of peak flows has occurred. Temporal sequencing of circumpolar freshet events will also be examined.

(II) Investigate the MOLY freshet flows entering the Arctic Ocean at a finer scale, by determining the trends in peak magnitude, volume, and timing of spring freshets in regulated, minimally regulated and unregulated sub-basins as well as changes in hydrograph shape. Trends on a sub-basin level will be compared to trends which have occurred at the outlets.

(III) Examine relationships of variability in spring freshets with regional temperature and precipitation patterns, as well as, several large-scale atmospheric/oceanic

teleconnection indices including the Arctic Oscillation (AO), North Atlantic Oscillation (NAO), Pacific Decadal Oscillation (PDO) and El Niño-Southern Oscillation (ENSO)

Results were presented as three separate, stand-alone journal-style manuscripts. Additionally, a literature review was provided to introduce background and set the context of the outlined research. Specifically, the literature review of Chapter 2 discussed the major freshwater budget components of the Arctic Ocean and its linkages with the global hydrological cycle with special emphasis placed on potential impacts of spring freshet variability. Other implications of Arctic freshwater and terrestrial runoff variability were discussed; for example, regional biological effects and sea-ice impacts. Atmospheric teleconnections indices were defined and related with respect to their regional climatic effects to the Mackenzie and Eurasian basins. Future climate scenarios and their flow and budget predictions were mentioned; specifically, how climate change occurs more rapidly in Arctic regions than elsewhere, and may result in a shift from a nival regime to a more pluvial one. Basin characteristics including physiography, climatology and flow regulation were discussed in detail. Finally, accuracy issues related to collecting hydrometric data in sparsely populated Arctic regions were discussed as a disclaimer to the subsequent research.

Thesis objective (I) was addressed in Chapter 3. Daily discharge data for MOLY outlet stations were used to quantify trends in freshet timing and magnitude for the entire available length of record for each station, as well as during 1980 – 2009. Over the longer records, pulse dates were found to be significantly decreasing in the Mackenzie and Lena stations, while peak freshet magnitudes showed non-significant decreasing trends. Freshet volumes did not exhibit any significant changes in any station over the longer term records. During 1980 – 2009,

however, freshet volumes increased in all stations, with only the Yenisei basin showing a non-statistically significant increase. Pulse dates were generally becoming earlier, whilst peak freshet magnitudes decreased (non-significantly) in the Lena and Yenisei basins. No change in peak freshet magnitude was observed in the Mackenzie basin during 1980 – 2009, while the Ob showed a minor increase. Freshet lengths increased in all stations during 1980 – 2009, although none of the increases were statistically significant. Circumpolar freshet volume contribution during the period 1980 – 2009 was dominated by the Lena River, followed by the Yenisei, Ob and Mackenzie. Freshet onset occurred on the Mackenzie River first, followed by the Ob, Yenisei and Lena rivers.

Importantly, total annual freshwater influx to the Arctic Ocean increased by 14% during 1980 – 2009. While this estimate was comparatively larger than the 7% increase found in a previous study using records from the six largest Eurasian rivers during 1936 – 2009 (see Peterson et al., 2002), the results found here were consistently more drastic during the shorter window of analysis. The increase was distributed throughout the year. Freshet contribution expressed as a percentage of annual flow decreased by 1.7% during 1980 – 2009, suggesting that despite total freshet volume showing a net increase, its proportional contribution to annual flow had decreased. Hence, annual increases were not solely due to increasing freshet volume. Winter, spring and fall expressed as proportions of annual flow showed increases (1.3%, 2.5% and 2.5%, respectively), while summer showed a strong decrease (5.8%) in proportional discharge during 1980 – 2009. Rising winter, spring and fall discharge proportions, combined with lower peak freshet magnitudes, potentially increased freshet durations, and lower summer proportions are indicative of a shift to a flatter, more gradual annual hydrograph with an earlier

pulse onset. This shift in seasonality has potential implications to Arctic Ocean freshwater circulation and is an important finding from Chapter 3.

Chapter 4 addressed thesis objective (II). Discharge was assessed on a sub-basin and regional level in order to determine the effects of the dominant controls of elevation and latitude, as well as flow regulation, on freshet trends and how these compared to outlet flow characteristics as obtained in Chapter 3. Comparisons of hydrographs revealed differences in hydrograph shape from 1962 – 2000 compared to 1980 – 2000. In many sub-basins, the annual hydrograph and specifically the spring freshet period trends were observed to have undergone a general "flattening", with earlier pulse onset dates, longer freshet durations and sometimes decreased peak freshet magnitudes. In some cases, early winter and late-fall low-flows rose, a possible result of changes in seasonal precipitation. Late summer rainfall peaks have increased in frequency and magnitude in many alpine, pluvial-dominated basins. These sub-basin trends suggested an overall shifting seasonality of flow, which propagated downstream to the outlet stations. Regionally, the high-relief western and southern areas of the Mackenzie basin as well as the southern Ob and southern and western Yenisei showed most similarity to flow at the outlets.

Notably, unregulated stations, regardless of region, had observed relationships with freshet volumes at the outlets, although those relationships could be negated in the larger encompassing basins if there was upstream regulation. No sub-basin relationships with freshet volume at the outlet were observed in any regulated station. High peak freshet magnitudes in regulated stations still related to high peak magnitudes at the outlets, particularly if there was only one dam impounding flow. This suggests that regulation impacted the volume of water released during the spring freshet but did not necessarily suppress the highest short-term peak

flows. Since the majority of all significant trends occurred in H_U stations, flow regulation may have impacted the timing of peak flows as well as moderated the effects of climatic drivers such as temperature and precipitation on H_R and H_M basins.

To separate the effects of regulation and climate, Chapter 5 addressed thesis objective (III) by assessing climatic drivers of trends obtained in Chapter 3 and Chapter 4. This was achieved by performing a correlation analysis of cumulative winter precipitation and spring temperatures to freshet measures. To supplement this, a composite teleconnections analysis related the highest or lowest 25% of values of four major climate indices (AO, NAO, PDO and ENSO) to corresponding freshet measures. This composite analysis essentially evaluated each phase of the climate indices separately, since climate signals from the large-scale teleconnections may not have displayed a linear relationship to the hydro-climatic variables.

Timing and peak magnitude of the freshets within sub-basins were found to be strongly linked to spring temperatures. Significant trends were found where significant climatic correlations existed, regardless of regulation status. Regulation did, however, appear to limit climatic relationships of cold season precipitation accumulation with freshet volume V_1 and V_2, since few significant correlations with volume were found in regulated stations. This reinforces the notion that flow impoundment did act to suppress some natural climatic drivers of freshet generation, with potential impact to seasonal runoff regimes. However, volume relationships with cold season precipitation were less clear than temperature linkages with freshet timing.

Significant relationships ($p < 0.05$) were found with all four major teleconnections indices. Relationships were generally less apparent during the shorter period of 1980 – 2000 compared to 1962 – 2000, possibly due to small sample sizes. Where statistically significant

relationships existed, only one phase of a particular climate signal was typically associated with the relationship, with few exceptions. Positive AO and NAO leading to warmer, wetter winters were most often associated with earlier pulse dates, decreased peak freshet magnitude and lower freshet volume. Positive ENSO (El Niño), associated with warmer, wetter winters over the Mackenzie and colder, drier winters over the Eurasian basins (with some regional variability), demonstrated relationships with earlier onset of pulse dates in the Mackenzie, later onset in the Eurasian sub-basins, and decreased peak freshet magnitude in the southern Mackenzie basin. El Niño had strong associations with decreased freshet volume in the southern Mackenzie but had little effect on Eurasian volumes. Meanwhile, positive PDO, associated with positive SAT anomalies and mixed, mostly positive precipitation anomalies in all basins, showed significant relationships with later pulse dates and lower freshet magnitudes in all basins. The unexpected relationships of PDO with delayed pulse onset, particularly during 1980 – 2000, may be due to the study period entirely occurring in a warm PDO phase. Significant relationships were predominantly found in unregulated basins, with fewer significant relationships observed in impounded stations.

In conclusion, the results of this research provide an expanded knowledge base of the significance of the spring freshet as an important component of atmospheric freshwater contribution to the Arctic Ocean. Importantly, it is found that the seasonality of the spring freshet is shifting, and that the freshet is sensitive to changes and variability in climatic conditions. Pulse onsets are occurring earlier, followed by an increase in freshet durations and generally lower peak magnitudes. Despite lower peak magnitudes, volume contribution during the freshet from the four major circumpolar basins has significantly increased over a recent time period. However, freshet volumes as a fraction of annual flow have decreased, while winter,

spring and fall proportions have increased. A key finding of this study is that increases in total annual freshwater contribution to the Arctic Ocean cannot be solely attributed to increases in circumpolar freshet volume; regardless of freshet volumes having increased, flow contribution during the winter, spring and fall seasons have increased at a greater rate. Rising winter and fall discharge proportions may be a result of an upward trend in precipitation changes, and should be investigated in more detail. Flow regulation appears to affect trends on a sub-basin level by suppressing climatic drivers of freshet volume, but may not have a substantial impact on freshet timing and peak magnitude. This is a preliminary result and further work is required to isolate the effects of flow regulation on freshet measures.

Although this research has provided valuable information regarding the dominant controls of freshet generation and has highlighted the potential impacts to Arctic Ocean freshwater balance, further investigation is required. This study can be expanded to include additional drainage areas that provide contribution to the Arctic Ocean, such as Hudson Bay. Future work should consider geochemical differences amongst basins. Basin geochemistry can be used as an indicator of changing permafrost thaw depth, which has subsequent effects on discharge seasonality. Since freshet volume relationships with cold season precipitation were less clear than temperature relationships with freshet timing, an integrated multi-variable approach incorporating both temperature and precipitation is needed to clarify these freshet volume relationships. The correlations analysis of Chapter 5 discovered some climatic and atmospheric relationships with freshet measures; however, a basin-scale synoptic climatological approach should be used to better identify atmospheric processes associated with regional variation in freshet measures. Trends in temperature and precipitation must be compared side-by-side to freshet trends, using a suite of re-analysis and observed climatic data sets, in order to fully reveal

the complex climatic interactions driving trends in freshet characteristics. Climatic variability and its relationship with extreme discharge events must also be investigated in greater detail.

Furthermore, since there were significant differences in climatic and large-scale atmospheric variability relationships with unregulated stations versus those stations incorporating an upstream regulation signal, the effects of flow regulation on the timing and magnitude of freshet response need to be more fully evaluated. Future climate as well as other human activities causing impacts to discharge behaviour, such as forestry and agriculture, should be considered alongside flow regulation. Hydraulic flow modelling, some datasets of which already exist, can be used to remove the effect of regulation and thereby permit clearer identification of climatic-induced long term trends as well as clarify the role of climate-atmosphere interactions at the regional scale. Likewise, flow modelling can be used to determine whether regulation can actually mitigate the effects of climatic variation on discharge seasonality and magnitude at the outlets. Lastly, implementation of a hydraulic flow-routing model will permit determination of travel time of flow from each sub-basin station along its channel to the mouth of the major river outlet. This will allow for accurate determination of proportional sub-basin contributions and identification of major regional freshet drivers. This discussion could be extended to include local climatic effects on key contributing sub-basins, with subsequent implications to the seasonality of relative contribution amongst major Arctic Ocean freshwater flow drivers.

APPENDIX A

Basin Hypsometry

Hypsometric curves for individual sub-basins in each of the four major basins are given below. Hypsometry for the entire gauged basin (i.e., at the outlet) is shown in the hypsometry of station ID 10LC014 (Mackenzie River at Arctic Red River) for the Mackenzie, 11801 (Ob at Salekhard) for the Ob, 9803 (Yenisei at Igarka) for the Yenisei and 3821 (Lena at Kusur) for the Lena. The Mackenzie basin shows a gradual hypsometric curve with 20% or more of the area above 900 m elevation. The Ob reveals the flattest and lowest elevation in its hypsometric curve, with approximately 90% of the basin below 500 m elevation. The Yenisei and Lena basins show greater percentages (40 – 50 %) above 500 m elevation, with much of the higher elevation terrain occurring in mountainous regions or plateaus.

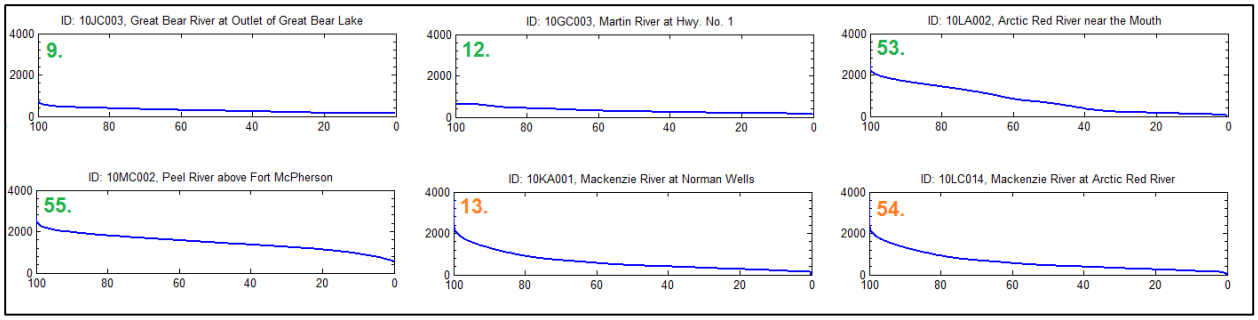

Figure A.1.1 Hypsometric curves (elevation versus % area) of Mackenzie station sub-basins, labelled and grouped by northern regions.

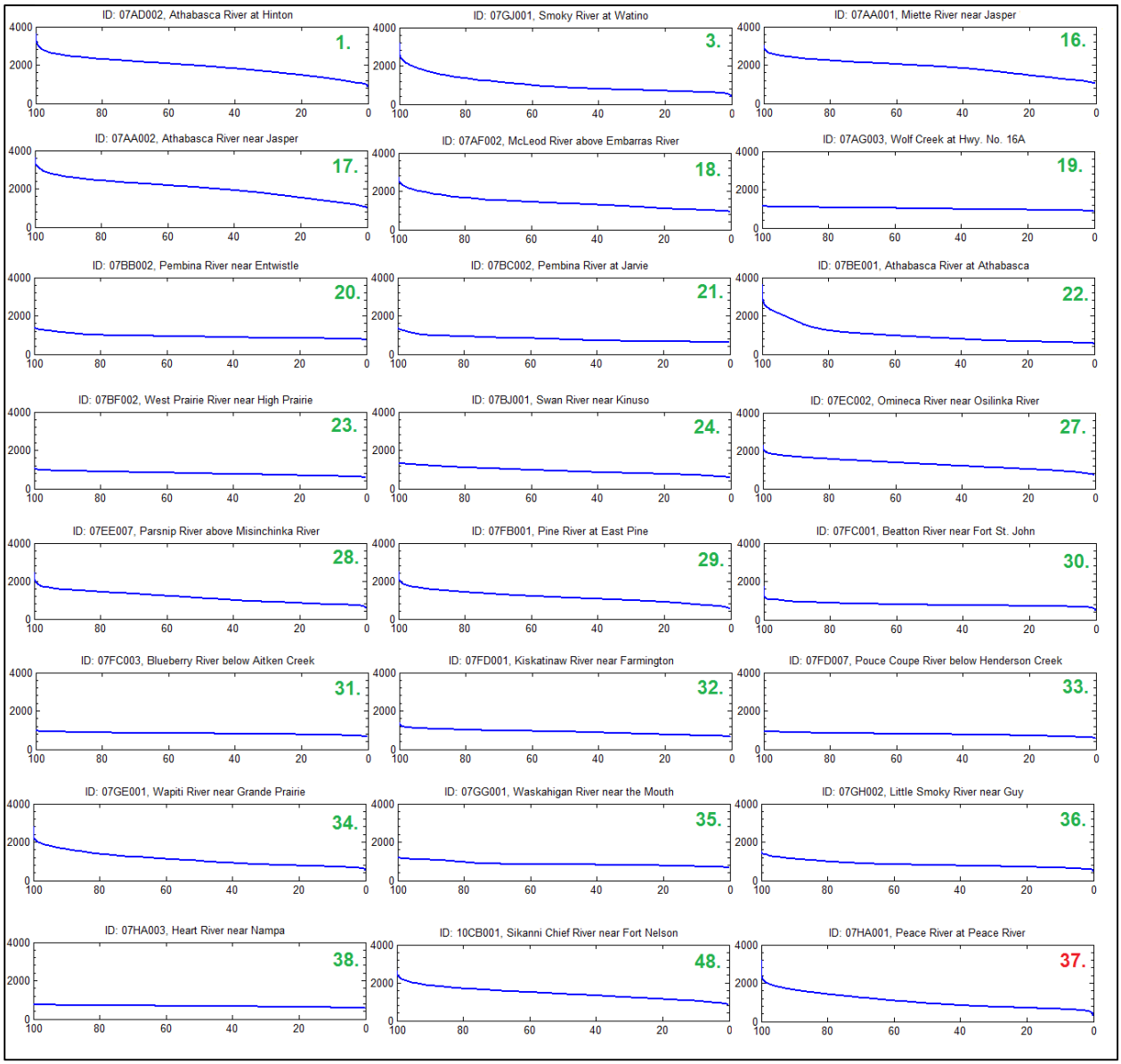

Figure A.1.2 Hypsometric curves (elevation versus % area) of Mackenzie station sub-basins, labelled and grouped by southern regions.

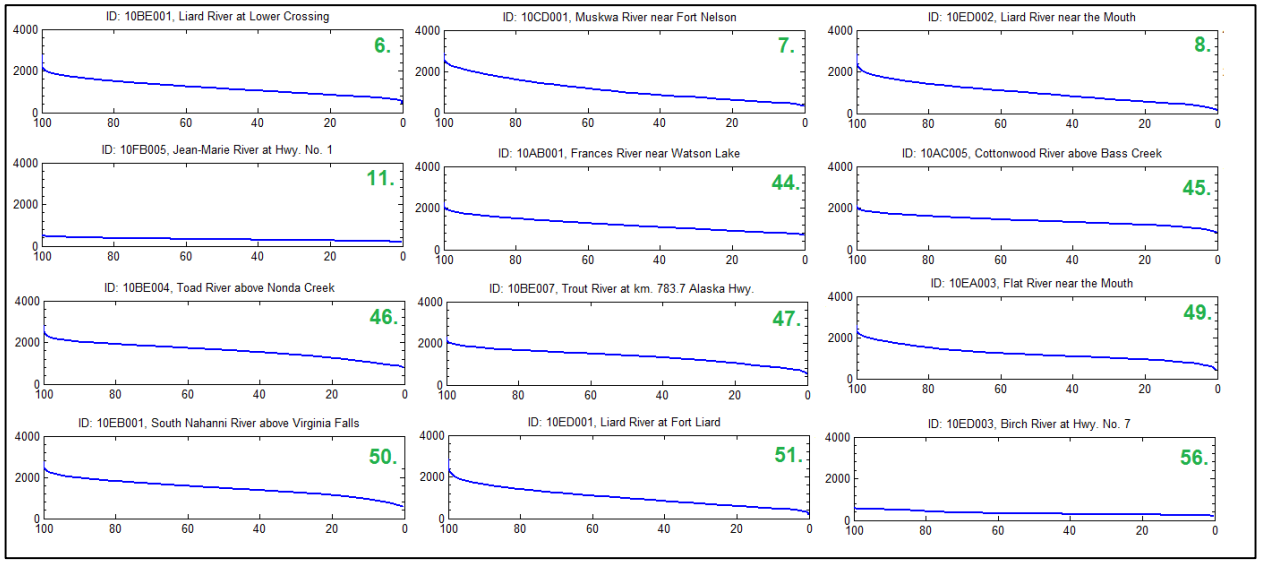

Figure A.1.3 Hypsometric curves (elevation versus % area) of Mackenzie station sub-basins, labelled and grouped by western regions.

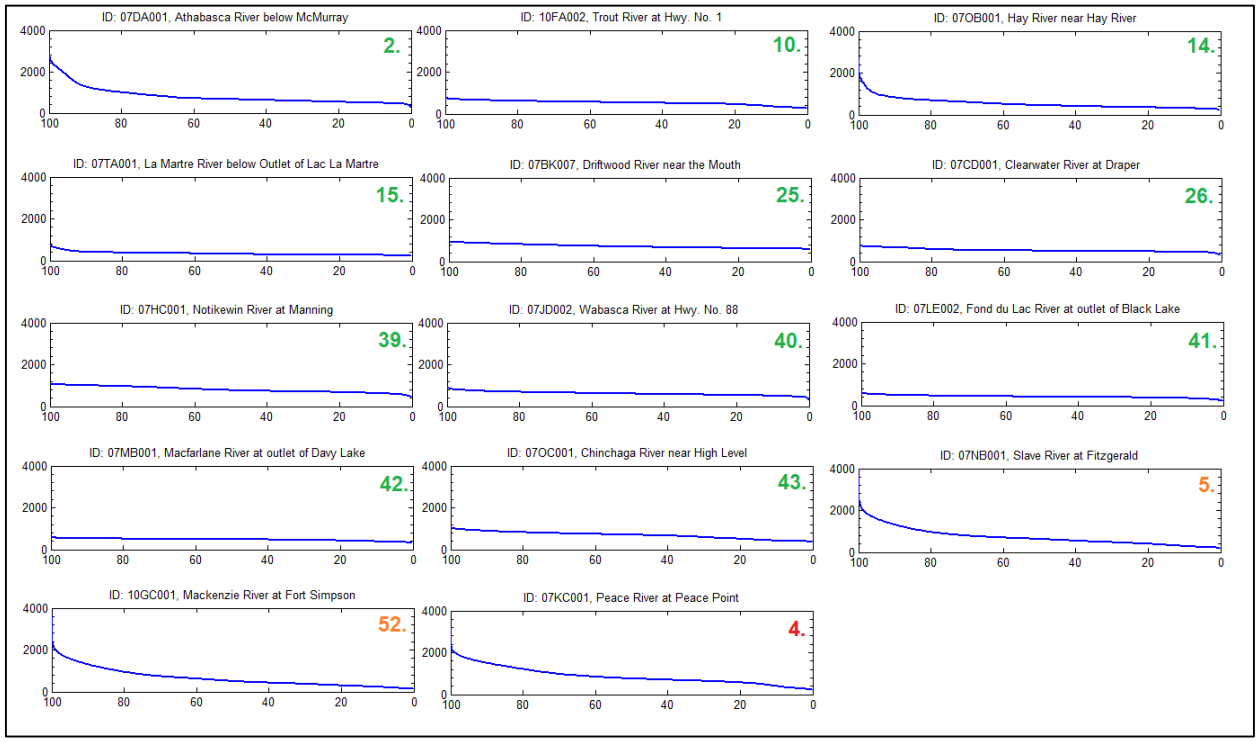

Figure A.1.4 Hypsometric curves (elevation versus % area) of Mackenzie station sub-basins, labelled and grouped by eastern regions.

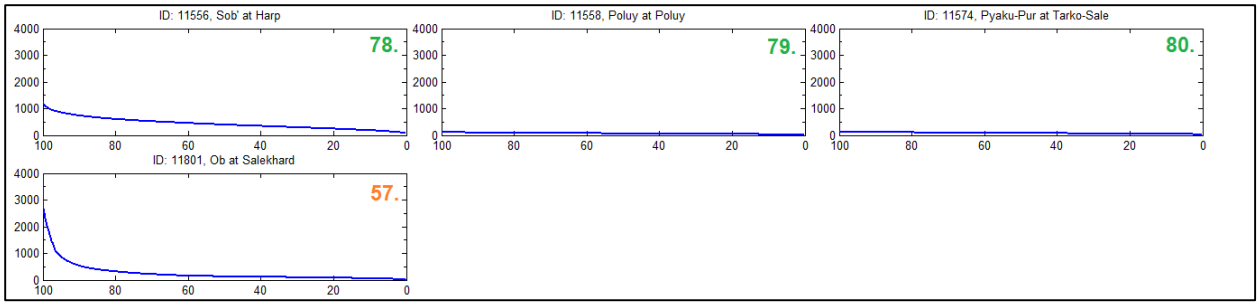

Figure A.2.1 Hypsometric curves (elevation versus % area) of Ob station sub-basins, labelled and grouped by northern regions.

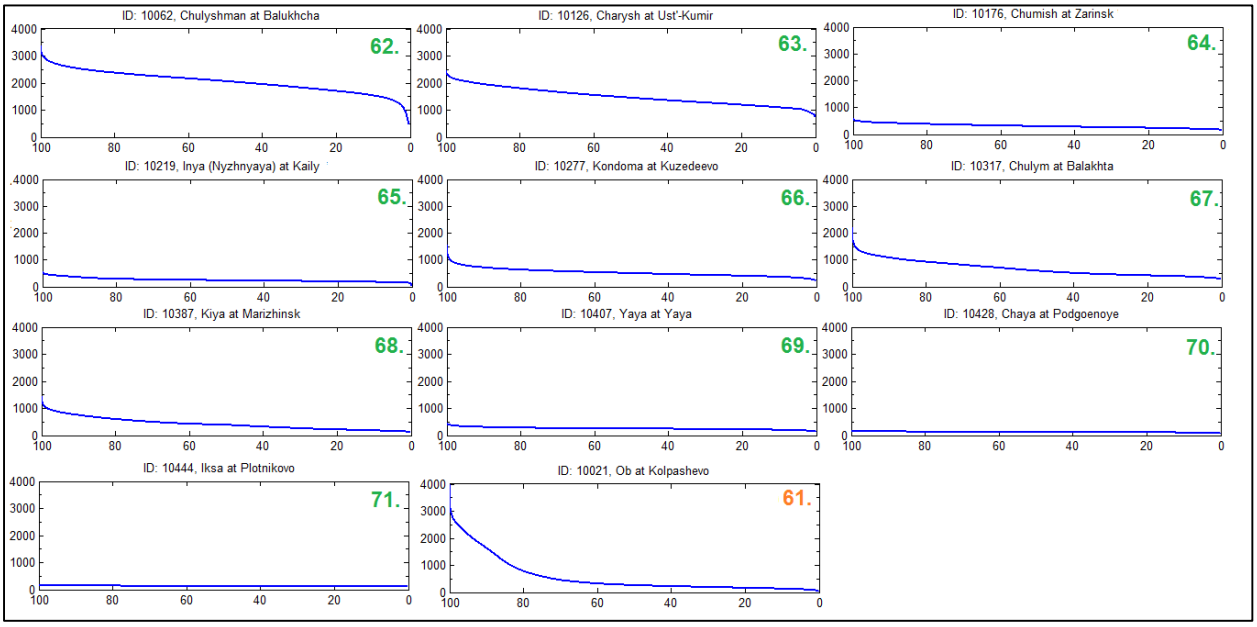

Figure A.2.2 Hypsometric curves (elevation versus % area) of Ob station sub-basins, labelled and grouped by southern regions.

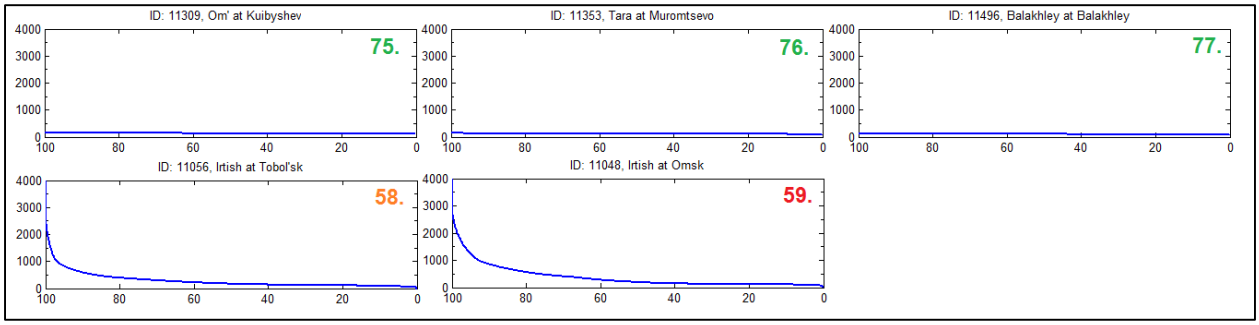

Figure A.2.3 Hypsometric curves (elevation versus % area) of Ob station sub-basins, labelled and grouped by western regions.

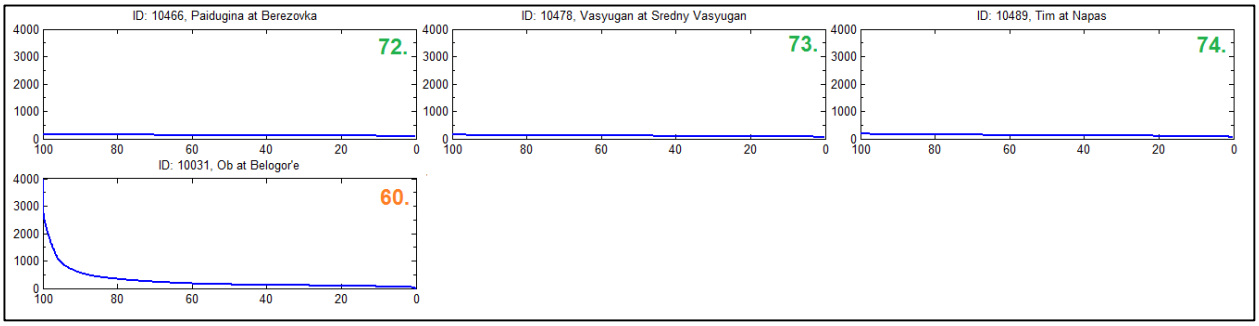

Figure A.2.4 Hypsometric curves (elevation versus % area) of Ob station sub-basins, labelled and grouped by eastern regions.

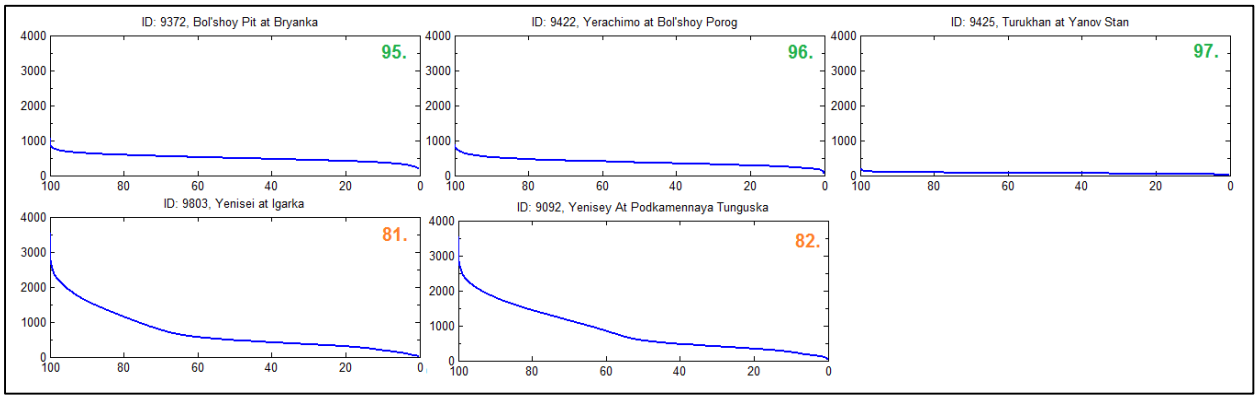

Figure A.3.1 Hypsometric curves (elevation versus % area) of Yenisei station sub-basins, labelled and grouped by northern regions.

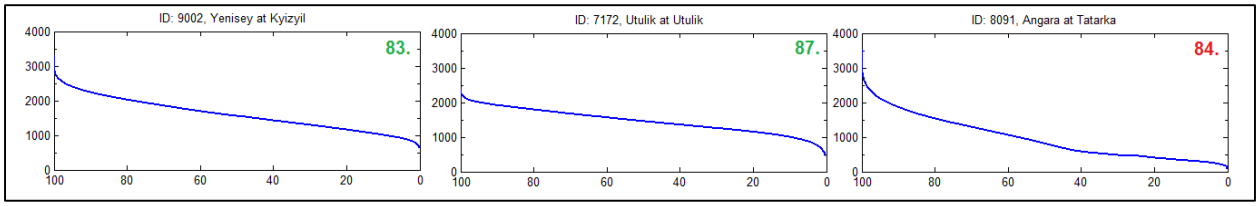

Figure A.3.2 Hypsometric curves (elevation versus % area) of Yenisei station sub-basins, labelled and grouped by southern regions.

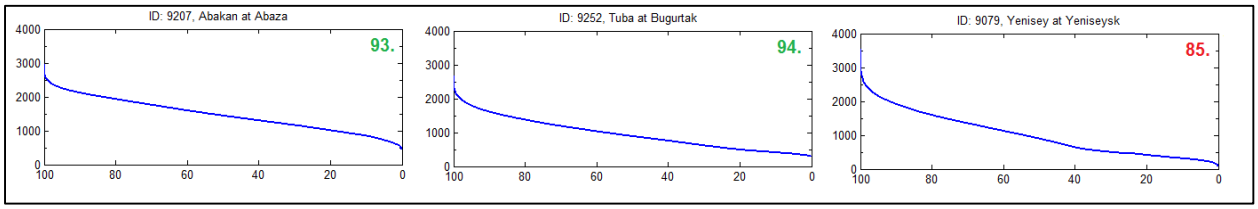

Figure A.3.3 Hypsometric curves (elevation versus % area) of Yenisei station sub-basins, labelled and grouped by western regions.

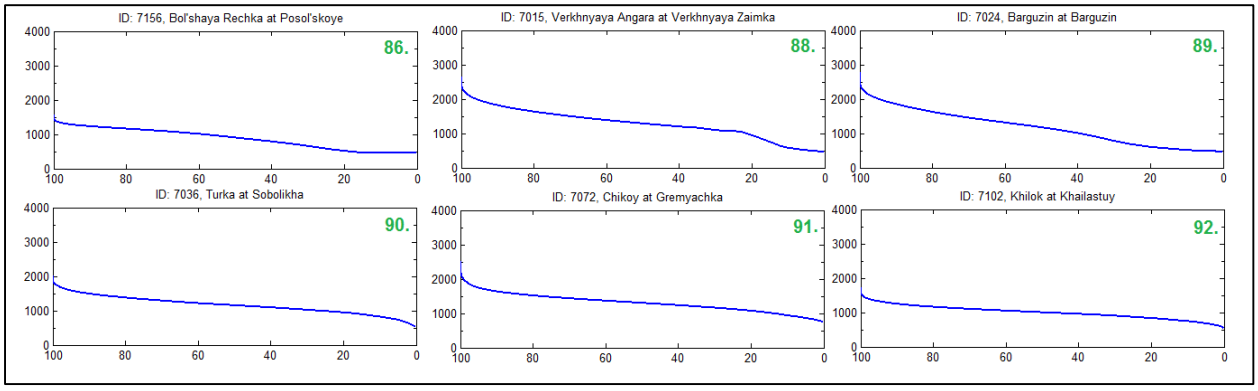

Figure A.3.4 Hypsometric curves (elevation versus % area) of Yenisei station sub-basins, labelled and grouped by eastern regions.

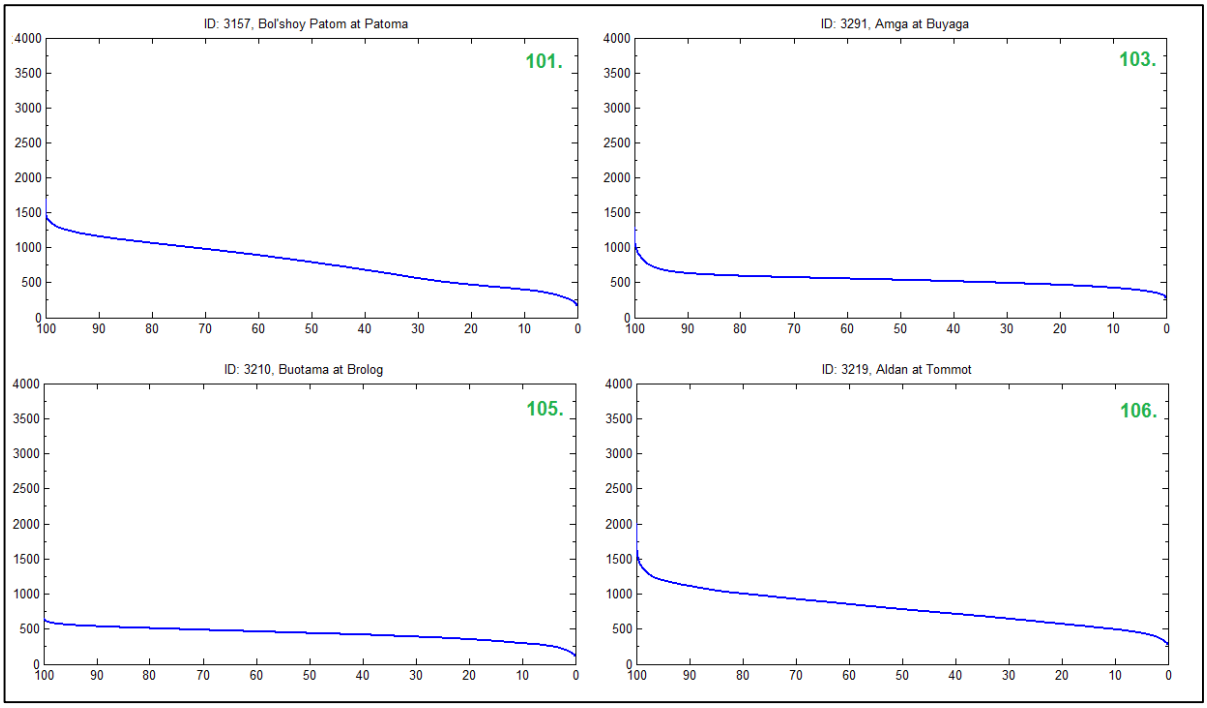

Figure A.4.1 Hypsometric curves (elevation versus % area) of Lena station sub-basins, labelled and grouped by southern regions.

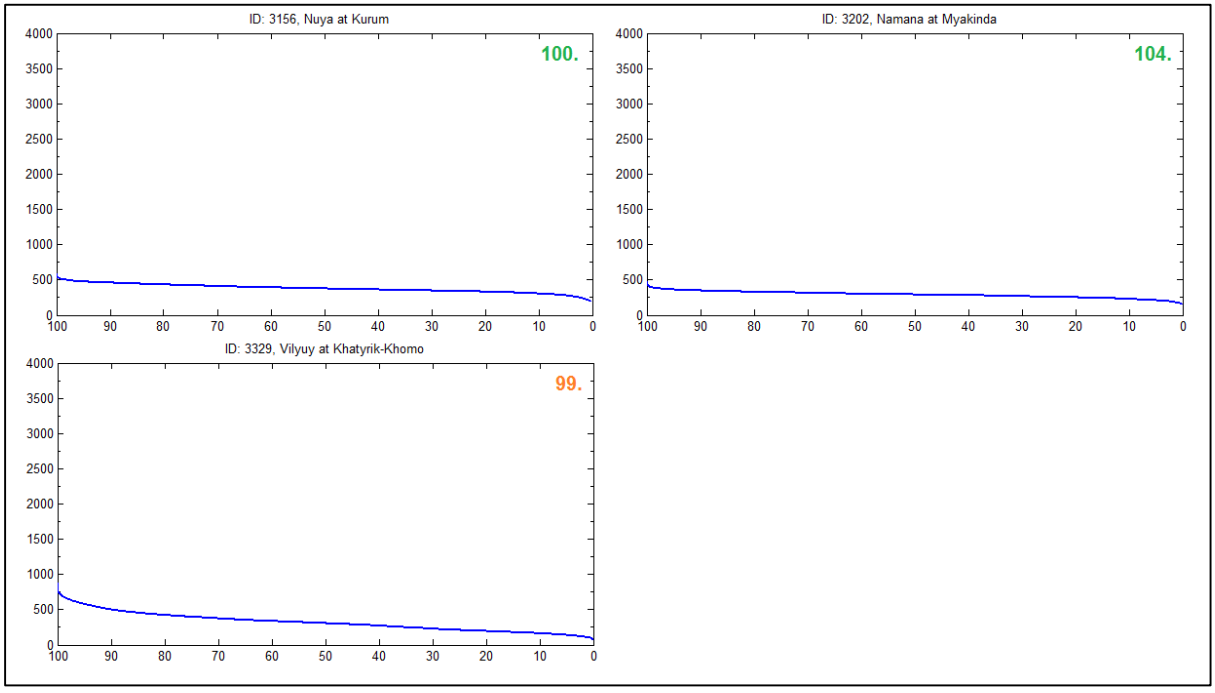

Figure A.4.2 Hypsometric curves (elevation versus % area) of Lena station sub-basins, labelled and grouped by western regions.

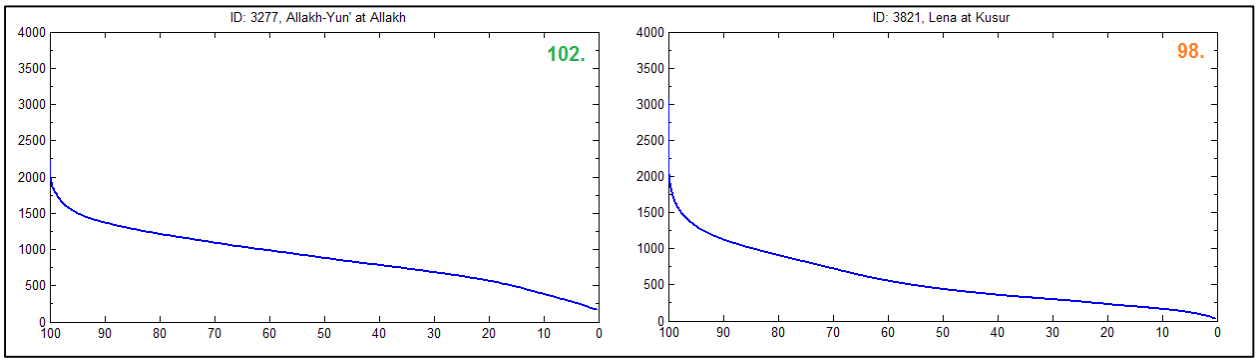

Figure A.4.3 Hypsometric curves (elevation versus % area) of Mackenzie station sub-basins, labelled and grouped by eastern regions.

APPENDIX B

Daily flow (upper curve) and cumulative departure from mean flow (lower curve) for the Yenisei River, 2000. The date at which cumulative departure is at a minimum defines the onset of the spring pulse, occurring on May 17 (Julian day 137) in this case (Cayan et al., 2001). Also shown is the annual hydrograph centre of mass date used to define the freshet end date; the freshet duration between the date of onset and the freshet end date; and the peak flow occurring during freshet. Shaded grey regions denote the time periods used to integrate flows occurring from April through July (V_1) and during freshet duration (V_2).

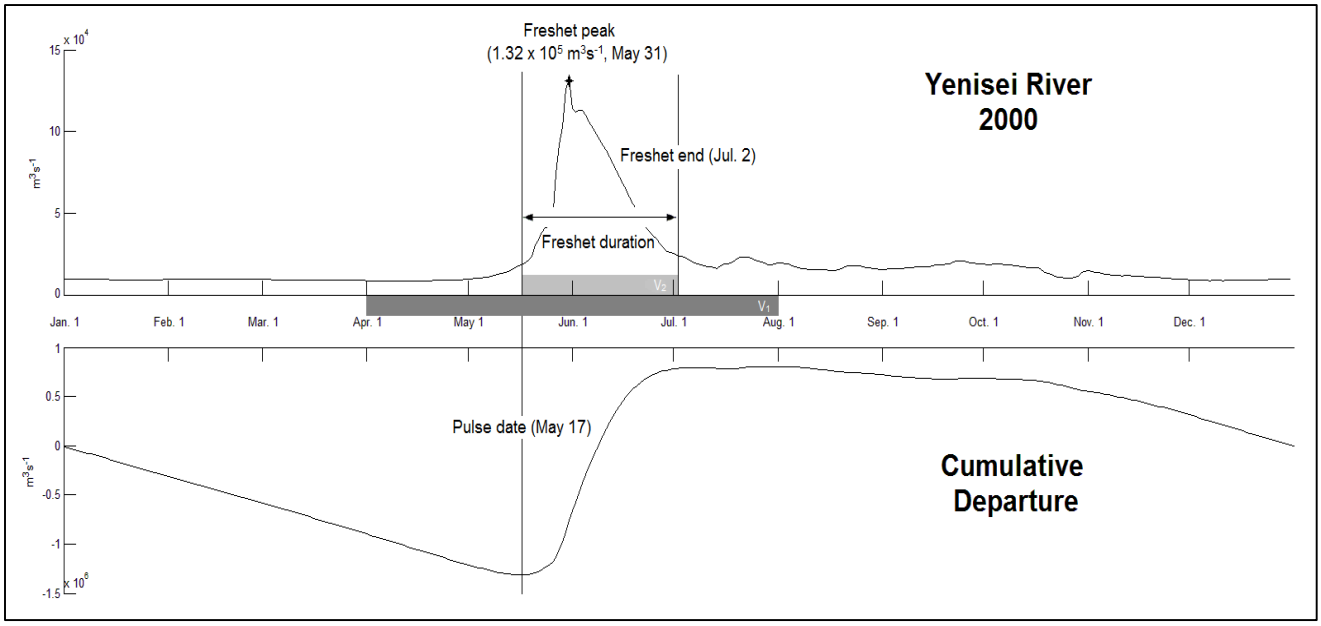

APPENDIX C

Climatic Relationships using Alternative Datasets

For the Mackenzie basin, climatic relationships were also performed using a 10 x10 km resolution, spline-interpolated dataset of daily precipitation and maximum and minimum daily temperature covering the period 1950 – 2010, referred to as NRCAN (2012) (Hutchinson et al., 2009; McKenney et al., 2011). The ERA-40 dataset was utilized for the Eurasian basins. ERA-40 is a re-analysis product of meteorological observations covering the period September 1957 to August 2002, produced by the European Centre for Medium-Range Weather Forcasts (ECMWF) (Uppala et al., 2005). Resolution is based on the T159 Gaussian grid, corresponding to a spatial resolution of approximately 1.125° x 1.125°.

Table C-1 and C-2 give the number of significant correlations (5% level) for all sub-basins obtained when using the CRU TS3.21 dataset versus NRCAN (2012) for the Mackenzie basin and ERA-40 for the Eurasian basins, respectively. Correlation results obtained using CRU TS 3.21 are further discussed in Chapter 5. In the Mackenzie basin, temperature-related correlations (F_P, F_L and F_M) using CRU TS3.21 improve, despite the higher resolution of NRCAN (2012). Precipitation-related correlations (V_1 and V_2) show worse overall performance using CRU TS3.21. In Eurasian basins, F_P correlations using CRU TS 3.21 show a vast improvement in significant results over ERA-40, although other variables show little improvement or worse performance. Because of the limited spatial resolution of the ERA-40 re-analysis dataset and limited spatial coverage of NRCAN (2012), CRU TS3.21 was chosen as the best available climatic dataset with the required spatial and temporal coverage and variables.

Table C-1. Number of significant correlations (5% level) with freshet measures obtained using different climatic datasets during the period 1980 – 2000 for Mackenzie stations. Shown in brackets are the percent changes in significant results when using the alternate climatic datasets compared to CRU TS3.21.

	F_P	F_L	F_M	V_1	V_2
CRU TS3.21	23 (+10%)	11 (+38%)	10 (+67%)	7 (-50%)	9 (-36%)
NRCAN	21	8	6	14	14

Table C-2. Number of significant correlations (5% level) with freshet measures obtained using different climatic datasets during the period 1980 – 2000 for Eurasian stations. Shown in brackets are the percent changes in significant results when using the alternate climatic datasets compared to CRU TS3.21.

	F_P	F_L	F_M	V_1	V_2
CRU TS3.21	35 (+3400%)	7 (+600%)	2 (-33%)	0 (-100%)	2 (+100%)
ERA-40	1	1	3	1	1

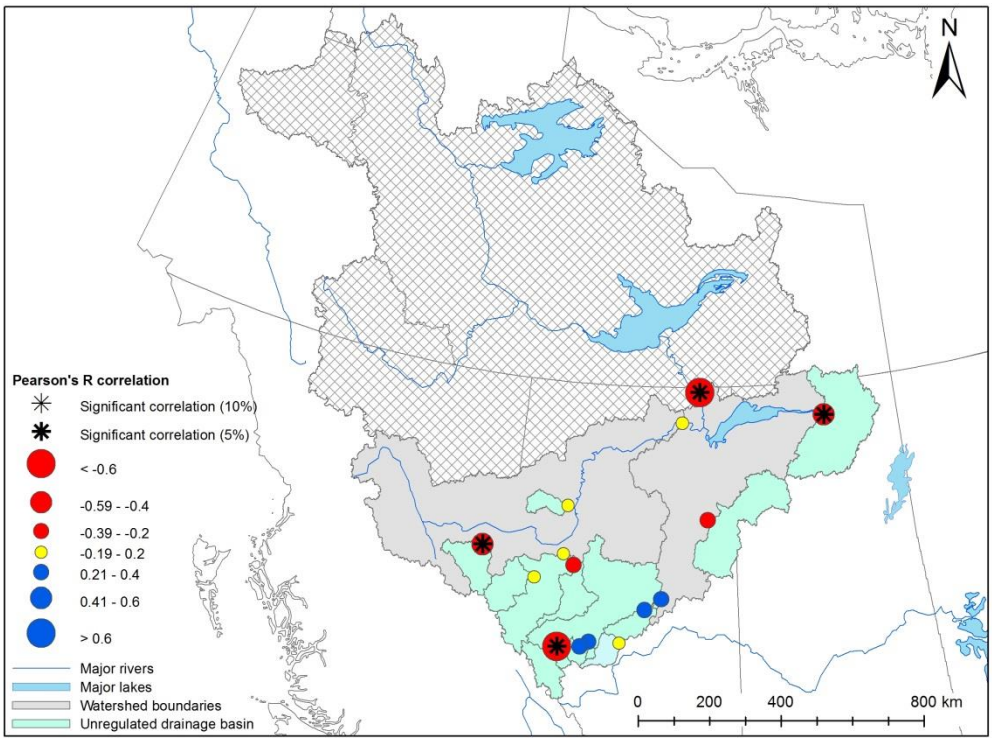

Figure C.1. Pulse date correlations with April through June average temperature (NRCAN) during the period 1962 – 2000 for Mackenzie stations.

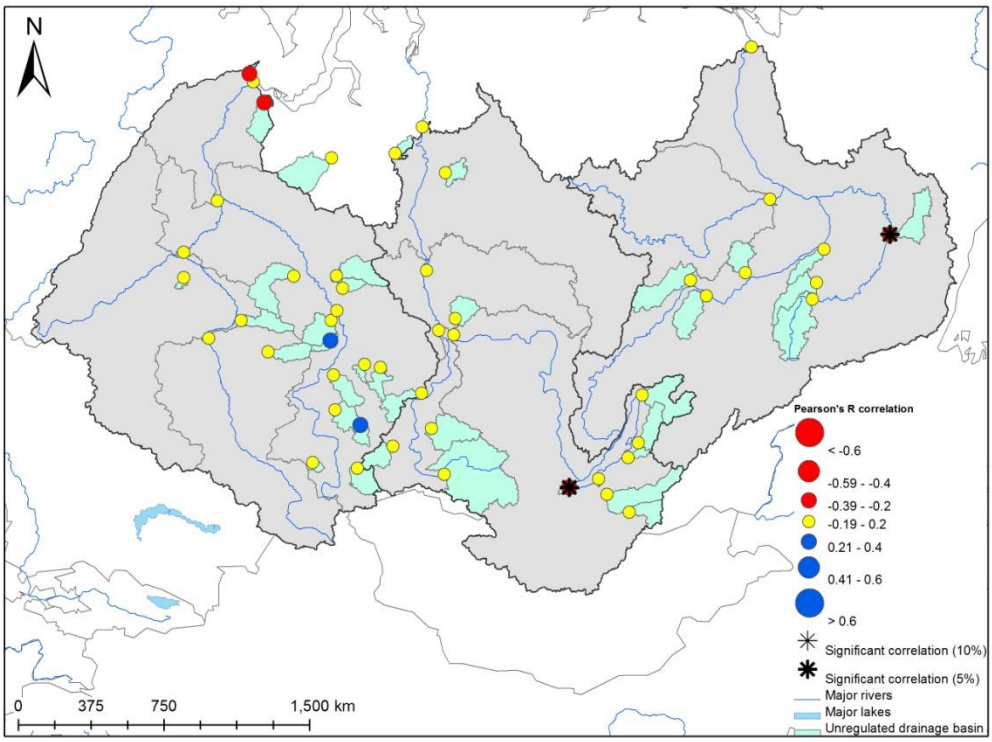

Figure C.2. Pulse date correlations with April through June average temperature (ERA-40) during the period 1962 – 2000 for Eurasian stations.

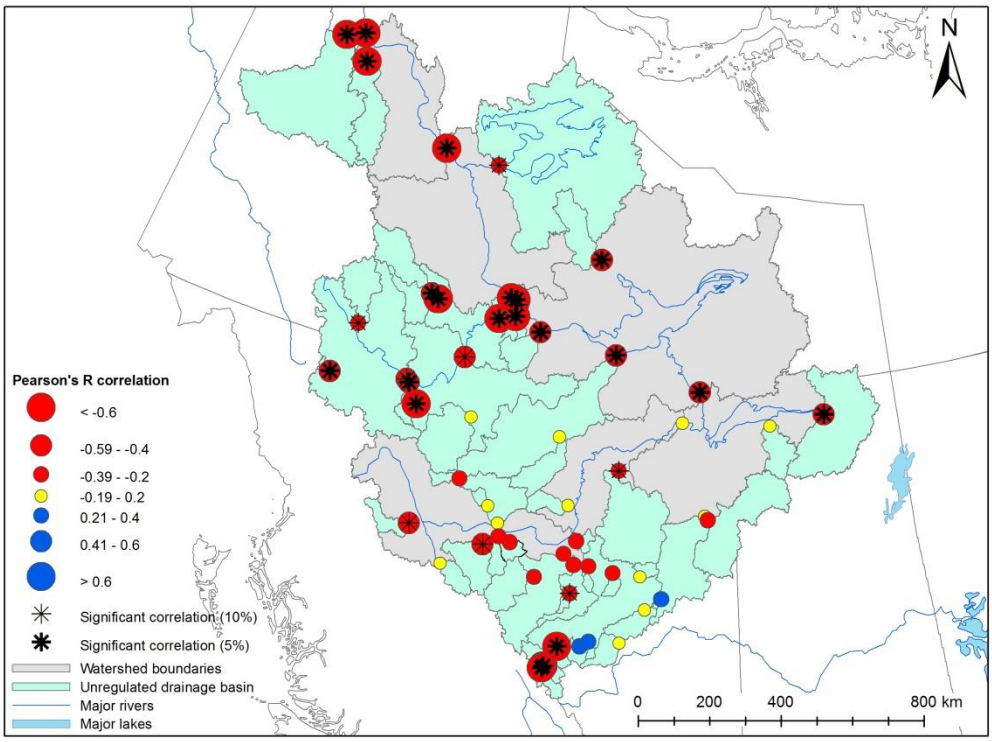

Figure C.3. Pulse date correlations with April through June average temperature (NRCAN) during the period 1980 – 2000 for Mackenzie stations.

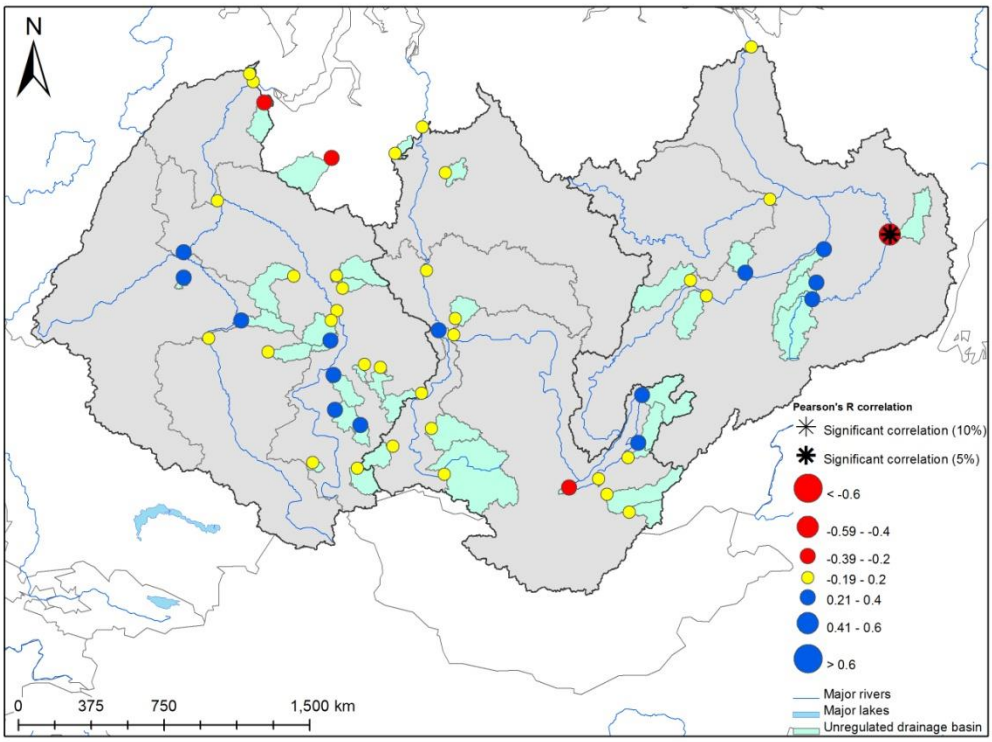

Figure C.4. Pulse date correlations with April through June average temperature (ERA-40) during the period 1980 – 2000 for Eurasian stations.

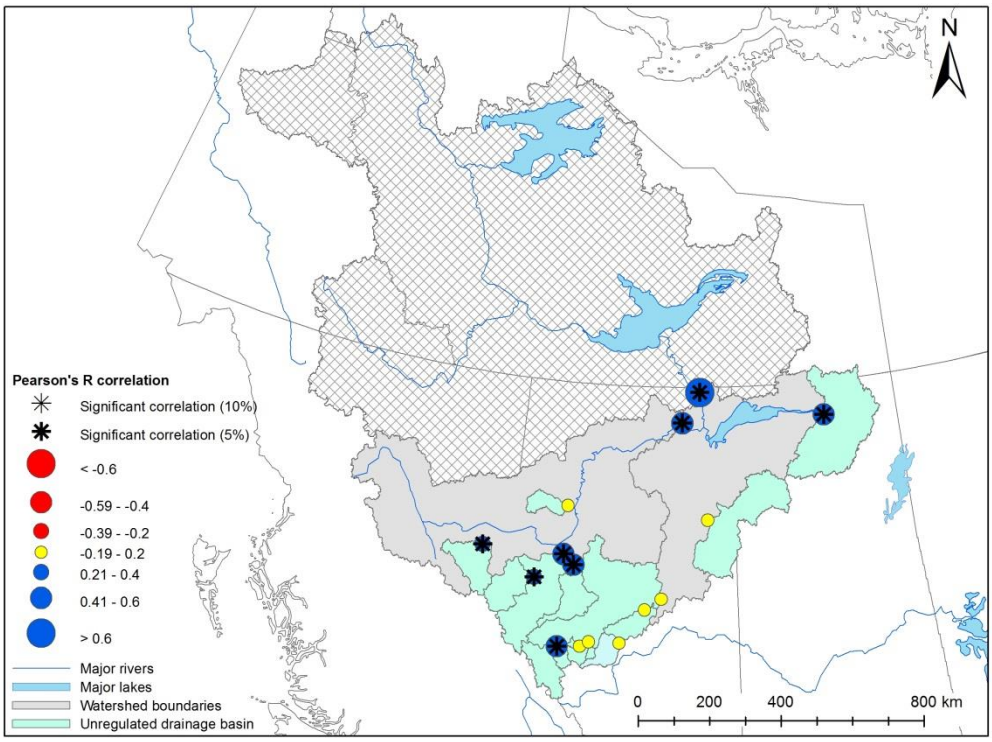

Figure C.5. Freshet length correlations with April through June average temperature (NRCAN) during the period 1962 – 2000 for Mackenzie stations.

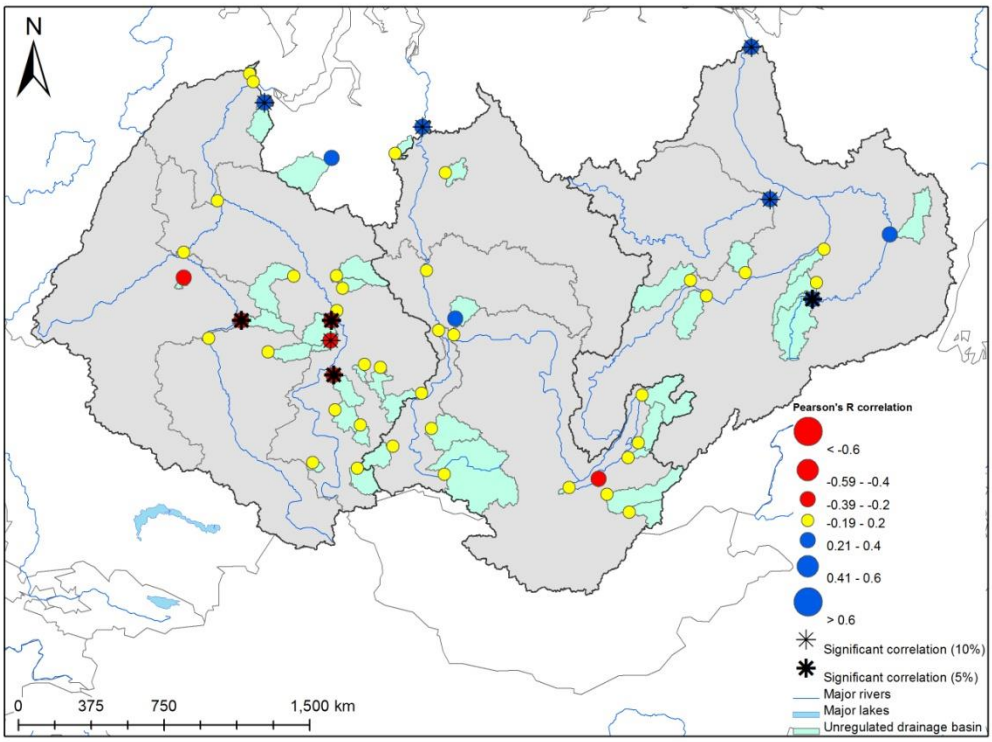

Figure C.6. Freshet length correlations with April through June average temperature (ERA-40) during the period 1962 – 2000 for Eurasian stations.

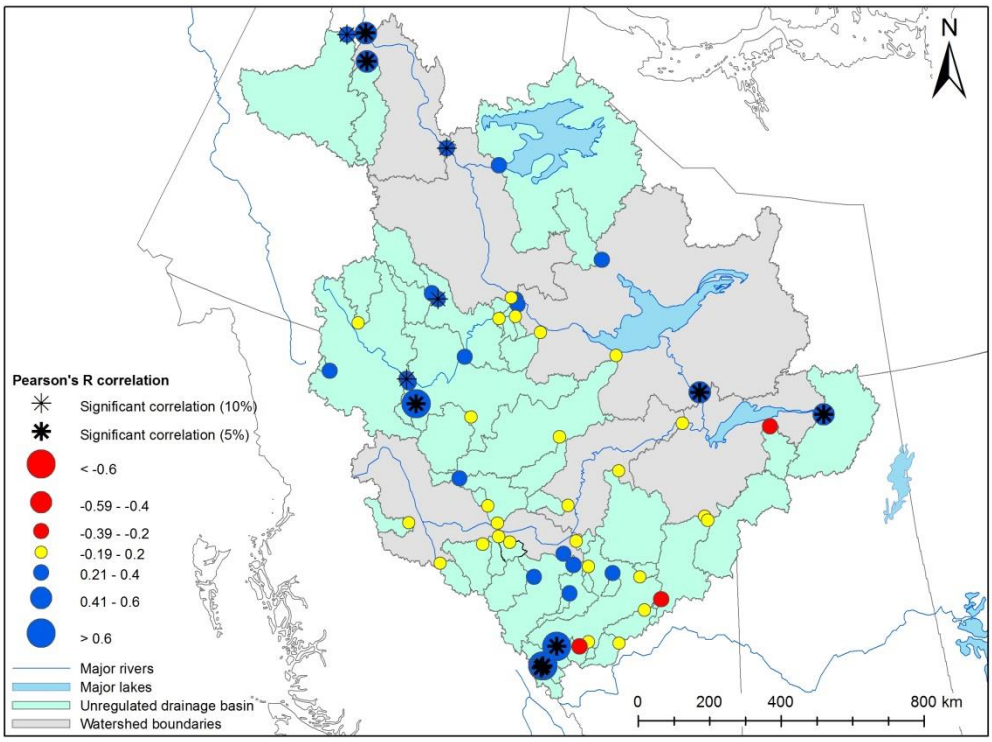

Figure C.7. Freshet length correlations with April through June average temperature (NRCAN) during the period 1980 – 2000 for Mackenzie stations.

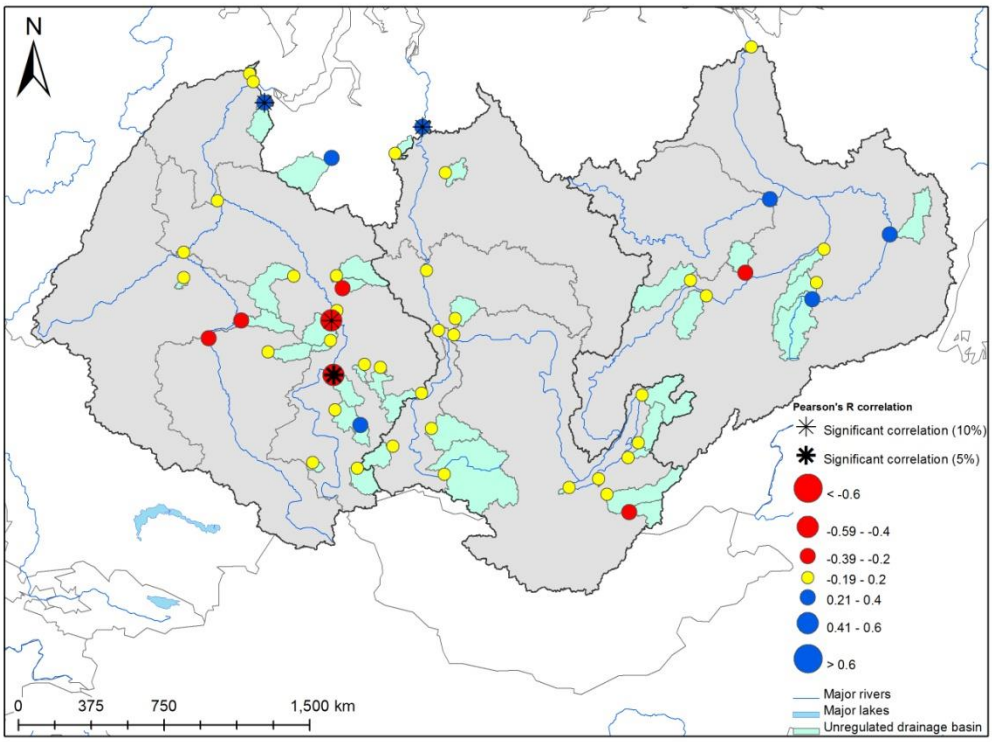

Figure C.8. Freshet length correlations with April through June average temperature (ERA-40) during the period 1980 – 2000 for Eurasian stations.

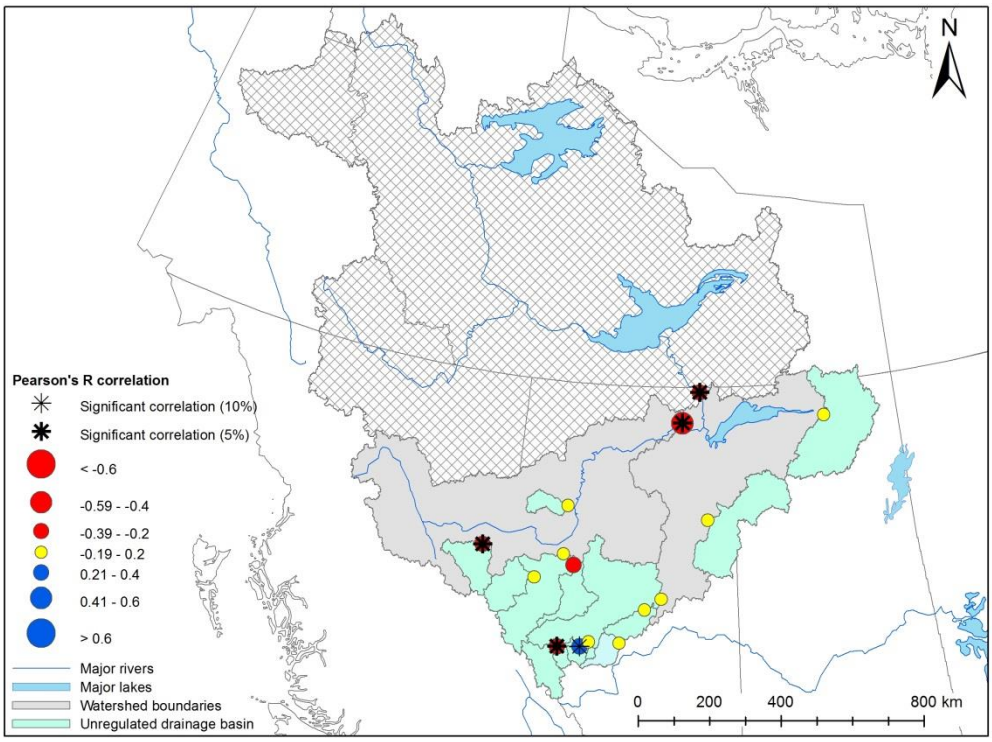

Figure C.9. Freshet magnitude correlations with April through June average temperature (NRCAN) during the period 1962 – 2000 for Mackenzie stations.

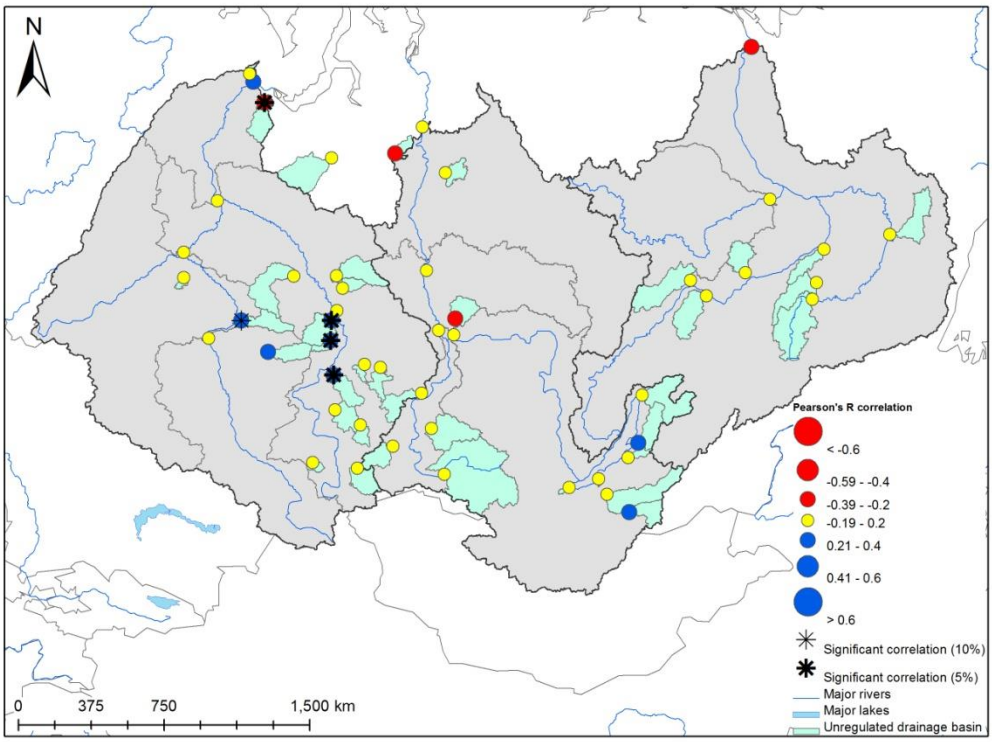

Figure C.10. Freshet magnitude correlations with April through June average temperature (ERA-40) during the period 1962 – 2000 for Eurasian stations.

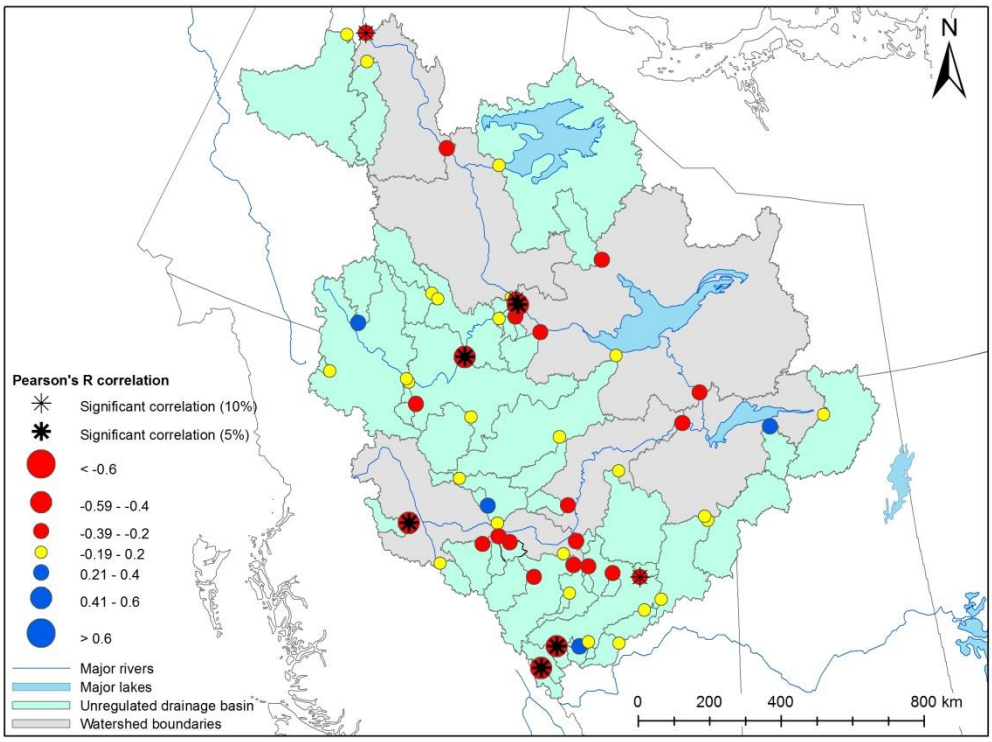

Figure C.11. Freshet magnitude correlations with April through June average temperature (NRCAN) during the period 1980 – 2000 for Mackenzie stations.

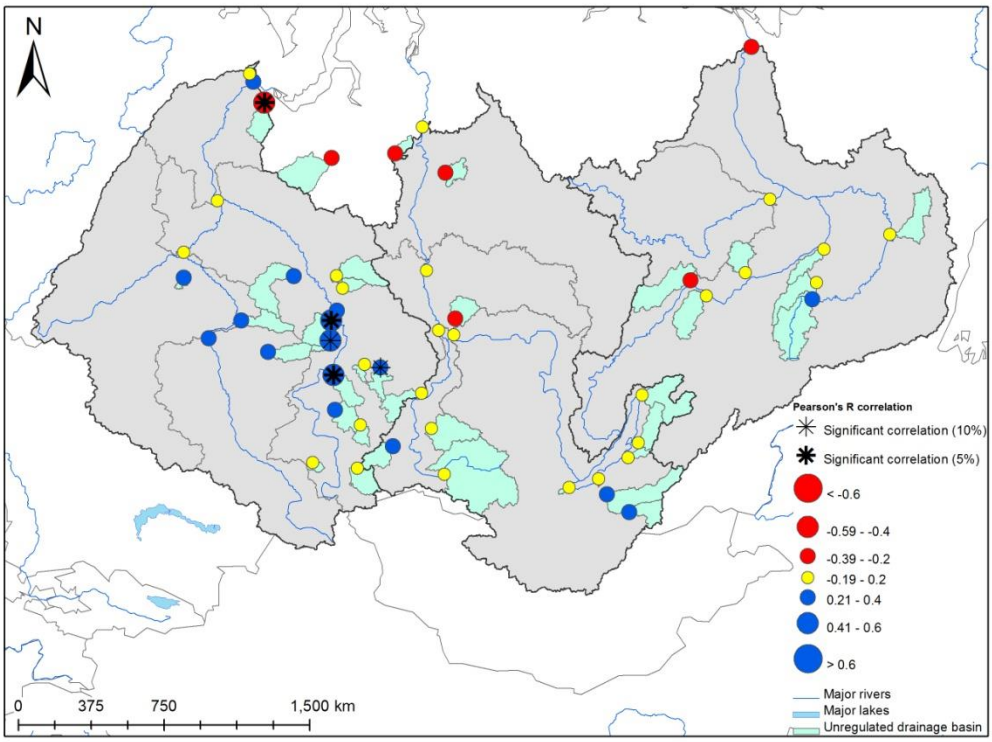

Figure C.12. Freshet magnitude correlations with April through June average temperature (ERA-40) during the period 1980 – 2000 for Eurasian stations.

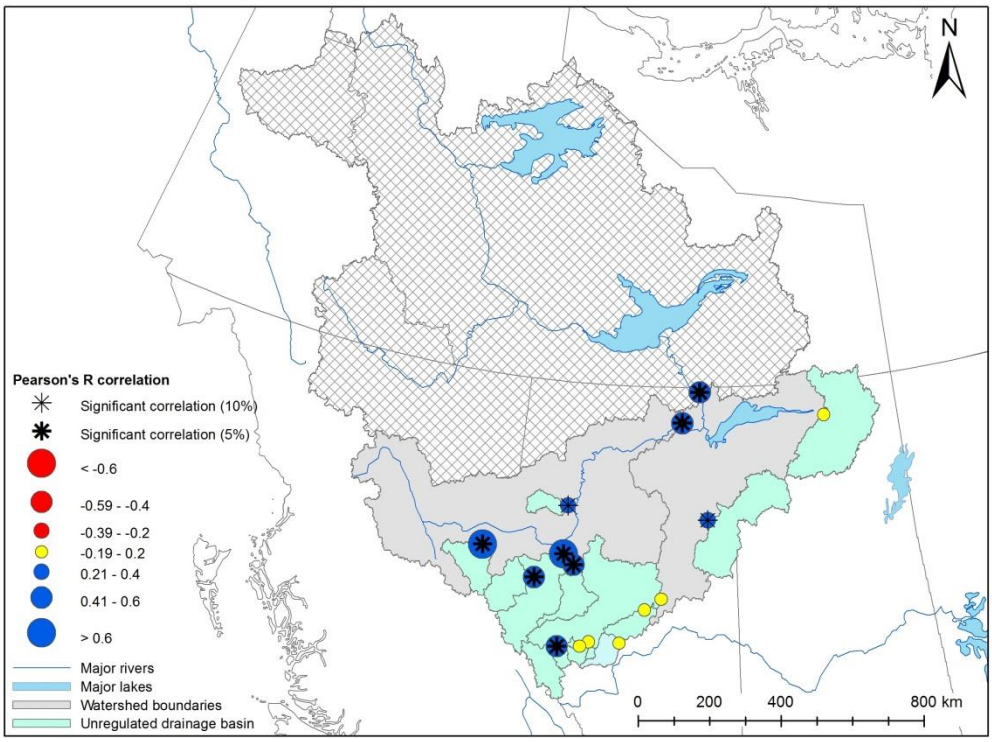

Figure C.13 Freshet volume correlations with November through March cumulative precipitation (NRCAN) during the period 1962 – 2000 for Mackenzie stations.

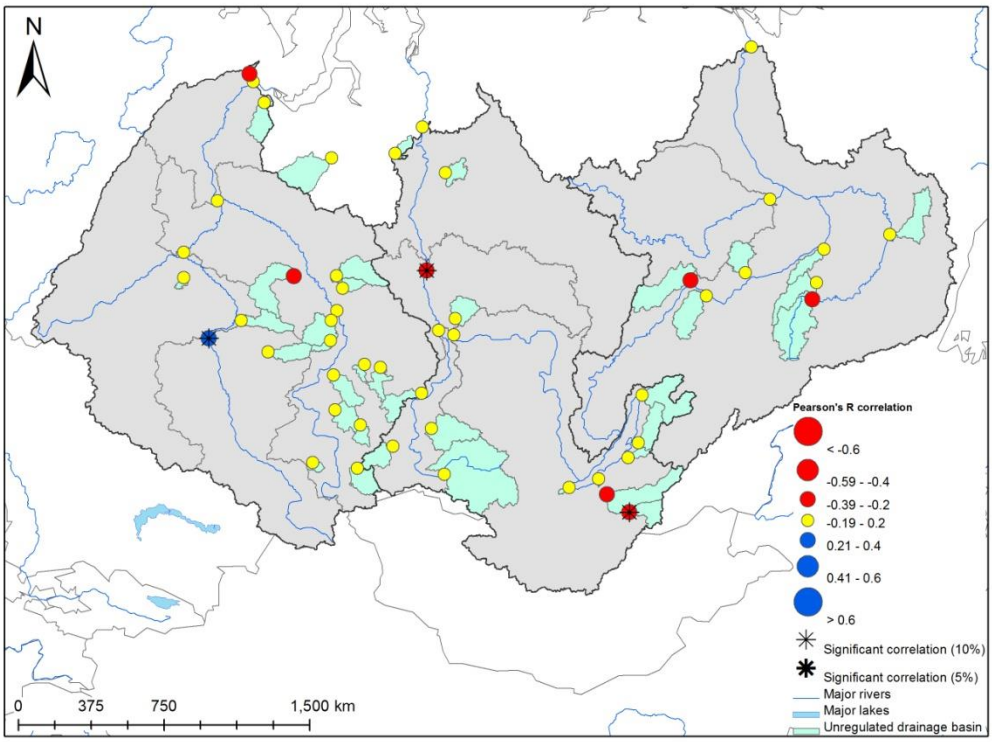

Figure C.14. Freshet volume correlations with November through March cumulative precipitation (ERA-40) during the period 1962 – 2000 for Eurasian stations.

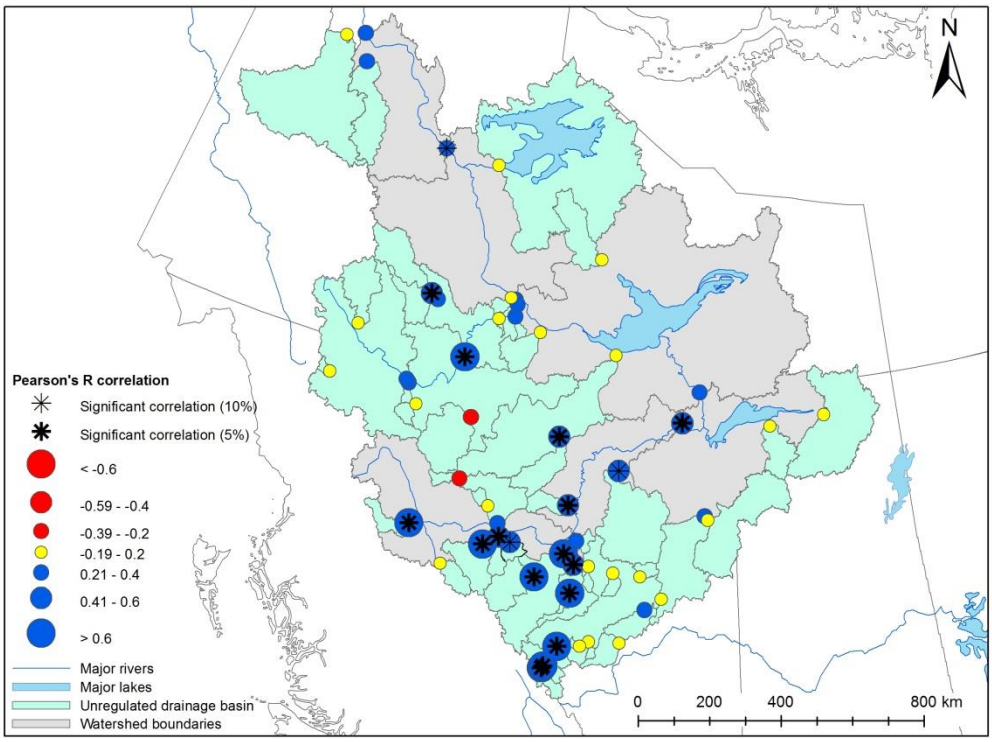

Figure C.15. Freshet volume correlations with November through March cumulative (NRCAN) precipitation during the period 1980 – 2000 for Mackenzie stations.

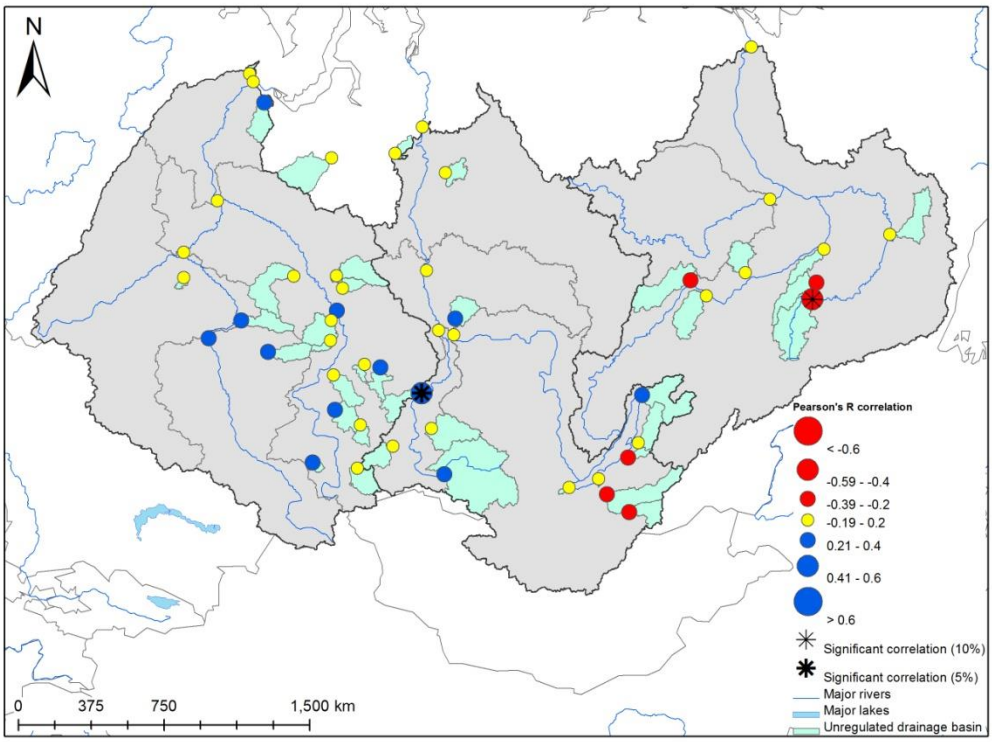

Figure C.16. Freshet volume correlations with November through March cumulative precipitation (ERA-40) during the period 1980 – 2000 for Eurasian stations.

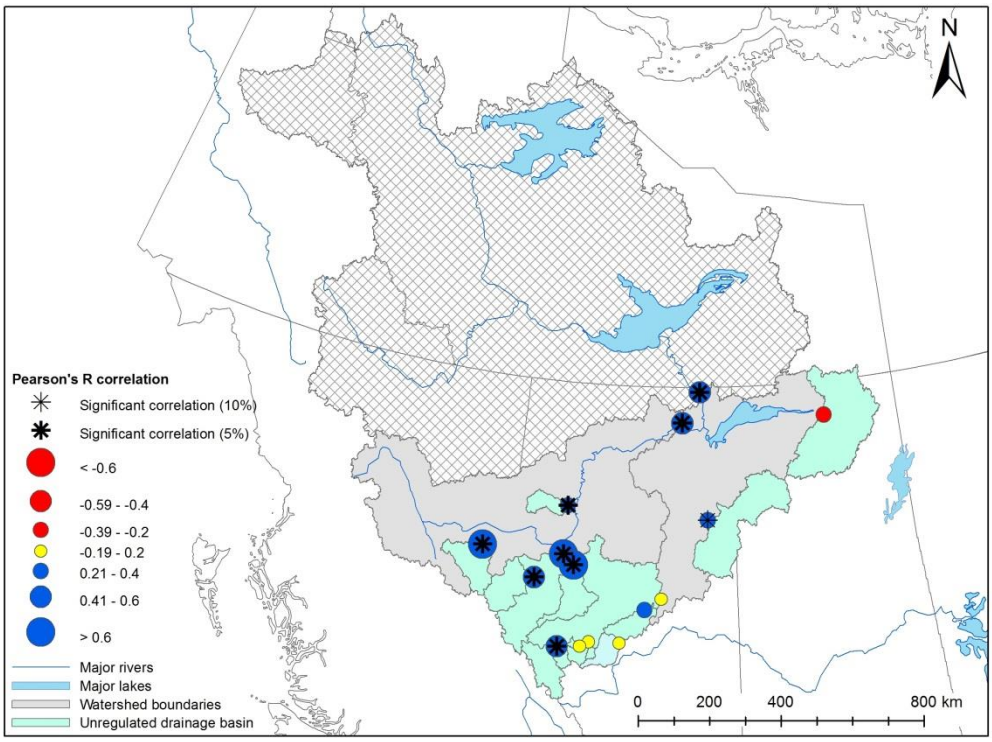

Figure C.17. April through July volume correlations with November through March cumulative precipitation (NRCAN) during the period 1962 – 2000 for Mackenzie stations.

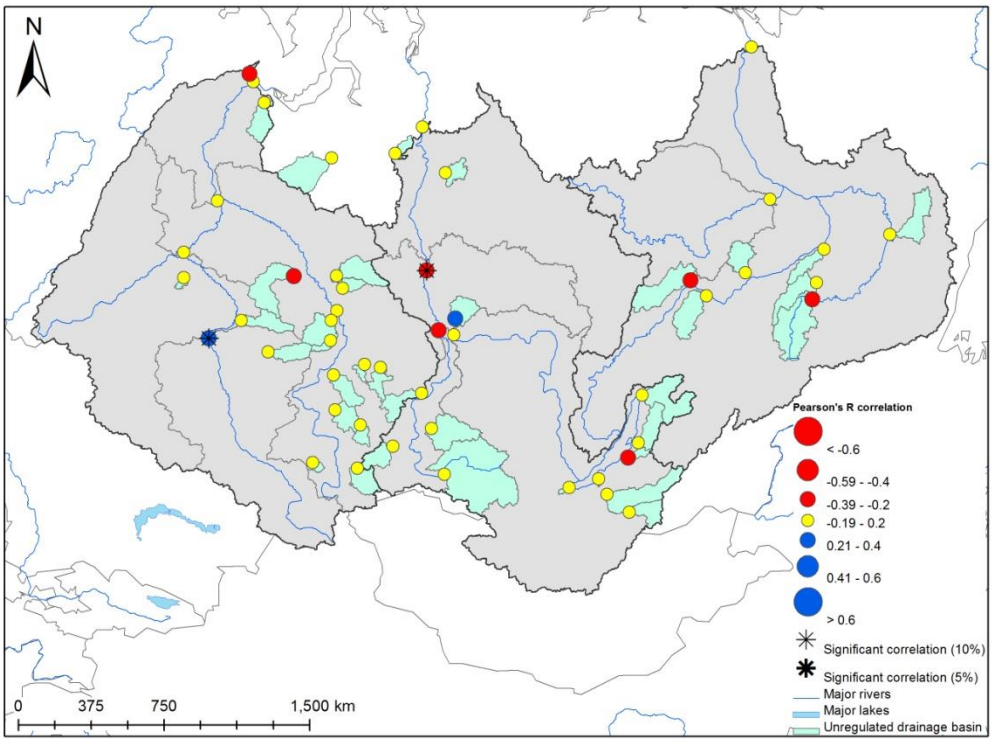

Figure C.18. April through July volume correlations with November through March cumulative precipitation (ERA-40) during the period 1962 – 2000 for Eurasian stations.

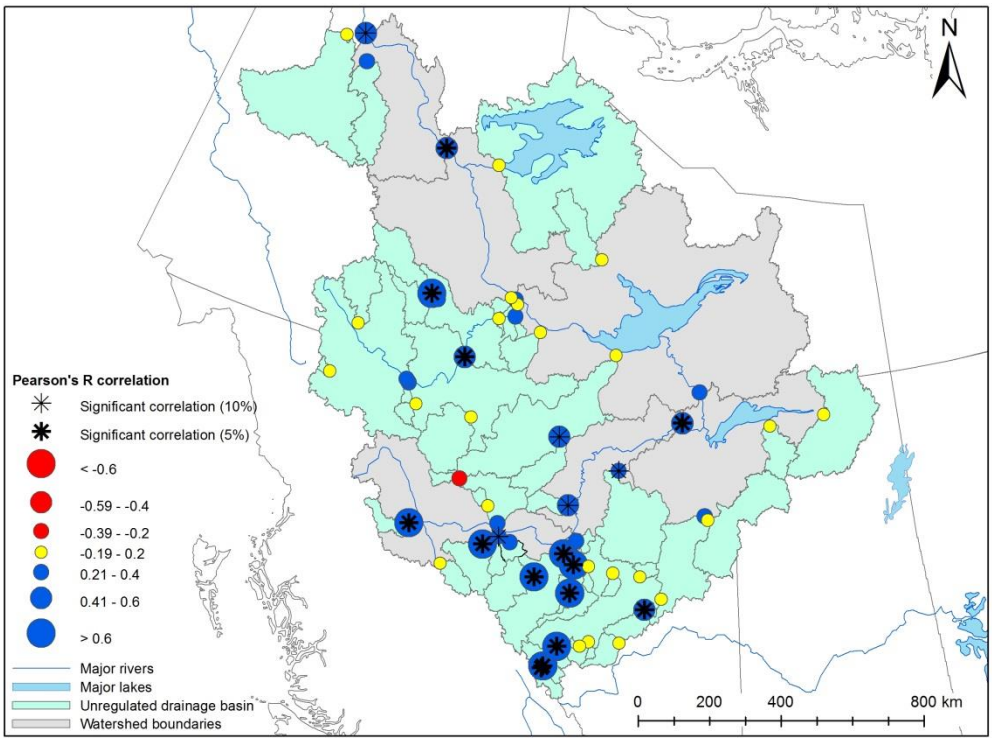

Figure C.19. April through July volume correlations with November through March cumulative precipitation (NRCAN) during the period 1980 – 2000 for Mackenzie stations.

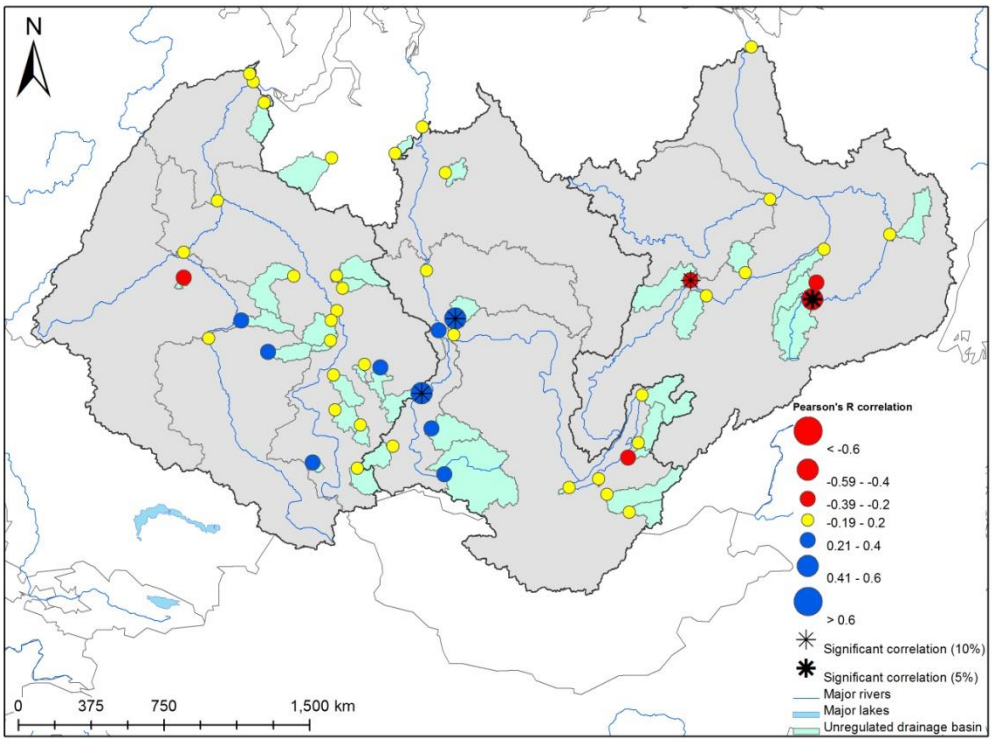

Figure C.20. April through July volume correlations with November through March cumulative precipitation (ERA-40) during the period 1980 – 2000 for Eurasian stations.